AD-A061 862 CITY COLL NEW YORK DEPT OF MECHANICAL ENGINEERING F/G 13/9
OPTIMIZATION OF STEP-UP GEAR TRAINS WITH DIFFERENT KINEMATIC PR--ETC(U)
MAY 78 G G LOWEN DAAG29-77-G-0037
UNCLASSIFIED ARO-14743.1-R-E NL

1 OF 4
ADA
061862

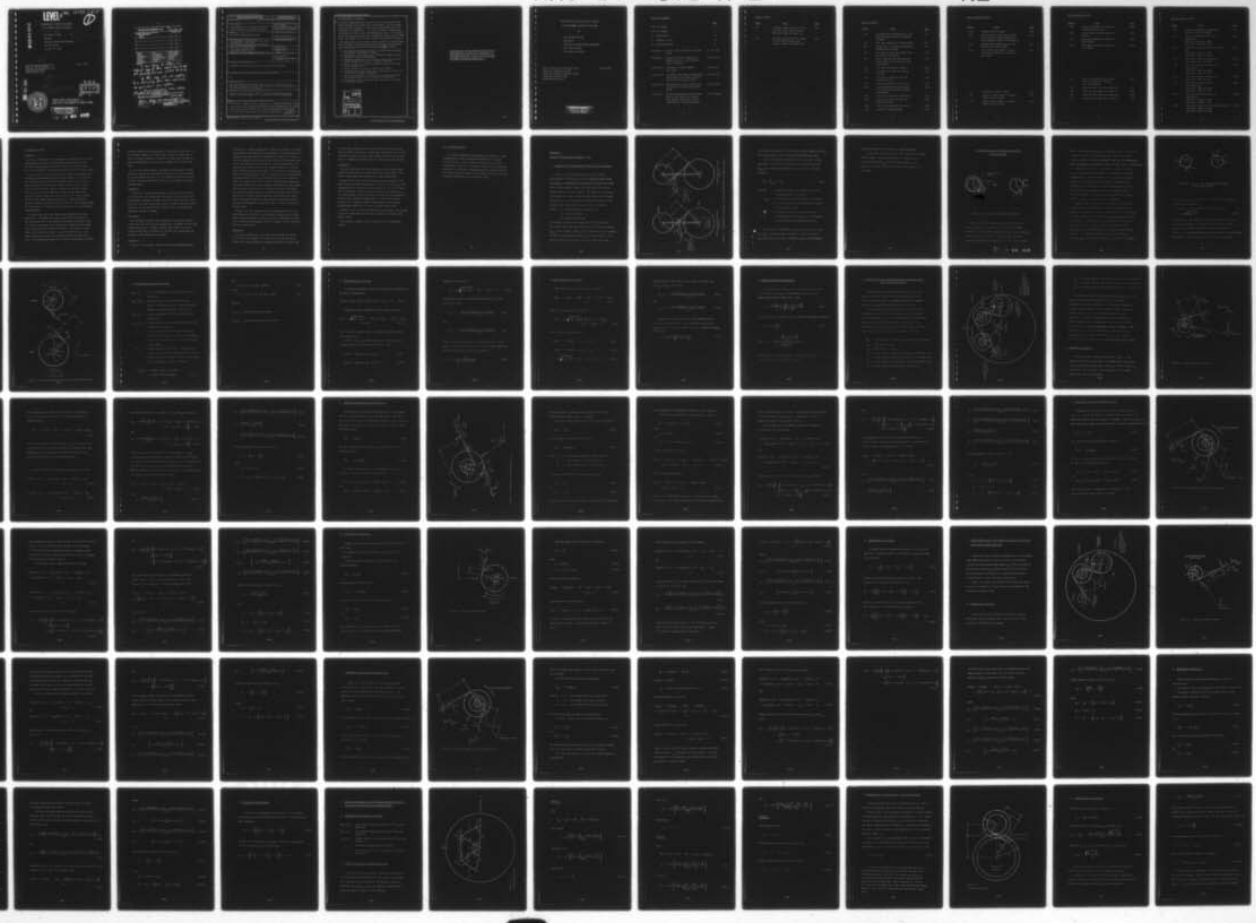

LEVEL II ARO 14743.1-R-E

(1)

AD A061862

(6) OPTIMIZATION OF STEP-UP GEAR TRAINS WITH DIFFERENT KINEMATIC PROFILES.

BY

(10) Dr. Gerard G. Lowen

Professor

Mechanical Engineering Department

The City College

New York, NY 10031

(9) Final rept. 20 Nov 76-31 May 78

(11) 31 May 78

(12) 316p

This research was conducted under
Grant No. DAAG29-77-G-0037
with the U.S. Army Research Office
Research Triangle Park
North Carolina 27709

May 31, 1978

(15) DAAG29-77-G-0037

(18) ARO

(19) 14743.1-R-E

DDC FILE COPY

DDC RECEIVED DEC 6 1978 D

THE CITY COLLEGE OF THE CITY UNIVERSITY of NEW YORK

DISTRIBUTION STATEMENT A
Approved for public release;
Distribution Unlimited

78 12 04 233

404 095

JOB

ROUTING AND TRANSMITTAL SLIP

Date: 20 Oct 78

TO: (Name, office symbol, room number, building, Agency/Post)	Initials	Date
1. DDC		
2.		
3.		
4.		
5.		

	Action		File		Note and Return
	Approval		For Clearance		Per Conversation
	As Requested		For Correction		Prepare Reply
	Circulate		For Your Information		See Me
	Comment		Investigate		Signature
	Coordination		Justify		

REMARKS

I was trying to obtain an original copy of this report due to the poor quality, but was unable to do so.

If this copy will not suffice; (it is still pretty poor) then eliminate the report from your system.

If any questions arise, please feel free to contact me.

DO NOT use this form as a RECORD of approvals, concurrences, disposals, clearances, and similar actions

FROM: (Name, org. symbol, Agency/Post)	Room No.—Bldg.
Robin Haley, AKO Library	Phone No. 433-3331 (Autov)

5041-102

OPTIONAL FORM 41 (Rev. 7-76)
Prescribed by GSA
FPMR (41 CFR) 101-11.206

GPO c48—16—83546-1

SECURITY CLASSIFICATION OF THIS PAGE *(When Data Entered)*

REPORT DOCUMENTATION PAGE		READ INSTRUCTIONS BEFORE COMPLETING FORM
1. REPORT NUMBER	2. GOVT ACCESSION NO.	3. RECIPIENT'S CATALOG NUMBER
4. TITLE *(and Subtitle)* Optimization of Step-up Gear Trains with Different Kinematic Profiles		5. TYPE OF REPORT & PERIOD COVERED Final Report 20 Nov.1976-31 May 1978 6. PERFORMING ORG. REPORT NUMBER
7. AUTHOR(s) Dr.Gerard G.Lowen,Professor		8. CONTRACT OR GRANT NUMBER(s) DAAG29-77-G-0037
9. PERFORMING ORGANIZATION NAME AND ADDRESS The Research Foundation of The City University of New York The City College,New York,N.Y.10031		10. PROGRAM ELEMENT, PROJECT, TASK AREA & WORK UNIT NUMBERS
11. CONTROLLING OFFICE NAME AND ADDRESS U.S.Army Research Office Post Office Box 12211 Research Triangle Park,NC 27709		12. REPORT DATE 31 May 1978 13. NUMBER OF PAGES 309
14. MONITORING AGENCY NAME & ADDRESS *(if different from Controlling Office)*		15. SECURITY CLASS. *(of this report)* Unclassified 15a. DECLASSIFICATION/DOWNGRADING SCHEDULE NA

16. DISTRIBUTION STATEMENT *(of this Report)*

Approved for public release. Distribution unlimited

17. DISTRIBUTION STATEMENT *(of the abstract entered in Block 20, if different from Report)*

NA

18. SUPPLEMENTARY NOTES

The findings in this report are not to be construed as an official Department of the Army position,unless so designated by other authorized documents

19. KEY WORDS *(Continue on reverse side if necessary and identify by block number)*

Gear train efficiency. Involute step-up gearing. Clock or ogival step-up gearing. Gear friction in spin environment.

20. ABSTRACT *(Continue on reverse side if necessary and identify by block number)*

It was the purpose of this project to provide the tools which allow efficiency comparisons between fuze related two and three pass step-up gear trains of different tooth geometries which are subject to operation in a spin environment. —> next page (cont'd.)

DD FORM 1 JAN 73 1473 EDITION OF 1 NOV 65 IS OBSOLETE

SECURITY CLASSIFICATION OF THIS PAGE *(When Data Entered)*

Continuation of Block 20

cont'd To this end, mathematical models of such gear trains with both involute and ogival tooth shapes have been developed. These models allow, by way of moment input-output relationships, the determination of point and cycle efficiencies of the gear trains. Pivot friction, partly due to the centrifugal forces, is considered in addition to tooth contact friction. All models allow a wide variety of parameter changes.

The appendices of this final report contain the derivations for the moment input-output relationships. In addition, they give derivations for the following associated topics:

a. Directions of friction forces at tooth contact points in involute and ogival gearing.

b. Assumptions concerning pivot friction moments of gear trains in a spin environment.

c. Auxiliary geometric and kinematic expressions for involute trains as basis for computer controls.

d. Design of unequal addendum involute gear meshes with unity contact ratio.

e. Basic geometry of clock (ogival) gear tooth.

f. Kinematics of clock tooth gear mesh: round on round and round on flat phase of motion.

g. Moment input-output relationships of single involute and ogival meshes in a stationary environment.

h. Kinematics of two and three pass step-up gear trains with ogival teeth.

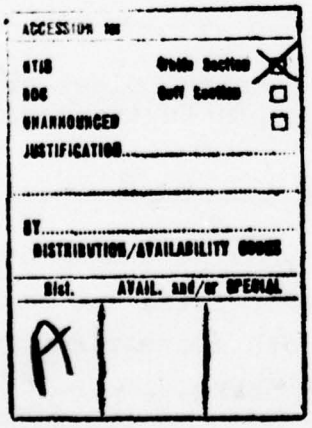

THE FINDINGS IN THIS REPORT ARE NOT TO BE CONSTRUED AS AN OFFICIAL DEPARTMENT OF THE ARMY POSITION, UNLESS SO DESIGNATED BY OTHER AUTHORIZED DOCUMENTS.

OPTIMIZATION OF STEP-UP GEAR TRAINS WITH DIFFERENT KINEMATIC PROFILES

BY

Dr. Gerard G.Lowen
Professor
Mechanical Engineering Department
The City College
New York,N.Y. 10031

This research was conducted under
Grant No. DAAG29-77-G-0037
with the U.S.Army Research Office
Research Triangle Park,
North Carolina 27709

May 31,1978

DISTRIBUTION STATEMENT A
Approved for public release;
Distribution Unlimited

TABLE OF CONTENTS

		Page
List of Tables		2
List of Figures		3
1. Introduction		8
2. Summary of Work		9
3. Acknowledgements		13
Appendix A:	Step-up Gear Trains with Involute Teeth	A-1 to A-83
Appendix B:	Design of Unequal Addendum Involute Gear Sets with Standard Center Distances	B-1 to B-15
Appendix D:	Geometry of General Ogival Gear Tooth	D-1 to D-5
Appendix E:	Kinematics and Moment Input-Output Relationship for Single Step-up Gear Mesh with Ogival Teeth	E-1 to E-39
Appendix G:	Kinematics of Two and Three Pass Step-up Gear Trains with Ogival Teeth	G-1 to G-46
Appendix H:	Moment Input-Output Relationships for Two and Three Pass Step-up Gear Trains with Ogival Teeth Operating in a Spin Environment	H-1 to H-108

LIST OF TABLES

Table	Title	Page
H-1	Possible Combinations of Phases for Three Pass Step-up Gear Train as Shown in Figure G-1	H-2
H-2	Possible Combinations of Phases for Two Pass Step-up Gear Train as Shown in Figure A-10	H-3

LIST OF FIGURES

Figure	Title	Page
A-1	Determination of Direction of Contact Friction Forces by Velocity Analysis	A-2
A-2	Free Body Diagrams of Pivot Shafts	A-5
A-3	Moments due to Friction Components Always Oppose Motion	A-7
A-4	Free Body Diagram for Single Step-Up Involute Gear Mesh	A-10
A-5	Basic Configuration for Involute Three Step-Up Gear Train in Spin Environment	A-19
A-6	Free Body Diagram of Pinion 4	A-21
A-7	Equilibrium of Gear and Pinion Set No.3	A-28
A-8	Free Body Diagram of Gear and Pinion Set No.2	A-35
A-9	Free Body Diagram of Gear No.1	A-42
A-10	Basic Configuration for Involute Two Step-Up Gear Train in Spin Environment	A-48
A-11	Free Body Diagram of Pinion No.3	A-49
A-12	Free Body Diagram of Gear and Pinion Set No.2	A-56
A-13	Free Body Diagram of Gear No.1	A-64
A-14	Pivot Hole Relationships	A-70

LIST OF FIGURES CONT'D

Figure	Title	Page
A-15	Involute Mesh Geometry	A-75
B-1	Relationship between Pinion Pitch Radius r_p, Rack Cutter Addendum A and Resulting Pinion Root Radius r_r	B-4
B-2	Minimum Root Radius r_{rm} for Rack Cutter with Sharp Corner	B-5
B-3	Rack Cutter with Corner Radius r_c (Effective Addendum of Cutter is Decreased)	B-6
D-1	Geometry of Ogival Tooth	D-2
E-1	Round on Round Phase of Contact (Gear Drives Pinion)	E-2
E-2	Round on Flat Phase of Contact (Gear Drives Pinion)	E-11

LIST OF FIGURES CONT'D

Figure	Title	Page
E-3	Sensing Geometry for Contact of Subsequent Tooth Mesh	E-19
E-4	Flat of Gear Contacts Round of Pinion	E-23
E-5	Free Body Diagram for Round on Round Phase	E-27
E-6	Free Body Diagram for Round on Flat Phase	E-34
G-1	Basic Configuration for Ogival Three Step-Up Gear Train in Spin Environment	G-2
G-2	Round on Round Phase for Mesh No.1	G-5
G-3	Round on Flat Phase for Mesh No.1	G-13
G-4	Round on Round Phase for Mesh No.2	G-24
G-5	Round on Flat Phase for Mesh No.2	G-31

LIST OF FIGURES CONT'D

Figure	Title	Page
H-1	Free Body Diagram of Pinion No.4 Mesh No.3:Round on Round	H-7
H-2	Free Body Diagram of Gear and Pinion No.3 Mesh No.3: Round on Round Mesh No.2: Round on Round	H-12
H-3	Free Body Diagram of Gear and Pinion No.2 Mesh No.2: Round on Round Mesh No.1 Round on Round	H-19
H-4	Free Body Diagram of Gear No.1 Mesh No.1: Round on Round	H-26
H-5	Free Body Diagram of Gear and Pinion No.2 Mesh No.2: Round on Round Mesh No.1: Round on Flat	H-32
H-6	Free Body Diagram of Gear No.1 Mesh No.1: Round on Flat	H-39
H-7	Free Body Diagram of Gear and Pinion No.3 Mesh No.3: Round on Round Mesh No.2: Round on Flat	H-45
H-8	Free Body Diagram of Gear and Pinion No.2 Mesh No.2: Round on Flat Mesh No.1: Round on Flat	H-52
H-9	Free Body Diagram of Gear and Pinion No.2 Mesh No.2: Round on Flat Mesh No.1: Round on Round	H-60

LIST OF FIGURES CONT'D

Figure	Title	Page
H-10	Free Body Diagram of Pinion No.4 Mesh No.3: Round on Flat	H-68
H-11	Free Body Diagram of Gear and Pinion No.3 Mesh No.3: Round on Flat Mesh No.2: Round On Flat	H-74
H-12	Free Body Diagram of Gear and Pinion No.3 Mesh No.3: Round on Flat Mesh No.2: Round on Round	H-83
H-13	Free Body Diagram of Pinion No.3 Mesh No.2: Round on Round	H-94
H-14	Free Body Diagram of Pinion No.3 Mesh No.2: Round on Flat	H-103

1. Introduction

It was the purpose of this project to provide the tools which allow efficiency comparisons between fuze-related two and three pass step-up gear trains of different tooth geometries which are subject to operation in a spin environment.

To this end, mathematical models of such gear trains with both involute and ogival (circular arc) tooth shapes have been developed. These models allow,by way of moment input-output relationships, the determination of point and cycle efficiencies of the gear trains. Pivot friction,partly due to the centrifugal forces,is considered in addition to tooth contact friction. All models allow a wide variety of parameter changes.

Various appendices of this final report contain the derivations of the moment relationships together with all associated work on pivot friction,geartooth geometry and direct contact mechanism kinematics. The following section gives a summary of this work.(There are no Appencices C or F).

2. Summary of Work

Appendix A

Appendix A furnishes the background, as well as gives the derivations, for the moment input-output expressions for two and three pass step-up gear trains (where in each mesh the gear is the driver) with involute teeth and unity contact ratio.

Section 1 shows the development of a sign convention for the direction of the contact point friction force. It is based on the direction of the relative velocity between the contact points on the gear and pinion teeth. Section 2 gives a discussion on how to deal with the normal and friction forces at the gear and pinion pivots of single and multiple mesh trains. Section 3 shows the application of the above results to the moment input-output analysis of a single mesh. The frame is assumed stationary for this case and the external loads are confined to the driving input moment and the equilibrating output moment.

The basic geometry of the three pass step-up gear train, mounted on a rotating fuze body, is formulated in section 4 for subsequent use in the moment input-output analysis. Force and moment equilibria of the individual component gears, which also account for the centrifugal forces, lead to the desired expression. Section 5 gives a similar derivation for a two pass step-up gear train with involute teeth. In order to be able to continuously compute the moment relationships for these

trains,a method for determining the simultaneous locations of the contact points of all the meshes had to be worked out. Such a method is given in section 6 together with certain angular relationships of the pivot locations on the model fuze body.

It is to be noted that,the kinematic relationships in involute gear trains are relatively simple,when compared to those in ogival trains, because of the constant transmission ratio and the invariant direction of the line of action in each individual mesh.

Appendix B

To avoid the severe undercutting of pinions which generally is associated with step-up gear meshes,it is necessary to use non-standard involute gearing. Appendix B shows both the theory as well as all necessary steps for the design of unequal addendum gears and pinions of unity contact ratio. In addition,a numerical example is given.

Appendix D

This Appendix describes the geometry of an ogival tooth in which each side of the tooth profile has a circular arc blending tangentially into a radial straight line flank. The basic tooth nomenclature is defined and methods for determining the required tooth parameters are given.

Appendix E

Section 1 of Appendix E gives all necessary kinematic deri-

vations for a single step-up mesh with ogival teeth. The motion of an ogival mesh consists of two phases. On first contact, the circular arc portion of the driving gear tooth makes contact with the circular arc portion of the driven pinion tooth. Later in the cycle,and up to the point of final disengagement, the circular arc portion of the gear tooth contacts the straight line portion of the pinion tooth. These phases of motion were named '' round on round '' and '' round on flat '' respectively. Equivalent four link mechanism models were used for both regimes to obtain expressions for the pinion output angles,for transition angles,for output angular velocities and for contact point relative velocities. In addition,a sensing expression was developed which allows the computer determination of that position of a given mesh at which the subsequent mesh comes into engagement. (Because of the variable transmission ratio of ogival meshes,there is only one set of teeth in contact at any one time).

Section 2 of this Appendix shows derivations of moment input-output expressions for both phases of contact of a single ogival mesh. Again,while pivot friction is considered in addition to contact friction,the frame is assumed to be stationary for this single mesh.

Appendix G

When one considers the kinematic relationships of ogival meshes which are mounted on a fuze body as parts of two or three pass step-up trains,it becomes necessary to account for

the relative positions of the individual meshes on the fuze body. Appendix G gives the appropriate derivations for each of the three meshes of a three pass train. The model of the fuze body is identical with that used for involute step-up trains.

Appendix H

This Appendix shows the derivations of moment input-output expressions for two and three pass step-up gear trains with ogival teeth which must operate in a spin environment.

Because of the increase in rotational speed associated with each tooth mesh, increasingly more sets of teeth will come into engagement in the second and third meshes as one set of teeth moves through one complete contact cycle in the first (i.e. the input) mesh. With two phases of motion for each mesh, there will be eight contact combinations in a three pass train. Section 1 of Appendix H gives a derivation for the moment input-output expression of each of these eight cases.

Section 2 shows similar work for the four contact combinations which are associated with two pass step-up gear trains with ogival teeth.

Both analyses account for the effects of the centrifugal forces.

5. Acknowledgements

The author gratefully acknowledges the support of this research due to Grant No.DAAG29-77-G-0037 by the Army Research Office. Special thanks for his great help and cooperation is due to Dr.Frederick R.Tepper of the Armament Research and Development Command,Dover,New Jersey. Finally, the author wishes to thank his students,Mr.Richard Chin and Mr.Shmuel Kayam,for their invaluable help.

APPENDIX A

STEP-UP GEAR TRAINS WITH INVOLUTE TEETH

1. DIRECTION OF FRICTION FORCE AT TOOTH TO TOOTH CONTACT

Figure A-1 uses the base circle - line of action configuration of an involute mesh, in which the gear drives the pinion, to determine the direction of the friction forces at the contact point C before and after the contact point passes through the pitch point P. The distance d represents the length of the line of action between base circle tangent points L and L'. The length a measures the distance of the contact point C from point L along the line of action.

Further: θ = actual (rolling) pressure angle

R_b = gear base radius

r_b = pinion base radius

The friction force of the pinion tooth on the gear tooth, for example, will have the direction of the relative velocity $\overline{V}_{C_p/C_g}$ of the contact point C_p of the pinion tooth with respect to the coincident contact point C_g of the gear tooth. (The friction force of the gear tooth on the pinion tooth has

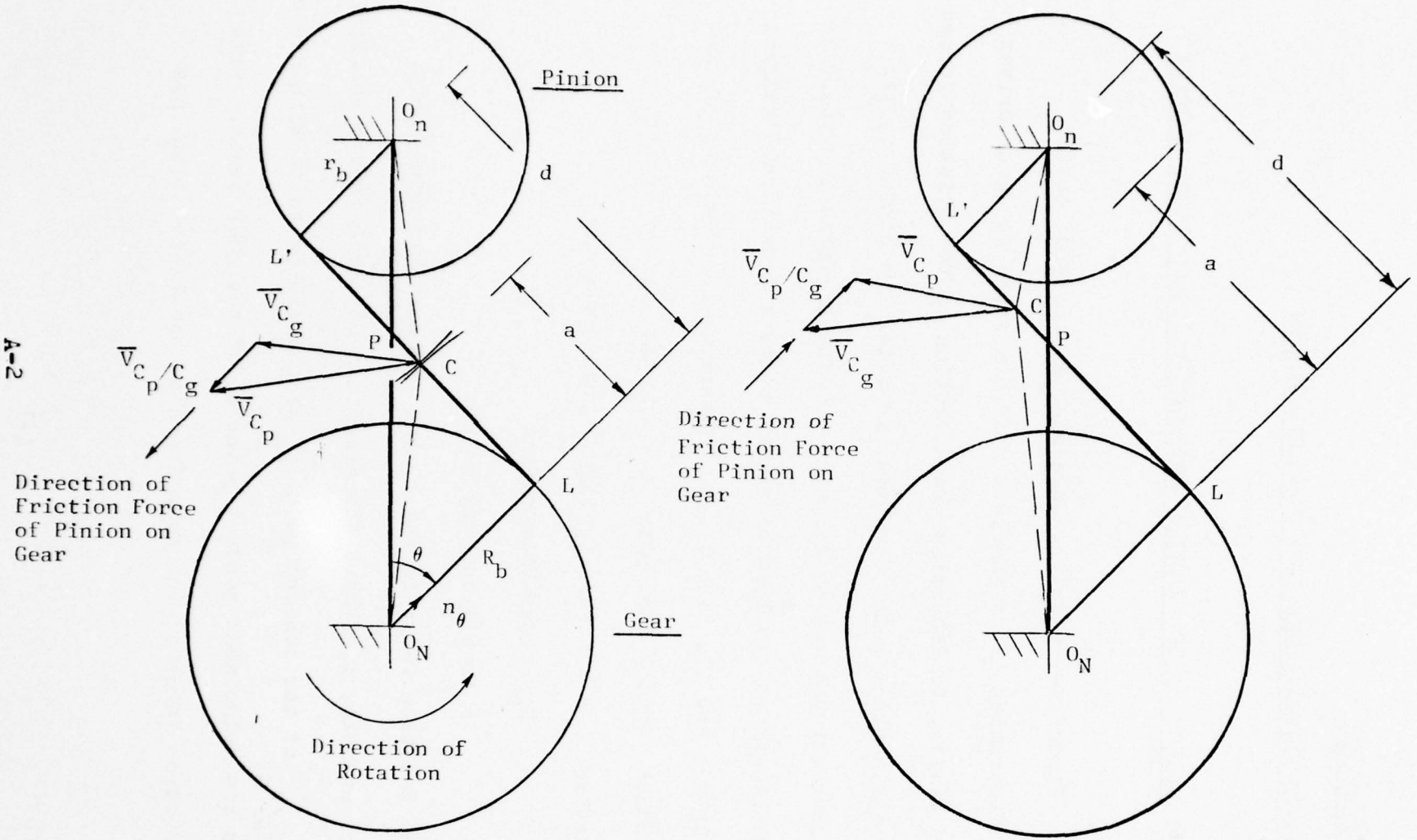

a. Contact Before Pitch Point (Approach)

b. Contact After Pitch Point (Recess)

FIGURE A-1 DETERMINATION OF DIRECTION OF CONTACT FRICTION FORCES BY VELOCITY ANALYSIS

the opposite direction.) This relative velocity changes direction at the pitch point, where it becomes instantaneously zero.

Figure A-1a shows contact before the pitch point (during approach). To obtain the direction of the relative velocity $\overline{V}_{C_p/C_g}$ by a graphical analysis one makes use of the velocity equation:

$$\overline{V}_{C_p} = \overline{V}_{C_p/C_g} + \overline{V}_{C_g} \qquad \text{(A-1)}$$

where $\overline{V}_{C_p}$ = velocity of point C_p on pinion tooth with direction normal to line O_n- C

$\overline{V}_{C_p/C_g}$ = relative velocity between point C_p and point C_g. The direction of this velocity is normal to the line of action.

$\overline{V}_{C_g}$ = velocity of point C_g on gear tooth with direction normal to line O_N- C. The magnitude of this velocity was arbitrarily chosen.

The graphical construction, according to Equ. (A1), shows that $\overline{V}_{C_p/C_g}$ has the direction opposite to that of the unit vector $\overline{n}_\theta$ shown at point O_N. As stated earlier this represents

the friction force on the gear tooth during approach.

Figure A-1b shows the same graphical analysis for contact during recess. Once the pitch point is passed, both the relative velocity $\overline{V}_{C_p/C_g}$ and the friction force of the pinion on the gear have the direction of the positive unit vector $\overline{n}_\theta$.

2. ASSUMPTIONS CONCERNING NORMAL AND FRICTION FORCES AT PIVOTS

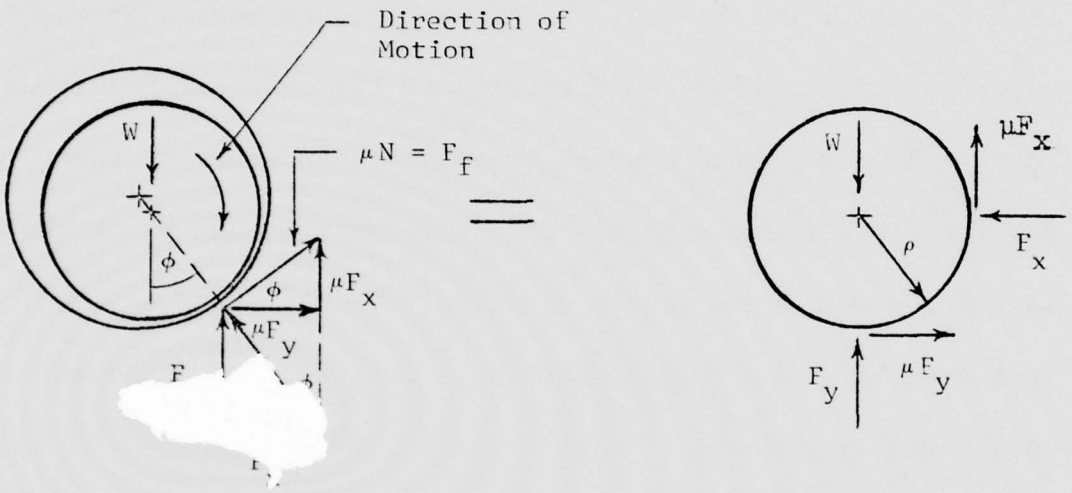

a. b.

FIGURE A-2 FREE-BODY DIAGRAMS OF PIVOT SHAFTS

Figure A-2a shows a pivot shaft which is loaded by a known external force W and which rotates in a clockwise direction. Due to friction between the shaft and the bearing, contact is made at an angle $\phi = \tan^{-1}\mu$, where μ is the associated coefficient of friction. N is the normal contact

68 12 04 228

force. The friction force $F_f = \mu N$ acts such that the clockwise rotation is opposed by a resulting counterclockwise moment. N may be resolved into the components F_x and F_y. The associated x and y components of the friction force are μF_y and μF_x, respectively.

The directions of the components of N and F_f are drawn in the same manner in Fig. A-2b in a somewhat more convenient representation. When the direction of the external resultant force W is not known, contact is possible anywhere on the periphery of the bearing and the components F_x and F_y of the normal contact force cannot be drawn with certainty in the free body diagram. The direction of the friction components still must be such that motion will be opposed.

Figures A-3a and A-3b show two general possibilities of drawing the free body diagram of a pivot which rotates in a clockwise direction. In either case the moments of the friction components oppose the rotation while F_x and F_y may be positive or negative. Assume now, for example, that Fig. A-3a shows the wrong direction for F_x and that the solution of the applicable equilibrium equation will reverse the sign of F_x. This will automatically reverse the sign of the friction component μF_x also. Since contact is now made on the opposite

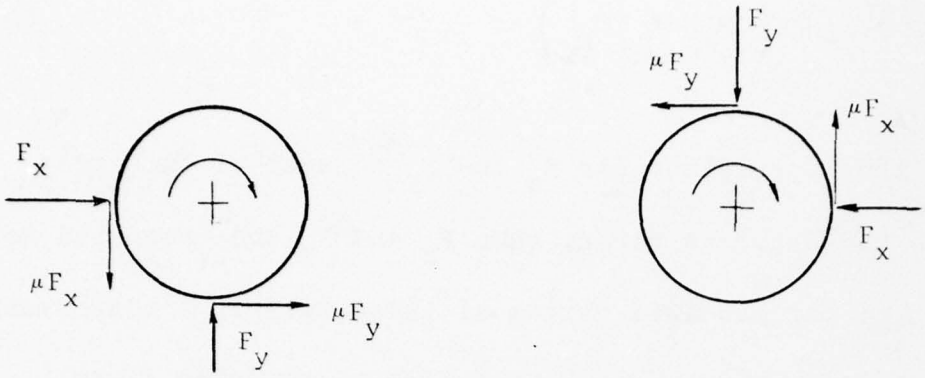

a. b.

FIGURE A-3 MOMENTS DUE TO FRICTION COMPONENTS ALWAYS OPPOSE MOTION

side of the pivot, the correct sign of the friction component is automatically assured.

The total friction moment then is expressed by:

$$M_f = \pm \mu \rho \sqrt{F_x^2 + F_y^2} \qquad (A\text{-}2)$$

where ρ is the pivot radius. The sign of the above is chosen such that the rotation is opposed. In case that F_x and F_y contain required terms that cannot be factored out of the square root of equation (A-2), the friction moment is conservatively overstated by the use of the absolute values of F_x and F_y;

$$M_f = \pm \mu \rho \left(|F_x| + |F_y| \right) \qquad \text{(A-3a)}$$

If the expressions for F_x and F_y consist of sums of positive and negative terms, then F_x and F_y are presented as the sums of the absolute values of these terms. A conservative pivot friction moment becomes, similar to equation (A-3a):

$$M_f = \pm \mu \rho \left(\tilde{F}_x + \tilde{F}_y \right) \qquad \text{(A-3b)}$$

The tildas represent the sums of the absolute values of the component terms.

3. MOMENT INPUT-OUTPUT RELATIONSHIP FOR SINGLE STEP-UP GEAR MESH WITH INVOLUTE TEETH

Figure A-4 shows free body diagrams of the gear and the pinion of a single mesh where the gear is driven by a counterclockwise input moment M_{in}. It is desired to find the equilibrating output moment M_o.

a. UNIT VECTORS

The unit vector directed from point O_N to point L is given by:

$$\bar{n}_{\theta} = \sin\theta\bar{i} + \cos\theta\bar{j} \qquad \text{(A-4)}$$

where θ represents the actual pressure angle, regardless of tooth modification. The unit vector directed along the line of action from point L to point L' is given by:

$$\bar{n}_{\theta T} = -\cos\theta\bar{i} + \sin\theta\bar{j} \qquad \text{(A-5)}$$

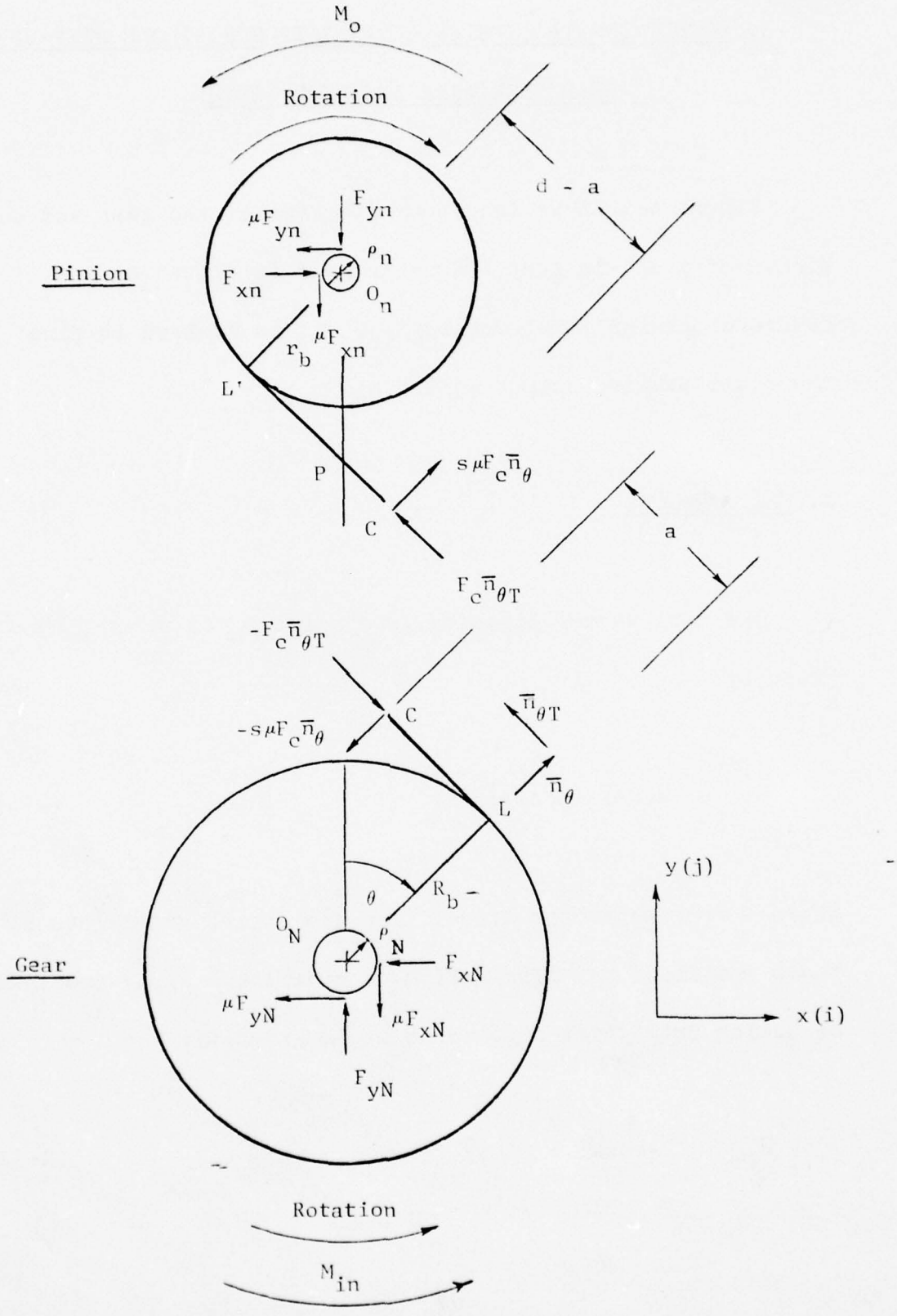

FIGURE A-4 FREE BODY DIAGRAM FOR SINGLE STEP-UP INVOLUTE GEAR MESH

b. *NOMENCLATURE AND SIGNUM CONVENTION*

F_{xN}, F_{yN} = x and y components of normal force acting on gear pivot

μF_{xN}, μF_{yN} = friction force components acting on gear pivot. Directions chosen to result in friction moments which oppose motion. (See part 2).

F_{xn}, F_{yn} = x and y components of normal force acting on pinion pivot.

μF_{xn}, μF_{yn} = friction force components acting on pinion pivot.

μ = coefficient of friction.

F_c = normal contact force between gear and pinion. The force of the pinion on the gear is $(-)F_c\bar{n}_{\theta T}$, while the normal force of the gear on the pinion becomes $F_c\bar{n}_{\theta T}$.

μF_c = tooth contact friction force. The analysis in Section 1 shows that the friction force of the pinion on the gear, before the pitch point, acts in the direction of $(-)\bar{n}_\theta$. Therefore:

$-s\mu F_c\bar{n}_\theta$ = friction force on gear with

s = +1 for a $< \overline{LP}$ (approach) (A-6)

and

$$s = -1 \quad \text{for } a > \overline{LP} \quad \text{(recess)} \tag{A-7}$$

while

$$s = 0 \text{ for } a = \overline{LP} \quad \text{(at pitch point)} \tag{A-8}$$

Further,

ρ_N, ρ_n = gear and pinion pivot radii

R_b, r_b = gear and pinion base circle radii

c. FORCE ANALYSIS OF THE GEAR

By inspecting Figure A-4, one sees that force equilibrium of the gear is expressed by:

$$-F_c\bar{n}_{\theta T} - s\mu F_c\bar{n}_\theta - F_{xN}\bar{i} - \mu F_{xN}\bar{j} + F_{yN}\bar{j} - \mu F_{yN}\bar{i} = 0 \qquad (A\text{-}9)$$

Similarly, moment equilibrium of the gear is given by:

$$M_{in}\bar{k} - \rho_N\mu\sqrt{F_{xN}^2 + F_{yN}^2}\,\bar{k} + R_b\bar{n}_\theta \times (-)F_c\bar{n}_{\theta T} + (R_b\bar{n}_\theta + a\bar{n}_{\theta T}) \times (-)s\mu F_c\bar{n}_\theta = 0 \qquad (A\text{-}10)$$

Note the use of equation (A-2) to express the friction moment at the gear pivot.

With the help of equations (A-4) and (A-5) one may write equations (A-9) and (A-10) in scalar form. Thus,

$$F_c\cos\theta - \mu s F_c\sin\theta - F_{xN} - \mu F_{yN} = 0 \qquad (A\text{-}11)$$

$$-F_c\sin\theta - \mu s F_c\cos\theta + F_{yN} - \mu F_{xN} = 0 \qquad (A\text{-}12)$$

Equation (A-10) becomes

$$M_{in} - \rho_N \mu \sqrt{F_{xN}^2 + F_{yN}^2} - R_b F_c + \mu s a F_c = 0 \qquad \text{(A-13)}$$

Simultaneous solution of equations (A-11) and (A-12) for F_{xN} and F_{yN} gives:

$$F_{xN} = F_c \frac{(1 - \mu^2 s)\cos\theta - \mu(1 + s)\sin\theta}{1 + \mu^2} \qquad \text{(A-14)}$$

and

$$F_{yN} = F_c \frac{(1 - \mu^2 s)\sin\theta + \mu(1 + s)\cos\theta}{1 + \mu^2} \qquad \text{(A-15)}$$

When the above expressions are substituted into the moment equation (A-13) and if one notes that s^2 always equals +1, the following expression for F_c is obtained:

$$F_c = \frac{M_{in}}{R_b + \mu(\rho_N - as)} \qquad \text{(A-16)}$$

d. FORCE ANALYSIS OF THE PINION

Force equilibrium of the pinion is assured by:

$$F_c\bar{n}_{\theta T} + \mu s F_c\bar{n}_\theta + F_{xn}\bar{i} - F_{yn}\bar{j} - \mu F_{xn}\bar{j} - \mu F_{yn}\bar{i} = 0, \qquad \text{(A-17)}$$

while moment equilibrium is given by:

$$M_o\bar{k} + \rho_n \mu \sqrt{F_{xn}^2 + F_{yn}^2}\,\bar{k} + \left[-r_b\bar{n}_\theta - (d - a)\bar{n}_{\theta T}\right] \times (F_c\bar{n}_{\theta T} + \mu s F_c\bar{n}_\theta) = 0 \qquad \text{(A-18)}$$

In scalar form, the above become:

$$-F_c\cos\theta + \mu s F_c\sin\theta + F_{xn} - \mu F_{yn} = 0 \qquad \text{(A-19)}$$

$$F_c\sin\theta + \mu s F_c\cos\theta - \mu F_{xn} - F_{yn} = 0 \qquad \text{(A-20)}$$

$$M_o + \mu\rho_n\sqrt{F_{xn}^2 + F_{yn}^2} - r_b F_c + \mu s(d - a)F_c = 0 \qquad \text{(A-21)}$$

Equations (A-19) and (A-20) are now solved simultaneously for F_{xn} and F_{yn}. This gives

$$F_{xn} = F_c \frac{(1 + \mu^2 s)\cos\theta + \mu(1 - s)\sin\theta}{1 + \mu^2} \qquad \text{(A-22)}$$

and

$$F_{yn} = F_c \frac{(1 + \mu^2 s)\sin\theta - \mu(1 - s)\cos\theta}{1 + \mu^2} \qquad \text{(A-23)}$$

Equations (A-22) and (A-23) are then substituted into the moment equation (A-21). This furnishes the following expression for the normal contact force F_c. (Again, s^2 always equals +1.)

$$F_c = \frac{M_o}{r_b - \mu\left[\rho_n + s(d - a)\right]} \qquad \text{(A-24)}$$

e. MOMENT INPUT-OUTPUT RELATIONSHIP

The equilibrant moment M_o may be expressed as a function of the input moment M_{in} after equations (A-16) and (A-24) have been set equal to each other. Thus,

$$M_o = \frac{M_{in}\left\{r_b - \mu\left[\rho_n + s(d - a)\right]\right\}}{R_b + \mu\left[\rho_N - sa\right]} \qquad \text{(A-25)}$$

The input-output relationship may also then be expressed in terms of

$$M_o = M_{in}\frac{r_b}{R_b}E_2 \qquad \text{(A-26)}$$

where $$E_2 = \frac{1 - \dfrac{\mu\left[\rho_n + s(d - a)\right]}{r_b}}{1 + \dfrac{\mu(\rho_N - sa)}{R_b}} ,$$

and represents the efficiency of moment transmission of a single step-up mesh with involute teeth.

4. MOMENT INPUT-OUTPUT RELATIONSHIP FOR THREE STEP-UP GEAR TRAIN IN SPIN ENVIRONMENT

Figure A-5 shows the basic configuration of the three step-up gear train for which the relationship between the equilibrant output moment M_{o4}, acting on pinion 4, and the input moment M_{in}, acting on gear 1, is to be found.

The body-fixed x-y coordinate system has its origin at the spin axis C of the fuze body, and its x-axis coincides with the line C-O_1, where O_1 represents the pivot axis of the input gear-spin rotor combination. Points O_2, O_3 and O_4 represent the pivot axes of gear and pinion no. 2, gear and pinion no. 3, and pinion no. 4 respectively. Further,

$\mathcal{R}_i$ = distance from the spin axis to the various pivot axes

R_{bi} = base radii of gears

r_{bi} = base radii of pinions

β_1 = angle between positive x-axis and line of centers O_1-O_2

β_2 = angle between positive x-axis and line of centers O_2-O_3

β_3 = angle between positive x-axis and line of centers O_3-O_4

γ_i = angle between positive x-axis and lines C-O_i

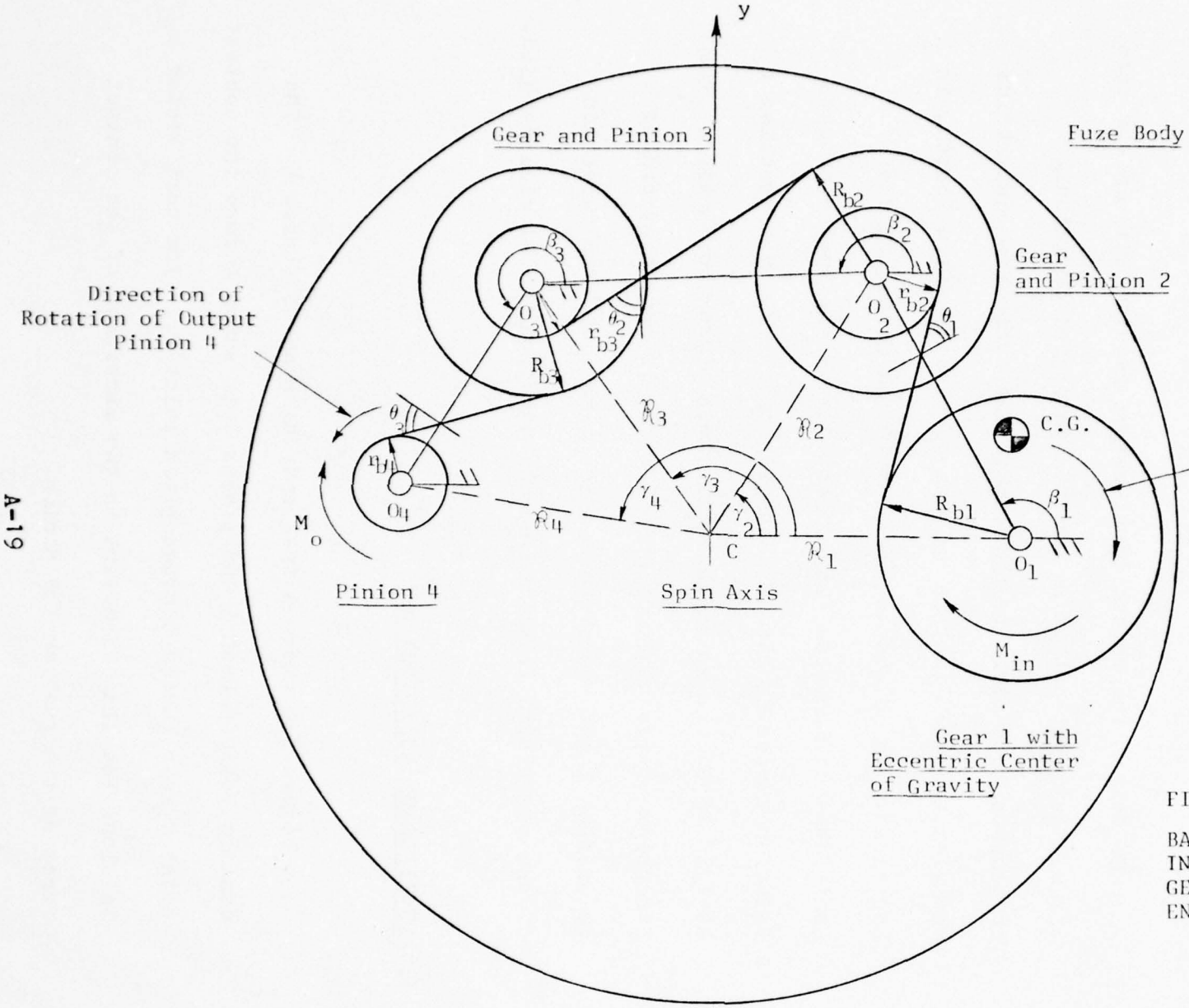

FIGURE A5

BASIC CONFIGURATION FOR INVOLUTE THREE STEP-UP GEAR TRAIN IN SPIN ENVIRONMENT

θ_1 = pressure angle of mesh between gear no. 1 and pinion no. 2

θ_2 = pressure angle of mesh between gear no. 2 and pinion no. 3

θ_3 = pressure angle of mesh between gear no. 3 and pinion no. 4

To obtain the moment input-output relationship of the total train, the input-output relationships of the individual components must first be obtained. The following equilibrium analyses include pivot as well as contact friction forces, in addition to loads due to the centrifugal forces on the individual components. The directions of the tooth-to-tooth friction forces is chosen according to the rules of Section 1 of this appendix, using an appropriate signum convention. The direction of the pivot friction forces is chosen according to Section 2 and, to avoid difficulties with the direction of the associated friction moment, equation (A-3b) will be used.

a. EQUILIBRIUM OF PINION 4

Figure A-6 shows a free body diagram of pinion 4. The contact between gear 3 and pinion 4 is shown before the contact point C_3 has passed through pitch point P_3. The unit vector $\bar{n}_{34}$ is along the line of action in the direction of the contact force of the gear on the pinion.

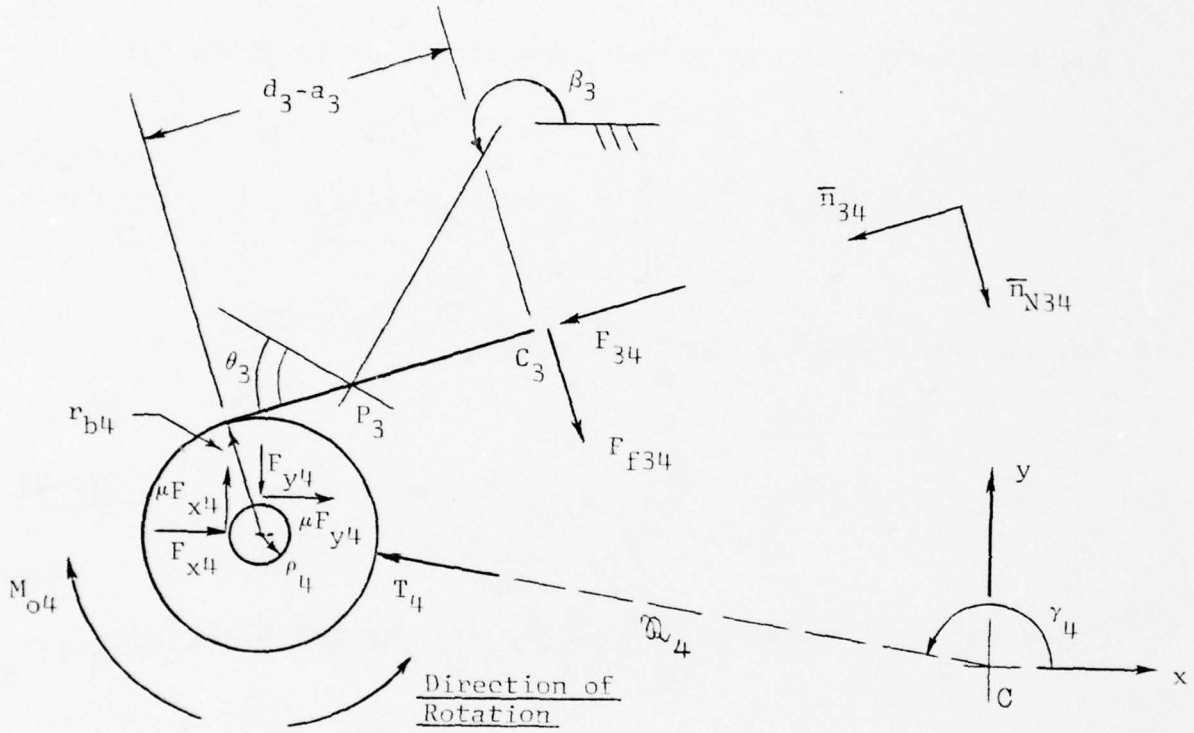

FIGURE A-6 FREE BODY DIAGRAM OF PINION 4

Thus,

$$\bar{n}_{34} = \sin(\beta_3 + \theta_3)\bar{i} - \cos(\beta_3 + \theta_3)\bar{j} \qquad \text{(A-27)}$$

The unit vector normal to the line of action is given by:

$$\bar{n}_{N34} = \cos(\beta_3 + \theta_3)\bar{i} + \sin(\beta_3 + \theta_3)\bar{j} \qquad \text{(A-28)}$$

The contact force $\bar{F}_{34}$ then becomes:

$$\bar{F}_{34} = F_{34}\,\bar{n}_{34} \qquad \text{(A-29)}$$

The friction force of gear 3 on pinion 4 is given by:

$$\bar{F}_{f34} = \mu s_3 F_{34}\,\bar{n}_{N34} \qquad \text{(A-30)}$$

where $s_3 = +1$, for contact before the pitch point

$s_3 = 0$, for contact at the pitch point

$s_3 = -1$, for contact after the pitch point

(See also Section 1.)

The normal forces on the pivot shaft are given by:

$$\overline{F}_{x4} = F_{x4}\,\overline{i} \tag{A-31}$$

and

$$\overline{F}_{y4} = -F_{y4}\,\overline{j} \tag{A-32}$$

The associated pivot friction forces are given by $\mu F_{x4}\,\overline{j}$ and $\mu F_{y4}\,\overline{i}$ for the indicated direction of rotation. The centrifugal force $\overline{T}_4$ on the pinion is represented by:

$$\overline{T}_4 = T_4(\cos\gamma_4\,\overline{i} + \sin\gamma_4\,\overline{j}) \tag{A-33}$$

where

$$T_4 = \mathcal{R}_4\omega^2 m_4 \tag{A-34a}$$

with

$$\omega = \text{spin angular velocity} \tag{A-34b}$$

and

$$m_4 = \text{mass of pinion 4} \tag{A-34c}$$

The force equilibrium equation is given by:

$$F_{34}\overline{n}_{34} + \mu s_3 F_{34}\overline{n}_{N34} + T_4(\cos\gamma_4\,\overline{i} + \sin\gamma_4\,\overline{j}) + F_{x4}\,\overline{i} + \mu F_{y4}\,\overline{i} + \mu F_{x4}\,\overline{j} - F_{y4}\,\overline{j} = 0 \tag{A-35}$$

Moment equilibrium is given by the following expression, in which the pivot friction moment is expressed according to Equation (A-3b):

$$-M_{o4} - \rho_4\mu(\tilde{F}_{x4} + \tilde{F}_{y4}) + r_{b4}F_{34} - \mu s_3(d_3 - a_3)F_{34} = 0 \qquad \text{(A-36)}$$

where ρ_4 represents the pivot radius. d_3 is the length of the line of action of the mesh from points of tangency to the base circles. a_3 is the distance on the line of action from the gear point of tangency to the contact point C_3.

Equation (A-35) gives the following component equations:

$$F_{34}\sin(\beta_3 + \theta_3) + \mu s_3 F_{34}\cos(\beta_3 + \theta_3) + T_4\cos\gamma_4 + F_{x4} + \mu F_{y4} = 0 \qquad \text{(A-37)}$$

$$-F_{34}\cos(\beta_3 + \theta_3) + \mu s_3 F_{34}\sin(\beta_3 + \theta_3) + T_4\sin\gamma_4 - F_{y4} + \mu F_{x4} = 0 \qquad \text{(A-38)}$$

Simultaneous solution of the above for F_{x4} and F_{y4} results in:

$$F_{x4} = \frac{1}{1 + \mu^2}\left\{-T_4\left[\cos\gamma_4 + \mu\sin\gamma_4\right] - F_{34}\left[(1 + \mu^2 s_3)\sin(\beta_3 + \theta_3) - \mu(1 - s_3)\cos(\beta_3 + \theta_3)\right]\right\} \quad \text{(A-39)}$$

and

$$F_{y4} = \frac{1}{1 + \mu^2}\left\{T_4\left[\sin\gamma_4 - \mu\cos\gamma_4\right] - F_{34}\left[(1 + \mu^2 s_3)\cos(\beta_3 + \theta_3) + \mu(1 - s_3)\sin(\beta_3 + \theta_3)\right]\right\} \quad \text{(A-40)}$$

To obtain conservative values for the pivot friction moment in equation (A-36) according to equation (A-3b), one substitutes the largest possible values for F_{x4} and F_{y4}. This is accomplished by making the signs of T_4 and F_{34} positive and by using the absolute values of their respective coefficients in Equations (A-39) and (A-40). Equation (A-36) then becomes:

$$-M_{o4} - \mu\rho_4(T_4A_1 + F_{34}A_2 + T_4A_3 + F_{34}A_4) + r_{b4}F_{34} - \mu s_3(d_3 - a_3)F_{34} = 0 \quad \text{(A-41)}$$

where

$$A_1 = \left|\frac{\sin\gamma_4 - \mu\cos\gamma_4}{1 + \mu^2}\right| \quad \text{(A-42)}$$

$$A_2 = \left| \frac{(1 + \mu^2 s_3)\cos(\beta_3 + \theta_3) + \mu(1 - s_3)\sin(\beta_3 + \theta_3)}{1 + \mu^2} \right| \quad \text{(A-43)}$$

$$A_3 = \left| \frac{\cos\gamma_4 + \mu\sin\gamma_4}{1 + \mu^2} \right| \quad \text{(A-44)}$$

$$A_4 = \left| \frac{(1 + \mu^2 s_3)\sin(\beta_3 + \theta_3) - \mu(1 - s_3)\cos(\beta_3 + \theta_3)}{1 + \mu^2} \right| \quad \text{(A-45)}$$

Finally equation (A-41) is solved for F_{34}:

$$F_{34} = \frac{M_{o4}}{D_1} + \frac{T_4 C_1}{D_1} \quad \text{(A-46)}$$

where

$$C_1 = \mu\rho_4(A_1 + A_3) \quad \text{(A-47)}$$

$$D_1 = r_{b4} - \mu\left[s_3(d_3 - a_3) + \rho_4(A_2 + A_4)\right] \quad \text{(A-48)}$$

b. EQUILIBRIUM OF GEAR AND PINION SET NO. 3

Figure A-7 shows the free body diagram of gear and pinion set no. 3. The contact point C_3, between pinion 4 and gear 3 is, as shown previously in Figure A-6, before the pitch point P_3. The normal force, along the line of action, is given by: (See equation (A-29).)

$$\overline{F}_{43} = -F_{34}\overline{n}_{34} \tag{A-49}$$

and the associated friction force $\overline{F}_{f43}$ is given by: (See equation (A-30).)

$$\overline{F}_{f43} = -s_3\mu F_{34}\overline{n}_{N34} \tag{A-50}$$

The unit vectors along and perpendicular to the line of action of gear 2 and pinion 3 are given by:

$$\overline{n}_{23} = -\sin(\beta_2 - \theta_2)\,\overline{i} + \cos(\beta_2 - \theta_2)\,\overline{j} \tag{A-51}$$

and

$$\overline{n}_{N23} = -\cos(\beta_2 - \theta_2)\,\overline{i} - \sin(\beta_2 - \theta_2)\,\overline{j} \tag{A-52}$$

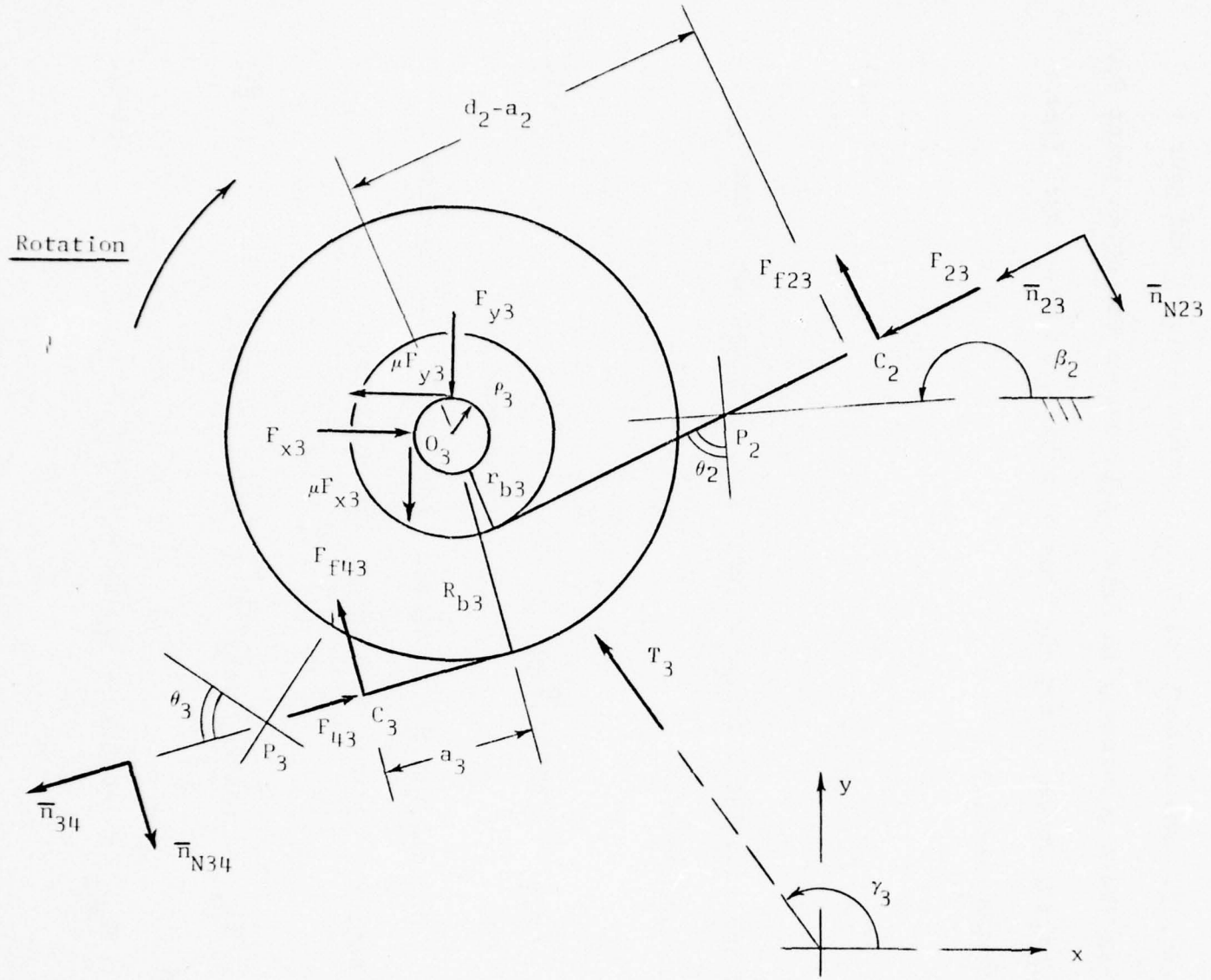

FIGURE A-7 EQUILIBRIUM OF GEAR AND PINION SET NO. 3

The contact point C_2 between gear 2 and pinion 3 is also shown before the pitch point P_2 is passed.

The normal contact force between these teeth then becomes:

$$\bar{F}_{23} = F_{23}\bar{n}_{23} \tag{A-53}$$

The associated friction force is given by:

$$\bar{F}_{f23} = -\mu s_2 F_{23}\bar{n}_{23} \tag{A-54}$$

where $s_2 = +1$ for contact before the pitch point P_2

$s_2 = 0$ for contact at the pitch point P_2

$s_2 = -1$ for contact after the pitch point P_2

The normal forces on the pivot shaft are given by:

$$\bar{F}_{x3} = F_{x3}\bar{I} \tag{A-55}$$

and

$$\bar{F}_{y3} = -F_{y3}\bar{j} \tag{A-56}$$

The associated pivot friction forces are represented by $(-)\mu F_{y3}\bar{i}$

and $(-)\mu F_{x3}\bar{j}$ for the indicated direction of gear rotation.

The centrifugal force $\bar{T}_3$ on the assembly is given by:

$$\bar{T}_3 = T_3(\cos\gamma_3\bar{i} + \sin\gamma_3\bar{j}) \qquad \text{(A-57)}$$

where

$$T_3 = \mathcal{R}_3\omega^2 m_3 \qquad \text{(A-58a)}$$

with

$$m_3 = \text{mass of pinion and gear 3} \qquad \text{(A58b)}$$

Force equilibrium is given by:

$$F_{23}\bar{n}_{23} - \mu s_2 F_{23}\bar{n}_{N23} - F_{34}\bar{n}_{34} - \mu s_3 F_{34}\bar{n}_{N34} + T_3(\cos\gamma_3\bar{i} + \sin\gamma_3\bar{j}) + F_{x3}\bar{i} - \mu F_{y3}\bar{i} - F_{y3}\bar{j} - \mu F_{x3}\bar{j} = 0 \qquad \text{(A-59)}$$

Moment equilibrium requires:

$$R_{b3}F_{34} - \mu s_3 a_3 F_{34} - r_{b3}F_{23} + \mu s_2(d_2 - a_2)F_{23} + \mu\rho_3(\tilde{F}_{x3} + \tilde{F}_{y3}) = 0 \qquad \text{(A-60)}$$

Note the use of equation (A-3b) for the pivot friction moment. ρ_3 represents the pivot radius and length d_2 is the length of the

line of action between the points of tangency to the base circles. a_2 is the distance along the line of action from the gear point of tangency to the contact point C_2.

The component form of equation (A-59) is represented by the following two expressions:

$$-F_{23}\sin(\beta_2 - \theta_2) + \mu s_2 F_{23}\cos(\beta_2 - \theta_2) - F_{34}\sin(\beta_3 + \theta_3) - \mu s_3 F_{34}\cos(\beta_3 + \theta_3) + T_3\cos\gamma_3 + F_{x3} - \mu F_{y3} = 0 \qquad \text{(A-61)}$$

and

$$F_{23}\cos(\beta_2 - \theta_2) + \mu s_2 F_{23}\sin(\beta_2 - \theta_2) + F_{34}\cos(\beta_3 + \theta_3) - \mu s_3 F_{34}\sin(\beta_3 + \theta_3) + T_3\sin\gamma_3 - F_{y3} - \mu F_{x3} = 0 \qquad \text{(A-62)}$$

Simultaneous solution of the above for F_{x3} and F_{y3} leads to:

$$F_{x3} = \frac{1}{1 + \mu^2}\left\{F_{23}\left[(1 + \mu^2 s_2)\sin(\beta_2 - \theta_2) + \mu(1 - s_2)\cos(\beta_2 - \theta_2)\right] + T_3\left[\mu\sin\gamma_3 - \cos\gamma_3\right] + F_{34}\left[(1 - \mu^2 s_3)\sin(\beta_3 + \theta_3) + \mu(1 + s_3)\cos(\beta_3 + \theta_3)\right]\right\} \qquad \text{(A-63)}$$

and

$$F_{y3} = \frac{1}{1+\mu^2}\left\{F_{23}\left[(1+\mu^2 s_2)\cos(\beta_2-\theta_2) + \mu(s_2-1)\sin(\beta_2-\theta_2)\right] + T_3\left[\sin\gamma_3 + \cos\gamma_3\right] + F_{34}\left[(1-\mu^2 s_3)\cos(\beta_3+\theta_3) - \mu(s_3+1)\sin(\beta_3+\theta_3)\right]\right\} \quad \text{(A-64)}$$

Now, equations (A-63) and (A-64) are substituted into the moment equation (A-60) with consideration of the pivot friction moment according to equation (A-3b). This gives:

$$R_{b3}F_{34} - \mu s_3 a_z F_{34} - r_{b3}F_{23} + \mu s_2(d_2-a_2)F_{23} + \mu\rho_3\left[F_{23}(A_5+A_8) + T_3(A_6+A_9) + F_{34}(A_7+A_{10})\right] = 0 \quad \text{(A-65)}$$

where

$$A_5 = \left|\frac{(1+\mu^2 s_2)\cos(\beta_2-\theta_2) + \mu(s_2-1)\sin(\beta_2-\theta_2)}{1+\mu^2}\right| \quad \text{(A-66)}$$

$$A_6 = \left|\frac{\sin\gamma_3 + \mu\cos\gamma_3}{1+\mu^2}\right| \quad \text{(A-67)}$$

$$A_7 = \left| \frac{(1 - \mu^2 s_3)\cos(\beta_3 + \theta_3) - \mu(1 + s_3)\sin(\beta_3 + \theta_3)}{1 + \mu^2} \right| \quad \text{(A-68)}$$

$$A_8 = \left| \frac{(1 + \mu^2 s_2)\sin(\beta_2 - \theta_2) + \mu(1 - s_2)\cos(\beta_2 - \theta_2)}{1 + \mu^2} \right| \quad \text{(A-69)}$$

$$A_9 = \left| \frac{\mu \sin\gamma_3 - \cos\gamma_3}{1 + \mu^2} \right| \quad \text{(A-70)}$$

$$A_{10} = \left| \frac{(1 - \mu^2 s_3)\sin(\beta_3 + \theta_3) + \mu(1 + s_3)\cos(\beta_3 + \theta_3)}{1 + \mu^2} \right| \quad \text{(A-71)}$$

Finally equation (A-65) is solved for F_{23}:

$$F_{23} = \frac{F_{34}C_2 + T_3C_3}{D_2} \quad \text{(A-72)}$$

where

$$C_2 = R_{b3} - \mu\left[s_3 a_3 - \rho_3(A_7 + A_{10})\right] \quad \text{(A-73)}$$

$$C_3 = \mu\rho_3(A_6 + A_9) \quad \text{(A-74)}$$

$$D_2 = r_{b3} - \mu\left[s_2(d_2 - a_2) + \rho_3(A_5 + A_8)\right] \quad \text{(A-75)}$$

c. EQUILIBRIUM OF GEAR AND PINION SET NO. 2

Figure A-8 shows the free body diagram of gear and pinion set no. 2. The contact point C_2, between gear 2 and pinion 3, is again shown before the pitch point P_2 is passed. (See also Figure A-7.) The normal force, along the line of action, becomes with equation (A-72):

$$\overline{F}_{32} = -F_{23}\overline{n}_{23} \tag{A-76}$$

The associated friction force $\overline{F}_{f32}$ is given by:

$$\overline{F}_{f32} = \mu s_2 F_{23}\overline{n}_{N23} \tag{A-77}$$

The unit vectors along and perpendicular to the line of action of gear 1 and pinion 2 are given by:

$$\overline{n}_{12} = \sin(\beta_1 + \theta_1)\overline{i} - \cos(\beta_1 + \theta_1)\overline{j} \tag{A-78}$$

and

$$\overline{n}_{N12} = \cos(\beta_1 + \theta_1)\overline{i} + \sin(\beta_1 + \theta_1)\overline{j} \tag{A-79}$$

The contact point C_1 between gear 1 and pinion 2 is also shown before the pitch point P_1 is passed.

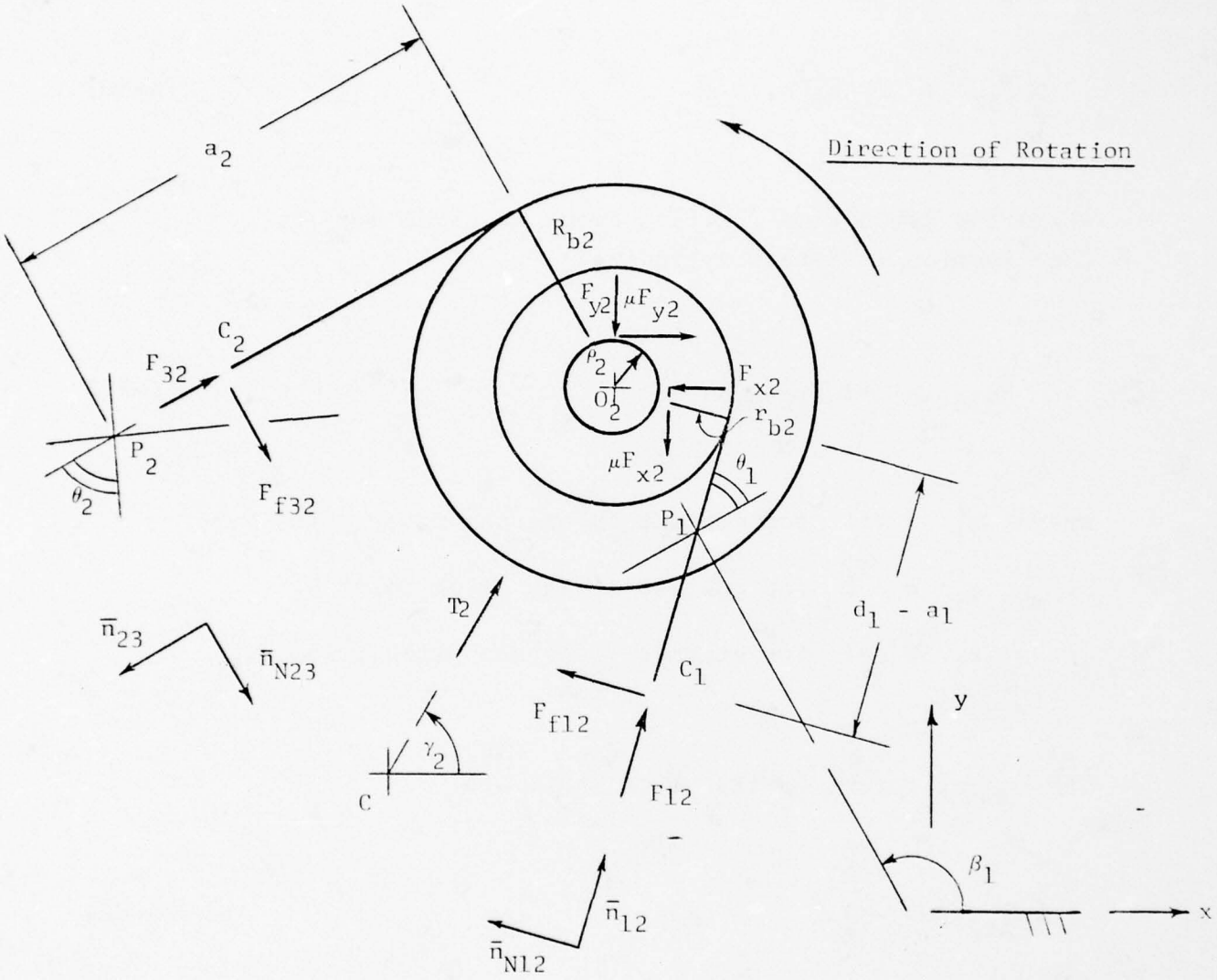

FIGURE A8 FREE BODY DIAGRAM OF GEAR AND PINION SET NO. 2

The normal contact force between the teeth of this mesh becomes:

$$\overline{F}_{12} = F_{12}\overline{n}_{12} , \qquad \text{(A-80)}$$

while the associated friction force is given by:
(See Section 1 of this Appendix.)

$$\overline{F}_{f12} = \mu s_1 F_{12}\overline{n}_{N12} \qquad \text{(A-81)}$$

where $s_1 = +1$ for contact before the pitch point P_1

$s_1 = 0$ for contact at the pitch point P_1

$s_1 = -1$ for contact after the pitch point P_1

The normal forces on the pivot shaft are:

$$\overline{F}_{x2} = -F_{x2}\overline{I} \qquad \text{(A-82)}$$

and

$$\overline{F}_{y2} = -F_{y2}\overline{J} \qquad \text{(A-83)}$$

The associated pivot friction forces are again chosen such that

their friction moments oppose the indicated rotation.

The centrifugal force $\bar{T}_2$ on this gear and pinion assembly is given by:

$$\bar{T}_2 = T_2(\cos\gamma_2\bar{i} + \sin\gamma_2\bar{j}) \qquad \text{(A-84)}$$

where $T_2 = \mathcal{R}_2\omega^2 m_2$ (A-85a)

with

m_2 = mass of gear and pinion set no. 2 (A-85b)

Force equilibrium is given by:

$$-F_{23}\bar{n}_{23} + \mu s_2 F_{23}\bar{n}_{N23} + F_{12}\bar{n}_{12} + \mu s_1 F_{12}\bar{n}_{N12} + T_2(\cos\gamma_2\bar{i} + \sin\gamma_2\bar{j}) - F_{x2}\bar{i} - F_{y2}\bar{j} + \mu F_{y2}\bar{i} - \mu F_{x2}\bar{j} = 0 \qquad \text{(A-86)}$$

Moment equilibrium is given by:

$$-R_{b2}F_{23} + \mu s_2 a_2 F_{23} + r_{b2}F_{12} - \mu s_1(d_1 - a_1)F_{12} - \mu\rho_2(\tilde{F}_{x2} + \tilde{F}_{y2}) = 0 \qquad \text{(A-87)}$$

Again, equation (A-3b) is used to account for the pivot friction moment. ρ_2 represents the pivot radius. d_1 is the length of the line of action between the points of tangency to the base circles, and a_1 is the distance from the point of tangency of the gear to the contact point C_1.

The component form of equation (A-86) is given by:

$$F_{23}\sin(\beta_2 - \theta_2) - \mu s_2 F_{23}\cos(\beta_2 - \theta_2) + F_{12}\sin(\beta_1 + \theta_1) + \mu s_1 F_{12}\cos(\beta_1 + \theta_1) + T_2\cos\gamma_2 - F_{x2} + \mu F_{y2} = 0 \qquad \text{(A-88)}$$

$$-F_{23}\cos(\beta_2 - \theta_2) - \mu s_2 F_{23}\sin(\beta_2 - \theta_2) - F_{12}\cos(\beta_1 + \theta_1) + \mu s_1 F_{12}\sin(\beta_1 + \theta_1) + T_2\sin\gamma_2 - F_{y2} - \mu F_{x2} = 0 \qquad \text{(A-89)}$$

Simultaneous solution of the above furnishes:

$$F_{x2} = \frac{1}{1 + \mu^2}\Big\{-F_{12}\Big[\mu(1 - s_1)\cos(\beta_1 + \theta_1) - (1 + \mu^2 s_1)\sin(\beta_1 + \theta_1)\Big] + T_2\Big[\mu\sin\gamma_2 + \cos\gamma_2\Big] + F_{23}\Big[(1 - \mu^2 s_2)\sin(\beta_2 - \theta_2) - \mu(1 + s_2)\cos(\beta_2 - \theta_2)\Big]\Big\} \qquad \text{(A-90)}$$

and

$$F_{y2} = \frac{1}{1+\mu^2}\left\{-F_{12}\left[\mu(1-s_1)\sin(\beta_1+\theta_1) + (1+\mu^2 s_1)\cos(\beta_1+\theta_1)\right] + T_2\left[\sin\gamma_2 - \mu\cos\gamma_2\right] + F_{23}\left[-\mu(1+s_2)\sin(\beta_2-\theta_2) - (1-\mu^2 s_2)\cos(\beta_2-\theta_2)\right]\right\} \quad \text{(A-91)}$$

Now, equations (A-90) and (A-91) are substituted into the moment equation (A-87). With consideration of the pivot friction moment according to equation (A-3b), this gives:

$$-R_{b2}F_{23} + \mu s_2 a_2 F_{23} + r_{b2}F_{12} - \mu s_1(d_1 - a_1)F_{12} - \mu\rho_2\left[F_{12}(A_{11}+A_{14}) + T_2(A_{12}+A_{15}) + F_{23}(A_{13}+A_{16})\right] = 0 \quad \text{(A-92)}$$

In the above

$$A_{11} = \left| \frac{\mu(1-s_1)\sin(\beta_1+\theta_1) + (1+\mu^2 s_1)\cos(\beta_1+\theta_1)}{1+\mu^2} \right| \quad \text{(A-93)}$$

$$A_{12} = \left| \frac{\sin\gamma_2 - \mu\cos\gamma_2}{1+\mu^2} \right| \quad \text{(A-94)}$$

$$A_{13} = \left| \frac{\mu(1 + s_2)\sin(\beta_2 - \theta_2) + (1 - \mu^2 s_2)\cos(\beta_2 - \theta_2)}{1 + \mu^2} \right| \quad \text{(A-95)}$$

$$A_{14} = \left| \frac{\mu(1 - s_1)\cos(\beta_1 + \theta_1) - (1 + \mu^2 s_1)\sin(\beta_1 + \theta_1)}{1 + \mu^2} \right| \quad \text{(A-96)}$$

$$A_{15} = \left| \frac{\mu \sin\gamma_2 + \cos\gamma_2}{1 + \mu^2} \right| \quad \text{(A-97)}$$

$$A_{16} = \left| \frac{(1 - \mu^2 s_2)\sin(\beta_2 - \theta_2) - \mu(1 + s_2)\cos(\beta_2 - \theta_2)}{1 + \mu^2} \right| \quad \text{(A-98)}$$

Finally, equation (A-92) is solved for F_{12}:

$$F_{12} = \frac{F_{23}C_4 + T_2C_5}{D_3} \quad \text{(A-99)}$$

where

$$C_4 = R_{b2} - \mu\left[s_2 a_2 - \rho_2(A_{13} + A_{16})\right] \quad \text{(A-100)}$$

$$C_5 = \mu\rho_2(A_{12} + A_{15}) \quad \text{(A-101)}$$

$$D_3 = r_{b2} - \mu\left[s_1(d_1 - a_1) + \rho_2(A_{11} + A_{14})\right] \quad \text{(A-102)}$$

d. EQUILIBRIUM OF GEAR NO. 1

Figure A-9 shows the free body diagram of gear no. 1, the input gear.

The contact point C_1 is identical with that shown in Figure A-8.

The normal force on gear no. 1 is given by: (See equation (A-80).)

$$\bar{F}_{21} = -F_{12}\bar{n}_{12} \tag{A-103}$$

The associated friction force is:

$$\bar{F}_{f21} = -\mu s_1 F_{12}\bar{n}_{N12} \tag{A-104}$$

The normal forces on the pivot shaft are given by:

$$\bar{F}_{x1} = -F_{x1}\bar{i} \tag{A-105}$$

and

$$\bar{F}_{y1} = F_{y1}\bar{j} \tag{A-106}$$

The associated pivot friction forces are chosen in such a direction that their moments oppose the indicated rotation.

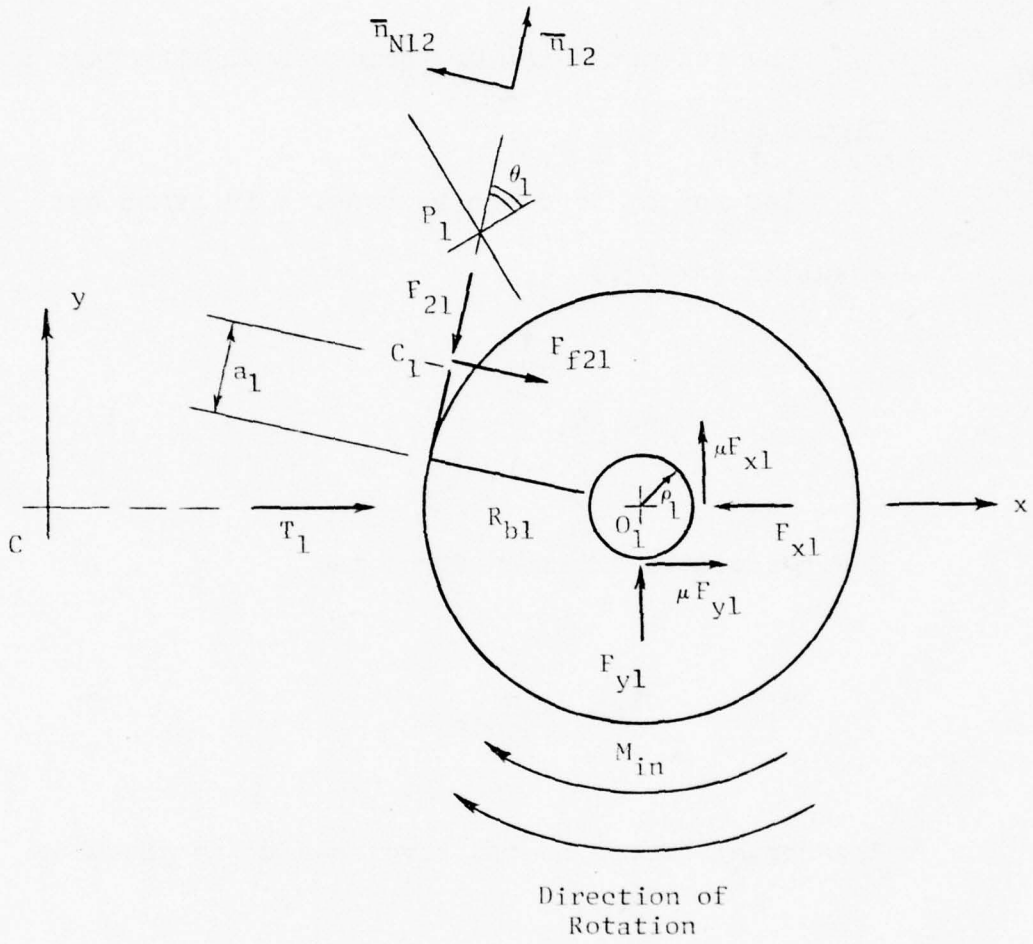

FIGURE A9 FREE BODY DIAGRAM OF GEAR 1

The centrifugal force $\overline{T}_1$ on gear 1 is given by:

$$\overline{T}_1 = T_1\overline{i} \tag{A-107}$$

where

$$T_1 = \mathcal{R}_1\omega^2 m_1 \tag{A-108a}$$

$$m_1 = \text{mass of gear 1} \tag{A-108b}$$

Force equilibrium is given by:

$$-F_{12}\overline{n}_{12} - \mu s_1 F_{12}\overline{n}_{N12} + T_1\overline{i} - F_{x1}\overline{i} + F_{y1}\overline{j} + \mu F_{y1}\overline{i} + \mu F_{x1}\overline{j} = 0 \tag{A-109}$$

Moment equilibrium is found from:

$$R_{b1}F_{12} - \mu s_1 a_1 F_{12} - M_{in} + \mu\rho_1(\widetilde{F}_{x1} + \widetilde{F}_{y1}) = 0 \tag{A-110}$$

The form of equation (A-3b) is again utilized to obtain the pivot friction moment. ρ_1 represents the pivot radius of gear 1.

The component form of equation (A-109) becomes:

$$-F_{12}\sin(\beta_1 + \theta_1) - \mu s_1 F_{12}\cos(\beta_1 + \theta_1) - F_{x1} + \mu F_{y1} + T_1 = 0 \qquad \text{(A-111)}$$

and

$$F_{12}\cos(\beta_1 + \theta_1) - \mu s_1 F_{12}\sin(\beta_1 + \theta_1) + F_{y1} + \mu F_{x1} = 0 \qquad \text{(A-112)}$$

Simultaneous solution of equations (A-111) and (A-112) furnishes the forces on the pivot, i.e.

$$F_{x1} = \frac{-F_{12}\left[(1 - \mu^2 s_1)\sin(\beta_1 + \theta_1) + \mu(1 + s_1)\cos(\beta_1 + \theta_1)\right] + T_1}{1 + \mu^2} \qquad \text{(A-113)}$$

$$F_{y1} = \frac{F_{12}\left[\mu(1 + s_1)\sin(\beta_1 + \theta_1) - (1 - \mu^2 s_1)\cos(\beta_1 + \theta_1)\right] - \mu T_1}{1 + \mu^2} \qquad \text{(A-114)}$$

Equations (A-113) and (A-114) are now substituted into the moment equation (A-110) in the following manner: (Again, the method of equation (A-3b) is applied.)

$$R_{b1}F_{12} - \mu s_1 a_1 F_{12} - M_{in} + \mu \rho_1 \left[F_{12}(A_{17} + A_{19}) + T_1(A_{18} + A_{20}) \right] = 0 \qquad \text{(A-115)}$$

where

$$A_{17} = \left| \frac{(1 - \mu^2 s_1)\sin(\beta_1 + \theta_1) + \mu(1 + s_1)\cos(\beta_1 + \theta_1)}{1 + \mu^2} \right| \qquad \text{(A-116)}$$

$$A_{18} = \left| \frac{1}{1 + \mu^2} \right| \qquad \text{(A-117)}$$

$$A_{19} = \left| \frac{\mu(1 + s_1)\sin(\beta_1 + \theta_1) - (1 - \mu^2 s_1)\cos(\beta_1 + \theta_1)}{1 + \mu^2} \right| \qquad \text{(A-118)}$$

$$A_{20} = \left| \frac{\mu}{1 + \mu^2} \right| \qquad \text{(A-119)}$$

Finally, equation (A-115) is solved for F_{12}:

$$F_{12} = \frac{M_{in}}{D_4} - \frac{T_1 C_6}{D_4} \qquad \text{(A-120)}$$

where

$$C_6 = \mu \rho_1 (A_{18} + A_{20}) \qquad \text{(A-121)}$$

$$D_4 = R_{b1} - \mu \left[s_1 a_1 - \rho_1 (A_{17} + A_{19}) \right] \qquad \text{(A-122)}$$

e. INPUT-OUTPUT RELATIONSHIP

To obtain the input-output relationship for the complete gear train, equation (A-120) is now equated to equation (A-99). This furnishes:

$$F_{23} = \frac{D_3}{C_4 D_4} (M_{in} - T_1 C_6) - T_2 \frac{C_5}{C_4} \qquad \text{(A-123)}$$

Further, the above is equated to equation (A-72). This results in the following expression for F_{34}:

$$F_{34} = \frac{D_2 D_3}{C_2 C_4 D_4} (M_{in} - T_1 C_6) - T_2 \frac{C_5 D_2}{C_2 C_4} - T_3 \frac{C_3}{C_2} \qquad \text{(A-124)}$$

Finally, equation (A-124) is equated to equation (A-46). This establishes the input-output relationship:

$$M_{o4} = \frac{D_1 D_2 D_3}{C_2 C_4 D_4} (M_{in} - T_1 C_6) - T_2 \frac{C_5 D_1 D_2}{C_2 C_4} - T_3 \frac{C_3 D_1}{C_2} - T_4 C_1 \qquad \text{(A-125)}$$

5. MOMENT INPUT-OUTPUT RELATIONSHIP FOR INVOLUTE TWO STEP-UP GEAR TRAIN IN SPIN ENVIRONMENT

Figure A-10 shows the basic configuration of a two step-up gear train with involute teeth for which the relationship between the equilibrant output moment M_{o3}, acting on pinion 3, and the input moment M_{in}, acting on gear 1 is to be found. All nomenclature is identical with that used in Section 4 in connection with the three step-up gear train.

Again, the general relationship between input and output is found by assembling the input-output relationships of the individual component gears.

a. EQUILIBRIUM OF PINION 3

Figure A-11 shows the free body diagram of pinion 3. The contact point C_2 between gear 2 and pinion 3 is shown before the pitch point P_2 is passed.

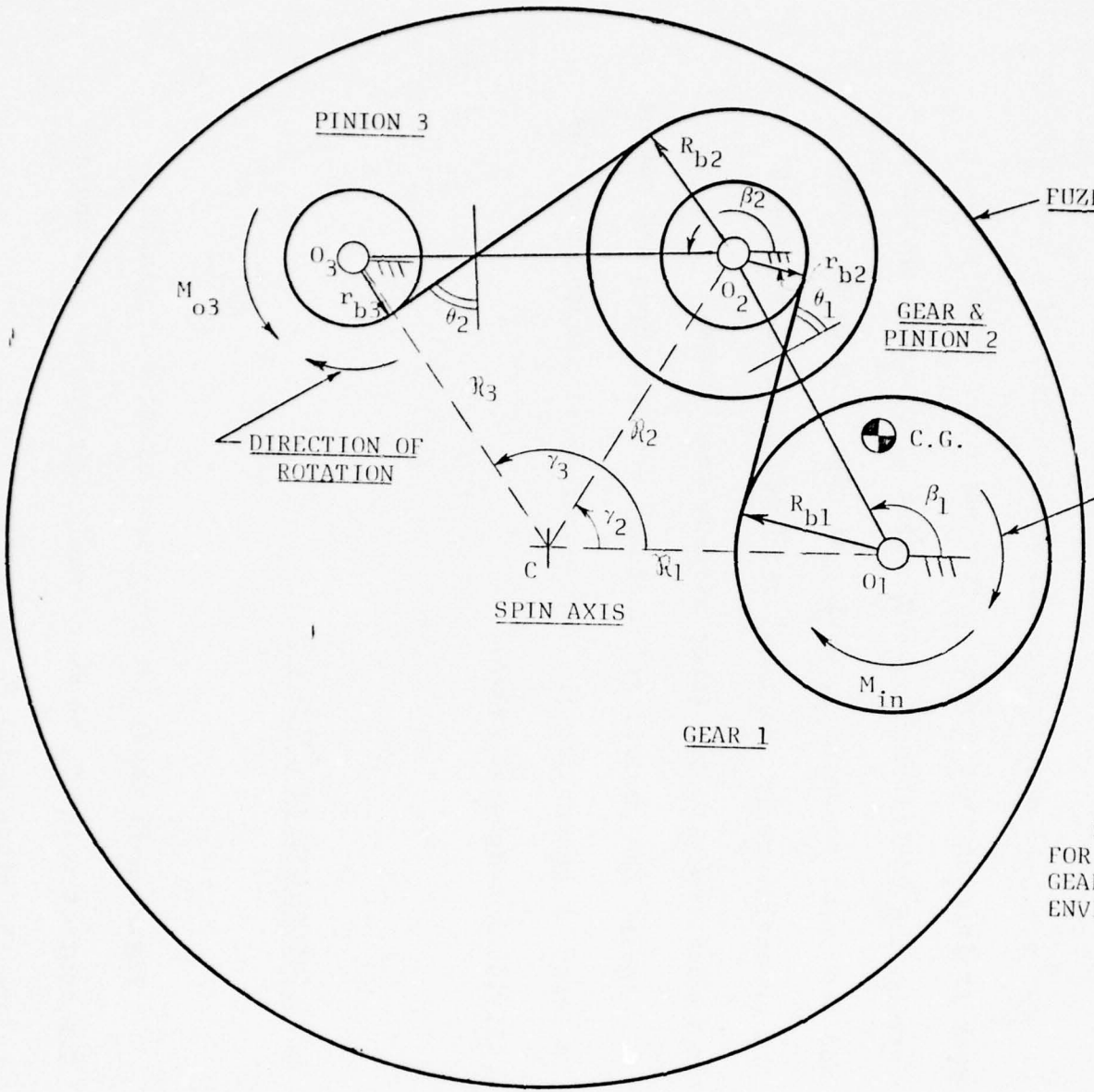

FIGURE A-10

BASIC CONFIGURATION FOR INVOLUTE TWO STEP-UP GEAR TRAIN IN SPIN ENVIRONMENT

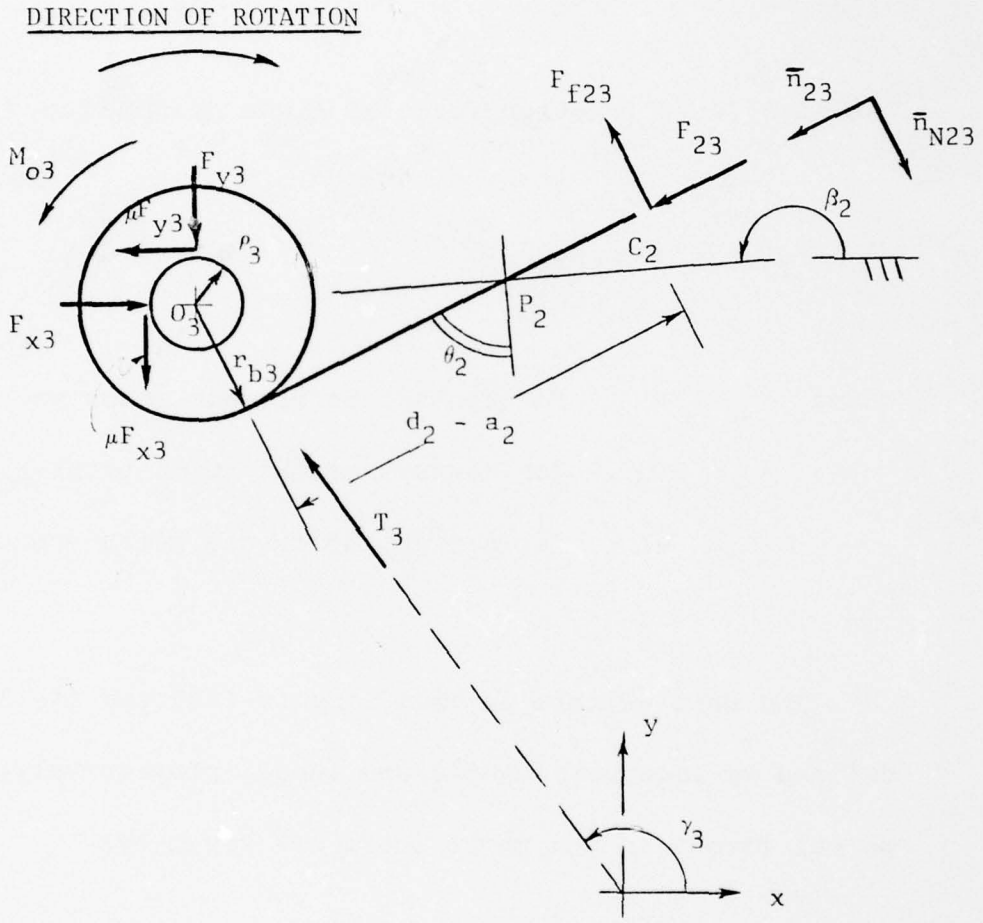

FIGURE A-11 FREE BODY DIAGRAM OF PINION 3

As in equation (A-53), the normal force between the teeth of gear 2 and pinion 3 is given by:

$$\bar{F}_{23} = F_{23}\bar{n}_{23} \tag{A-126}$$

The associated friction force is given by equation (A-54), i.e.

$$\bar{F}_{f23} = -\mu s_2 F_{23}\bar{n}_{N23} \tag{A-127}$$

where $s_2 = +1$, for contact before the pitch point P_2

$s_2 = 0$, for contact at the pitch point P_2

$s_2 = -1$, for contact after the pitch point P_2

The unit vectors in equations (A-126) and (A-127) were defined by equations (A-51) and (A-52) respectively. The normal forces on the pivot shaft are given by:

$$\bar{F}_{x3} = F_{x3}\bar{i} \tag{A-128}$$

and

$$\bar{F}_{y3} = -F_{y3}\bar{j} \tag{A-129}$$

The pivot friction forces become $(-)\mu F_{y3}\bar{i}$ and $(-)\mu F_{x3}\bar{j}$ for the indicated direction of rotation.

As in equation (A-57), the centrifugal force on the pinion is given by:

$$\bar{T}_3 = T_3(\cos\gamma_3\bar{i} + \sin\gamma_3\bar{j}) \qquad \text{(A-130)}$$

where

$$T_3 = \mathcal{R}_3\omega^2 m_3 \qquad \text{(A-131)}$$

with

$$m_3 = \text{mass of pinion 3} \qquad \text{(A-132)}$$

Force equilibrium is given by:

$$F_{23}\bar{n}_{23} - \mu s_2 F_{23}\bar{n}_{H23} + T_3(\cos\gamma_3\bar{i} + \sin\gamma_3\bar{j}) + F_{x3}\bar{i} - \mu F_{y3}\bar{i} - F_{y3}\bar{j} - \mu F_{x3}\bar{j} = 0 \qquad \text{(A-133)}$$

Moment equilibrium is obtained from:

$$M_{o3} - r_{b3}F_{23} + \mu s_2(d_2 - a_2)F_{23} + \mu p_3(\tilde{F}_{x3} + \tilde{F}_{y3}) = 0 \qquad \text{(A-134)}$$

Note the use of equation (A-3b) for the pivot friction moment. ρ_3 represents the pivot radius. d_2 is the length of the line of action between the points of tangency to the base circles of pinion 3 and gear 2. a_2 is the distance along the line of action from the gear point of tangency to the contact point C_2.

The x and y components of equation (A-133) are given by:

$$-F_{23}\sin(\beta_2 - \theta_2) + \mu s_3 F_{23}\cos(\beta_2 - \theta_2) + T_3\cos\gamma_3 + F_{x3} - \mu F_{y3} = 0 , \quad \text{(A-135)}$$

and

$$F_{23}\cos(\beta_2 - \theta_2) + \mu s_3 F_{23}\sin(\beta_2 - \theta_2) + T_3\sin\gamma_3 - F_{y3} - \mu F_{x3} = 0 \quad \text{(A-136)}$$

Simultaneous solution of these expressions for F_{x3} and F_{y3} furnishes:

$$F_{x3} = \frac{1}{1 + \mu^2}\left\{ F_{23}\left[(1 + \mu^2 s_2)\sin(\beta_2 - \theta_2) + \mu(1 - s_2)\cos(\beta_2 - \theta_2)\right] + T_3\left[\mu\sin\gamma_3 - \cos\gamma_3\right]\right\} \quad \text{(A-137)}$$

and

$$F_{y3} = \frac{1}{1+\mu^2}\left\{ F_{23}\left[(1+\mu^2 s_2)\cos(\beta_2-\theta_2) + \mu(s_2-1)\sin(\beta_2-\theta_2)\right] + T_3\left[\sin\gamma_3 + \mu\cos\gamma_3\right]\right\} \quad \text{(A-138)}$$

Now, equations (A-137) and (A-138) are substituted into the moment equation (A-134), with the pivot friction moment given according to the formulation of equation (A-3b):

$$M_{o3} - r_{b3}F_{23} + \mu s_2(d_2 - a_2)F_{23} + \mu\rho_3\left[F_{23}(A_1 + A_3) + T_3(A_2 + A_4)\right] = 0 \quad \text{(A-139)}$$

where

$$A_1 = \left| \frac{(1+\mu^2 s_2)\cos(\beta_2-\theta_2) + \mu(s_2-1)\sin(\beta_2-\theta_2)}{1+\mu^2} \right| \quad \text{(A-140)}$$

$$A_2 = \left| \frac{\sin\gamma_3 + \mu\cos\gamma_3}{1+\mu^2} \right| \quad \text{(A-141)}$$

$$A_3 = \left| \frac{(1+\mu^2 s_2)\sin(\beta_2-\theta_2) + \mu(1-s_2)\cos(\beta_2-\theta_2)}{1+\mu^2} \right| \quad \text{(A-142)}$$

$$A_4 = \left| \frac{\mu \sin\gamma_3 - \cos\gamma_3}{1 + \mu^2} \right| \qquad \text{(A-143)}$$

Finally equation (A-139) is solved for F_{23}:

$$F_{23} = \frac{M_{o3}}{D_1} + T_3 \frac{C_1}{D_1} \qquad \text{(A-144)}$$

where

$$C_1 = \mu\rho_3(A_2 + A_4) \qquad \text{(A-145)}$$

$$D_1 = r_{b3} - \mu\left[s_2(d_2 - a_2) + \rho_3(A_1 + A_3)\right] \qquad \text{(A-146)}$$

b. EQUILIBRIUM OF GEAR AND PINION SET NO. 2

Figure A-12 shows the free body diagram of gear and pinion set no. 2. The contact point C_2, between gear 2 and pinion 3 is again shown before the pitch point P_2. With equation (A-126), the normal force between the teeth of this mesh becomes:

$$\bar{F}_{32} = -F_{23}\bar{n}_{23} \tag{A-147}$$

The associated friction force is the negative of equation (A-127), i.e.

$$\bar{F}_{f32} = \mu_{s_2} F_{23} \bar{n}_{N23} \tag{A-148}$$

Similar to equation (A-80), the normal force between gear 1 and pinion 2 is given by:

$$\bar{F}_{12} = F_{12}\bar{n}_{12} \tag{A-149}$$

(See equation (A-78) for the definition of the unit vector $\bar{n}_{12}$.)

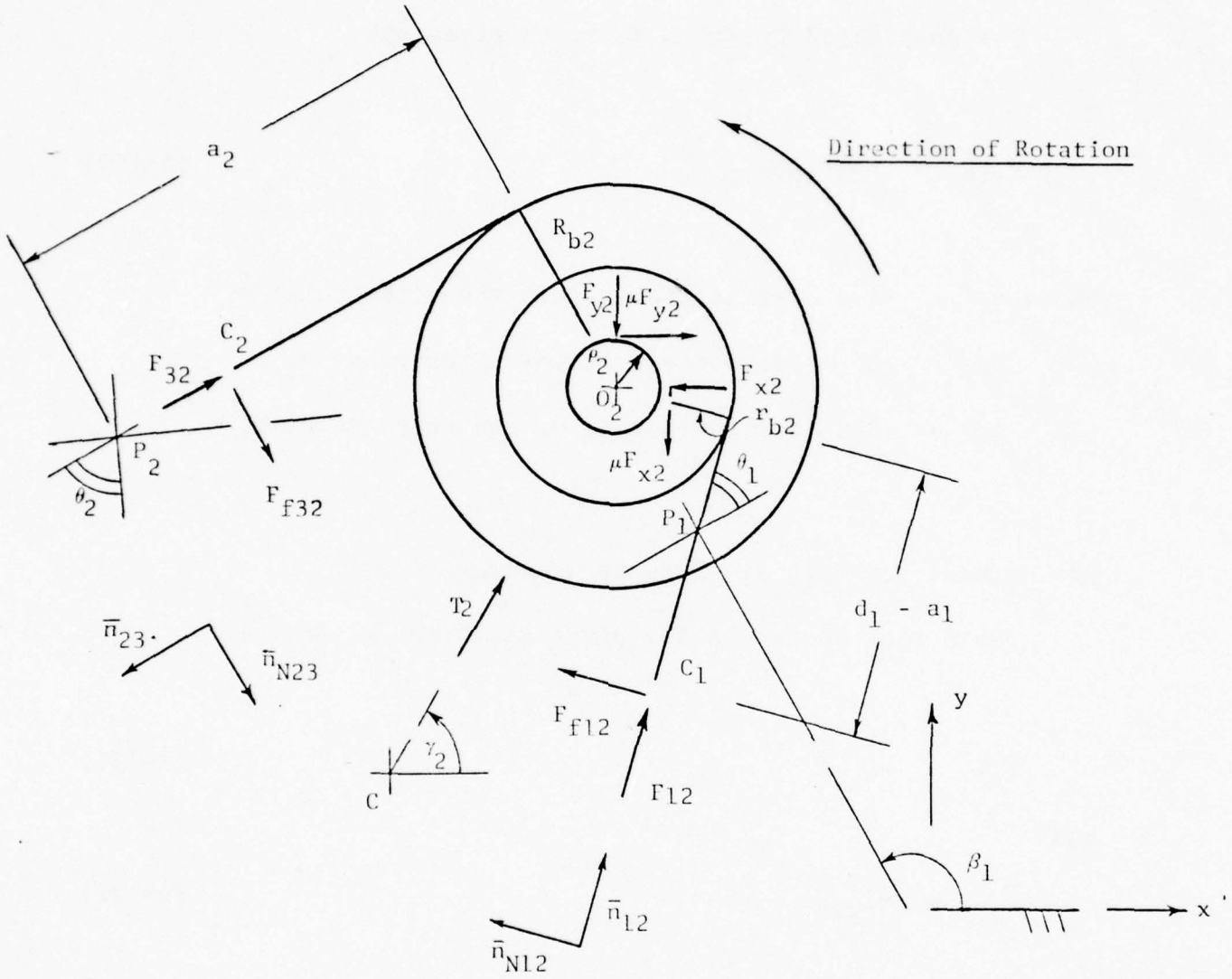

FIGURE A-12 FREE BODY DIAGRAM OF GEAR AND PINION SET NO. 2

Figure A-12 shows the contact point C_1 before the pitch point P_1 is passed.

The associated friction force is given by:

$$\bar{F}_{f12} = \mu s_1 F_{12} \bar{n}_{N12} \tag{A-150}$$

where $s_1 = +1$, for contact before the Pitch point P_1

$s_1 = 0$, for contact at the pitch point P_1

$s_1 = -1$, for contact after the pitch point P_1

The unit vector $\bar{n}_{N12}$ is given by equation (A-79).

The normal forces on the pivot shaft are given by:

$$\bar{F}_{x2} = -F_{x2}\bar{i} \tag{A-151}$$

and

$$\bar{F}_{y2} = -F_{y2}\bar{j} \tag{A-152}$$

The associated friction forces $\mu F_{y2}\bar{i}$ and $(-)\mu F_{x2}\bar{j}$ were chosen such that their moments oppose the indicated rotation.

The centrifugal force on this gear and pinion assembly is expressed by:

$$\bar{T}_2 = T_2(\cos\gamma_2\bar{i} + \sin\gamma_2\bar{j}) \tag{A-153}$$

where $T_2 = \mathcal{R}_2\omega^2 m_2$ (A-154)

m_2 = mass of gear and pinion set no. 2 (A-155)

Force equilibrium is given by:

$$-F_{23}\bar{n}_{23} + \mu s_2 F_{23}\bar{n}_{N23} + F_{12}\bar{n}_{12} + \mu s_1 F_{12}\bar{n}_{N12}$$
$$+ T_2(\cos\gamma_2\bar{i} + \sin\gamma_2\bar{j}) - F_{x2}\bar{i} + \mu F_{y2}\bar{i} - F_{y2}\bar{j} - \mu F_{x2}\bar{j}$$
$$= 0 \tag{A-156}$$

Moment equilibrium is given by:

$$-R_{b2}F_{23} + \mu s_2 a_2 F_{23} + r_{b2}F_{12} - \mu s_1(d_1 - a_1)F_{12}$$
$$- \mu\rho_2(\tilde{F}_{x2} + \tilde{F}_{y2}) = 0 \tag{A-157}$$

Again, equation (A-3b) is used to obtain a conservative pivot friction moment. ρ_2 represents the pivot radius. d_1 and a_1 are similar to the previously used distances along the lines of action of the other meshes.

The component form of equation (A-156) becomes:

$$F_{23}\sin(\beta_2 - \theta_2) - \mu s_2 F_{23}\cos(\beta_2 - \theta_2) + F_{12}\sin(\beta_1 + \theta_1)$$
$$+ \mu s_1 F_{12}\cos(\beta_1 + \theta_1) + T_2\cos\gamma_2 - F_{x2} + \mu F_{y2} = 0 \qquad \text{(A-158)}$$

and

$$-F_{23}\cos(\beta_2 - \theta_2) - \mu s_2 F_{23}\sin(\beta_2 - \theta_2) - F_{12}\cos(\beta_1 + \theta_1)$$
$$+ \mu s_1 F_{12}\sin(\beta_1 + \theta_1) + T_2\sin\gamma_2 - F_{y2} - \mu F_{x2} = 0 \qquad \text{(A-159)}$$

Simultaneous solution of the above expressions for F_{x2} and F_{y2} gives:

$$F_{x2} = \frac{1}{1 + \mu^2}\Big\{ -F_{12}\Big[\mu(1 - s_1)\cos(\beta_1 + \theta_1) - (1 + \mu^2 s_1)\sin(\beta_1 + \theta_1)\Big]$$
$$+ T_2\Big[\mu\sin\gamma_2 + \cos\gamma_2\Big]$$
$$+ F_{23}\Big[(1 - \mu^2 s_2)\sin(\beta_2 - \theta_2) - \mu(1 + s_2)\cos(\beta_2 - \theta_2)\Big]\Big\} \qquad \text{(A-160)}$$

$$F_{y2} = \frac{1}{1+\mu^2}\Big\{-F_{12}\Big[\mu(1-s_1)\sin(\beta_1+\theta_1)+(1+\mu^2 s_1)\cos(\beta_1+\theta_1)\Big] + T_2\Big[\sin\gamma_2 - \mu\cos\gamma_2\Big] + F_{23}\Big[-\mu(1+s_2)\sin(\beta_2-\theta_2)-(1-\mu^2 s_2)\cos(\beta_2-\theta_2)\Big]\Big\} \quad \text{(A-161)}$$

Now equations (A-160) and (A-161) are substituted into the moment equation (A-157) with the pivot friction moment formulated again according to equation (A-3b):

$$-R_{b2}F_{23} + \mu s_2 a_2 F_{23} + r_{b2}F_{12} - \mu s_1(d_1 - a_1)F_{12} - \mu\rho_2\left[F_{12}(A_5 + A_8) + T_2(A_6 + A_9) + F_{23}(A_7 + A_{10})\right] = 0 \tag{A-162}$$

where

$$A_5 = \left| \frac{\mu(1 - s_1)\sin(\beta_1 + \theta_1) + (1 + \mu^2 s_1)\cos(\beta_1 + \theta_1)}{1 + \mu^2} \right| \tag{A-163}$$

$$A_6 = \left| \frac{\sin\gamma_2 - \mu\cos\gamma_2}{1 + \mu^2} \right| \tag{A-164}$$

$$A_7 = \left| \frac{\mu(1 + s_2)\sin(\beta_2 - \theta_2) + (1 - \mu^2 s_2)\cos(\beta_2 - \theta_2)}{1 + \mu^2} \right| \tag{A-165}$$

$$A_8 = \left| \frac{\mu(1 - s_1)\cos(\beta_1 + \theta_1) - (1 + \mu^2 s_1)\sin(\beta_1 + \theta_1)}{1 + \mu^2} \right| \tag{A-166}$$

$$A_9 = \left| \frac{\mu\sin\gamma_2 + \cos\gamma_2}{1 + \mu^2} \right| \tag{A-167}$$

$$A_{10} = \left| \frac{(1 - \mu^2 s_2)\sin(\beta_2 - \theta_2) - \mu(1 + s_2)\cos(\beta_2 - \theta_2)}{1 + \mu^2} \right| \qquad \text{(A-168)}$$

Finally equation (A-162) is solved for F_{12}:

$$F_{12} = \frac{F_{23}C_2}{D_2} + \frac{T_2C_3}{D_2} \qquad \text{(A-169)}$$

where

$$C_2 = R_{b2} - \mu\left[s_2a_2 - \rho_2(A_7 + A_{10})\right] \qquad \text{(A-170)}$$

$$C_3 = \mu\rho_2(A_6 + A_9) \qquad \text{(A-171)}$$

$$D_2 = r_{b2} - \mu\left[s_1(d_1 - a_1) + \rho_2(A_5 + A_8)\right] \qquad \text{(A172)}$$

c. EQUILIBRIUM OF GEAR NO. 1

Figure A-13 shows the free body diagram of gear no. 1, the input gear.

The contact point C_1 corresponds to that shown in Figure A-12.

According to equation (A-149), the normal contact force between pinion 2 and gear 1 becomes:

$$\bar{F}_{21} = -F_{12}\bar{n}_{12} \tag{A-173}$$

The associated friction force is the negative of equation (A-150), i.e.:

$$\bar{F}_{f21} = -\mu s_1 F_{12}\bar{n}_{N12} \tag{A-174}$$

The normal forces on the pivot shaft are given by:

$$\bar{F}_{x1} = -F_{x1}\bar{i} \tag{A-175}$$

and

$$\bar{F}_{y1} = F_{y1}\bar{j} \tag{A-176}$$

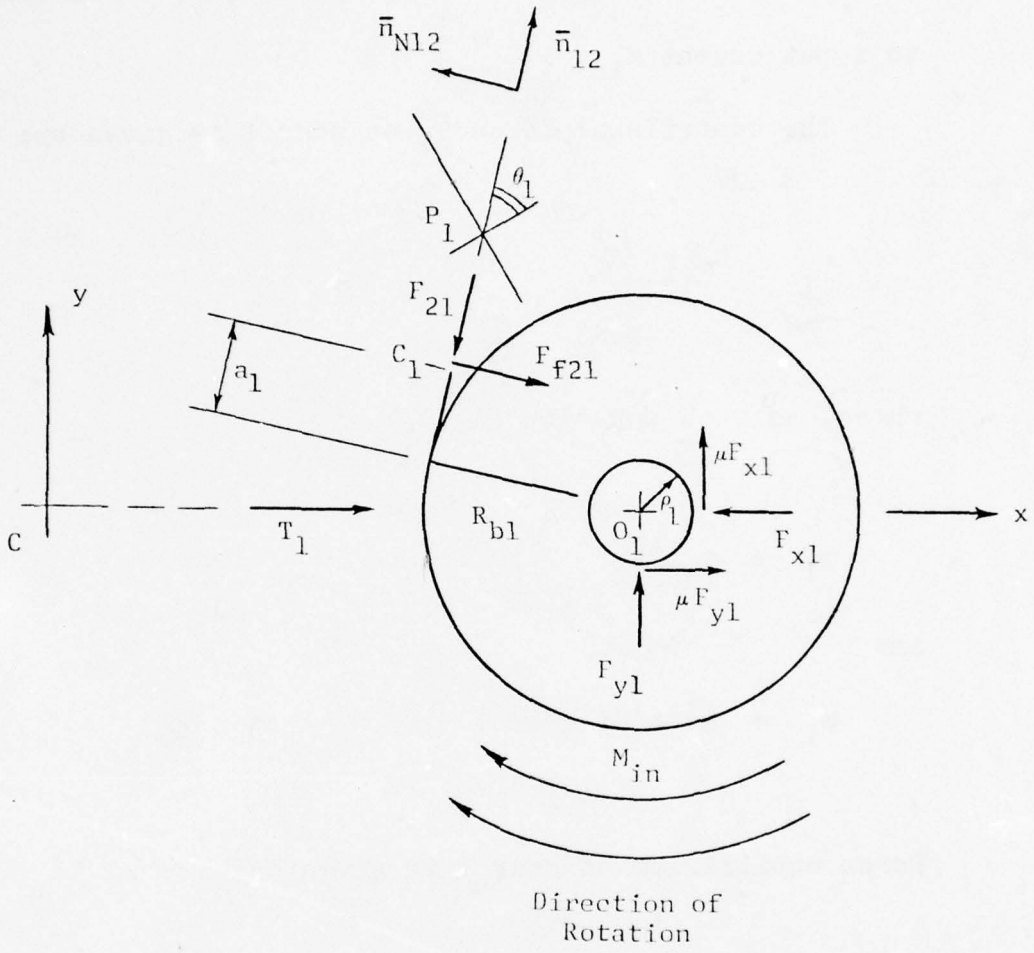

FIGURE A-13 FREE BODY DIAGRAM OF GEAR 1

The associated friction forces $\mu F_{y1}\bar{i}$ and $\mu F_{x1}\bar{j}$ were chosen with such directions that their moments oppose rotation due to input moment M_{in}.

The centrifugal force $\bar{T}_1$ on gear 1 is given by:

$$\bar{T}_1 = T_1\bar{i} \tag{A-177}$$

where, as with equation (A-107)

$$T_1 = \mathcal{R}_1\omega^2 m_1 \tag{A-178}$$

and

$$m_1 = \text{mass of gear 1} \tag{A-179}$$

Force equilibrium of gear 1 is given by:

$$-F_{12}\bar{n}_{12} - \mu s_1 F_{12}\bar{n}_{N12} + T_1\bar{i} - F_{x1}\bar{i} + F_{y1}\bar{j} + \mu F_{y1}\bar{i} + \mu F_{x1}\bar{j} = 0 \tag{A-180}$$

Moment equilibrium is given by:

$$R_{b1}F_{12} - \mu s_1 a_1 F_{12} - M_{in} + \mu\rho_1(\tilde{F}_{x1} + \tilde{F}_{y1}) = 0 \tag{A-181}$$

Note that equations (A-180) and (A-181) have the same forms as equations (A-109) and (A-110).

The force component expressions are the same as given by equations (A-111) and (A-112), and their simultaneous solution for the pivot forces is identical to that given by equations (A-113) and (A-114), i.e.

$$F_{x1} = \frac{-F_{12}\left[(1 - \mu^2 s_1)\sin(\beta_1 + \theta_1) + \mu(1 + s_1)\cos(\beta_1 + \theta_1)\right] + T_1}{1 + \mu^2} \tag{A-182}$$

and

$$F_{y1} = \frac{F_{12}\left[\mu(1 + s_1)\sin(\beta_1 + \theta_1) - (1 - \mu^2 s_1)\cos(\beta_1 + \theta_1)\right] - \mu T_1}{1 + \mu^2} \tag{A-183}$$

Equations (A-182) and (A-183) are now substituted into equation (A-181) according to the method of equation (A-3b):

$$R_{b1}F_{12} - \mu s_1 a_1 F_{12} - M_{in} + \mu\rho_1\left[F_{12}(A_{11} + A_{13}) + T_1(A_{12} + A_{14})\right] = 0 \tag{A-184}$$

where

$$A_{11} = \left| \frac{(1 - \mu^2 s_1)\sin(\beta_1 + \theta_1) + \mu(1 + s_1)\cos(\beta_1 + \theta_1)}{1 + \mu^2} \right| \quad \text{(A-185)}$$

$$A_{12} = \left| \frac{1}{1 + \mu^2} \right| \quad \text{(A-186)}$$

$$A_{13} = \left| \frac{\mu(1 + s_1)\sin(\beta_1 + \theta_1) - (1 - \mu^2 s_1)\cos(\beta_1 + \theta_1)}{1 + \mu^2} \right| \quad \text{(A-187)}$$

$$A_{14} = \left| \frac{\mu}{1 + \mu^2} \right| \quad \text{(A-188)}$$

Finally, equation (A-184) is solved for F_{12}:

$$F_{12} = \frac{M_{in}}{D_3} - \frac{T_1 C_4}{D_3} \quad \text{(A-189)}$$

where

$$C_4 = \mu \rho_1 (A_{12} + A_{14}) \quad \text{(A-190)}$$

$$D_3 = R_{b1} - \mu \left[s_1 a_1 - \rho_1 (A_{11} + A_{13}) \right] \quad \text{(A-191)}$$

d. INPUT-OUTPUT RELATIONSHIP

To obtain the input-output relationship for the complete gear train, equation (A-189) is now set equal to equation (A-169). This furnishes:

$$F_{23} = \frac{D_2}{C_2 D_3}\left[M_{in} - T_1 C_4\right] - T_2 \frac{C_3}{C_2} \qquad \text{(A-192)}$$

The above is then set equal to equation (A-144). This results in the input-output moment relationship:

$$M_{o3} = \frac{D_1 D_2}{C_2 D_3}\left[M_{in} - T_1 C_4\right] - T_2 \frac{C_3 D_1}{C_2} - T_3 C_1 \qquad \text{(A-193)}$$

6. AUXILIARY GEOMETRIC AND KINEMATIC EXPRESSIONS FOR TWO AND THREE STEP-UP GEAR TRAINS WITH INVOLUTE TEETH

a. NOMENCLATURE FOR INVOLUTE GEAR TEETH

R_{pi}, r_{pi} = pitch radii of gear and pinion of i^{th} gear and pinion set

R_{bi}, r_{bi} = base radii of gear and pinion of i^{th} gear and pinion set

R_{oi}, r_{oi} = outside radii of gear and pinion of i^{th} gear and pinion set

θ_j = effective pressure angle of j^{th} mesh

$\mathcal{R}_i$ = distance from spin axis to pivot of i^{th} gear and pinion set

b. ANGULAR RELATIONSHIPS BETWEEN PIVOT HOLES

Figure A-14 shows the angular relationships between the lines connecting the pivot holes as well as the spin center. (See also Figures A-5 and A-10.) The following serves to determine the angles γ_i and β_i for certain combinations of gears and pinions as well as spin radii $\mathcal{R}_i$.

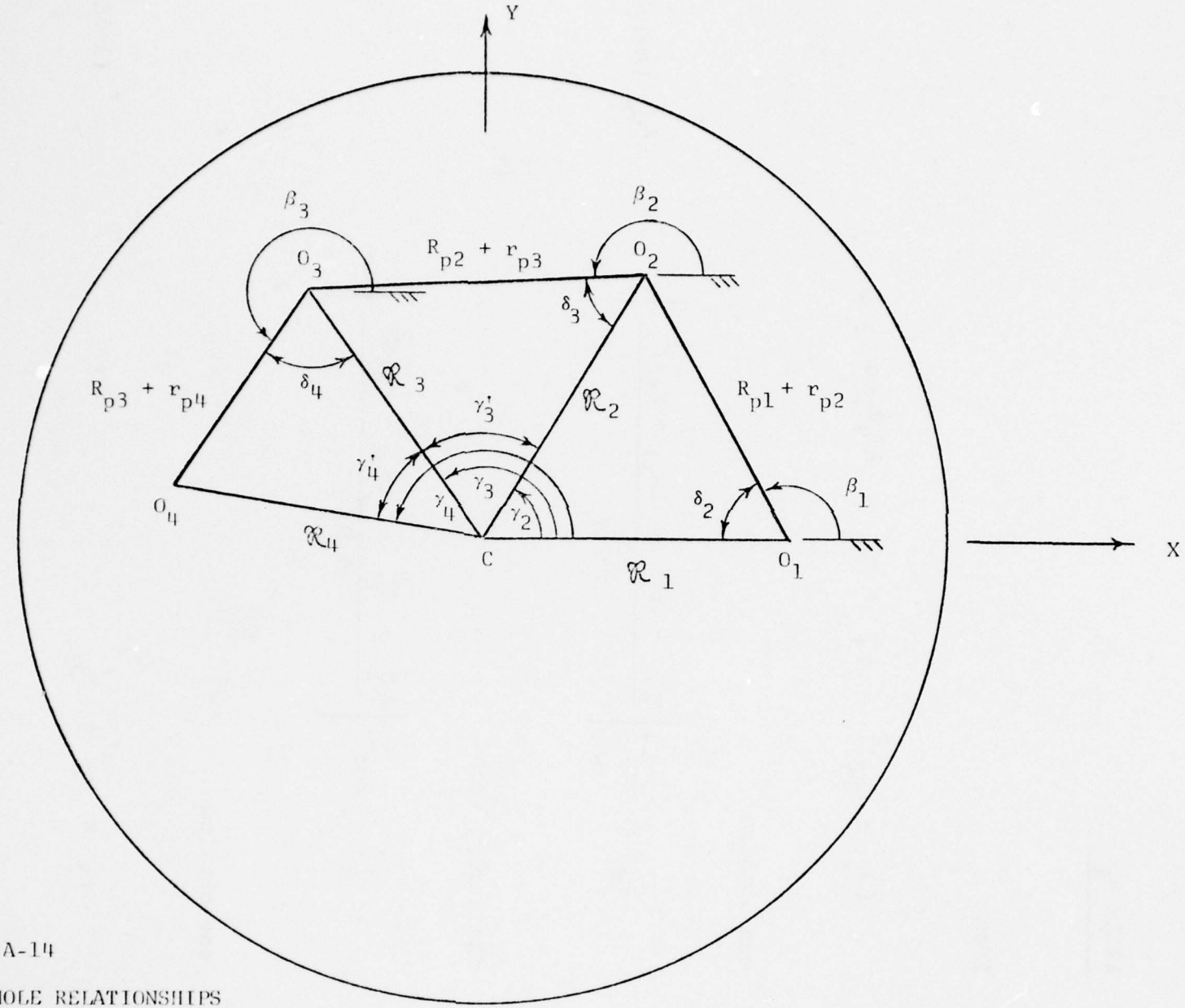

FIGURE A-14

PIVOT HOLE RELATIONSHIPS

ANGLE γ_i

From

$$(R_{p1} + r_{p2})^2 = \mathcal{R}_1^2 + \mathcal{R}_2^2 - 2\mathcal{R}_1\mathcal{R}_2\cos\gamma_2$$

one obtains

$$\gamma_2 = \cos^{-1}\left[\frac{\mathcal{R}_1^2 + \mathcal{R}_2^2 - (R_{p1} + r_{p2})^2}{2\mathcal{R}_1\mathcal{R}_2}\right] \qquad \text{(A-194)}$$

Similarly, from

$$\gamma_3' = \cos^{-1}\left[\frac{\mathcal{R}_2^2 + \mathcal{R}_3^2 - (R_{p2} + r_{p3})^2}{2\mathcal{R}_2\mathcal{R}_3}\right]$$

one obtains

$$\gamma_3 = \gamma_2 + \gamma_3' \qquad \text{(A-195)}$$

Also with

$$\gamma_4' = \cos^{-1}\left[\frac{\mathcal{R}_3^2 + \mathcal{R}_4^2 - (R_{p3} + r_{p4})^2}{2\mathcal{R}_3\mathcal{R}_4}\right]$$

one obtains

$$\gamma_4 = \gamma_3 + \gamma_4' \tag{A-196}$$

ANGLES δ_i

Since

$$\mathcal{R}_2^2 = (R_{p1} + r_{p2})^2 + \mathcal{R}_1^2 - 2(R_{p1} + r_{p2})\mathcal{R}_1\cos\delta_2$$

$$\delta_2 = \cos^{-1}\left[\frac{(R_{p1} + r_{p2})^2 + \mathcal{R}_1^2 - \mathcal{R}_2^2}{2\mathcal{R}_1(R_{p1} + r_{p2})}\right] \tag{A-197}$$

Similarly,

$$\delta_3 = \cos^{-1}\left[\frac{(R_{p2} + r_{p3})^2 + \mathcal{R}_2^2 - \mathcal{R}_3^2}{2\mathcal{R}_2(R_{p2} + r_{p3})}\right] \tag{A-198}$$

and

$$\delta_4 = \cos^{-1}\left[\frac{(R_{p3} + r_{p4})^2 + \mathcal{R}_3^2 - \mathcal{R}_4^2}{2\mathcal{R}_3(R_{p3} + r_{p4})}\right] \qquad \text{(A-199)}$$

ANGLES β_i

With Equation (A-197)

$$\beta_1 = \pi - \delta_2 \qquad \text{(A-200)}$$

Further, with Equations (A-194) and (A-198)

$$\beta_2 = \gamma_2 + (\pi - \delta_3) \qquad \text{(A-201)}$$

Finally, with Equations (A-195) and (A-199)

$$\beta_3 = \gamma_3 + (\pi - \delta_4) \qquad \text{(A-202)}$$

c. DETERMINATION OF CONTACT POINT C FOR VARIOUS MESHES

Figure A-15 shows the points of interest along the line of action of an involute gear which drives an involute pinion.

Points L and L' are the points of tangency to the base circles of radius R_b and r_b respectively and the distance d = LL'. Initial contact is made at point M, where the line of action intersects the pinion addendum circle of radius r_o. Final contact corresponds to point N. Here the line of action intersects the gear addendum circle of radius R_o.

The position of the instantaneous contact point C with respect to point L, i.e. the length a, is expressed with the help of the instantaneous angle α which has its origin at the line O_1L. Then,

$$a = LC = R_b\alpha \qquad \text{(A-203)}$$

A computer procedure for the determination of the instantaneous angle α of any mesh must first find the associated initial and final angles of contact α_{in} and α_{fin}. In addition it must contain a method for incrementing the angle α. The following shows such a procedure for each of the meshes of a two pass and a three pass step-up gear train, together with a means of obtaining the signs of the signum terms.

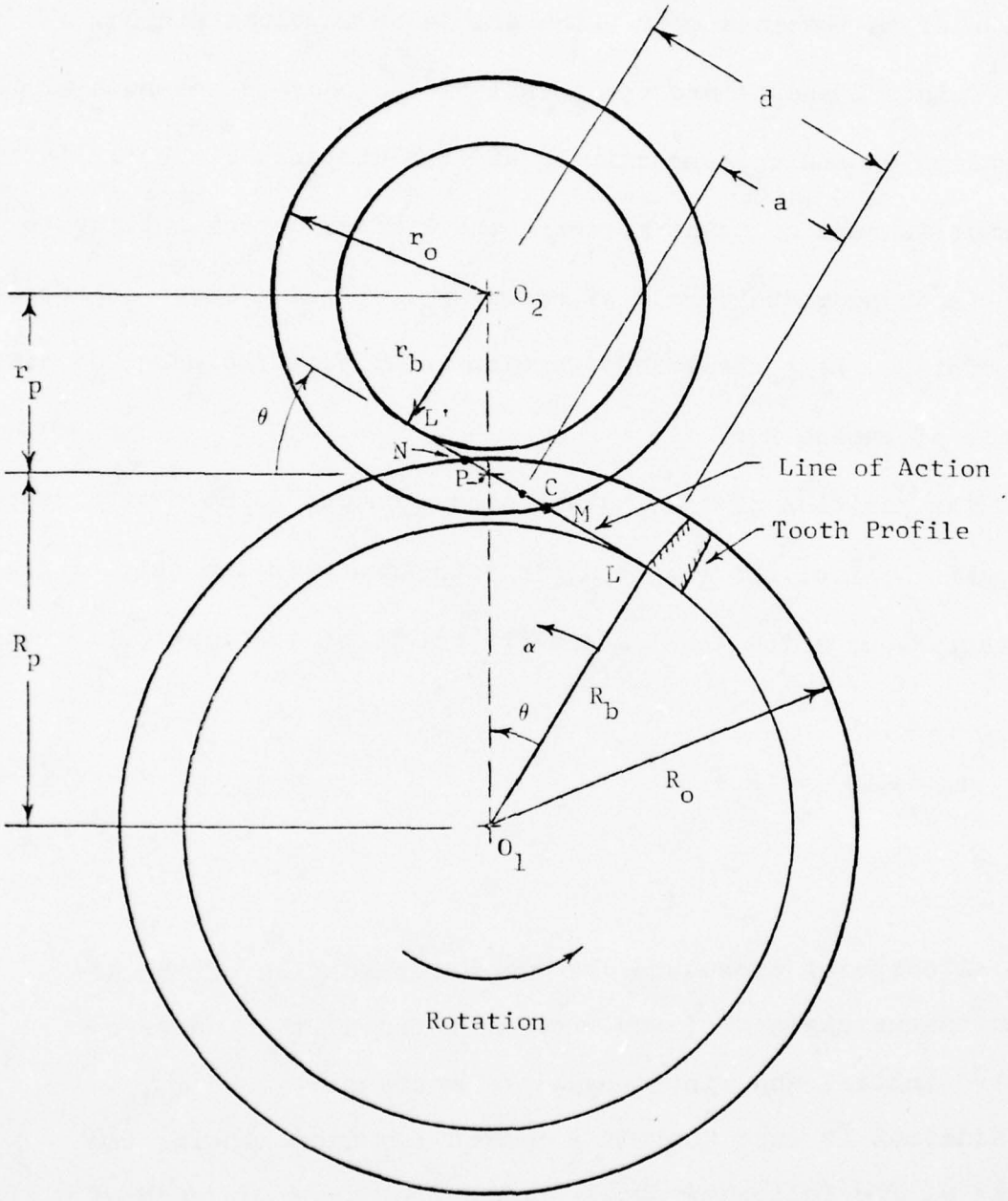

FIGURE A-15

INVOLUTE MESH GEOMETRY

1.) MESH OF GEAR 1 AND PINION 2

The total length $d_1 = LL'$ is given by:

$$d_1 = (R_{b1} + r_{b1})\tan\theta_1 \tag{A-204}$$

The initial angle of contact α_{1IN} is obtained from:

$$\alpha_{1\,in} = \frac{ML}{R_{b1}} = \frac{(R_{b1} + r_{b2})\tan\theta_1 - \sqrt{r_{o2}^2 - r_{b2}^2}}{R_{b1}} \tag{A-205}$$

Similarly, the final angle of contact α_{1FIN} is given by:

$$\alpha_{1\,fin} = \frac{\sqrt{R_{o1}^2 - R_{b1}^2}}{R_{b1}} \tag{A-206}$$

The magnitude of the increment $\Delta\alpha_1$ depends on whether one deals with a two step-up or a three step-up gear train.

Assuming that a two step-up train is involved and that one wishes to compute the length a_2 of mesh 2 K_2 times after the first contact, the angular increment $\Delta\alpha_{22}$ has the magnitude

$$\Delta\alpha_{22} = \frac{\alpha_{2fin} - \alpha_{2in}}{K_2} \qquad \text{(A-207)}$$

(The second subscript refers to a two step-up configuration.) Because of the transmission ratio between gear sets 1 and 2, the associated angular increment of gear 1 will be smaller than $\Delta\alpha_{22}$, i.e.

$$\Delta\alpha_{12} = \Delta\alpha_{22} \frac{r_{b2}}{R_{b1}} \qquad \text{(A-208)}$$

The instantaneous angle α_1 will then be given by:

$$\alpha_1 = \alpha_{1in} + j_{12}\Delta\alpha_{12} \qquad \text{(A-209)}$$

and, the instantaneous distance a_1 becomes:

$$a_1 = R_{b1}(\alpha_{1in} + j_{12}\Delta\alpha_{12}) \qquad \text{(A-210)}$$

In the above, j_{12} represents the number of times the angle α_1 has been incremented. While the total number of increments depends on the length of contact, the incrementing of α_1 comes to an end when $\alpha_1 \geq \alpha_{1fin}$. This also corresponds to a complete mechanism

AD-A061 862 CITY COLL NEW YORK DEPT OF MECHANICAL ENGINEERING F/G 13/9 F/G 13/9
OPTIMIZATION OF STEP-UP GEAR TRAINS WITH DIFFERENT KINEMATIC PR~~INEMATIC~~ PR--ETC(U)
MAY 78 G G LOWEN DAAG29-77-G-0037
UNCLASSIFIED ARO-14743.1-R-E NL NL

2 OF 4
ADA
061862

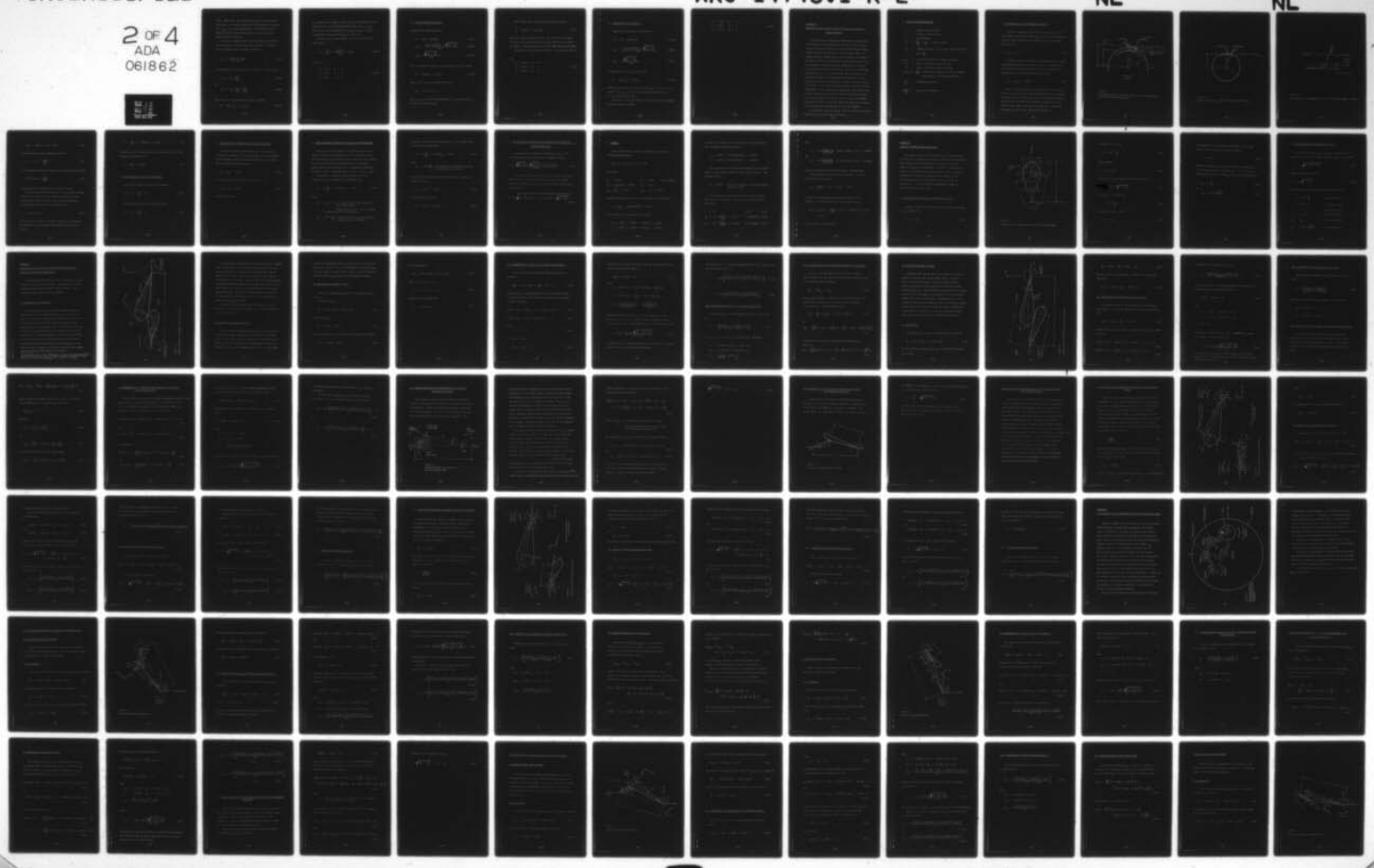

cycle. Since mesh 2 goes through R_{b1}/r_{b2} times as many cycles as mesh no. 1, the angle α_2 has to be re-initialized to α_{2in} when $\alpha_2 \geq \alpha_{2fin}$, i.e. after K_2 increments. (For simplicity it is assumed that the motion starts when all meshes are at their initial contact angles α_{in}.)

When a three step-up gear train is involved, one must make sure that enough computations are made for mesh 3. Assuming that K_3 increments are to be made, one obtains

$$\Delta\alpha_{33} = \frac{\alpha_{3fin} - \alpha_{3in}}{K_3} \tag{A-211}$$

The associated angular increments for meshes 2 and 1 then become:

$$\Delta\alpha_{23} = \Delta\alpha_{33} \frac{r_{b3}}{R_{b2}} \tag{A-212}$$

and

$$\Delta\alpha_{13} = \Delta\alpha_{33} \frac{r_{b3}}{R_{b2}} \times \frac{r_{b2}}{R_{b1}} \tag{A-213}$$

For this case the instantaneous distance a_1 becomes

$$a_1 = R_{b1}(\alpha_{1in} + j_{13}\Delta\alpha_{13}) \tag{A-214}$$

j_{13} stands for the number of times α_1 has been incremented at any given instant. This incrementing again ends when $\alpha_1 \geq \alpha_{1fin}$. Meshes 2 and 3 are re-initialized to α_{2in} and α_{3in} as often as is necessary to complete one cycle for mesh no. 1.

The sign of s_1 is best obtained from the fact that at the pitch point P_1

$$\alpha_{1p} = \frac{LP}{R_{b1}} = \frac{R_{b1}\tan\theta_1}{R_{b1}} = \tan\theta_1 \qquad \text{(A-215)}$$

then for:

$$\begin{aligned} \alpha_1 < \tan\theta_1 &: \quad s_1 = +1 \\ \alpha_1 = \tan\theta_1 &: \quad s_1 = 0 \\ \alpha_1 > \tan\theta_1 &: \quad s_1 = -1 \end{aligned} \qquad \text{(A-216)}$$

2.) MESH OF GEAR 2 AND PINION 3

Similar to the previous section:

$$d_2 = (R_{b2} + r_{b3})\tan\theta_2 \tag{A-217}$$

$$\alpha_{2in} = \frac{(R_{b2} + r_{b3})\tan\theta_2 - \sqrt{r_{o3}^2 - r_{b3}^2}}{R_{b2}} \tag{A-218}$$

$$\alpha_{2fin} = \frac{\sqrt{R_{o2}^2 - R_{b2}^2}}{R_{b2}} \tag{A-219}$$

For a 2 step-up gear train the instantaneous length a_2 becomes:

$$a_2 = R_{b2}(\alpha_{2in} + j_{22}\Delta\alpha_{22}) \tag{A-220}$$

where $\Delta\alpha_{22}$ is given by Equation (A-207) and

$$j_{22} = 1, 2, \ldots, K_2.$$

When $\alpha_2 \geq \alpha_{2fin}$ it must be re-initialized to α_{2in} until mesh no. 1 has completed its full cycle.

For a three step-up gear train the length a_2 becomes:

$$a_2 = R_{b2}(\alpha_{2in} + j_{23}\Delta\alpha_{23}) \qquad \text{(A-221)}$$

with $\Delta\alpha_{23}$ given by Equation (A-212). j_{23} stands for the number of times α_2 has been incremented and again depends on the length of contact. Re-initialization follows the same rule as given above.

The sign of s_2 is obtained as follows: (See Equation (A-215).)

For

$$\begin{aligned} \alpha_2 < \tan\theta_2 &: \quad s_2 = +1 \\ \alpha_2 = \tan\theta_2 &: \quad s_2 = 0 \\ \alpha_2 > \tan\theta_2 &: \quad s_2 = -1 \end{aligned} \qquad \text{(A-222)}$$

3.) MESH OF GEAR 3 AND PINION 4

Again, in the same vein as in Section 1:

$$d_3 = (R_{b3} + r_{b4})\tan\theta_3 \tag{A-223}$$

$$\alpha_{3in} = \frac{(R_{b3} + r_{b4})\tan\theta_3 - \sqrt{r_{o4}^2 - r_{b4}^2}}{R_{b3}} \tag{A-224}$$

$$\alpha_{3fin} = \frac{\sqrt{R_{o3}^2 - R_{b3}^2}}{R_{b3}} \tag{A-225}$$

The instantaneous length a_3 is given by:

$$a_3 = R_{b3}(\alpha_{3in} + j_{33}\Delta\alpha_{33}) \tag{A-226}$$

where $\Delta\alpha_{33}$ is given by Equation (A-211) and $j_{33} = 1, 2, \ldots, K_3$. Whenever $\alpha_3 \geq \alpha_{3fin}$ it must be re-initialized until mesh no. 1 has completed its full cycle.

The sign of s_3 is again obtained with the help of an expression similar to Equation (A-215):

$$\alpha_3 < \tan\theta_3 : \quad s_3 = +1$$
$$\alpha_3 = \tan\theta_3 : \quad s_3 = 0 \qquad \text{(A-227)}$$
$$\alpha_3 > \tan\theta_3 : \quad s_3 = -1$$

APPENDIX B

DESIGN OF UNEQUAL ADDENDUM INVOLUTE GEAR SETS WITH STANDARD CENTER DISTANCES

One of the ways of preventing undercutting in pinions with small numbers of teeth, which must mesh with gears of unequal and larger numbers of teeth, is to decrease the pinion dedendum together with the gear addendum by the necessary amount. To maintain standard working depth for such a mesh, the addendum of the pinion as well as the dedendum of the gear are increased by the same amount. (This, of course, presupposes that the gear is not undercut by this modification.) This can be accomplished without any change in the standard base and pitch radii or the associated standard center distance by "withdrawing" the hob during the cutting of the pinion and feeding it "deeper" when the gear is cut. In this way the pinion, which has its ouside radius increased by the hob withdrawal distance, will have a larger than standard circular tooth thickness at its standard pitch circle. The outside radius of the gear is decreased by the same amount. Because the cutter is fed to full depth, the gear tooth thickness at the standard pitch circle will be less than standard.

The following gives the design steps for this type of gearing and illustrates them by way of an example.

1. STANDARD GEAR NOMENCLATURE

N = number of teeth of gear

n = number of teeth of pinion

θ = pressure angle

$P_d = \frac{N}{2R_p} = \frac{n}{2r_p}$ = diametral pitch

p_{cs} = standard circular pitch at pitch circle, where also

$$p_{cs} = \frac{\pi}{P_d}$$

R_p, r_p = pitch radii of gear and pinion respectively

$R_b = R_p\cos\theta$, base circle radius of gear

$r_b = r_p\cos\theta$, base circle radius of pinion

T_{cs}, $t_{cs} = \frac{p_{cs}}{2}$, circular tooth thickness of gear and pinion respectively at standard pitch circles

$\frac{1}{P_d}$ = standard gear addendum

$\frac{1.157}{P_d}$ = standard gear dedendum

2. DETERMINATION OF HOB WITHDRAWAL DISTANCE C

Figure B-1 indicates the relationship between the pinion pitch radius r_p, its root radius r_r and the rack cutter addendum A. The root radius is formed by the addendum line of the cutter tooth, so that

$$r_r = r_p - A \tag{B-1}$$

In order to avoid undercutting, the addendum line of a sharp cornered cutter must not pass below point L, the tangent point of the line of action and the base circle (see Figure B-2). The minimum root radius r_{rm} becomes for this case:

$$r_{rm} = r_b \cos\theta = r_p \cos^2\theta \tag{B-2}$$

When the rack tooth corner is rounded off with a radius r_c, as shown in Figure B-3, the effective addendum line of the cutter tooth moves up the distance $r_c(1 - \sin\theta)$. To avoid undercutting with this type of cutter, the effective addendum line must not pass the base circle below point L in Figure B-2. This allows a reduction of the minimum allowable root radius to:

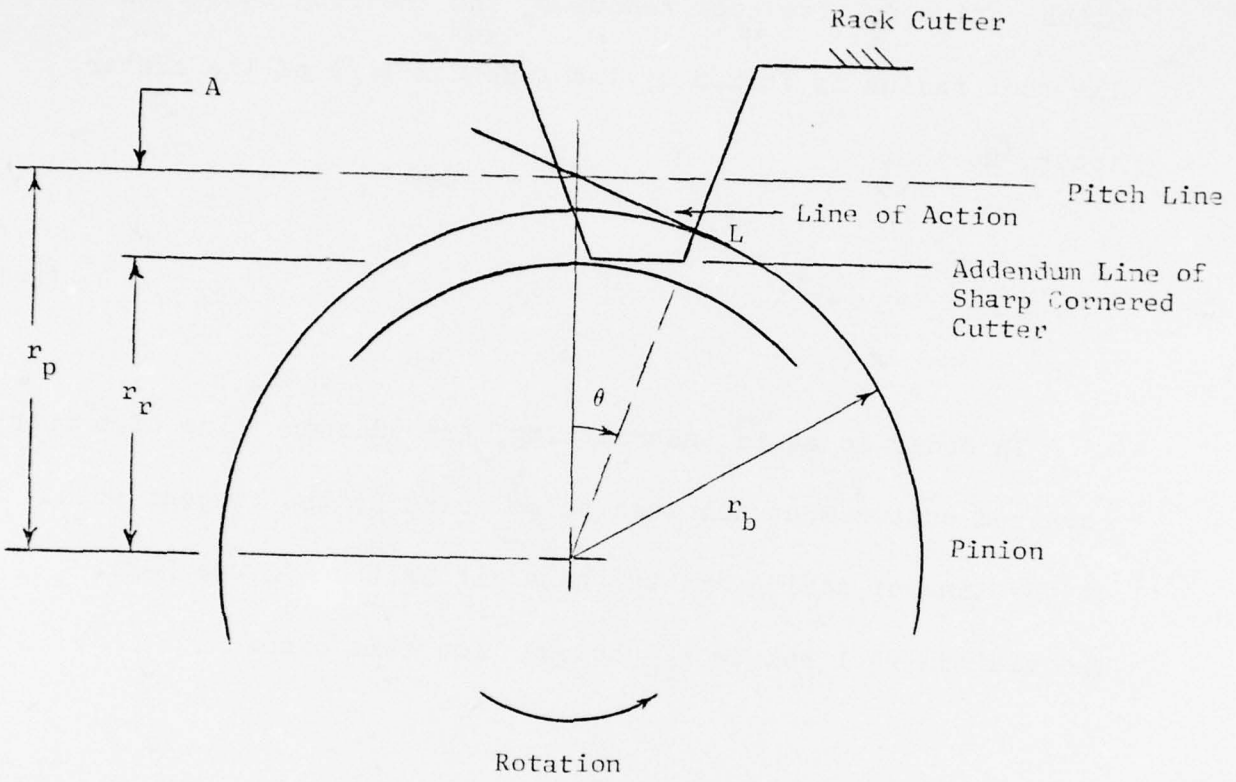

FIGURE B-1

RELATIONSHIP BETWEEN PINION PITCH RADIUS r_p, RACK CUTTER ADDENDUM A AND RESULTING PINION ROOT RADIUS r_r

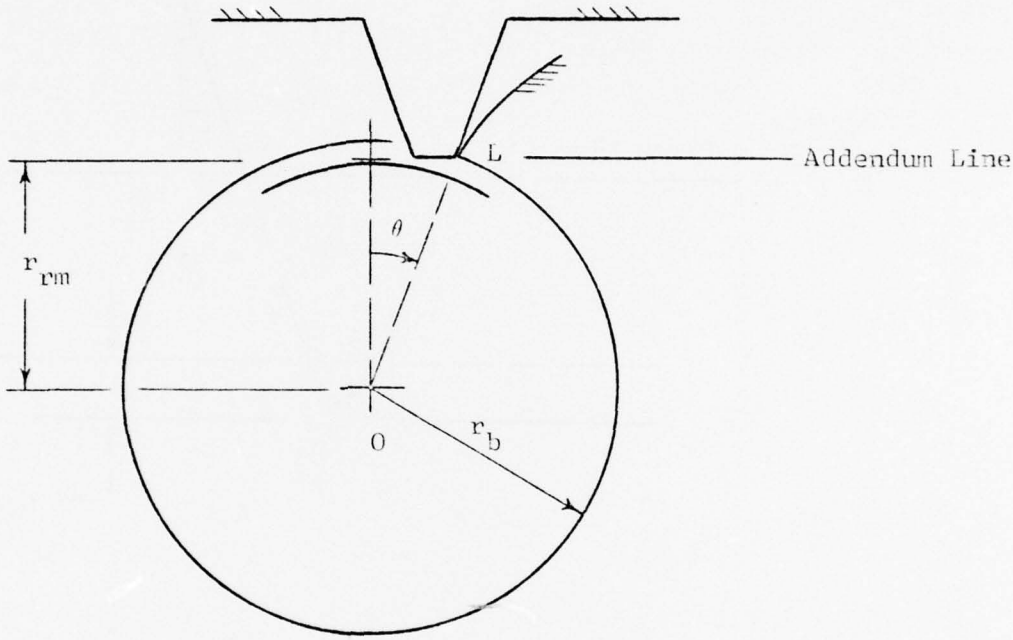

FIGURE B-2

MINIMUM ROOT RADIUS r_{rm} FOR RACK CUTTER WITH SHARP CORNER

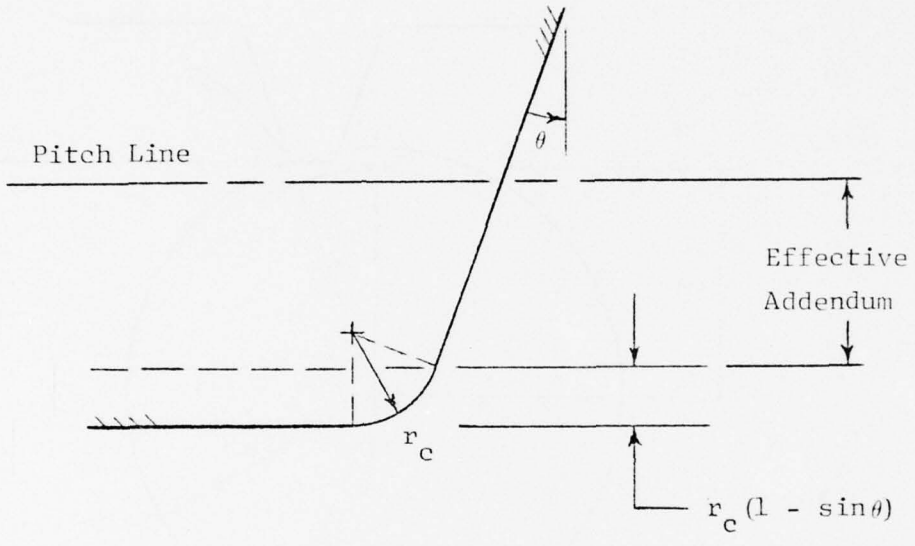

FIGURE B-3

RACK CUTTER WITH CORNER RADIUS r_c (EFFECTIVE ADDENDUM OF CUTTER IS DECREASED)

$$r_{rmc} = r_p\cos^2\theta - r_c(1 - \sin\theta) \qquad \text{(B-3)}$$

By common usage the corner radius may either be

$$r_c = .1\, t_s = \frac{.05\pi}{P_d}\,, \qquad \text{(B-4)}$$

or it is chosen such that the second term in Equation (B-3) becomes

$$r_c(1 - \sin\theta) \approx \frac{.157}{P_d} \qquad \text{(B-5)}$$

(This makes for an effective cutter addendum of $1/P_d$.)

Hob withdrawal becomes necessary if the root radius, obtained by setting the cutter to standard depth, is smaller than the minimum given by Equation (B-3). Thus, the hob withdrawal C is obtained from Equations (B-1) and (B-3), i.e. :

$$C = r_{rmc} - r_r \qquad \text{(B-6)}$$

With the cutter addendum $A = 1.157/P_d$, and using the expression of Equation (B-4) for the rack corner radius, Equation (B-6) becomes:

$$C = \frac{1}{P_d}(1 + .157\sin\theta) - r_p\sin^2\theta \qquad (B\text{-}7)$$

If Equation (B-5) is used, with the same definition of the cutter addendum, one obtains for C:

$$C = \frac{1}{P_d} - r_p\sin^2\theta \qquad (B\text{-}7)$$

3. OUTSIDE RADII OF PINION AND GEAR BLANKS

The outside radius of the pinion blank becomes:

$$r_o = r_p + \frac{1}{P_d} + C \qquad (B\text{-}8)$$

The outside radius of the gear blank becomes:

$$R_o = R_p + \frac{1}{P_d} - C \qquad (B\text{-}9)$$

4. TOOTH THICKNESS AT PITCH CIRCLES OF PINION AND GEAR

Since the thickness of the hobtooth at the pinion pitch circle will be reduced by the amount $2C\tan\theta$, due to the withdrawal C, the circular thickness of the pinion tooth at this location will be increased by this amount, i.e. :

$$t_c = t_{cs} + 2C\tan\theta \qquad \text{(B-10)}$$

The gear tooth thickness will be decreased to:

$$T_c = T_{cs} - 2C\tan\theta \qquad \text{(B-11)}$$

at its pitch circle.

5. TOOTH THICKNESS AT OUTSIDE AND BASE RADII BY INVOLUTOMETRY

The circular tooth thickness at an arbitrary radius of an involute tooth may be obtained if the tooth thickness, radius, and pressure angle of any other location, such as the pitch circle, are known together with the pressure angle at the arbitrary radius. [See Equation (5-5), pg. 80, E. Buckingham: Analytical Mechanics of Gears, McGraw-Hill Book Co., Inc. New York, 1949.]

Accordingly, the circular tooth thickness t_o, at the outside radius of the pinion, may be obtained from:

$$t_o = t_c \frac{r_o}{r_p} - 2r_o(INV\theta_{OP} - INV\theta) \qquad (B\text{-}12)$$

where

$INV\theta = \tan\theta - \theta$, the involute function corresponding to the pressure angle θ

θ = pressure angle of mesh. This is also the pressure angle at the pitch circle.

$\theta_{OP} = \cos^{-1} \frac{r_b}{r_o}$, the pressure angle associated with the outside radius of the pinion

Similarly, the circular tooth thickness T_o at the outside radius of the gear is obtained from:

$$T_o = T_c \frac{R_o}{R_p} - 2R_o(INV\theta_{OG} - INV\theta) \qquad (B\text{-}13)$$

where

$\theta_{OG} = \cos^{-1} \frac{R_b}{R_o}$, the pressure angle associated with the outside radius of the gear

The tooth thickness at the base circle radius of the modified pinion is given by:

$$t_b = t_c \cos\theta + 2r_b INV\theta \qquad (B\text{-}14)$$

This becomes for the gear:

$$T_b = T_c \cos\theta + 2R_b INV\theta \qquad (B\text{-}15)$$

6. EXPRESSIONS FOR CONTACT RATIO AND PINION OUSIDE RADIUS FOR UNITY CONTACT RATIO

The expression for contact ratio [Equation 4-19, pg. 72, E. Buckingham: Analytical Mechanics of Gears] is given by:

$$m_p = \frac{\sqrt{R_o^2 - R_b^2} + \sqrt{r_o^2 - r_b^2} - (R_b + r_b)\tan\theta}{p_{cs}\cos\theta} \qquad \text{(B-16)}$$

If the contact ratio of a certain mesh is larger than unity, and one wishes to reduce it to unity by reducing the outside radius of the pinion, one may find this new pinion outside radius with the help of

$$r_o' = \sqrt{r_b^2 + \left[p_{cs}\cos\theta + (R_b + r_b)\tan\theta - \sqrt{R_o^2 - R_b^2} \right]^2} \qquad \text{(B-17)}$$

7. EXAMPLE

Let it be required to design a pinion and a gear with the following specifications:

$$P_d = 44, \quad N = 42, \quad n = 8, \quad \theta = 20^\circ$$

This gives:

$R_p = .47727$ $\qquad$ $r_p = .09091$ $\qquad$ (all in inches)

$R_b = R_p \cos 20^\circ = .44848$ $\qquad$ $r_b = .08542$

$p_{cs} = \frac{\pi}{44} = .07140$ $\qquad$ $T_{cs} = t_{cs} = .03570$

According to Equation (B-7), the hob withdrawal C is computed as

$$C = \frac{1}{44} - .09091 \sin^2 20^\circ = .012093$$

Then, according to Equations (B-8) and (B-9):

$$r_o = .09091 + .022727 + .012093 = .12573"$$

$$R_o = .47727 + .022727 - .012093 = .48790"$$

The new tooth thickness at the pitch radii are found with the help of Equations (B-10) and (B-11):

$$t_c = .03570 + 2(.012093)\tan 20^\circ = .04450"$$

$$T_c = .03570 - 2(.012093)\tan 20^\circ = .02689"$$

For the purposes of the present analysis, the pinion outside radius is now reduced to obtain a contact ratio of unity. With Equation (B-17):

$r_o' = .110''$ (This is essentially the unmodified pinion radius of .113".)

Now compute the circular tooth thickness at the outside radii r_o' and R_o using the following data in Equations (B-12) and (B-13):

$\theta = 20^\circ$ INV $20^\circ = .01490$

$\theta_{OP} = \cos^{-1} \frac{.08542}{.110} = 39.0509^\circ$ INV $39.0509^\circ = .12969$

$\theta_{OG} = \cos^{-1} \frac{.44848}{.48790} = 23.1889^\circ$ INV $23.1889^\circ = .02365$

Then

$$t_o = .04450\left(\frac{.110}{.09091}\right) - 2(.110)(.12969 - .0149) = .02860''$$

and

$$T_o = .02689\left(\frac{.4879}{.47727}\right) - 2(.4879)(.02365 - .0149) = .01896''$$

These are sufficient to allow for rounding off of the teeth.

Finally check that the gear is not undercut. The actual root radius of the gear is:

$$R_o - \frac{2.157}{P_d} = .4879 - .04902 = .4389"$$

The minimum permissible root radius without undercutting according to Equations (B-3) and (B-4) is computed from:

$$R_{rm} = R_p\cos^2\theta - \frac{.05\pi}{P_d}(1 - \sin\theta) = .47727(.883) - .0023$$

$$= .419"$$

Thus, the gear is not undercut.

APPENDIX D

GEOMETRY OF GENERAL OGIVAL GEAR TOOTH

The general ogival tooth of thickness t and outside radius r_o consists of a circular arc of radius ρ which blends tangentially into a radial tooth flank, as shown in Figure D-1 (only one center of curvature is indicated). The center of curvature C is located at a distance a from the center of the gear or pinion. Frequently this distance a equals the pitch radius r_p. The tooth geometry may either be described with the help of the parameters t, ρ and a, or with the combination t, ρ and r_o. Both approaches are shown below.

1. TOOTH GEOMETRY WITH HELP OF PARAMETERS t, ρ AND a

C_x and C_y represent the coordinates of the center of curvature C. C_x is defined by:

$$C_x = \rho - \frac{t}{2} \qquad \text{(D-1)}$$

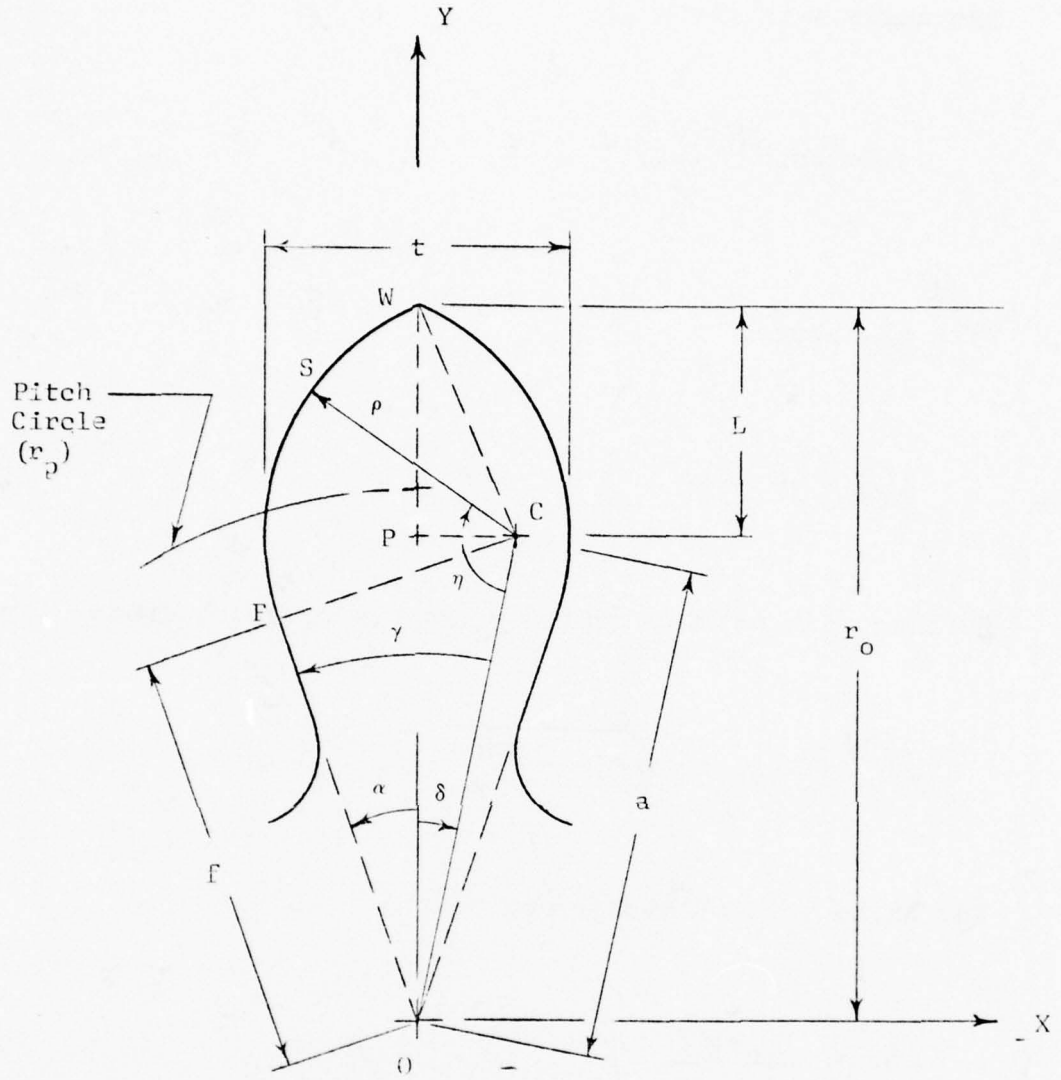

FIGURE D-1

GEOMETRY OF OGIVAL TOOTH (ONLY ONE CENTER OF CURVATURE SHOWN)

The angle δ is given by:

$$\delta = \sin^{-1} \frac{C_x}{a} \qquad \text{(D-2)}$$

With the above,

$$C_y = a \cos\delta \qquad \text{(D-3)}$$

Further, the outside radius r_o may be computed from:

$$C_y + \sqrt{\rho^2 - C_x^2} \qquad \text{(D-4)}$$

The angle γ is obtained from

$$\gamma = \sin^{-1} \frac{\rho}{a} \quad , \qquad \text{(D-5)}$$

and the flank angle α from:

$$\alpha = \gamma - \delta \qquad \text{(D-6)}$$

The distance f, from the center of rotation O to the blend point F of the flank of the tooth, is given by:

$$f = a \cos\gamma \tag{D-7}$$

The angle η defines the tooth contact point S on the ogival, i.e. circular, portion of the tooth with the lines OC and CS. The minimum and maximum angles η_{min} and η_{max} are respectively:

$$\eta_{min} = \frac{\pi}{2} - \gamma \tag{D-8}$$

and

$$\eta_{max} = \sin^{-1} \frac{r_o \sin\delta}{\rho} \tag{D-9}$$

2. TOOTH GEOMETRY FROM PARAMETERS ρ, t AND r_o

If the outside radius r_o is given, the distance a must be computed. The length C_x is still given by Equation (D-1), while

$$a = \sqrt{(r_o - L)^2 + C_x^2} \qquad \text{(D-10)}$$

where, according to Figure D-1:

$$L = \sqrt{\rho^2 - C_x^2} \qquad \text{(D-11)}$$

All other quantities of interest remain as before, i.e.

$$\delta = \sin^{-1} \frac{C_x}{a} \qquad \text{See Equation (D-2)}$$

$$\gamma = \sin^{-1} \frac{\rho}{a} \qquad \text{See Equation (D-5)}$$

$$\alpha = \gamma - \delta \qquad \text{See Equation (D-6)}$$

$$f = a \cos\gamma \qquad \text{See Equation (D-7)}$$

$$\eta_{min} = \frac{\pi}{2} - \gamma \qquad \text{See Equation (D-8)}$$

$$\eta_{max} = \sin^{-1} \frac{r_o \sin \delta}{\rho} \qquad \text{See Equation (D-9)}$$

APPENDIX E

KINEMATICS AND MOMENT INPUT-OUTPUT RELATIONSHIP FOR SINGLE STEP-UP GEAR MESH WITH OGIVAL TEETH

The present appendix first shows the kinematics of a single step-up gear mesh with ogival teeth. Subsequently, the moment input-output relationship for such a mesh is derived. Both contact and pivot friction will be included.

1. KINEMATICS OF AN OGIVE MESH

Figure E-1 indicates the condition of initial contact in ogival meshes when the circular arc portion of the gear tooth drives the circular arc portion of the pinion tooth.[1] This type of direct contact will be called "round on round". As the motion progresses, the circular arc of the gear tooth moves into contact with the straight flank of the pinion tooth, as shown in Figure E-2. During this "round on flat" phase, the distance g at first decreases and then increases again. Before round on round contact can again occur for a given mesh, i.e. g has become equal to f_p again, the subsequent mesh comes into engagement with round on round contact. (See below.)

[1] See section b-VII of this appendix for a check that indicates whether the initial contact is round on round or whether possibly the round portion of the pinion touches the flat portion of the gear.

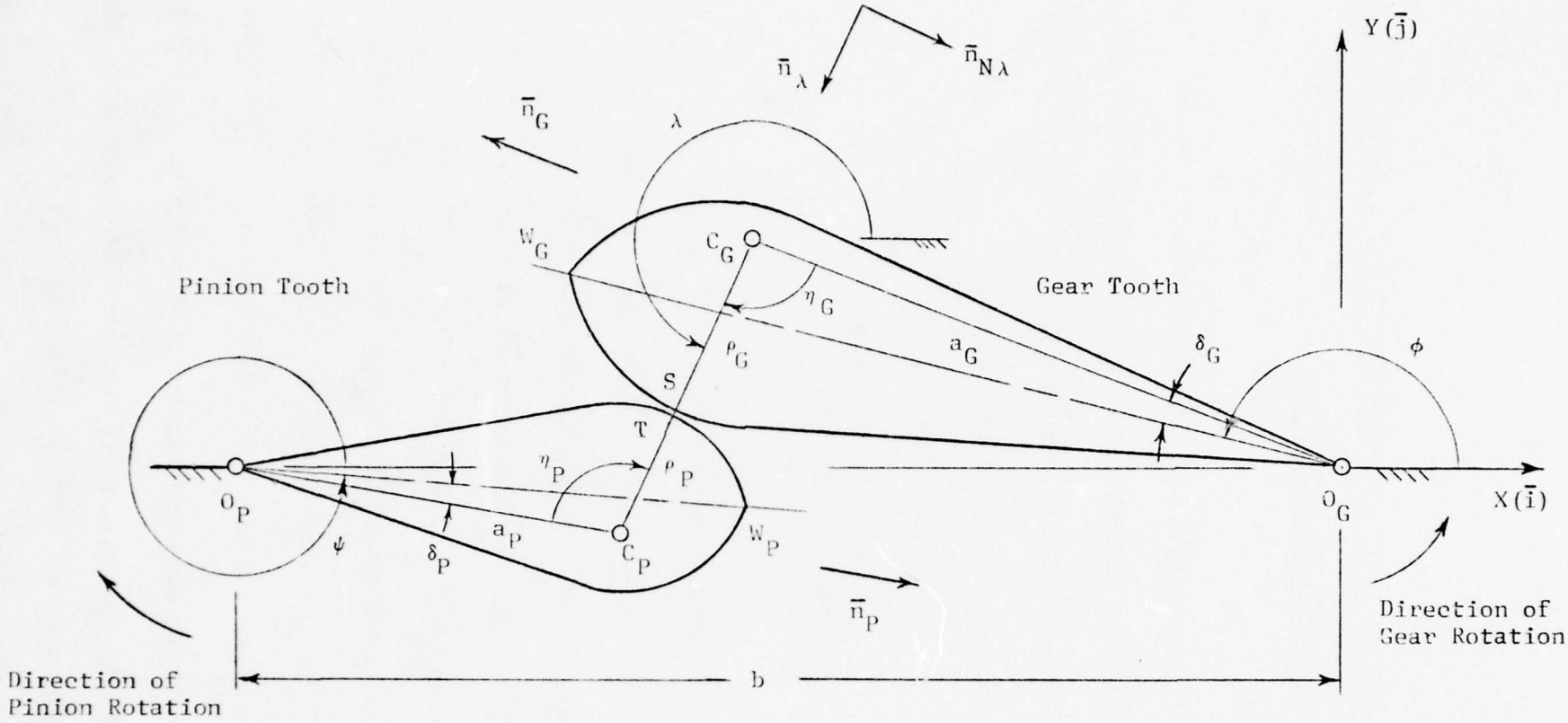

FIGURE E-1

ROUND ON ROUND PHASE OF CONTACT (GEAR DRIVES PINION)

The kinematics of both round on round and round on flat phases will be given first. Further it will be shown how to determine those gear angles ϕ at which the regime changes from round on round to round on flat, and at which contact is taken over by the subsequent set of teeth. Since the ratio of angular velocities between gear and pinion varies with contact point, and the pinion moves faster for a given gear speed for round on round than for round on flat, the original set of teeth disengages as soon as the subsequent one makes contact. Thus, the contact ratio is unity for this type of gearing.

The gear tooth nomenclature given in Appendix D is used throughout. The additional subscripts G and P refer to gear and pinion respectively.

a. ROUND ON ROUND PHASE OF MOTION

Figure E-1 shows the input angle ϕ as the angle between the x-axis and the center line $O_G W_G$ of the gear tooth. The output angle ψ is the angle between the x-axis and the centerline $O_P W_P$. During this phase of motion, the line connecting the centers of curvature C_G and C_P is of constant length $L = \rho_G + \rho_P$ and passes

through the instantaneous contact points S on the gear and T on the pinion. Because of this constant length one may obtain both the output angle ψ and the "coupler" angle λ from the equivalent four-bar linkage O_G-C_C-C_P-O_P, with ground pivot distance b.

I. UNIT VECTORS AND ANGLES η_G AND η_P

The unit vectors associated with round on round phase are given now.

In direction O_G-C_G:

$$\bar{n}_G = \cos(\phi - \delta_G)\bar{i} + \sin(\phi - \delta_G)\bar{j} \qquad \text{(E-1)}$$

In direction C_G-C_P:

$$\bar{n}_\lambda = \cos\lambda\bar{i} + \sin\lambda\bar{j} \qquad \text{(E-2)}$$

The unit vector normal to $\bar{n}_\lambda$ (in the right hand sense) becomes:

$$\bar{n}_{N\lambda} = -\sin\lambda\bar{i} + \cos\lambda\bar{j} \qquad \text{(E-3)}$$

In direction O_P-C_P:

$$\bar{n}_P = \cos(\psi - \delta_P)\bar{I} + \sin(\psi - \delta_P)\bar{J} \qquad \text{(E-4)}$$

Since $\lambda - (\phi - \delta_G) = \pi - \eta_G$

$$\eta_G = \pi + \phi - \lambda - \delta_G \qquad \text{(E-5)}$$

The angle η_P is obtained from

$$\eta_P = (\psi - \delta_P) - \lambda \qquad \text{(E-6)}$$

II. DETERMINATION OF OUTPUT ANGLE ψ AND "COUPLER" ANGLE λ

The loop equation of the equivalent four-bar linkage is given by:

$$a_G\bar{n}_G + (\rho_G + \rho_P)\bar{n}_\lambda - a_P\bar{n}_P + b\bar{i} = 0 \qquad \text{(E-7)}$$

With appropriate substitutions for the unit vectors, according to Equations (E-1), (E-2), and (E-4), one obtains the following component equation:

$$a_G\cos(\phi - \delta_G) + L\cos\lambda + b - a_P\cos(\psi - \delta_P) = 0 \qquad \text{(E-8)}$$

$$a_G\sin(\phi - \delta_G) + L\sin\lambda - a_P\sin(\psi - \delta_P) = 0 \qquad \text{(E-9)}$$

where

$$L = \rho_G + \rho_P \qquad \text{(E-10)}$$

To eliminate λ, let

$$\sin^2\lambda + \cos^2\lambda = 1 \qquad \text{(E-11)}$$

Substitution of expressions for $\sin\lambda$ and $\cos\lambda$ from Equations (E-9) and (E-8) respectively leads to:

$$A_R \sin\psi + B_R \cos\psi = C_R \qquad \text{(E-12)}$$

where

$$A_R = \sin(\phi - \delta_G) + \cos(\phi - \delta_G)\tan\delta_P + \frac{b}{a_G}\tan\delta_P$$

$$B_R = \cos(\phi - \delta_G) + \frac{b}{a_G} - \sin(\phi - \delta_G)\tan\delta_P$$

$$C_R = \frac{a_P^2 + a_G^2 + b^2 - L^2}{2a_P a_G \cos\delta_P} + \frac{b\cos(\phi - \delta_G)}{a_P \cos\delta_P}$$

Equation(E-12) is solved for ψ by a method similar to the one given on pg. 296 of R. S. Hartenberg and J. Denavit; Kinematic Synthesis of Linkages, McGraw-Hill Book Co., New York, 1964. Thus,

$$\psi = 2\tan^{-1} \frac{A_R \pm \sqrt{A_R^2 + B_R^2 - C_R^2}}{B_R + C_R} \qquad \text{(E-13)}$$

The correct sign in Equation (E-13) must be found from the geometric conditions of the equivalent four-bar linkage.

The "coupler" angle λ may now be determined either from Equation (E-8) or from Equation (E-9), i.e.

$$\lambda = \cos^{-1}\left[\frac{a_P\cos(\psi - \delta_P) - a_G\cos(\phi - \delta_G) - b}{L}\right] \qquad \text{(E-14)}$$

or

$$\lambda = \sin^{-1}\left[\frac{a_P\sin(\psi - \delta_P) - a_G\sin(\phi - \delta_G)}{L}\right] \qquad \text{(E-15)}$$

III. DETERMINATION OF OUTPUT PINION ANGULAR VELOCITY $\dot{\psi}$

Differentiation of Equation (E-12) with respect to time leads to:

$$\dot{\psi} = \dot{\phi}\left[\frac{A_{RD}\sin\psi + B_{RD}\cos\psi - C_{RD}}{A_R\cos\psi - B_R\sin\psi}\right] \qquad \text{(E-16)}$$

where A_R and B_R are given with Equation (E-12), and where

$$A_{RD} = \tan\delta_P\sin(\phi - \delta_G) - \cos(\phi - \delta_G)$$

$$B_{RD} = \sin(\phi - \delta_G) + \tan\delta_P\cos(\phi - \delta_G)$$

$$C_{RD} = \frac{b}{a_P\cos\delta_P}\sin(\phi - \delta_G)$$

IV. RELATIVE VELOCITY AT CONTACT POINT BETWEEN GEAR AND PINION

With point S on the gear and point T on the pinion, as shown by Figure E-1, the relative velocity between gear and pinion at the contact point is given by:

$$\bar{V}_{S/T} = \bar{V}_{S/O_G} - \bar{V}_{T/O_P} \tag{E-17}$$

This relative velocity is tangent to the contacting surfaces and can therefore be expressed in terms of the unit vector $\bar{n}_{N\lambda}$ (see Figure E-1). Then, the above becomes:

$$\bar{V}_{S/T} = \left[(\bar{V}_{S/O_G} \cdot \bar{n}_{N\lambda}) - (\bar{V}_{T/O_P} \cdot \bar{n}_{N\lambda})\right] \bar{n}_{N\lambda} \tag{E-18}$$

or

$$\bar{V}_{S/T} = \left\{\left[\dot{\phi}\bar{k} \times (a_G\bar{n}_G + \rho_G\bar{n}_\lambda)\right] \cdot \bar{n}_{N\lambda} - \left[\dot{\psi}\bar{k} \times (a_P\bar{n}_P - \rho_P\bar{n}_\lambda)\right] \cdot \bar{n}_{N\lambda}\right\} \bar{n}_{N\lambda} \tag{E-19}$$

Appropriate substitution of unit vectors and simplification results in:

$$\bar{V}_{S/T} = \left\{\dot{\phi}\left[a_G\cos(\phi - \delta_G - \lambda) + \rho_G\right] - \dot{\psi}\left[a_P\cos(\psi - \delta_P - \lambda) - \rho_P\right]\right\} \bar{n}_{N\lambda} \tag{E-20}$$

b. ROUND ON FLAT PHASE OF MOTION

Figure E-2 gives the details of the round on flat contact between the driving gear and the driven pinion. The input angle ϕ and the output angle ψ are again defined counter-clockwise between the x-axis and the respective tooth center lines $O_G W_G$ and $O_P W_P$. Since contact is always made on the straight radial flank of the pinion, the line SC_G of the gear is always normal to the flank of the pinion. The contact point is at a distance g from the pinion center O_P, and this distance is always smaller than, or equal to the distance f_P (which is defined by Equation (D-7) in Appendix D). Again, the subscripts G and P are used for gear and pinion tooth parameters respectively.

I. UNIT VECTORS

As before, the unit vector in direction $O_G C_G$ is given by:

$$\bar{n}_G = \cos(\phi - \delta_G)\bar{i} + \sin(\phi - \delta_G)\bar{j} \qquad \text{(E-21)}$$

The unit vector in direction $O_P T$, along the flank of the pinion is given by:

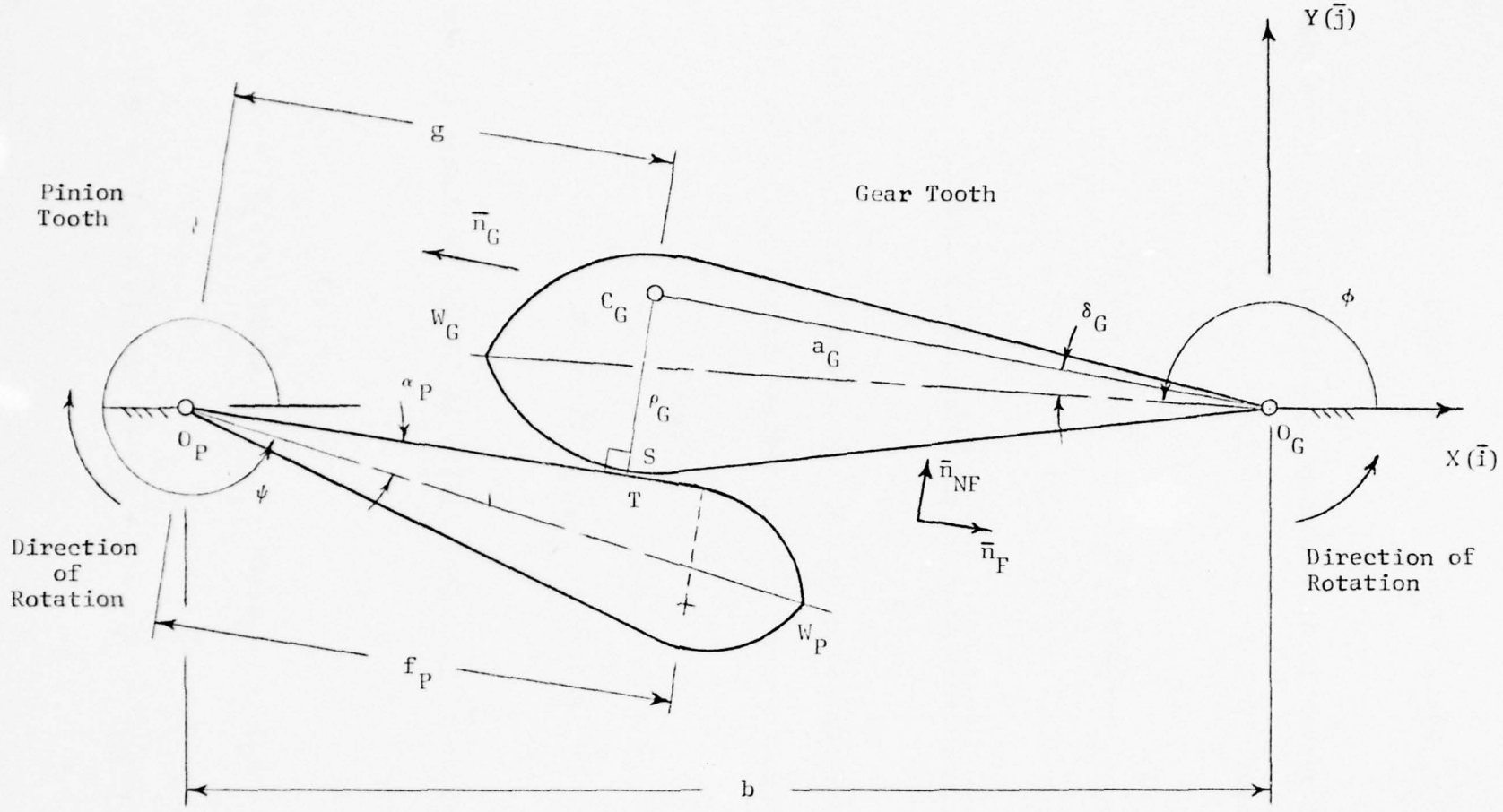

FIGURE E-2

ROUND ON FLAT PHASE OF CONTACT (GEAR DRIVES PINION)

$$\bar{n}_F = \cos(\psi + \alpha_P)\bar{i} + \sin(\psi + \alpha_P)\bar{j} \qquad \text{(E-22)}$$

The unit vector in direction SC_G is normal to $\bar{n}_F$ in the right hand sense:

$$\bar{n}_{NF} = -\sin(\psi + \alpha_P)\bar{i} + \cos(\psi + \alpha_P)\bar{j} \qquad \text{(E-23)}$$

II. DETERMINATION OF OUTPUT ANGLE ψ AND DISTANCE g

The vector equation for the mechanism loop O_G-C_G-S-T-O_P, which forms the basis of the desired solution, has the following form:

$$a_G\bar{n}_G - \rho_G\bar{n}_{NF} - g\bar{n}_F + b\bar{i} = 0 \qquad \text{(E-24)}$$

Substitution of Equations (E-21) to (E-23) furnishes the component equations:

$$a_G\cos(\phi - \delta_G) + \rho_G\sin(\psi + \alpha_P) - g\cos(\psi + \alpha_P) + b = 0 \qquad \text{(E25)}$$

$$a_G\sin(\phi - \delta_G) - \rho_G\cos(\psi + \alpha_P) - g\sin(\psi + \alpha_P) = 0 \qquad \text{(E26)}$$

From Equation (E-26) one obtains for g:

$$g = \frac{a_G \sin(\phi - \delta_G) - \rho_G \cos(\psi + \alpha_P)}{\sin(\psi + \alpha_P)} \qquad \text{(E-27)}$$

This expression for g is now substituted into Equation(E-25). Rearrangement and simplification lead to :

$$A_F \sin\psi + B_F \cos\psi = C_F \qquad \text{(E-28)}$$

where

$$A_F = b\cos\alpha_P + a_G\cos(\phi - \delta_G - \alpha_P)$$

$$B_F = b\sin\alpha_P - a_G\sin(\phi - \delta_G - \alpha_P)$$

$$C_F = -\rho_G$$

The solution of Equation (E-28) for ψ is obtained in the same way as that of Equation (E-13), i.e.

$$\psi = 2\tan^{-1}\frac{A_F \pm \sqrt{A_F^2 + B_F^2 - C_F^2}}{B_F + C_F} \qquad \text{(E-29)}$$

The correct sign in Equation (E-29) depends on the geometric conditions of the mechanism position as in all four-bar linkage solutions of this type.

III. DETERMINATION OF PINION ANGULAR VELOCITY $\dot{\psi}$

Differentiation of Equation (E-28) with respect to time gives:

$$\dot{\psi} = \dot{\phi}\left[\frac{A_{FD}\sin\psi + B_{FD}\cos\psi}{A_F\cos\psi - B_F\sin\psi}\right] \qquad \text{(E-30)}$$

where A_F and B_F are given with Equation (E-28) and where

$$A_{FD} = a_G\sin(\phi - \delta_G - \alpha_P)$$

$$B_{FD} = a_G\cos(\phi - \delta_G - \alpha_P)$$

IV. RELATIVE VELOCITY AT CONTACT POINT BETWEEN GEAR AND PINION

As for round on round contact, the relative velocity between point S on the gear tooth and point T on the pinion tooth is tangent to the contacting surfaces. In this case it will have the direction of unit vector $\bar{n}_F$ (see Figure E-2). Then,

$$\bar{V}_{S/T} = \bar{V}_{S/O_G} - \bar{V}_{T/O_P} = \left[(\bar{V}_{S/O_G} \cdot \bar{n}_F) - (\bar{V}_{T/O_P} \cdot \bar{n}_F) \right] \bar{n}_F \tag{E-31}$$

Since, because of the radial flank of the pinion, the velocity of the contact point T is normal to unit vector $\bar{n}_F$.

$$\bar{V}_{T/O_P} \cdot \bar{n}_F = 0 \tag{E-32}$$

Therefore,

$$\bar{V}_{S/T} = \left[\bar{V}_{S/O_G} \cdot \bar{n}_F \right] \bar{n}_F \tag{E-33}$$

or

$$\bar{V}_{S/T} = \left\{ \left[\dot{\phi} \bar{k} \times (a_G \bar{n}_P - \rho_G \bar{n}_{NF}) \right] \cdot \bar{n}_F \right\} \bar{n}_F \tag{E-34}$$

Appropriate substitution of unit vectors gives:

$$\bar{V}_{S/T} = \dot{\phi} \left[\rho_G + a_G \sin(\psi - \phi + \alpha_P + \delta_G) \right] \bar{n}_F \tag{E-35}$$

V. DETERMINATION OF TRANSITION ANGLES FROM ROUND ON ROUND TO ROUND ON FLAT MOTION

The transition angles ϕ_T and ψ_T, which occur when the round on flat phase follows the round on round one, may be determined with the help of the modified component equations (E-25) and (E-26), i.e. one lets $\phi = \phi_T$, $\psi = \psi_T$ and $g = f_P$. This results in:

$$a_G\cos(\phi_T - \delta_G) + \rho_G\sin(\psi_T + \alpha_P) - f_P\cos(\psi_T + \alpha_P) + b = 0 \tag{E-36}$$

and

$$a_G\sin(\phi_T - \delta_G) - \rho_G\cos(\psi_T + \alpha_P) - f_P\sin(\psi_T + \alpha_P) = 0 \tag{E-37}$$

From the above,

$$\cos(\phi_T - \delta_G) = \frac{1}{a_G}\left[f_P\cos(\psi_T + \alpha_P) - b - \rho_G\sin(\psi_T + \alpha_P)\right] \tag{E-38}$$

and

$$\sin(\phi_T - \delta_G) = \frac{1}{a_G}\left[f_P\sin(\psi_T + \alpha_P) + \rho_G\cos(\psi_T + \alpha_P)\right] \tag{E-39}$$

The angle ψ_T may now be obtained by first eliminating ϕ_T from Equations (E-38) and (E-39). This is accomplished with

$$\sin^2(\phi_T - \delta_G) + \cos^2(\phi_T - \delta_G) = 1 \qquad \text{(E-40)}$$

Substitution into the above leads to the following expression in ψ_T:

$$A_T \sin\psi_T + B_T \cos\psi_T = C_T \qquad \text{(E-41)}$$

where

$$A_T = \rho_G \cos\alpha_P + f_P \sin\alpha_P$$

$$B_T = \rho_G \sin\alpha_P - f_P \cos\alpha_P$$

$$C_T = \frac{a_G^2 - f_P^2 - b^2 - \rho_G^2}{2b}$$

Equation (E-41) is again solved in the manner of Equation (E-13):

$$\psi_T = 2 \tan^{-1} \frac{A_T \pm \sqrt{A_T^2 + B_T^2 - C_T^2}}{B_T + C_T} \qquad \text{(E-42)}$$

The correct sign must again be determined from the geometric conditions.

The associated transition angle ϕ_T can now be obtained either with the help of Equation (E-38) or Equation (E-39):

$$\phi_T = \cos^{-1}\left[\frac{f_P\cos(\psi_T + \alpha_P) - \rho_G\sin(\psi_T + \alpha_P) - b}{a_G}\right] + \delta_G \qquad \text{(E-43)}$$

or

$$\phi_T = \sin^{-1}\left[\frac{f_P\sin(\psi_T + \alpha_P) + \rho_G\cos(\psi_T + \alpha_P)}{a_G}\right] + \delta_G \qquad \text{(E-44)}$$

VI. SENSING GEOMETRY FOR THE DETERMINATION OF CONTACT OF SUBSEQUENT TOOTH MESH

The following derives a computer sensing equation which indicates when contact is transferred from one tooth mesh to the succeeding one. Figure E-3 illustrates the case. The active mesh is in the round on flat mode and the subsequent mesh will make its initial contact in the round on round mode. This

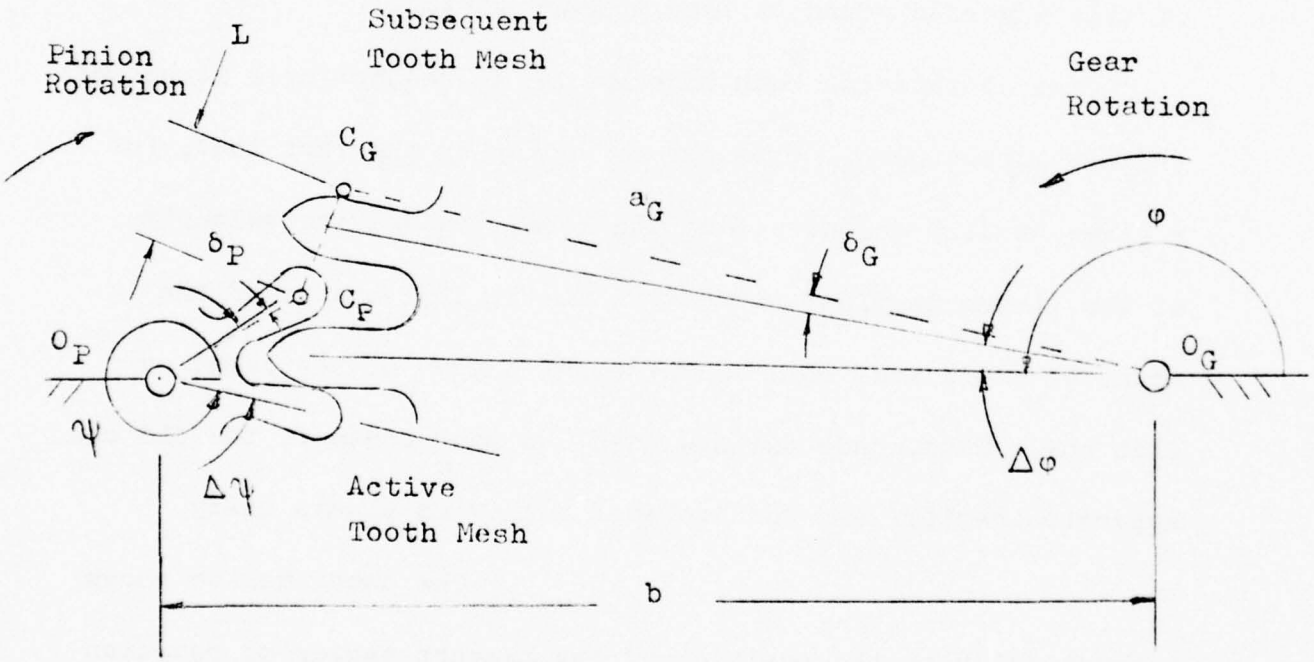

Figure E3
Sensing Geometry for Contact of Subsequent Tooth Mesh

assertion is based on experience with the three gear and pinion combinations of the M125A1 booster. In each of these instances, the subsequent mesh makes contact before the round of the gear has left the flat of the pinion in the active mesh, i.e. $g < f_p$. (See work in section V.) It has also been found that initial contact of the subsequent mesh is always in the round on round mode. Generally, contact between the flat of the gear and the round of the pinion does not occur, and it has not been considered in this report. Section VII gives a criterion for the existence of this inverted round on flat mode of contact.

Once contact has been made by the subsequent mesh it becomes the new active mesh. This can be proven by the fact that, for a given angular velocity $\dot{\phi}$ of the gear, the angular velocity of the pinion is always larger in the initial stages of the round on round mode than in the final stages of the round on flat one. Thus, once the new mesh has made contact, the old one separates rapidly and the "contact ratio" is always unity.

The above may be shown theoretically by the position of the instant center of rotation between the gear and the pinion on line $O_G O_p$.

If $\Delta\phi$ and $\Delta\psi$ represent the angles between the individual tooth center lines of the gear and pinion respectively (see Figure E-3), the

closure equation for the subequent mesh may be written in terms of the active mesh as follows:

$$a_P\left[\cos(\psi - \delta_P + \Delta\psi)\bar{i} + \sin(\psi - \delta_P + \Delta\psi)\bar{j}\right] + L_x\bar{i} + L_y\bar{j}$$

$$= b\bar{i} + a_G\left[\cos(\phi - \delta_G - \Delta\phi)\bar{i} + \sin(\phi - \delta_G - \Delta\phi)\bar{j}\right] \qquad \text{(E-45)}$$

where L_x, L_y = components of the distance $L = C_P C_G$

ψ = pinion angle determined from round on flat mode according to Equation (E-29)

The components L_x and L_y may be obtained from Equation (E-45):

$$L_x = b + a_G\cos(\phi - \delta_G - \Delta\phi) - a_P\cos(\psi - \delta_P + \Delta\psi) \qquad \text{(E-46)}$$

and

$$L_y = a_G\sin(\phi - \delta_G - \Delta\phi) - a_P\sin(\psi - \delta_P + \Delta\psi) \qquad \text{(E-47)}$$

Contact will have occurred when the distance L becomes equal to or slightly smaller than the sum of the two radii of curvature ρ_G and ρ_P. Thus, the criterion of contact becomes:

$$\sqrt{L_x^2 + L_y^2} \leq \rho_G + \rho_P \qquad \text{(E-48)}$$

VII. POSSIBILITY OF FLAT OF GEAR MAKING CONTACT WITH THE ROUND PORTION OF THE PINION

Figure E-4 shows a transition configuration in which the flat part of the gear tooth makes contact with the circular arc of the pinion, i.e. $\overline{O_G S} = f_G$. The radius of curvature ρ_P of of the pinion will only then be normal to the flat of the gear

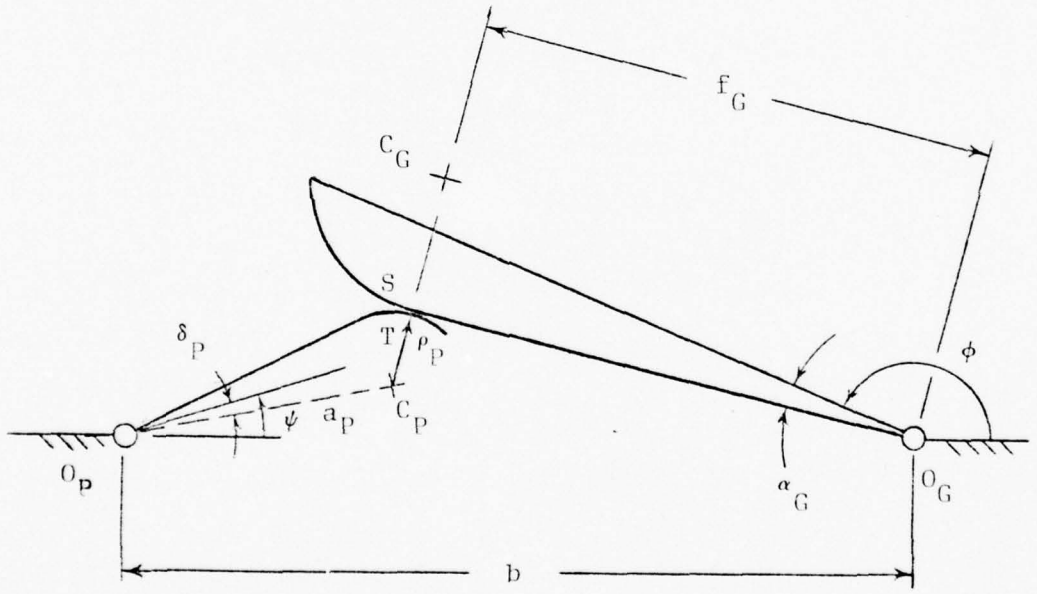

FIGURE E-4

FLAT OF GEAR CONTACTS ROUND OF PINION

when $\overline{O_G S} \leq f_G$. Accordingly, in order to avoid this type of contact, the following criterion must be met:

$$b > \left[a_P + \sqrt{f_G^2 + \rho_P^2} \right] \qquad \text{(E-49)}$$

The three gear meshes of the M125A1 booster always satisfy equation (E-49), and therefore the initial contact is made in the round on round mode.

2. MOMENT INPUT-OUTPUT RELATIONSHIP FOR SINGLE STEP-UP GEAR MESH WITH OGIVAL TEETH

The present section concerns itself with the determination of the equilibrant moment M_o, acting on the output pinion of a single ogival mesh, when the input moment M_{in}, which acts on the gear, is given. This relationship must be derived both for the round on round and for the round on flat phases of the motion. The directions of the pivot friction forces are again chosen such that the resulting moments oppose the motion of the respective component. (See Appendix A.) The magnitude of these friction moments is expressed in the manner of equation (A-2) of the aforementioned appendix. The direction of the friction force of the gear on the pinion is the same as the direction of the relative velocity $\bar{V}_{S/T}$, of the gear contact point S with respect to the pinion contact point T. This will be expressed by the appropriate signum convention. It must also be remembered that the kinematic expressions must conform to the motion phase under consideration.

a. INPUT-OUTPUT RELATIONSHIP FOR THE ROUND ON ROUND PHASE OF MOTION

Figure E-5 shows the free body diagrams for the round on round phase of motion with the gear considered to be component no. 1 and the pinion defined as component no. 2. The contact forces F_{12} and F_{21} are expressed with the help of the unit vector $\bar{n}_{\lambda}$ [see equation (E-2)] . This unit vector is always normal to both contacting surfaces at points S and T. The unit vector $\bar{n}_{N\lambda}$ is used to describe the direction of the friction forces at the contact point. The sense of these friction forces is determined with the help of

$$s = \frac{V_{S/T}}{\left|V_{S/T}\right|} \tag{E-50}$$

(See equation (E-20) for $\bar{V}_{S/T}$.) Since the friction force F_{f12} of the gear on the pinion has the same direction as the relative velocity $V_{S/T}$, one may write

$$\bar{F}_{f12} = \mu s F_{12} \bar{n}_{N\lambda} \tag{E-51}$$

where μ represents the coefficient of friction at the contact point.

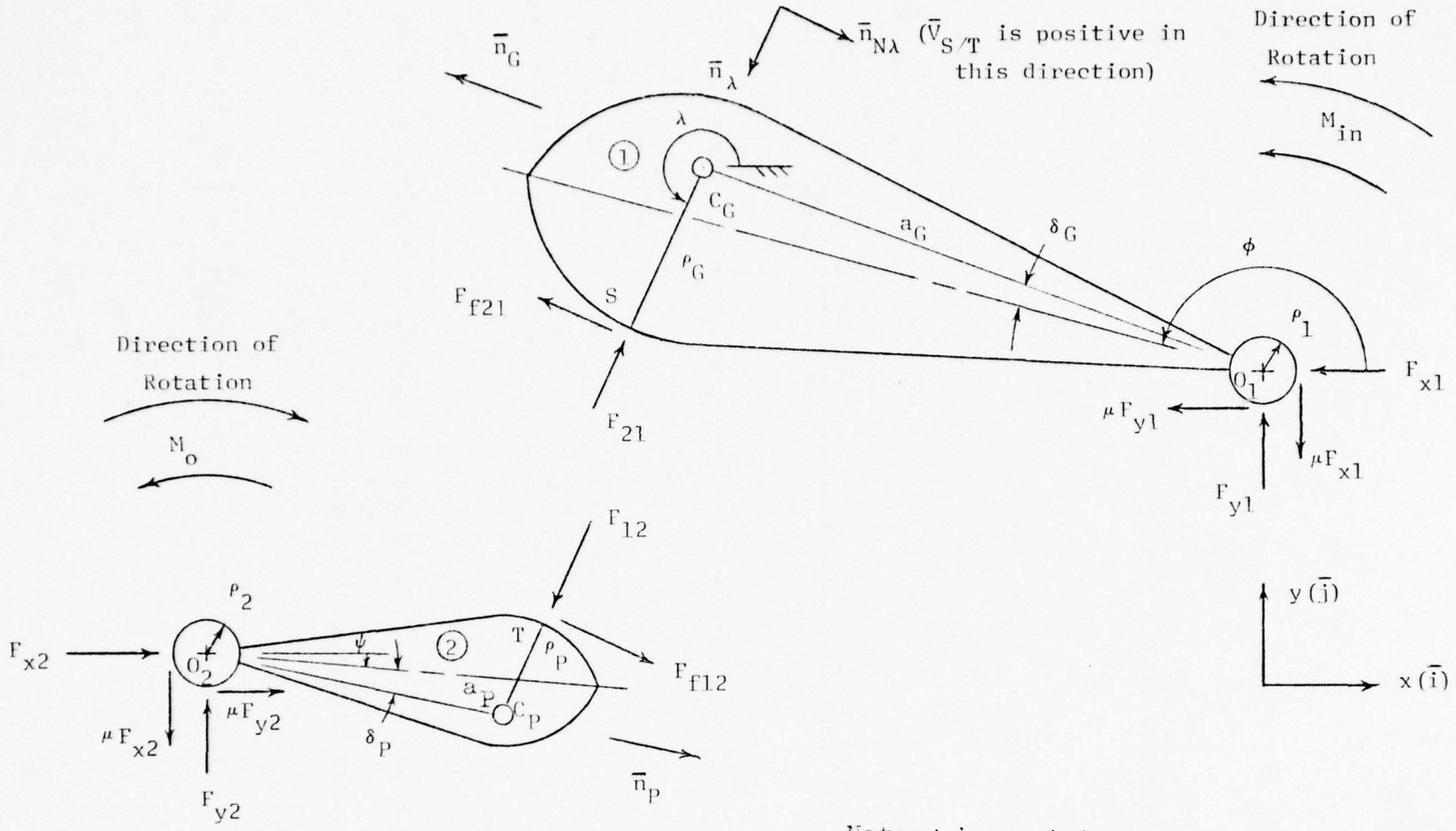

Note: ψ is positive in ccw direction

FIGURE E-5

FREE BODY DIAGRAM FOR ROUND ON ROUND PHASE

Since

$$\bar{F}_{21} = - F_{12}\bar{n}_{\lambda} \tag{E-52}$$

the friction force of the pinion on the gear becomes:

$$\bar{F}_{f21} = - \mu s F_{12}\bar{n}_{N\lambda} \tag{E-53}$$

I. FORCE AND MOMENT EQUILIBRIUM OF THE GEAR

The force equilibrium of the gear is assured when

$$-F_{12}\bar{n}_{\lambda} - \mu s F_{12}\bar{n}_{N\lambda} - F_{x1}\bar{i} + F_{y1}\bar{j} - \mu F_{y1}\bar{i} - \mu F_{x1}\bar{j} = 0 \tag{E-54}$$

In the above μ also stands for the pivot coefficient of friction.

Moment equilibrium is given by:

$$M_{in}\bar{k} - \mu\rho_1\sqrt{F_{x1}^2 + F_{y1}^2}\,\bar{k} + \left[a_G\bar{n}_G + \rho_G\bar{n}_{\lambda}\right] \times \left[-F_{12}\bar{n}_{\lambda} - \mu s F_{12}\bar{n}_{N\lambda}\right] = 0 \tag{E-55}$$

The unit vector $\bar{n}_G$ is defined by equation (E-1).

The following component equations may be obtained from equation (E-54):

$$-F_{12}\cos\lambda + \mu s F_{12}\sin\lambda - F_{x1} - \mu F_{y1} = 0 \qquad \text{(E-56)}$$

and

$$-F_{12}\sin\lambda - \mu s F_{12}\cos\lambda + F_{y1} - \mu F_{x1} = 0 \qquad \text{(E-57)}$$

After substitution and cross-multiplication, one obtains the moment expression, equation (E-55), in scalar form:

$$M_{in} - \mu\rho_1\sqrt{F_{x1}^2 + F_{y1}^2} + F_{12}\left[-\mu s\rho_G + a_G\sin(\phi - \delta_G - \lambda) - \mu s a_G\cos(\phi - \delta_G - \lambda)\right] = 0 \qquad \text{(E-58)}$$

Simultaneous solution of equations (E-56) and (E-57) for F_{x1} and F_{y1} results in:

$$F_{x1} = -F_{12}\left[\frac{(1 + \mu^2 s)\cos\lambda + \mu(1 - s)\sin\lambda}{1 + \mu^2}\right] \qquad \text{(E-59)}$$

and

$$F_{y1} = F_{12}\left[\frac{(1 + \mu^2 s)\sin\lambda - \mu(1 - s)\cos\lambda}{1 + \mu^2}\right] \qquad \text{(E-60)}$$

These results are now substituted in equation (E-53). Since s^2 is unity and always positive, the resulting expression for F_{12} has the following form:

$$F_{12} = \frac{M_{in}}{\mu(\rho_1 + s\rho_G) + a_G[\mu s\cos(\phi - \delta_G - \lambda) - \sin(\phi - \delta_G - \lambda)]} \qquad \text{(E-61)}$$

II. FORCE AND MOMENT EQUILIBRIUM OF THE PINION

Force equilibrium of the pinion is assured by:

$$F_{12}\bar{n}_\lambda + \mu s F_{12}\bar{n}_{N\lambda} + F_{x2}\bar{i} + F_{y2}\bar{j} + \mu F_{y2}\bar{i} - \mu F_{x2}\bar{j} = 0 \qquad \text{(E-62)}$$

Moment equilibrium must satisfy:

$$M_o\bar{k} + \mu\rho_2\sqrt{F_{x2}^2 + F_{y2}^2}\,\bar{k} + \left[a_p\bar{n}_p - \rho_p\bar{n}_\lambda\right] \times \left[F_{12}\bar{n}_\lambda + \mu s F_{12}\bar{n}_{N\lambda}\right] = 0 \qquad \text{(E-63)}$$

The unit vector $\bar{n}_p$ is defined by equation (E-4).

Equation (E-62) gives rise to the following component equations:

$$F_{12}\cos\lambda - \mu s F_{12}\sin\lambda + F_{x2} + \mu F_{y2} = 0 \qquad \text{(E-64)}$$

and

$$F_{12}\sin\lambda + \mu s F_{12}\cos\lambda + F_{y2} - \mu F_{x2} = 0 \qquad \text{(E-65)}$$

The moment equation (E-63) becomes, in scalar form:

$$M_o + \mu\rho_2\sqrt{F_{x2}^2 + F_{y2}^2} + F_{12}\left[-\mu s\rho_p - a_p\sin(\psi - \delta_p - \lambda) + \mu s a_p\cos(\psi - \delta_p - \lambda)\right] = 0 \qquad \text{(E-66)}$$

Simultaneous solution of equations (E-64) and (E-65) for F_{x2} and F_{y2} results in:

$$F_{x2} = F_{12}\left[\frac{\mu(1 + s)\sin\lambda - (1 - \mu^2 s)\cos\lambda}{1 + \mu^2}\right] \qquad \text{(E-67)}$$

and

$$F_{y2} = -F_{12}\left[\frac{\mu(1 + s)\cos\lambda + (1 + \mu^2 s)\sin\lambda}{1 + \mu^2}\right] \qquad \text{(E-68)}$$

The above expressions are now substituted into equation (E-66). Again, s^2 is unity and always positive, and the following expression may be obtained for the contact force F_{12} in terms of the equilibrant moment M_o:

$$F_{12} = \frac{M_o}{\mu(s\rho_P - \rho_2) - a_P\left[\mu s\cos(\psi - \delta_P - \lambda) - \sin(\psi - \delta_P - \lambda)\right]} \tag{E-69}$$

III. MOMENT INPUT-OUTPUT RELATIONSHIP

When equations (E-61) and (E-69) are set equal to each other, one obtains the following input-output relationship:

$$M_o = M_{in}\left[\frac{\mu(s\rho_P - \rho_2) - a_P\left[\mu s\cos(\psi - \delta_P - \lambda) - \sin(\psi - \delta_P - \lambda)\right]}{\mu(\rho_1 + s\rho_G) + a_G\left[\mu s\cos(\phi - \delta_G - \lambda) - \sin(\phi - \delta_G - \lambda)\right]}\right] \tag{E-70}$$

b. INPUT-OUTPUT RELATIONSHIP FOR ROUND ON FLAT PHASE OF MOTION

Figure E-6 gives the free body diagrams for the round on flat phase of the motion. Again, the gear is considered to be component no. 1, while the pinion is component no. 2. Using the unit vector $\bar{n}_{NF}$, of equation (E-22), which is normal to the flat side of the pinion to express the force $\bar{F}_{12}$ of the gear on the pinion, one obtains:

$$\bar{F}_{12} = - F_{12}\bar{n}_{NF} \tag{E-71}$$

The friction force of the gear on the pinion again has the same direction as the now applicable relative velocity $\bar{V}_{S/T}$ of equation (E-35). With

$$s = \frac{V_{S/T}}{\left|V_{S/T}\right|} \tag{E-72}$$

as the applicable signum convention, the friction force $\bar{F}_{f12}$ becomes:

$$\bar{F}_{f12} = \mu s F_{12}\bar{n}_{F} \tag{E-73}$$

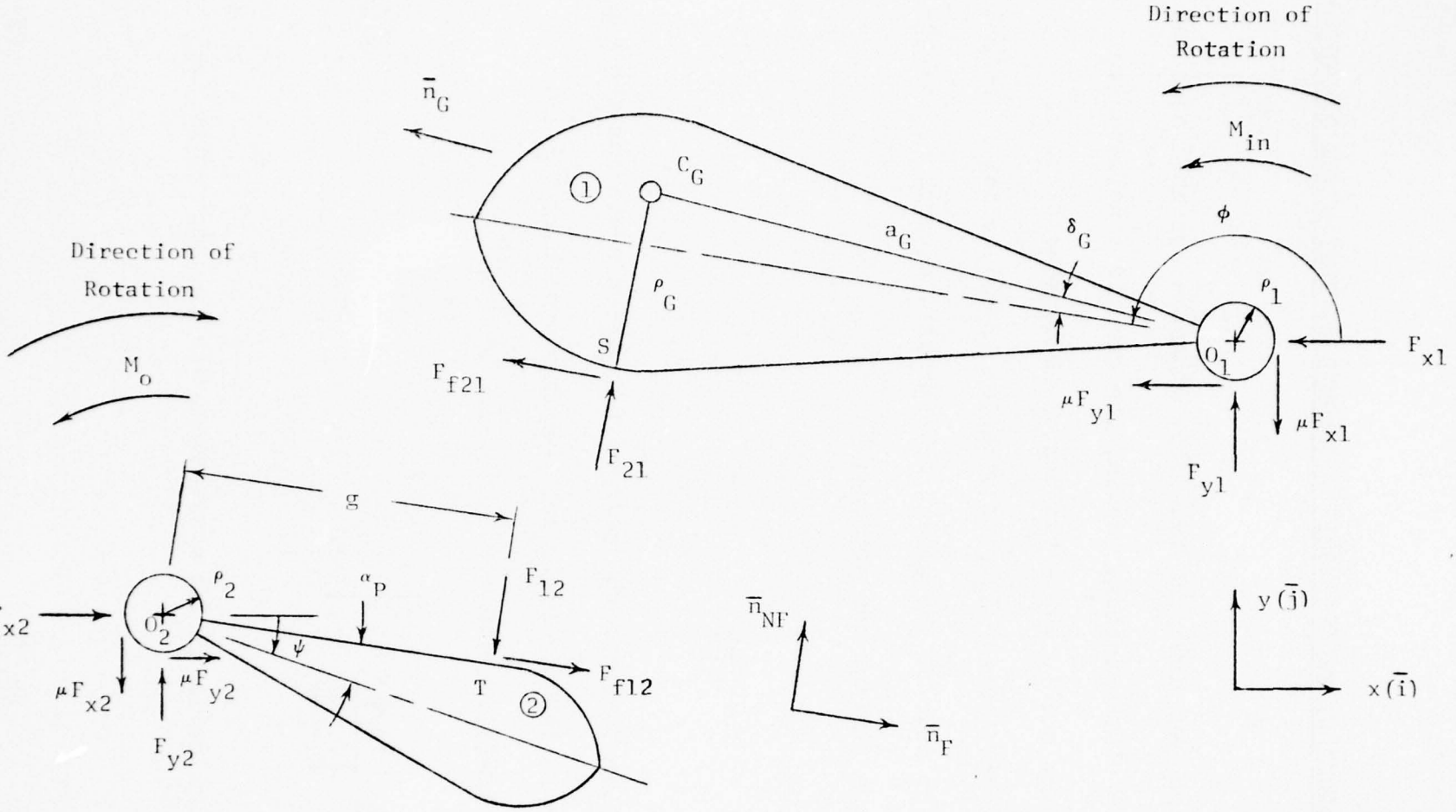

Note: ψ is positive in ccw direction

FIGURE E-6

FREE BODY DIAGRAM FOR ROUND ON FLAT PHASE

The contact force $\bar{F}_{21}$ of the pinion on the gear and the associated friction force are equal and opposite to the forces given by equations (E-71) and (E-73) respectively. Thus,

$$\bar{F}_{21} = F_{12}\bar{n}_{NF} \tag{E-74}$$

and

$$\bar{F}_{f21} = -\mu s F_{12}\bar{n}_{F} \tag{E-75}$$

Note that the kinematics of the round on flat phase must now be used.

I. FORCE AND MOMENT EQUILIBRIUM OF THE GEAR

Force equilibrium of the gear is given by:

$$F_{12}\bar{n}_{NF} - \mu s F_{12}\bar{n}_{F} - F_{x1}\bar{I} + F_{y1}\bar{j} - \mu F_{y1}\bar{i} - \mu F_{x1}\bar{j} = 0 \tag{E-76}$$

Moment equilibrium requires:

$$M_{in}\bar{k} - \mu\rho_1\sqrt{F_{x1}^2 + F_{y1}^2}\,\bar{k} + \left[a_G\bar{n}_G - \rho_G\bar{n}_{NF}\right] \times \left[F_{12}\bar{n}_{NF} - \mu s F_{12}\bar{n}_{F}\right] = 0 \tag{E-77}$$

Equation (E-76) furnishes the following component expressions:

$$-F_{12}\sin(\psi + \alpha_p) - \mu s F_{12}\cos(\psi + \alpha_p) - F_{x1} - \mu F_{y1} = 0 \tag{E-78}$$

and

$$F_{12}\cos(\psi + \alpha_p) - \mu s F_{12}\sin(\psi + \alpha_p) + F_{y1} - \mu F_{x1} = 0 \tag{E-79}$$

The scalar form of equation (E-77) is given by:

$$M_{in} - \mu\rho_1\sqrt{F_{x1}^2 + F_{y1}^2} + F_{12}\left[-\mu s\rho_G + a_G\cos(\phi - \delta_G - \psi - \alpha_p) + \mu s a_G\sin(\phi - \delta_G - \psi - \alpha_p)\right] = 0 \tag{E-80}$$

Simultaneous solution of equations (E-78) and (E-79) for F_{x1} and F_{y1} furnishes:

$$F_{x1} = F_{12}\left[\frac{\mu(1 - s)\cos(\psi + \alpha_p) - (1 + \mu^2 s)\sin(\psi + \alpha_p)}{1 + \mu^2}\right] \tag{E-81}$$

and

$$F_{y1} = -F_{12}\left[\frac{\mu(1 - s)\sin(\psi + \alpha_p) + (1 + \mu^2 s)\cos(\psi + \alpha_p)}{1 + \mu^2}\right] \tag{E-82}$$

The above results are now substituted into equation (E-80). Since s^2 is again unity and positive at all times, the resulting expression for F_{12} becomes in terms of M_{in}:

$$F_{12} = \frac{M_{in}}{\mu(\rho_1 + s\rho_G) - a_G\left[\cos(\phi - \delta_G - \psi - \alpha_p) + \mu s \sin(\phi - \delta_G - \psi - \alpha_p)\right]} \qquad \text{(E-83)}$$

II . FORCE AND MOMENT EQUILIBRIUM OF THE PINION

Force equilibrium of the pinion is expressed by:

$$-F_{12}\bar{n}_{NF} + \mu s F_{12}\bar{n}_F + F_{x2}\bar{i} + F_{y2}\bar{j} + \mu F_{y2}\bar{i} - \mu F_{x2}\bar{j} = 0 \qquad \text{(E-84)}$$

Moment equilibrium requires that

$$M_o\bar{k} + \mu\rho_2\sqrt{F_{x2}^2 + F_{y2}^2}\,\bar{k} + g\bar{n}_F \times (-F_{12}\bar{n}_{NF}) = 0 \qquad \text{(E-85)}$$

Equation (E-84) furnishes the following component equations:

$$F_{12}\sin(\psi + \alpha_p) + \mu s F_{12}\cos(\psi + \alpha_p) + F_{x2} + \mu F_{y2} = 0$$

and (E-86)

$$-F_{12}\cos(\psi + \alpha_p) + \mu s F_{12}\sin(\psi + \alpha_p) + F_{y2} - \mu F_{x2} = 0$$

(E-87)

The scalar form of the moment equation (E-85) becomes:

$$M_o + \mu \rho_2 \sqrt{F_{x2}^2 + F_{y2}^2} - sF_{12} = 0 \qquad \text{(E-88)}$$

Simultaneous solution of equations (E-86) and (E-87) for F_{x2} and F_{y2} leads to:

$$F_{x2} = -F_{12}\left[\frac{(1 - \mu^2 s)\sin(\psi + \alpha_p) + \mu(1 + s)\cos(\psi + \alpha_p)}{1 + \mu^2}\right]$$

(E-89)

and

$$F_{y2} = F_{12}\left[\frac{(1 - \mu^2 s)\cos(\psi + \alpha_p) - \mu(1 + s)\sin(\psi + \alpha_p)}{1 + \mu^2}\right]$$

(E-90)

The above expressions are now substituted into equation (E-88). Again, s^2 is unity and positive. The following expression for F_{12} is now obtained:

$$F_{12} = \frac{M_o}{\mathcal{E} - \mu\rho_2} \qquad \text{(E-91)}$$

III. MOMENT INPUT-OUTPUT RELATIONSHIP

When equations (E-83) and (E-91) are set equal to each other, one obtains the following input-output relationship:

$$M_o = M_{in}\left[\frac{\mathcal{E} - \mu\rho_2}{\mu(\rho_1 + s\rho_G) - a_G\left[\cos(\phi - \delta_G - \psi - \alpha_P) + \mu s\sin(\phi - \delta_G - \psi - \alpha_P)\right]}\right] \qquad \text{(E-92)}$$

APPENDIX G

KINEMATICS OF TWO AND THREE STEP-UP GEAR TRAINS WITH OGIVAL TEETH

Figure G-1 shows the basic configuration of a three step-up gear train used in certain fuze applications. The general layout is identical to that shown in Figure A-5 of Appendix A. Now, ogival type gear teeth are used instead of involute type ones. Again, it is required to find the equilibrant moment M_{o4}, acting on pinion no. 4 which holds the input moment M_{in}, acting on gear no. 1, in equilibrium when both pivot and contact friction are taken into account, and when the fuze body spins. Appendix H gives the force and moment analyses for the determination of this moment input-output relationship. The same appendix also shows the derivation of such an input-output relationship for a two step-up gear train with ogival gear teeth which must operate in a spin environment. (Figure A-10 of Appendix A shows this type of configuration with involute teeth.) The present appendix lays the groundwork for the moment relationships of Appendix H by providing the kinematics of the three ogival gear meshes involved.

In each case both round on round and round on flat phases

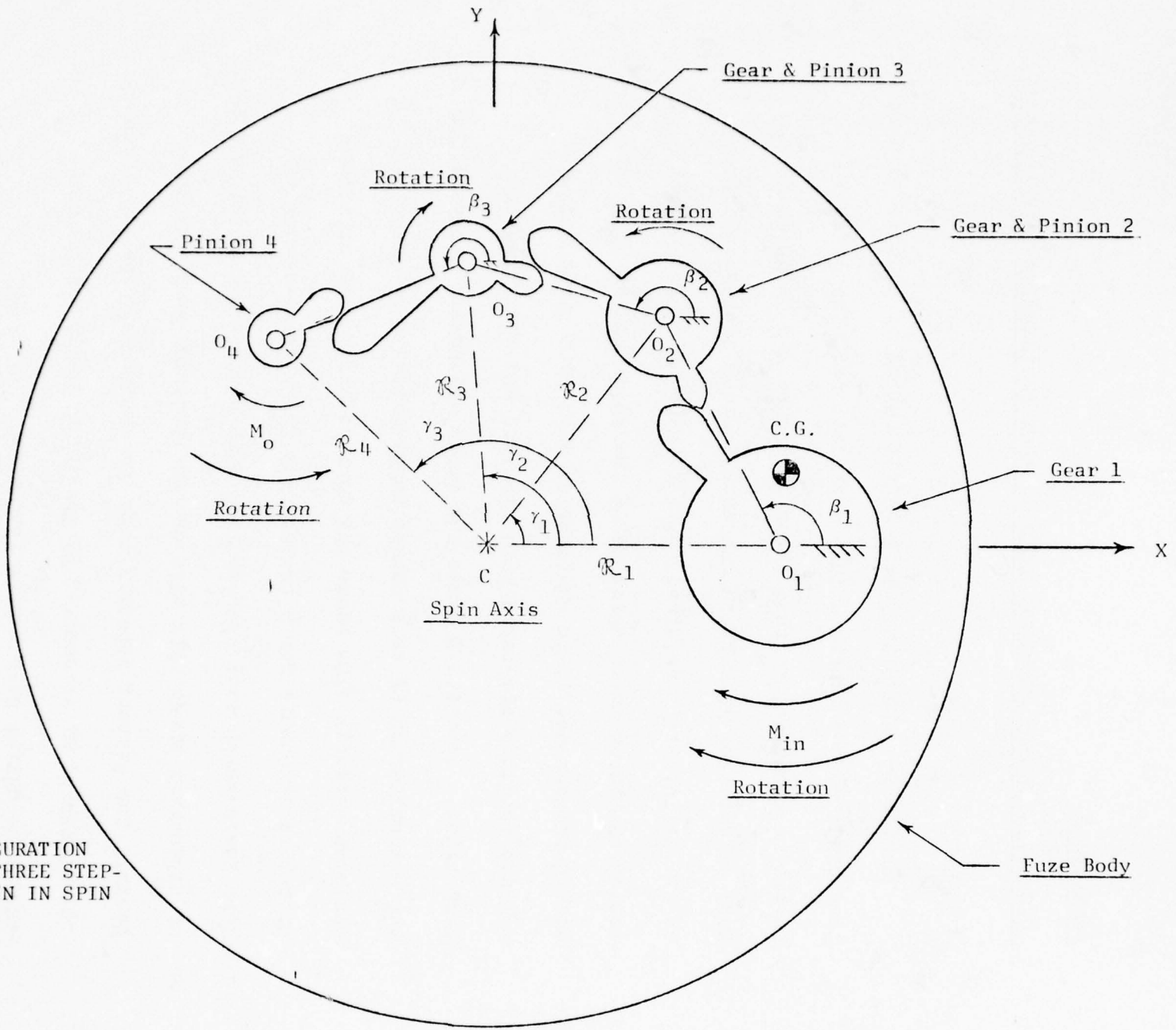

FIGURE G-1

BASIC CONFIGURATION FOR OGIVAL THREE STEP-UP GEAR TRAIN IN SPIN ENVIRONMENT

of motion have to be considered. All derivations follow the pattern set in Section 1 of Appendix E. The derivations must take into account that the driving gears of meshes no. 1 and no. 3, i.e. between gear no. 1 and pinion no. 2 and between gear no. 3 and pinion no. 4, respectively, have clockwise rotations. The driving gear of mesh no. 2, i.e. between gear no. 2 and pinion no. 3, has counterclockwise rotation.

Finally, the inclinations of the various pivot to pivot centerlines with respect to the body-fixed X-axes, as represented by the angles β_1, β_2 and β_3, must be considered.

For the sake of simplicity, the notation will in most cases not differentiate between round on round and round on flat phases of motion. For example, the output angle ψ_i and its derivatives will have the same symbol for both phases.

For definitions of angles β_i and γ_i as well as the distances ℓ_i, see Appendix A-6.

1. KINEMATICS OF MESH NO. 1 (GEAR NO. 1 AND PINION NO. 2)

a. ROUND ON ROUND PHASE OF MOTION

Figure G-2 shows the round on round phase of the motion of mesh no. 1 in a schematic manner. Only the contacting faces of the gear and the pinion are indicated.

I. UNIT VECTORS

The unit vector in the direction O_1C_{G1} of the gear is given by:

$$\bar{n}_{G1} = \cos(\phi_1 + \delta_{G1})\bar{i} + \sin(\phi_1 + \delta_{G1})\bar{j} \qquad (G\text{-}1)$$

The unit vector in the direction $C_{G1}C_{P1}$ is given by:

$$\bar{n}_{\lambda 1} = \cos\lambda_1\bar{i} + \sin\lambda_1\bar{j} \qquad (G\text{-}2)$$

The unit vector normal to $\bar{n}_{\lambda 1}$ (in the right hand sense) becomes:

$$\bar{n}_{N\lambda 1} = -\sin\lambda_1\bar{i} + \cos\lambda_1\bar{j} \qquad (G\text{-}3)$$

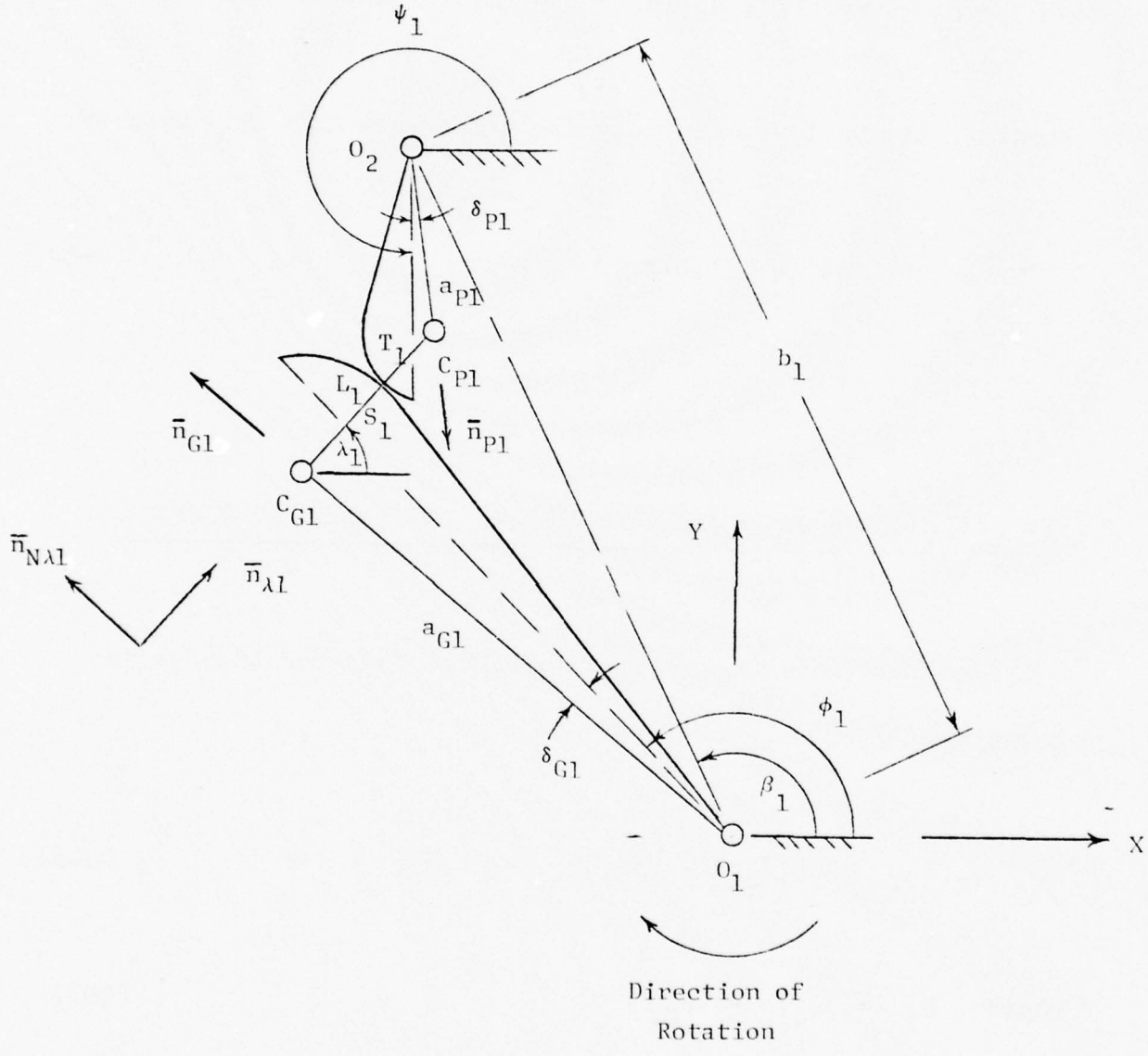

FIGURE G-2

ROUND ON ROUND PHASE FOR MESH NO. 1

The unit vector in the direction O_2C_{P1} is given by:

$$\bar{n}_{P1} = \cos(\psi_1 + \delta_{P1})\bar{i} + \sin(\psi_1 + \delta_{P1})\bar{j} \qquad (G\text{-}4)$$

Finally, the unit vector along the centerline O_1O_2 is given by:

$$\bar{n}_{\beta 1} = \cos\beta_1\bar{i} + \sin\beta_1\bar{j} \qquad (G\text{-}5)$$

II. DETERMINATION OF OUTPUT ANGLE ψ_1 AND "COUPLER" ANGLE λ_1

The loop equation of the equivalent four-bar linkage is given by:

$$a_{G1}\bar{n}_{G1} + L_1\bar{n}_{\lambda 1} - a_{P1}\bar{n}_{P1} - b_1\bar{n}_{\beta 1} = 0 \qquad (G\text{-}6)$$

where $L_1 = \rho_{G1} + \rho_{P1}$ (G-7)

With the appropriate substitution for the unit vectors, one obtains the following component equations:

$$a_{G1}\cos(\phi_1 + \delta_{G1}) + L_1\cos\lambda_1 - b_1\cos\beta_1 - a_{P1}\cos(\psi_1 + \delta_{P1}) = 0 \qquad (G\text{-}8)$$

and

$$a_{G1}\sin(\phi_1 + \delta_{G1}) + L_1\sin\lambda_1 - b_1\sin\beta_1 - a_{P1}\sin(\psi_1 + \delta_{P1}) = 0 \qquad (G\text{-}9)$$

To eliminate λ_1, let

$$\sin^2\lambda_1 + \cos^2\lambda_1 = 1 \qquad (G\text{-}10)$$

The above trigonometric functions are obtained from equations (G-8) and (G-9) respectively. Substitution into equation (G-10) furnishes:

$$A_{1R}\sin\psi_1 + B_{1R}\cos\psi_1 = C_{1R} \qquad (G\text{-}11)$$

where

$$A_{1R} = a_{G1}\sin(\phi_1 + \delta_{G1} - \delta_{P1}) - b_1\sin(\beta_1 - \delta_{P1})$$

$$B_{1R} = a_{G1}\cos(\phi_1 + \delta_{G1} - \delta_{P1}) - b_1\cos(\beta_1 - \delta_{P1})$$

$$C_{1R} = \frac{a_{P1}^2 + a_{G1}^2 + b_1^2 - L_1^2 - 2a_{G1}b_1\cos(\phi_1 + \delta_{G1} - \beta_1)}{2a_{P1}}$$

Equation (G-11) is now solved for ψ_1 in the manner described in Appendix E in connection with equation (E-12), i.e.:

$$\psi_1 = 2 \tan^{-1} \frac{A_{1R} \pm \sqrt{A_{1R}^2 + B_{1R}^2 - C_{1R}^2}}{B_{1R} + C_{1R}} \qquad \text{(G-12)}$$

The correct sign on equation (G-12) must be found from geometric considerations.

The coupler angle λ_1 may now be determined either from equation (G-8) or from equation (G-9). Thus,

$$\lambda_1 = \cos^{-1} \left[\frac{b_1 \cos\beta_1 + a_{P1} \cos(\psi_1 + \delta_{P1}) - a_{G1} \cos(\phi_1 + \delta_{G1})}{L_1} \right] \qquad \text{(G-13)}$$

or

$$\lambda_1 = \sin^{-1} \left[\frac{b_1 \sin\beta_1 + a_{P1} \sin(\psi_1 + \delta_{P1}) - a_{G1} \sin(\phi_1 + \delta_{G1})}{L_1} \right] \qquad \text{(G-14)}$$

III. DETERMINATION OF ANGULAR VELOCITY $\dot{\psi}_1$ OF PINION NO. 2

Differentiation of equation (G-11) with respect to time gives:

$$\dot{\psi}_1 = \dot{\phi}_1 \left[\frac{B_{1RD}\cos\psi_1 - A_{1RD}\sin\psi_1 + C_{1RD}}{A_{1R}\cos\psi_1 - B_{1R}\sin\psi_1} \right] \qquad (G\text{-}15)$$

where

$$A_{1RD} = a_{G1}\cos(\phi_1 + \delta_{G1} - \delta_{P1})$$

$$B_{1RD} = a_{G1}\sin(\phi_1 + \delta_{G1} - \delta_{P1})$$

$$C_{1RD} = \frac{a_{G1}b_1\sin(\phi_1 + \delta_{G1} - \beta_1)}{a_{P1}}$$

IV. RELATIVE VELOCITY AT THE CONTACT POINT

The relative velocity $\bar{V}_{S1/T1_R}$ of the contact point S_1 on gear no. 1 with respect to point T_1 on pinion no. 2, represents the vectorial difference between the absolute velocities of these points. Thus,

$$\bar{V}_{S1/T1_R} = \bar{V}_{S1/C} - \bar{V}_{T1/C} \tag{G-16}$$

where C represents the spin center of the fuze body. If $\bar{\omega}$ stands for the angular velocity of the fuze body, then appropriate substitution into equation (G-16) gives: (See also Figures G-1 and G-2)

$$\bar{V}_{S1/T1_R} = \left[\bar{\omega} \times \bar{\mathcal{R}}_1 + (\bar{\omega} + \dot{\bar{\phi}}_1) \times (\bar{a}_{G1} + \bar{\rho}_{G1})\right] - \left[\bar{\omega} \times \bar{\mathcal{R}}_2 + (\bar{\omega} + \dot{\psi}_1) \times (\bar{a}_{P1} + \bar{\rho}_{P1})\right] \tag{G-17}$$

Since

$$\bar{\omega} \times \left[\bar{\mathcal{R}}_1 + \bar{a}_{G1} + \bar{\rho}_{G1}\right] = \bar{\omega} \times \left[\bar{\mathcal{R}}_2 + \bar{a}_{P1} + \bar{\rho}_{P1}\right] \tag{G-18}$$

because the position vectors in brackets are equal, equation (G-17) may be written

$$\bar{V}_{S1/T1_R} = \bar{V}_{S1/O_1} - \bar{V}_{T1/O_2}$$

$$= \dot{\bar{\phi}}_1 \times (\bar{a}_{G1} + \bar{\rho}_{G1}) - \dot{\bar{\psi}}_1 \times (\bar{a}_{P1} + \bar{\rho}_{P1}) \qquad \text{(G-19)}$$

Note that $\bar{V}_{S1/T1_R}$ becomes the vectorial difference of the contact point velocities with respect to the fuze body.

Since this relative velocity is tangent to the contacting surfaces, it may be written as the vectorial difference of the velocity components along these surfaces. Accordingly, equation (G-19) becomes with the help of the unit vector $\bar{n}_{N\lambda 1}$:

$$\bar{V}_{S1/T1_R} = \left\{ \left[\dot{\phi}_1 \bar{k} \times (a_{G1}\bar{n}_{G1} + \rho_{G1}\bar{n}_{\lambda 1}) \right] \cdot \bar{n}_{N\lambda 1} - \left[\dot{\psi}_1 \bar{k} \times (a_{P1}\bar{n}_{P1} - \rho_{P1}\bar{n}_{\lambda 1}) \right] \cdot \bar{n}_{N\lambda 1} \right\} \bar{n}_{N\lambda 1}$$

(G-20)

Appropriate substitution of unit vectors given earlier in Section I and simplification results in:

$$\bar{V}_{S1/T1_R} = \left\{ \dot{\phi}_1 \left[a_{G1} \cos(\phi_1 + \delta_{G1} - \lambda_1) + \rho_{G1} \right] - \dot{\psi}_1 \left[a_{P1} \cos(\psi_1 + \delta_{P1} - \lambda_1) - \rho_{P1} \right] \right\} \bar{n}_{N\lambda 1} \tag{G-21}$$

b. ROUND ON FLAT PHASE OF MOTION

Figure G-3 shows a schematic view of mesh no. 1 in the round on flat phase of the motion.

I. UNIT VECTORS

The unit vector in the direction O_2T_1 is given by:

$$\bar{n}_{F1} = \cos(\psi_1 - \alpha_{P1})\bar{i} + \sin(\psi_1 - \alpha_{P1})\bar{j} \tag{G-22}$$

The unit vector $\bar{n}_{NF1}$, in the direction $C_{G1}S_1$, is always normal to $\bar{n}_{F1}$:

$$\bar{n}_{NF1} = -\sin(\psi_1 - \alpha_{P1})\bar{i} + \cos(\psi_1 - \alpha_{P1})\bar{j} \tag{G-23}$$

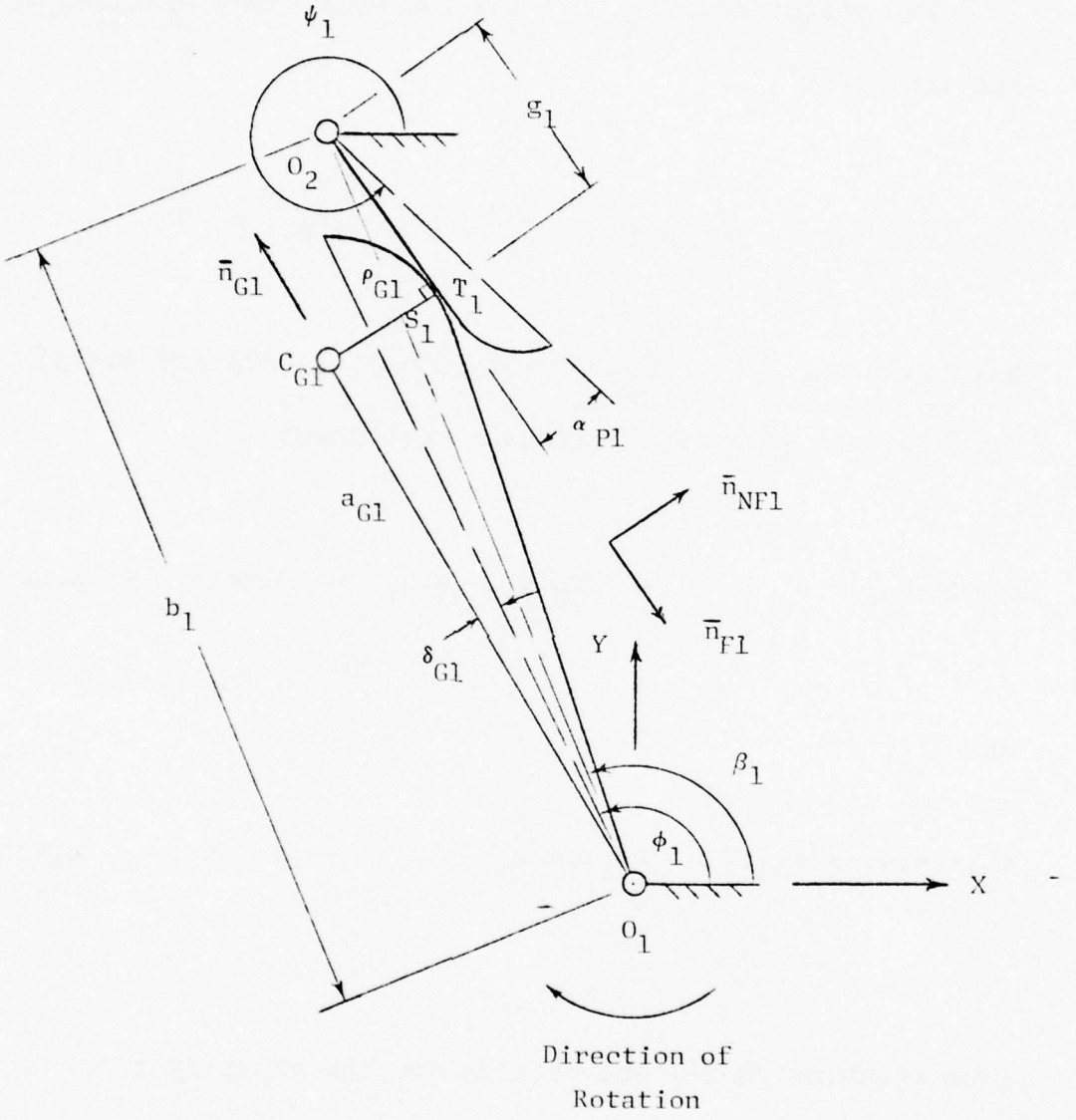

FIGURE G-3

ROUND ON FLAT PHASE FOR MESH NO. 1

II. DETERMINATION OF OUTPUT ANGLE ψ_1 AND DISTANCE s_1

The vector equation for the mechanism loop O_1-C_{G1}-S_1-T_1-O_2 has the form:

$$a_{G1}\bar{n}_{G1} + \rho_{G1}\bar{n}_{NF1} - s_1\bar{n}_{F1} - b_1\bar{n}_{\beta 1} = 0 \qquad (G\text{-}24)$$

Substitution of equations (G-1), (G-5), (G-22) and (G-23) leads to the following component equations:

$$a_{G1}\cos(\phi_1 + \delta_{G1}) - \rho_{G1}\sin(\psi_1 - \alpha_{P1}) - b_1\cos\beta_1 - s_1\cos(\psi_1 - \alpha_{P1}) = 0 \qquad (G\text{-}25)$$

and

$$a_{G1}\sin(\phi_1 + \delta_{G1}) + \rho_{G1}\cos(\psi_1 - \alpha_{P1}) - b_1\sin\beta_1 - s_1\sin(\psi_1 - \alpha_{P1}) = 0 \qquad (G\text{-}26)$$

From equation (G-26) one obtains for the quantity s_1:

$$s_1 = \frac{a_{G1}\sin(\phi_1 + \delta_{G1}) + \rho_{G1}\cos(\psi_1 - \alpha_{P1}) - b_1\sin\beta_1}{\sin(\psi_1 - \alpha_{P1})} \qquad (G\text{-}27)$$

This expression is now substituted in equation (G-25). This leads to the following:

$$A_{1F}\sin\psi_1 + B_{1F}\cos\psi_1 = C_{1F} \qquad \text{(G-28)}$$

where

$$A_{1F} = a_{G1}\cos(\phi_1 + \delta_{G1} + \alpha_{P1}) - b_1\cos(\beta_1 + \alpha_{P1})$$

$$B_{1F} = -a_{G1}\sin(\phi_1 + \delta_{G1} + \alpha_{P1}) + b_1\sin(\beta_1 + \alpha_{P1})$$

$$C_{1F} = \rho_{G1}$$

Equation (G-28) is solved for ψ_1 in the now customary manner:

$$\psi_1 = 2\tan^{-1}\frac{A_{1F} \pm \sqrt{A_{1F}^2 + B_{1F}^2 - C_{1F}^2}}{B_{1F} + C_{1F}} \qquad \text{(G-29)}$$

The appropriate sign is again found from geometric considerations.

III. DETERMINATION OF ANGULAR VELOCITY $\dot{\psi}_1$ DURING ROUND ON FLAT PHASE OF MOTION

Implicit differentiation of equation (G-28) with respect to time gives for $\dot{\psi}_1$:

$$\dot{\psi}_1 = \dot{\phi}_1 \left[\frac{A_{1FD}\sin\psi_1 + B_{1FD}\cos\psi_1}{A_{1F}\cos\psi_1 - B_{1F}\sin\psi_1} \right] \qquad \text{(G-30)}$$

where

$$A_{1FD} = a_{G1}\sin(\phi_1 + \delta_{G1} + \alpha_{P1})$$

$$B_{1FD} = a_{G1}\cos(\phi_1 + \delta_{G1} + \alpha_{P1})$$

IV. RELATIVE VELOCITY $\bar{V}_{S1/T1_F}$ AT CONTACT POINT DURING ROUND ON FLAT PHASE OF MOTION

For the round on flat phase, the relative velocity $\bar{V}_{S1/T1_F}$ may be expressed by:

$$\bar{V}_{S1/T1_F} = \bar{V}_{S1/O_1} - \bar{V}_{T1/O_2} \tag{G-31}$$

Now, this velocity has the direction of the unit vector $\pm \bar{n}_{F1}$. Since there is no velocity component along the pinion flank, equation (G-31) becomes:

$$\bar{V}_{S1/T1_f} = \bar{V}_{S1/O_1} \cdot \bar{n}_{F1}$$

$$= \left\{ \left[\dot{\phi}_1 \times (a_{G1}\bar{n}_{G1} + \rho_{G1}\bar{n}_{NF1}) \right] \cdot \bar{n}_{F1} \right\} \bar{n}_{F1} \tag{G-32}$$

Appropriate substitution of unit vectors furnishes:

$$\bar{V}_{S1/T1_F} = \dot{\phi}_1 \left[a_{G1} \sin(\psi_1 - \alpha_{P1} - \phi_1 - \delta_{G1}) - \rho_{G1} \right] \bar{n}_{F1} \tag{G-33}$$

V. DETERMINATION OF TRANSITION ANGLES

The transition angle ϕ_{1T} and the corresponding angle ψ_{1T} are reached when the round on round phase is followed by the round on flat one. They are obtained by letting $g_1 = f_{P1}$ in the component equations (G-25) and (G-26). This gives:

$$a_{G1}\cos(\phi_{1T} + \delta_{G1}) - \rho_{G1}\sin(\psi_{1T} - \alpha_{P1}) - b_1\cos\beta_1 - f_{P1}\cos(\psi_{1T} - \alpha_{P1}) = 0 \qquad \text{(G-34)}$$

and

$$a_{G1}\sin(\phi_{1T} + \delta_{G1}) + \rho_{G1}\cos(\psi_{1T} - \alpha_{P1}) - b_1\sin\beta_1 - f_{P1}\sin(\psi_{1T} - \alpha_{P1}) = 0 \qquad \text{(G-35)}$$

From the above, one obtains:

$$\cos(\phi_{1T} + \delta_{G1}) = \frac{1}{a_{G1}}\left[\rho_{G1}\sin(\psi_{1T} - \alpha_{P1}) + b_1\cos\beta_1 + f_{P1}\cos(\psi_{1T} - \alpha_{P1})\right] \qquad \text{(G-36)}$$

$$\sin(\phi_{1T} + \delta_{G1}) = \frac{1}{a_{G1}}\left[-\rho_{G1}\cos(\psi_{1T} - \alpha_{P1}) + b_1\sin\beta_1 + f_{P1}\sin(\psi_{1T} - \alpha_{P1})\right] \qquad \text{(G-37)}$$

The angle ψ_{1T} is now obtained by letting

$$\sin^2(\phi_{1T} + \delta_{G1}) + \cos^2(\phi_{1T} + \delta_{G1}) = 1$$

This results in:

$$A_{1T}\sin\psi_{1T} + B_{1T}\cos\psi_{1T} = C_{1T} \qquad \text{(G-38)}$$

where

$$A_{1T} = \rho_{G1}\cos(\beta_1 + \alpha_{P1}) + f_{P1}\sin(\beta_1 + \alpha_{P1})$$

$$B_{1T} = -\rho_{G1}\sin(\beta_1 + \alpha_{P1}) + f_{P1}\cos(\beta_1 + \alpha_{P1})$$

$$C_{1T} = \frac{a_{G1}^2 - \rho_{G1}^2 - b_1^2 - f_{P1}^2}{2b_1}$$

Finally,

$$\psi_{1T} = 2\tan^{-1}\frac{A_{1T} \pm \sqrt{A_{1T}^2 + B_{1T}^2 - C_{1T}^2}}{B_{1T} + C_{1T}} \qquad \text{(G-39)}$$

The appropriate sign must be found from geometric considerations. The associated angle ϕ_{1T} may be found with the help of either equation (G-36) or equation (G-37):

$$\phi_{1T} = \cos^{-1}\left[\frac{\rho_{G1}\sin(\psi_{1T} - \alpha_{P1}) + f_{P1}\cos(\psi_{1T} - \alpha_{P1}) + b_1\cos\beta_1}{a_{G1}}\right] - \delta_{G1} \qquad \text{(G-40)}$$

or

$$\phi_{1T} = \sin^{-1}\left[\frac{-\rho_{G1}\cos(\psi_{1T} - \alpha_{P1}) + f_{P1}\sin(\psi_{1T} - \alpha_{P1}) + b_1\sin\beta_1}{a_{G1}}\right] - \delta_{G1} \qquad \text{(G-41)}$$

VI. SENSING EQUATION FOR THE DETERMINATION OF CONTACT ON SUBSEQUENT TOOTH MESH

The following contact sensing equation is derived with the assumption that subsequent contact is made in the round on round phase of the motion, in the manner shown in Section VI of Appendix E. Now, the configuration is that of Figure G-2 where gear no. 1 rotates in a clockwise direction.

Before contact is made, the distance between the centers of curvature C_{G1} and C_{P1} is given by:

$$\overline{C_{G1}C_{P1}} = L_{x1}\bar{i} + L_{y1}\bar{j} \qquad (G\text{-}42)$$

If $\Delta\phi_1$ and $\Delta\psi_1$ represent the tooth spacing angles of gear no. 1 and pinion no. 2, respectively, the associated loop equation becomes (see Figures E-3 and G-2):

$$a_{G1}\left[\cos(\phi_1 + \Delta\phi_1 + \delta_{G1})\bar{i} + \sin(\phi_1 + \Delta\phi_1 + \delta_{G1})\bar{j}\right] + L_{x1}\bar{i} + L_{y1}\bar{j}$$

$$= b_1(\cos\beta_1\bar{i} + \sin\beta_1\bar{j}) + a_{P1}\left[\cos(\psi_1 - \Delta\psi_1 + \delta_{P1})\bar{i} + \sin(\psi_1 - \Delta\psi_1 + \delta_{P1})\bar{j}\right] \qquad (G\text{-}43)$$

where

ψ_1 = angle of pinion no. 2 as determined for the round on flat mode with equation (G-29)

The magnitudes of L_{x1} and L_{y1} are determined from the component form of equation (G-43), i.e.

$$L_{x1} = b_1\cos\beta_1 + a_{P1}\cos(\psi_1 - \Delta\psi_1 + \delta_{P1}) - a_{G1}\cos(\phi_1 + \Delta\phi_1 + \delta_{G1}) \qquad (G\text{-}44)$$

and

$$L_{y1} = b_1\sin\beta_1 + a_{P1}\sin(\psi_1 - \Delta\psi_1 + \delta_{P1}) - a_{G1}\sin(\phi_1 + \Delta\phi_1 + \delta_{G1}) \qquad (G\text{-}45)$$

Contact will have occurred as soon as

$$\sqrt{L_{x1}^2 + L_{y1}^2} \leq \rho_{G1} + \rho_{P1} \qquad \text{(G-46)}$$

2. KINEMATICS OF MESH NO. 2 (GEAR NO. 2 AND PINION NO. 3)

a. ROUND ON ROUND PHASE OF MOTION

Figure G-4 gives a schematic representation of the round on round phase of the motion. Only the contacting faces of the gear and the pinion are shown. It is to be noted that the input gear rotates in the counter-clockwise direction, and that the output angle ψ_1 of mesh no. 1 is identical to the input angle ϕ_2 of mesh no. 2.

I. UNIT VECTORS

The unit vector in the direction C_2C_{G2} of the gear is given by:

$$\bar{n}_{G2} = \cos(\phi_2 - \delta_{G2})\bar{i} + \sin(\phi_2 - \delta_{G2})\bar{j} \qquad \text{(G-47)}$$

The unit vector in the direction $C_{G2}C_{P2}$ is given by:

$$\bar{n}_{\lambda 2} = \cos\lambda_2\bar{i} + \sin\lambda_2\bar{j} \qquad \text{(G-48)}$$

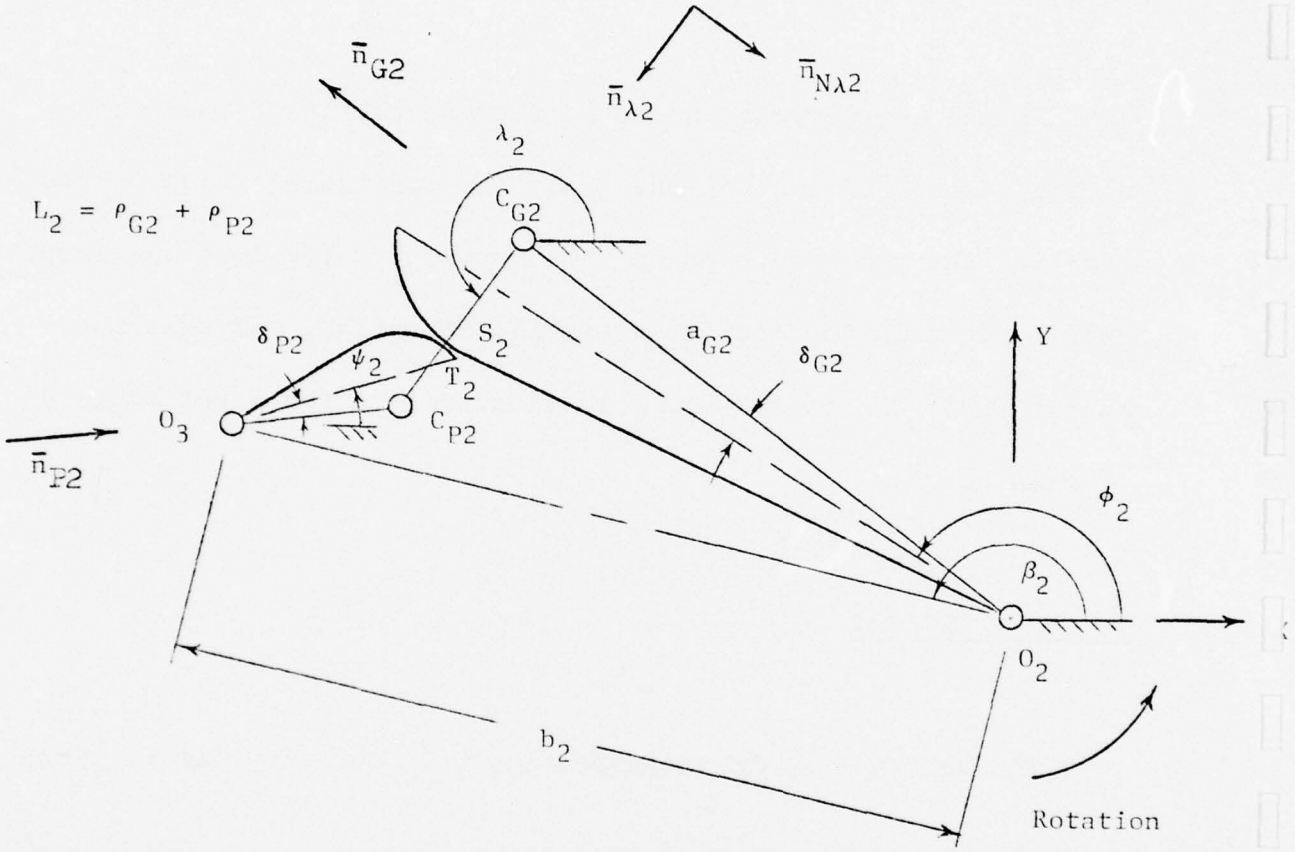

FIGURE G-4

ROUND ON ROUND PHASE FOR MESH NO. 2

The unit vector normal to $\bar{n}_{\lambda 2}$ in the right hand sense becomes:

$$\bar{n}_{N\lambda 2} = -\sin\lambda_2\bar{i} + \cos\lambda_2\bar{j} \qquad \text{(G-49)}$$

The pinion unit vector $\bar{n}_{P2}$, in the direction O_3C_{P2}, is represented by:

$$\bar{n}_{P2} = \cos(\psi_2 - \delta_{P2})\bar{i} + \sin(\psi_2 - \delta_{P2})\bar{j} \qquad \text{(G-50)}$$

Finally, the unit vector along the centerline O_2O_3 is given by:

$$\bar{n}_{\beta 2} = \cos\beta_2\bar{i} + \sin\beta_2\bar{j} \qquad \text{(G-51)}$$

II. DETERMINATION OF OUTPUT ANGLE ψ_2 AND "COUPLER" ANGLE λ_2

The loop equation of the equivalent four-bar linkage is given by:

$$a_{G2}\bar{n}_{G2} + L_2\bar{n}_{\lambda 2} - a_{P2}\bar{n}_{P2} - b_2\bar{n}_{\beta 2} = 0 \qquad \text{(G-52)}$$

where

$$L_2 = \rho_{G2} + \rho_{P2} \qquad \text{(G-53)}$$

After substitution of the unit vector, as given earlier, one obtains the following component equations:

$$a_{G2}\cos(\phi_2 - \delta_{G2}) + L_2\cos\lambda_2 - a_{P2}\cos(\psi_2 - \delta_{P2}) - b_2\cos\beta_2 = 0 \qquad \text{(G-54)}$$

and

$$a_{G2}\sin(\phi_2 - \delta_{G2}) + L_2\sin\lambda_2 - a_{P2}\sin(\psi_2 - \delta_{P2}) - b_2\sin\beta_2 = 0 \qquad \text{(G-55)}$$

To solve for the output angle ψ_2 in terms of the input angle ϕ_2, substitute the expressions for $\sin\lambda_2$ and $\cos\lambda_2$, as obtained from the component equations (G-54) and (G-55), into:

$$\sin^2\lambda_2 + \cos^2\lambda_2 = 1 \qquad \text{(G-56)}$$

This leads to:

$$A_{2R}\sin\psi_2 + B_{2R}\cos\psi_2 = C_{2R} \qquad \text{(G-57)}$$

where

$$A_{2R} = b_2\sin(\beta_2 + \delta_{P2}) - a_{G2}\sin(\phi_2 - \delta_{G2} + \delta_{P2})$$

$$B_{2R} = b_2\cos(\beta_2 + \delta_{P2}) - a_{G2}\cos(\phi_2 - \delta_{G2} + \delta_{P2})$$

$$C_{2R} = \frac{L_2^2 - b_2^2 - a_{G2}^2 - a_{P2}^2 + 2a_{G2}b_2\cos(\phi_2 - \delta_{G2} - \beta_2)}{2a_{P2}}$$

Equation (G-57) is then solved for ψ_2 in the manner discussed in Appendix E:

$$\psi_2 = 2\tan^{-1}\frac{A_{2R} \pm \sqrt{A_{2R}^2 + B_{2R}^2 - C_{2R}^2}}{B_{2R} + C_{2R}} \qquad \text{(G-58)}$$

The correct sign must again be determined from geometric considerations.

The angle λ_2 may now be determined either from equation (G-54) or equation (G-55):

$$\lambda_2 = \cos^{-1}\left[\frac{b_2\cos\beta_2 + a_{P2}\cos(\psi_2 - \delta_{P2}) - a_{G2}\cos(\phi_2 - \delta_{G2})}{L_2}\right] \qquad \text{(G-59)}$$

or

$$\lambda_2 = \sin^{-1}\left[\frac{b_2\sin\beta_2 + a_{P2}\sin(\psi_2 - \delta_{P2}) - a_{G2}\sin(\phi_2 - \delta_{G2})}{L_2}\right] \qquad \text{(G-60)}$$

III. DETERMINATION OF OUTPUT ANGULAR VELOCITY $\dot{\psi}_2$

Implicit differentiation of equation (G-57) with respect to time leads to:

$$\dot{\psi}_2 = \dot{\phi}_2 \left[\frac{A_{2RD}\sin\psi_2 - B_{2RD}\cos\psi_2 - C_{2RD}}{A_{2R}\cos\psi_2 - B_{2R}\sin\psi_2} \right] \qquad \text{(G-61)}$$

where

$$A_{2RD} = a_{G2}\cos(\phi_2 - \delta_{G2} + \delta_{P2})$$

$$B_{2RD} = a_{G2}\sin(\phi_2 - \delta_{G2} + \delta_{P2})$$

$$C_{2RD} = \frac{a_{G2}b_2\sin(\phi_2 - \delta_{G2} - \beta_2)}{a_{P2}}$$

IV. RELATIVE VELOCITY AT THE CONTACT POINT

The relative velocity $\bar{V}_{S2/T2_R}$, of point S_2 on gear no. 2 with respect to point T_2 on pinion no. 3 has the direction of the unit vector $\bar{n}_{N\lambda 2}$. Thus, in the manner of equation (G-20):

$$\bar{V}_{S2/T2_R} = \left\{ \left[\dot{\phi}_2 \bar{k} \times (a_{G2}\bar{n}_{G2} + \rho_{G2}\bar{n}_{\lambda 2}) \right] \cdot \bar{n}_{N\lambda 2} - \left[\dot{\psi}_2 \bar{k} \times (a_{P2}\bar{n}_{P2} - \rho_{P2}\bar{n}_{\lambda 2}) \right] \cdot \bar{n}_{N\lambda 2} \right\} \bar{n}_{N\lambda 2} \tag{G-62}$$

Substitution of unit vectors yields:

$$\bar{V}_{S2/T2_R} = \left\{ \dot{\phi}_2 \left[a_{G2}\cos(\phi_2 - \delta_{G2} - \lambda_2) + \rho_{G2} \right] - \dot{\psi}_2 \left[a_{P2}\cos(\psi_2 - \delta_{P2} - \lambda_2) - \rho_{P2} \right] \right\} \bar{n}_{N\lambda 2} \tag{G-63}$$

b. ROUND ON FLAT PHASE OF MOTION

Figure G-5 shows a schematic view of mesh no. 2 in the round on flat phase of the motion. Again, only the contacting sides of the gear teeth are indicated.

I. UNIT VECTORS

The unit vector in the direction O_3T_2, along the flank of pinion no. 3, is given by:

$$\bar{n}_{F2} = \cos(\psi_2 + \alpha_{P2})\bar{i} + \sin(\psi_2 + \alpha_{P2})\bar{j} \qquad \text{(G-64)}$$

The unit vector $\bar{n}_{NF2}$, in the direction S_2C_{G2}, is normal to $\bar{n}_{F2}$ in the right hand sense:

$$\bar{n}_{NF2} = -\sin(\psi_2 + \alpha_{P2})\bar{i} + \cos(\psi_2 + \alpha_{P2})\bar{j} \qquad \text{(G-65)}$$

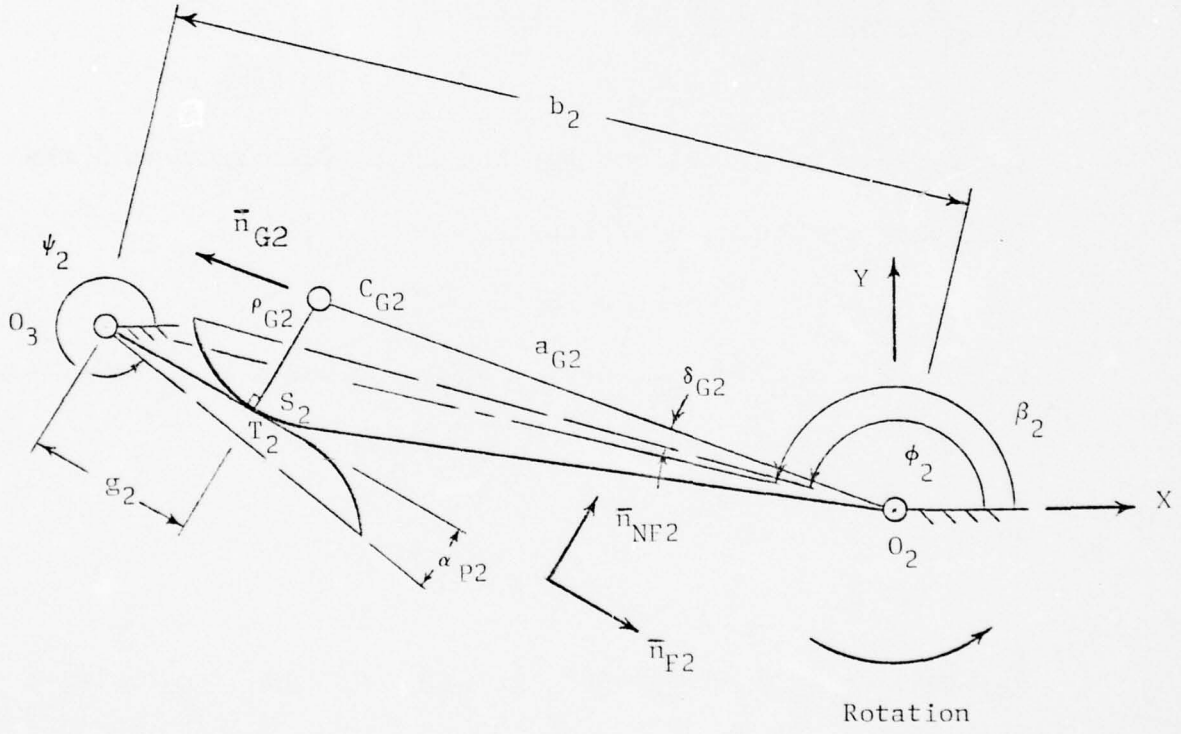

FIGURE G-5

ROUND ON FLAT PHASE OF MOTION OF MESH NO. 2

AD-A061 862 CITY COLL NEW YORK DEPT OF MECHANICAL ENGINEERING F/G 13/9
OPTIMIZATION OF STEP-UP GEAR TRAINS WITH DIFFERENT KINEMATIC PR--ETC(U)
MAY 78 G G LOWEN DAAG29-77-G-0037

UNCLASSIFIED ARO-14743.1-R-E NL

3 OF 4
ADA
061862

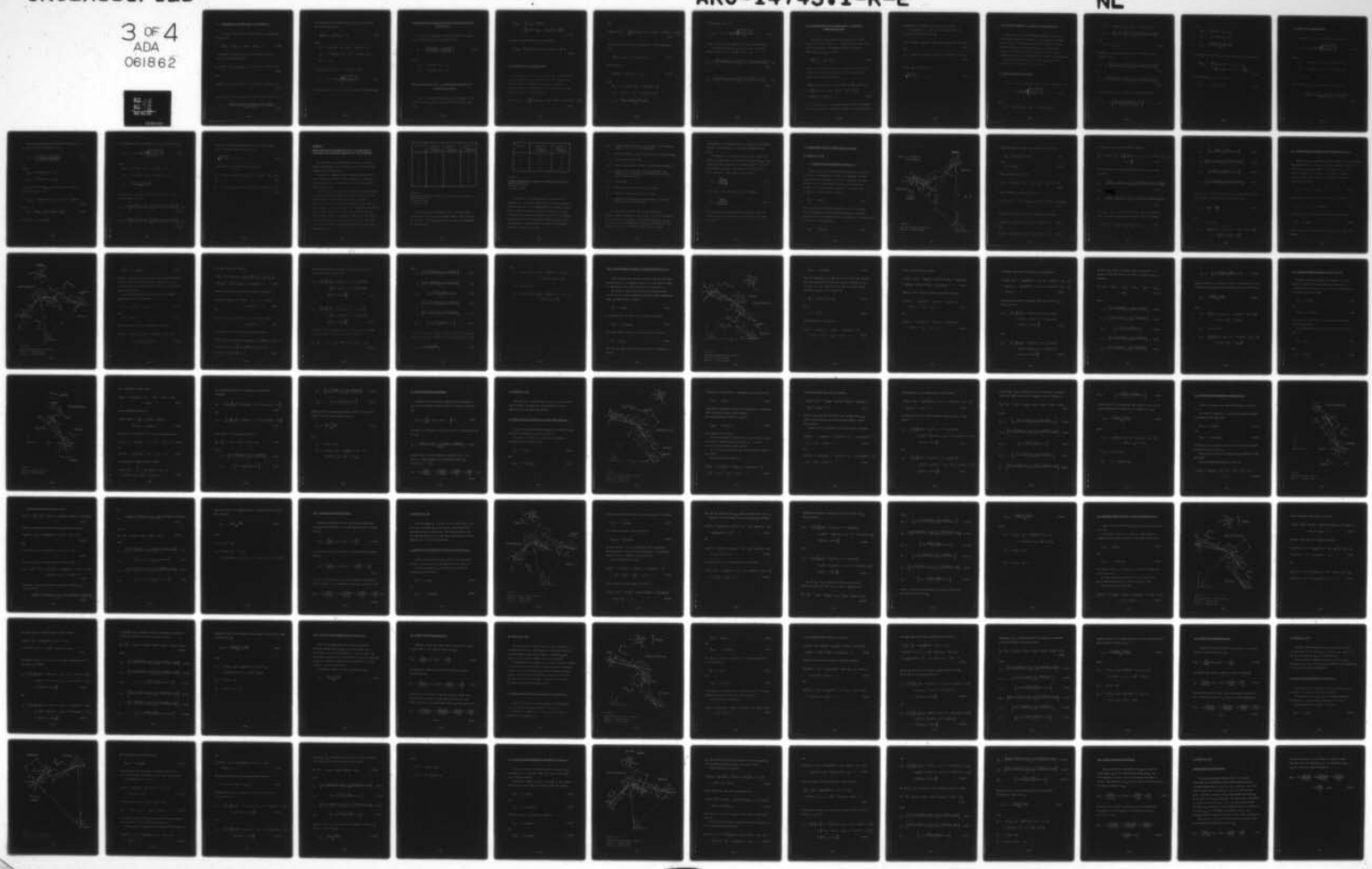

II. DETERMINATION OF OUTPUT ANGLE ψ_2 AND DISTANCE S_2

The vector equation for the mechanism loop O_2-C_{G2}-S_2-T_2-O_3 has the form:

$$a_{G2}\bar{n}_{G2} - \rho_{G2}\bar{n}_{NF2} - S_2\bar{n}_F - b_2\bar{n}_{\beta 2} = 0 \qquad \text{(G-66)}$$

Appropriate substitutions for the unit vectors furnish the following component equations:

$$a_{G2}\cos(\phi_2 - \delta_{G2}) + \rho_{G2}\sin(\psi_2 + \alpha_{P2}) - b_2\cos\beta_2 - S_2\cos(\psi_2 + \alpha_{P2}) = 0 \qquad \text{(G-67)}$$

and

$$a_{G2}\sin(\phi_2 - \delta_{G2}) - \rho_{G2}\cos(\psi_2 + \alpha_{P2}) - b_2\sin\beta_2 - S_2\sin(\psi_2 + \alpha_{P2}) = 0 \qquad \text{(G-68)}$$

From equation (G-68) one obtains the following expression for S_2:

$$S_2 = \frac{a_{G2}\sin(\phi_2 - \delta_{G2}) - \rho_{G2}\cos(\psi_2 + \alpha_{P2}) - b_2\sin\beta_2}{\sin(\psi_2 + \alpha_{P2})} \qquad \text{(G-69)}$$

This expression is now substituted into equation (G-67), and one obtains the following:

$$A_{2F}\sin\psi_2 + B_{2F}\cos\psi_2 = C_{2F} \qquad \text{(G-70)}$$

where

$$A_{2F} = a_{G2}\cos(\phi_2 - \delta_{G2} - \alpha_{P2}) - b_2\cos(\beta_2 - \alpha_{P2})$$

$$B_{2F} = -a_{G2}\sin(\phi_2 - \delta_{G2} - \alpha_{P2}) + b_2\sin(\beta_2 - \alpha_{P2})$$

$$C_{2F} = -\rho_{G2}$$

Equation (G-70) is solved in the customary manner:

$$\psi_2 = 2\tan^{-1}\frac{A_{2F} \pm \sqrt{A_{2F}^2 + B_{2F}^2 - C_{2F}^2}}{B_{2F} + C_{2F}} \qquad \text{(G-71)}$$

The appropriate sign is again found from geometric considerations.

III. DETERMINATION OF ANGULAR VELOCITY $\dot{\psi}_2$ DURING ROUND ON FLAT PHASE OF MOTION

Implicit differentiation of equation (G-70) with respect to time gives the following expression for $\dot{\psi}_2$:

$$\dot{\psi}_2 = \dot{\phi}_2 \left[\frac{A_{2FD}\sin\psi_2 + B_{2FD}\cos\psi_2}{A_{2F}\cos\psi_2 - B_{2F}\sin\psi_2} \right] \qquad \text{(G-72)}$$

where

$$A_{2FD} = a_{G2}\sin(\phi_2 - \delta_{G2} - \alpha_{P2})$$

$$B_{2FD} = a_{G2}\cos(\phi_2 - \delta_{G2} - \alpha_{P2})$$

IV. RELATIVE VELOCITY $\bar{V}_{S2/T2_F}$ AT CONTACT POINT DURING ROUND ON FLAT PHASE OF MOTION

Again, the relative velocity $\bar{V}_{S2/T2_F}$ consists only of that component of $\bar{V}_{S2/O_2}$ which is directed along the pinion flank. Thus,

$$\bar{V}_{S2/T2_F} = \left[\bar{V}_{S2/O_2} \cdot \bar{n}_{F2} \right] \bar{n}_{F2}$$

$$= \left\{ \left[\dot{\phi}_2 \bar{k} \times (a_{G2}\bar{n}_{G2} - \rho_{G2}\bar{n}_{NF2}) \right] \cdot \bar{n}_{F2} \right\} \bar{n}_{F2}$$

(G-73)

Appropriate substitution of unit vectors gives:

$$\bar{V}_{S2/T2_F} = \dot{\phi}_2 \left[a_{G2}\sin(\psi_2 + \alpha_{P2} - \phi_2 + \delta_{G2}) + \rho_{G2} \right] \bar{n}_{F2}$$

(G-74)

V. DETERMINATION OF TRANSITION ANGLES

The transition angle ϕ_{2T} and the angle ψ_{2T}, which correspond to the transition from the round on round to the round on flat phase of motion, are obtained by letting $\delta_2 = f_{P2}$ in the component equations (G-67) and (G-68). From this one finds the following with $\phi_2 = \phi_{2T}$ and $\psi_2 = \psi_{2T}$:

$$\cos(\phi_{2T} - \delta_{G2}) = \frac{1}{-a_{G2}} \left[-\rho_{G2}\sin(\psi_{2T} + \alpha_{P2}) + b_2\cos\beta_2 + f_{P2}\cos(\psi_{2T} + \alpha_{P2}) \right]$$

(G-75)

and

$$\sin(\phi_{2T} - \delta_{G2}) = \frac{1}{a_{G2}}\left[\rho_{G2}\cos(\psi_{2T} + \alpha_{P2}) + b_2\sin\beta_2 + f_{P2}\sin(\psi_{2T} + \alpha_{P2})\right] \quad \text{(G-76)}$$

The angle ψ_{2T} is now found by substituting the above expressions into:

$$\sin^2(\phi_{2T} - \delta_{G2}) + \cos^2(\phi_{2T} - \delta_{G2}) = 1 \quad \text{(G-77)}$$

This results in:

$$A_{2T}\sin\psi_{2T} + B_{2T}\cos\psi_{2T} = C_{2T} \quad \text{(G-78)}$$

where

$$A_{2T} = -\rho_{G2}\cos(\beta_2 - \alpha_{P2}) + f_{P2}\sin(\beta_2 - \alpha_{P2})$$

$$B_{2T} = \rho_{G2}\sin(\beta_2 - \alpha_{P2}) + f_{P2}\cos(\beta_2 - \alpha_{P2})$$

$$C_{2T} = \frac{a_{G2}^2 - \rho_{G2}^2 - b_2^2 - f_{P2}^2}{2\,b_2}$$

Finally, in the usual way:

$$\psi_{2T} = 2\tan^{-1}\frac{A_{2T} \pm \sqrt{A_{2T}^2 + B_{2T}^2 - C_{2T}^2}}{B_{2T} + C_{2T}} \qquad \text{(G-79)}$$

Again, the sign must be decided from geometric considerations.

The associated angle ϕ_{2T} may be found with the help of either equation (G-75) or equation (G-76), i.e.

$$\phi_{2T} = \cos^{-1}\left[\frac{-\rho_{G2}\sin(\psi_{2T} + \alpha_{P2}) + b_2\cos\beta_2 + f_{P2}\cos(\psi_{2T} + \alpha_{P2})}{a_{G2}}\right] + \delta_{G2} \qquad \text{(G-80)}$$

or

$$\phi_{2T} = \sin^{-1}\left[\frac{\rho_{G2}\cos(\psi_{2T} + \alpha_{P2}) + b_2\sin\beta_2 + f_{P2}\sin(\psi_{2T} + \alpha_{P2})}{a_{G2}}\right] + \delta_{G2} \qquad \text{(G-81)}$$

VI. SENSING EQUATION FOR THE DETERMINATION OF CONTACT ON SUBSEQUENT TOOTH MESH

The contact sensing equation for mesh no. 2 is derived similarly to that for mesh no. 1 before contact is made in the round on round mode. The distance between the centers of curvature C_{G2} and C_{P2} is given by:

$$\overline{C_{G2}C_{P2}} = L_{x2}\bar{i} + L_{y2}\bar{j} \qquad (G\text{-}82)$$

If $\Delta\phi_2$ and $\Delta\psi_2$ represent the tooth spacing angles of gear no. 2 and pinion no. 3 respectively, the associated loop equation becomes (see Figures E-3 and G-4):

$$a_{G2}\left[\cos(\phi_2 - \Delta\phi_2 - \delta_{G2})\bar{i} + \sin(\phi_2 - \Delta\phi_2 - \delta_{G2})\bar{j}\right] + L_{x2}\bar{i} + L_{y2}\bar{j}$$
$$- a_{P2}\left[\cos(\psi_2 + \Delta\psi_2 - \delta_{P2})\bar{i} + \sin(\psi_2 + \Delta\psi_2 - \delta_{P2})\bar{j}\right]$$
$$- b_2\left[\cos\beta_2\bar{i} + \sin\beta_2\bar{j}\right] = 0 \qquad (G\text{-}83)$$

Note that for mesh no. 2, the angular increment $\Delta\phi_2$ is negative while $\Delta\psi_2$ is positive. Further, as before, the angle ψ_2 must be

determined for the round on flat phase of the motion.

The magnitudes of L_{x2} and L_{y2} are determined from the components of equation (G-83), i.e.

$$L_{x2} = b_2\cos\beta_2 + a_{P2}\cos(\psi_2 + \Delta\psi_2 - \delta_{P2}) - a_{G2}\cos(\phi_2 - \Delta\phi_2 - \delta_{G2}) \tag{G-84}$$

while

$$L_{y2} = b_2\sin\beta_2 + a_{P2}\sin(\psi_2 + \Delta\psi_2 - \delta_{P2}) - a_{G2}\sin(\phi_2 - \Delta\phi_2 - \delta_{G2}) \tag{G-85}$$

Contact will occur as soon as

$$\sqrt{L_{x2}^2 + L_{y2}^2} \leq \rho_{G2} + \rho_{P2} \tag{G-86}$$

3. KINEMATICS OF MESH NO. 3 (GEAR NO. 3 AND PINION NO. 4)

Since mesh no. 3 is kinematically equivalent to mesh no. 1, the kinematic equations for mesh no. 3 may be obtained from those for mesh no. 1. The angle β_3 must replace the angle β_1 and the center distance b_3 is used instead of b_1. All parameters of gear no. 1 are replaced by those of gear no. 3 and the pinion parameters of pinion no. 4 are substituted for those of pinion no. 2.

It is to be noted that the input angle ϕ_3 of mesh no. 3 is identical to the output angle ψ_2 of mesh no. 2.

a. ROUND ON ROUND PHASE OF MOTION

The ouput angle ψ_3 is obtained with the help of equation (G-12):

$$\psi_3 = 2 \tan^{-1} \frac{A_{3R} \pm \sqrt{A_{3R}^2 + B_{3R}^2 - C_{3R}^2}}{B_{3R} + C_{3R}} \qquad \text{(G-87)}$$

where

$$A_{3R} = a_{G3}\sin(\phi_3 + \delta_{G3} - \delta_{P3}) - b_3\sin(\beta_3 - \delta_{P3})$$

$$B_{3R} = a_{G3}\cos(\phi_3 + \delta_{G3} - \delta_{P3}) - b_3\cos(\beta_3 - \delta_{P3})$$

$$C_{3R} = \frac{a_{P3}^2 + a_{G3}^2 + b_3^2 - L_3^2 - 2a_{G3}b_3\cos(\phi_3 + \delta_{G3} - \beta_3)}{2\,a_{P3}}$$

and

$$L_3 = \rho_{G3} + \rho_{P3} \qquad \text{(G-88)}$$

The angle λ_3 may be found with the help of equation (G-13) or equation (G-14):

$$\lambda_3 = \cos^{-1}\left[\frac{b_3\cos\beta_3 + a_{P3}\cos(\psi_3 + \delta_{P3}) - a_{G3}\cos(\phi_3 + \delta_{G3})}{L_3}\right] \qquad \text{(G-89)}$$

or

$$\lambda_3 = \sin^{-1}\left[\frac{b_3\sin\beta_3 + a_{P3}\sin(\psi_3 + \delta_{P3}) - a_{G3}\sin(\phi_3 + \delta_{G3})}{L_3}\right] \qquad \text{(G-90)}$$

The angular velocity $\dot{\psi}_3$ is obtained from equation (G-15):

$$\dot{\psi}_3 = \dot{\phi}_3\left[\frac{B_{3RD}\cos\psi_3 - A_{3RD}\sin\psi_3 + C_{3RD}}{A_{3R}\cos\psi_3 - B_{3R}\sin\psi_3}\right] \qquad \text{(G-91)}$$

where

$$A_{3RD} = a_{G3}\cos(\phi_3 + \delta_{G3} - \delta_{P3})$$

$$B_{3RD} = a_{G3}\sin(\phi_3 + \delta_{G3} - \delta_{P3})$$

$$C_{3RD} = \frac{a_{G3}b_3\sin(\phi_3 + \delta_{G3} - \beta_3)}{a_{P3}}$$

The relative velocity $\bar{V}_{S3/T3_R}$ becomes according to Equation (G-21):

$$\bar{V}_{S3/T3_R} = \left\{ \dot{\phi}_3\left[a_{G3}\cos(\phi_3 + \delta_{G3} - \lambda_3) + \rho_{G3}\right] - \dot{\psi}_3\left[a_{P3}\cos(\psi_3 + \delta_{P3} - \lambda_3) - \rho_{P3}\right]\right\}\bar{n}_{N\lambda 3} \quad \text{(G-92)}$$

where, according to equation (G-3),

$$\bar{n}_{N\lambda 3} = -\sin\lambda_3\bar{i} + \cos\lambda_3\bar{j} \quad \text{(G-93)}$$

b. ROUND ON FLAT PHASE OF MOTION

The output angle ψ_3 is obtained from equation (G-29):

$$\psi_3 = 2 \tan^{-1} \frac{A_{3F} \pm \sqrt{A_{3F}^2 + B_{3F}^2 - C_{3F}^2}}{B_{3F} + C_{3F}} \qquad \text{(G-94)}$$

where

$$A_{3F} = a_{G3}\cos(\phi_3 + \delta_{G3} + \alpha_{P3}) - b_3\cos(\beta_3 + \alpha_{P3})$$

$$B_{3F} = -a_{G3}\sin(\phi_3 + \delta_{G3} + \alpha_{P3}) + b_3\sin(\beta_3 + \alpha_{P3})$$

$$C_{3F} = \rho_{G3}$$

The distance s_3 becomes according to equation (G-27):

$$s_3 = \frac{a_{G3}\sin(\phi_3 + \delta_{G3}) + \rho_{G3}\cos(\psi_3 - \alpha_{P3}) - b_3\sin\beta_3}{\sin(\psi_3 - \alpha_{P3})} \qquad \text{(G-95)}$$

The angular velocity $\dot{\psi}_3$ for the round on flat phase of the motion is found from equation (G-30):

$$\dot{\psi}_3 = \dot{\phi}_3 \left[\frac{A_{3FD}\sin\psi_3 + B_{3FD}\cos\psi_3}{A_{3F}\cos\psi_3 - B_{3F}\sin\psi_3} \right] \qquad \text{(G-96)}$$

where

$$A_{3FD} = a_{G3}\sin(\phi_3 + \delta_{G3} + \alpha_{P3})$$

$$B_{3FD} = a_{G3}\cos(\phi_3 + \delta_{G3} + \alpha_{P3})$$

The relative velocity $\bar{V}_{S3/T3_F}$ for the round on flat phase comes from equation (G-33):

$$\bar{V}_{S3/T3_F} = \dot{\phi}_3 \left[a_{G3}\sin(\psi_3 - \alpha_{P3} - \phi_3 - \delta_{G3}) - \rho_{G3} \right] \bar{n}_{F3} \qquad \text{(G-97)}$$

where

$$\bar{n}_{F3} = \cos(\psi_3 - \alpha_{P3})\bar{i} + \sin(\psi_3 - \alpha_{P3})\bar{j} \qquad \text{(G-98)}$$

according to equation (G-22).

The transition angle ψ_{3T} is obtained by way of equation (G-39):

$$\psi_{3T} = 2 \tan^{-1} \frac{A_{3T} \pm \sqrt{A_{3T}^2 + B_{3T}^2 - C_{3T}^2}}{B_{3T} + C_{3T}} \qquad \text{(G-99)}$$

where

$$A_{3T} = \rho_{G3}\cos(\beta_3 + \alpha_{P3}) + f_{P3}\sin(\beta_3 + \alpha_{P3})$$

$$B_{3T} = -\rho_{G3}\sin(\beta_3 + \alpha_{P3}) + f_{P3}\cos(\beta_3 + \alpha_{P3})$$

$$C_{3T} = \frac{a_{G3}^2 - \rho_{G3}^2 - b_3^2 - f_{P3}^2}{2\, b_3}$$

The associated angle ϕ_{3T} may be obtained from equation (G-40) or from equation (G-41):

$$\phi_{3T} = \cos^{-1}\left[\frac{\rho_{G3}\sin(\psi_{3T} - \alpha_{P3}) + f_{P3}\cos(\psi_{3T} - \alpha_{P3}) + b_3\cos\beta_3}{a_{G3}}\right] - \delta_{G3} \qquad \text{(G-100)}$$

or

$$\phi_{3T} = \sin^{-1}\left[\frac{-\rho_{G3}\cos(\psi_{3T} - \alpha_{P3}) + f_{P3}\sin(\psi_{3T} - \alpha_{P3}) + b_3\sin\beta_3}{a_{G3}}\right] - \delta_{G3} \qquad \text{(G-101)}$$

Finally, the contact sensing equation is based on equations (G-44) - (G-46). Contact will occur, when

$$\sqrt{L_{x3}^2 + L_{y3}^2} \leq \rho_{G3} + \rho_{P3} \tag{G-102}$$

where with the tooth spacing angles $\Delta\phi_3$ and $\Delta\psi_3$,

$$L_{x3} = b_3\cos\beta_3 + a_{P3}\cos(\psi_3 - \Delta\psi_3 + \delta_{P3}) - a_{G3}\cos(\phi_3 + \Delta\phi_3 + \delta_{G3}) \tag{G-103}$$

and

$$L_{y3} = b_3\sin\beta_3 + a_{P3}\sin(\psi_3 - \Delta\psi_3 + \delta_{P3}) - a_{G3}\sin(\phi_3 + \Delta\phi_3 + \delta_{G3}) \tag{G-104}$$

APPENDIX H

MOMENT INPUT-OUTPUT RELATIONSHIPS FOR TWO AND THREE STEP-UP GEAR TRAINS WITH OGIVAL TEETH OPERATING IN A SPIN ENVIRONMENT

The following gives the derivations for the moment input-output relationships of two and three step-up gear trains which operate in a spin environment.

Figure G-1 of Appendix G shows the basic configuration of a three step-up gear train. The input moment M_{in}, which acts on gear no. 1, is held in equilibrium by the moment M_{o4} which acts on pinion no. 4.

Since in all three meshes there may either be round on round or round on flat type of contact, the force and moment analyses must account for various contact combinations. Table H-1 shows the eight different phase combinations which may occur in a three step-up gear train, and for which input-output relationships must be found. The two step-up gear train, which is shown in Figure A-10 of Appendix A for involute gearing, does not contain pinion 4 and gear no. 3. Here, the input moment M_{in}, which acts on gear no. 1, is held in equilibrium by moment M_{o3}, which acts on pinion no. 3.

Case no.	Mesh No. 3 (Gear 3 & Pinion 4)	Mesh No. 2 (Gear 2 & Pinion 3)	Mesh No. 1 (Gear 1 & Pinion 2)
1	R	R	R
2	R	R	F
3	R	F	F
4	R	F	R
5	F	F	F
6	F	F	R
7	F	R	R
8	F	R	F

TABLE H-1

POSSIBLE COMBINATIONS OF PHASES FOR THREE STEP-UP GEAR TRAIN AS SHOWN IN FIGURE G-1

R = Round on Round

F = Round on Flat

When ogival teeth are involved, there are four possible phase combinations of the two remaining meshes. These are shown in Table H-2. Again input-output relationships must be obtained for each of them.

Case No.	Mesh No. 2 (Gear 2 & Pinion 3)	Mesh No. 1 (Gear 1 & Pinion 2)
1	R	R
2	R	F
3	F	F
4	F	R

TABLE H-2

POSSIBLE COMBINATIONS OF PHASES FOR TWO STEP-UP GEAR TRAIN AS SHOWN IN FIGURE A-10
R = Round on Round
F = Round on Flat

The unit vectors, mechanism angles and kinematic terms necessary for the following analyses were derived in Appendix G. (See also Appendix D for a description of the geometry of ogival teeth.) Certain terms used in connection with mesh no. 3 may be obtained from expressions derived for mesh no. 1 in Appendix G by the replacement of the appropriate subscript numbers, since the kinematics of these meshes are identical. The following additional nomenclature is used:

$\mathcal{R}_i$ = distance from spin axis C to pivot points O_i of individual gears. (i = 1, 2, 3, 4 as applicalbe)

γ_i = angle of lines $\mathcal{R}_i = CO_i$ with respect to the body-fixed X-axis

ω = spin velocity of fuze body

m_i = mass of various gears, pinions and gear-pinion combinations

Q_i = $m_i \mathcal{R}_i \omega^2$, centrifugal force acting on individual gear components. (Now called Q_i to differentiate it from the pinion contact point T_i.)

ρ_i = pivot radius

ρ_{Pi} = radius of curvature of pinion tooth (ogival)

ρ_{Gi} = radius of curvature of gear tooth (ogival)

μ = coefficient of friction at pivots as well as at contact point between gears and pinions

The pivot friction moments are obtained according to equation (A-3b) of Appendix A. They always oppose motion regardless of the assumption of direction of the pivot reactions F_{xi} and F_{yi}. To this end the pivot forces $\tilde{F}_{xi}$ and $\tilde{F}_{yi}$, which represent the sums of the absolute values of their component parts, are added

algebraically. The algebraic addition of such modified reactions provides a conservative, i.e. a somewhat overstated friction moment.

The directions of the friction forces of the gears on the pinions are always those of the relative velocities $\bar{V}_{Si/Ti}$, where points S_i and T_i are located at the contact points of the gears and pinions respectively. This allows the introduction of a signum convention. For the round on round phases,

$$s_{iR} = \frac{V_{Si/Ti_R}}{\left|V_{Si/Ti_R}\right|} \qquad (H-1)$$

For the round on flat phase, the convention becomes:

$$s_{iF} = \frac{V_{Si/Ti_F}}{\left|V_{Si/Ti_F}\right|} \qquad (H-2)$$

The expressions for the above relative velocities, which are different for round on round and for round on flat, are given in Appendix G.

1. INPUT-OUTPUT ANALYSIS OF THREE STEP-UP GEAR TRAIN

a. CASE NO. 1: RRR

I. FORCE AND MOMENT EQUILIBRIA OF PINION NO. 4

Figure H-1 shows a schematic free body diagram of pinion no. 4 in the round on round mode of contact. The equivalent four-bar linkage associated with mesh no. 3 is also indicated. The pinion is acted upon by the equilibrant moment M_{o4} in the direction opposite to its counterclockwise rotation. The contact force of gear no. 3 on the pinion is given by:

$$\bar{F}_{34} = F_{34}\bar{n}_{\lambda 3} \tag{H-3}$$

The associated friction force exerted by the gear on the pinion has the direction of the relative velocity $\bar{V}_{S3/T3_R}$, as given by equation (G-92). With the use of the signum convention of equation (H-1) the friction force $\bar{F}_{f34}$ becomes:

$$\bar{F}_{f34} = \mu_{s_{3R}} F_{34}\bar{n}_{N\lambda 3} \tag{H-4}$$

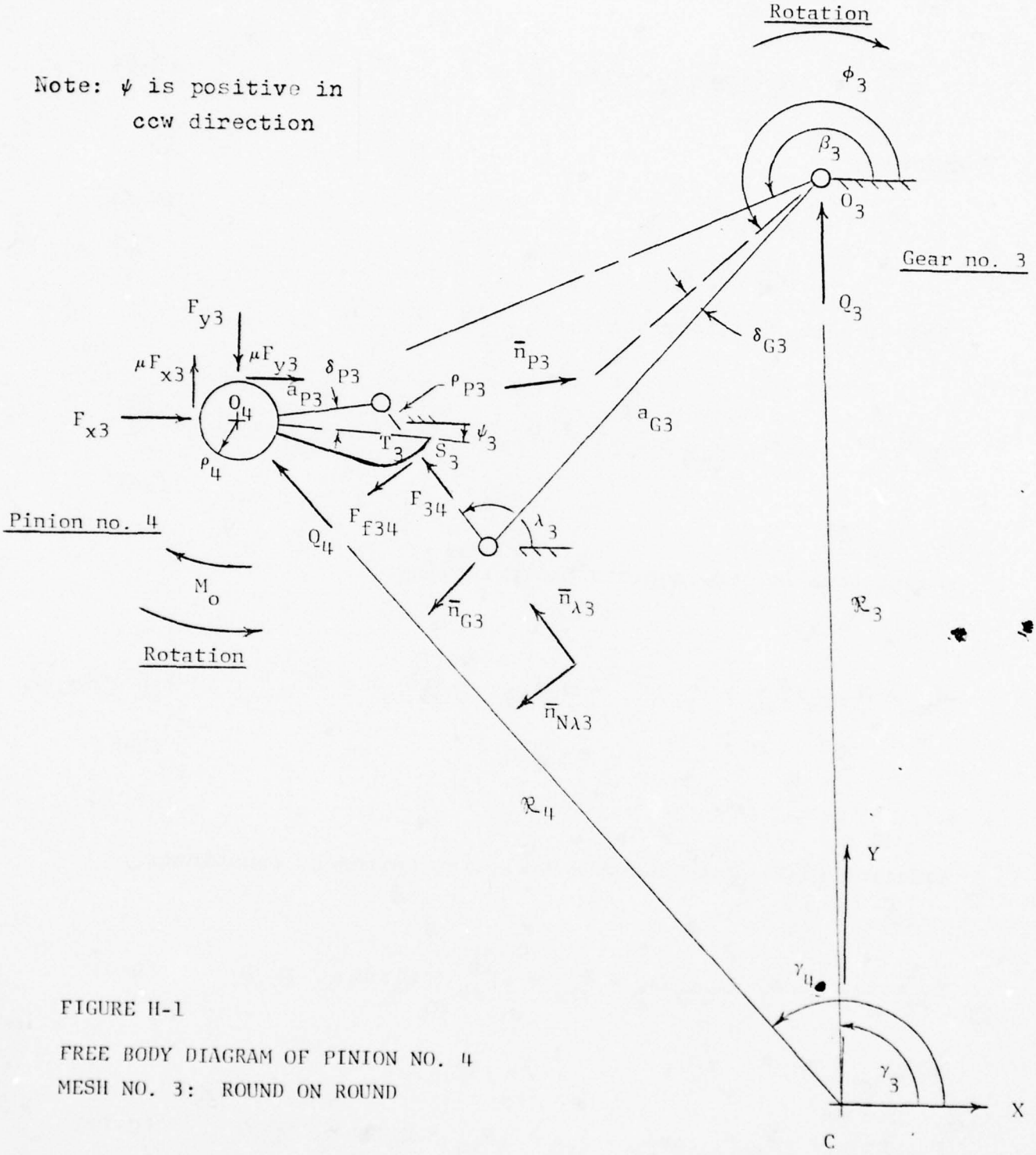

FIGURE H-1

FREE BODY DIAGRAM OF PINION NO. 4
MESH NO. 3: ROUND ON ROUND

The centrifugal force, due to the pinion mass, is given by:

$$\bar{Q}_4 = Q_4(\cos\gamma_4 \bar{i} + \sin\gamma_4 \bar{j}) \qquad \text{(H-5)}$$

where

$$Q_4 = \mathcal{R}_4 m_4 \omega^2 \qquad \text{(H-6)}$$

Force equilibrium is given by:

$$F_{34}\bar{n}_{\lambda 3} + \mu s_{3R} F_{34}\bar{n}_{N\lambda 3} + F_{x4}\bar{i} + \mu F_{y4}\bar{i} - F_{y4}\bar{j} + \mu F_{x4}\bar{j} + \bar{Q}_4 = 0 \qquad \text{(H-7)}$$

Moment equilibrium requires the following:

$$-M_{o4}\bar{k} - \mu\rho_4(\tilde{F}_{x4} + \tilde{F}_{y4})\bar{k} + (a_{P3}\bar{n}_{P3} - \rho_{P3}\bar{n}_{\lambda 3}) \times (F_{34}\bar{n}_{\lambda 3} + \mu s_{3R} F_{34}\bar{n}_{N\lambda 3}) = 0 \qquad \text{(H-8)}$$

Equation (H-7) furnishes the following component equations:

$$F_{34}\cos\lambda_3 - \mu s_{3R} F_{34}\sin\lambda_3 + F_{x4} + \mu F_{y4} + Q_4\cos\gamma_4 = 0 \qquad \text{(H-9)}$$

and

$$F_{34}\sin\lambda_3 + \mu s_{3R} F_{34}\cos\lambda_3 - F_{y4} + \mu F_{x4} + Q_4\sin\gamma_4 = 0 \qquad \text{(H-10)}$$

The scalar form of the moment equation becomes:

$$-M_{o4} - \mu\rho_4(\tilde{F}_{x4} + \tilde{F}_{y4}) - F_{34}\Big\{a_{P3}\Big[\sin(\psi_3 + \delta_{P3} - \lambda_3) - \mu s_{3R}\cos(\psi_3 + \delta_{P3} - \lambda_3)\Big] + \mu s_{3R}\rho_{P3}\Big\} = 0 \qquad \text{(H-11)}$$

Simultaneous solution of equations (H-9) and (H-10) for F_{x4} and F_{y4} gives:

$$F_{x4} = \frac{F_{34}\left[\mu(s_{3R} - 1)\sin\lambda_3 - (1 + \mu^2 s_{3R})\cos\lambda_3\right] - Q_4(\mu\sin\gamma_4 + \cos\gamma_4)}{1 + \mu^2} \qquad \text{(H-12)}$$

and

$$F_{y4} = \frac{F_{34}\left[(1 + \mu^2 s_{3R})\sin\lambda_3 + \mu(s_{3R} - 1)\cos\lambda_3\right] + Q_4(\sin\gamma_4 - \mu\cos\gamma_4)}{1 + \mu^2} \qquad \text{(H-13)}$$

The sum $\tilde{F}_{x4} + \tilde{F}_{y4}$ of equation (H-11) is now made up of equations (H-12) and (H-13) in the sense of equation (A-3b) of Appendix A:

$$\tilde{F}_{x4} + \tilde{F}_{y4} = Q_4 A_1 + F_{34} A_2 + Q_4 A_3 + F_{34} A_4 \qquad \text{(H-14)}$$

$$A_1 = \left| \frac{\mu \sin\gamma_4 + \cos\gamma_4}{1 + \mu^2} \right| \qquad \text{(H-15)}$$

$$A_2 = \left| \frac{\mu(s_{3R} - 1)\sin\lambda_3 - (1 + \mu^2 s_{3R})\cos\lambda_3}{1 + \mu^2} \right| \qquad \text{(H-16)}$$

$$A_3 = \left| \frac{\sin\gamma_4 - \mu\cos\gamma_4}{1 + \mu^2} \right| \qquad \text{(H-17)}$$

$$A_4 = \left| \frac{(1 + \mu^2 s_{3R})\sin\lambda_3 + \mu(s_{3R} - 1)\cos\lambda_3}{1 + \mu^2} \right| \qquad \text{(H-18)}$$

Equation (H-14) is now substituted into the moment equation (H-11) and the latter is solved for the contact force F_{34}:

$$F_{34} = \frac{M_{o4}}{C_2} + \frac{Q_4 C_1}{C_2} \qquad \text{(H-19)}$$

where

$$C_1 = \mu\rho_4(A_1 + A_3)$$

$$C_2 = a_{P3}\left[\mu s_{3R}\cos(\psi_3 + \delta_{P3} - \lambda_3) - \sin(\psi_3 + \delta_{P3} - \lambda_3)\right]$$

$$- \mu\left[\rho_{P3} s_{3R} + \rho_4(A_2 + A_4)\right]$$

II. FORCE AND MOMENT EQUILIBRIA OF GEAR AND PINION SET NO. 3

Figure H-2 gives a schematic free body diagram of the gear and pinion combination no. 3. Mesh no. 2 is also indicated to obtain the directions of the forces of gear no. 2 on pinion no. 3. The forces of pinion no. 4 on gear no. 3 are opposite to those given by equations (H-3) and (H-4) respectively. Thus, the contact force becomes:

$$\bar{F}_{43} = -\bar{F}_{34} = -F_{34}\bar{n}_{\lambda 3} \qquad \text{(H-20)}$$

The friction force of pinion no. 4 on gear no. 3 becomes:

$$\bar{F}_{f43} = -\bar{F}_{f34} = -\mu s_{3R} F_{34}\bar{n}_{N\lambda 3} \qquad \text{(H-21)}$$

The contact force of gear no. 2 on pinion no. 3 is given by:

$$\bar{F}_{23} = F_{23}\bar{n}_{\lambda 2} \qquad \text{(H-22)}$$

while the associated friction force of gear no. 2 on pinion no. 3 becomes:

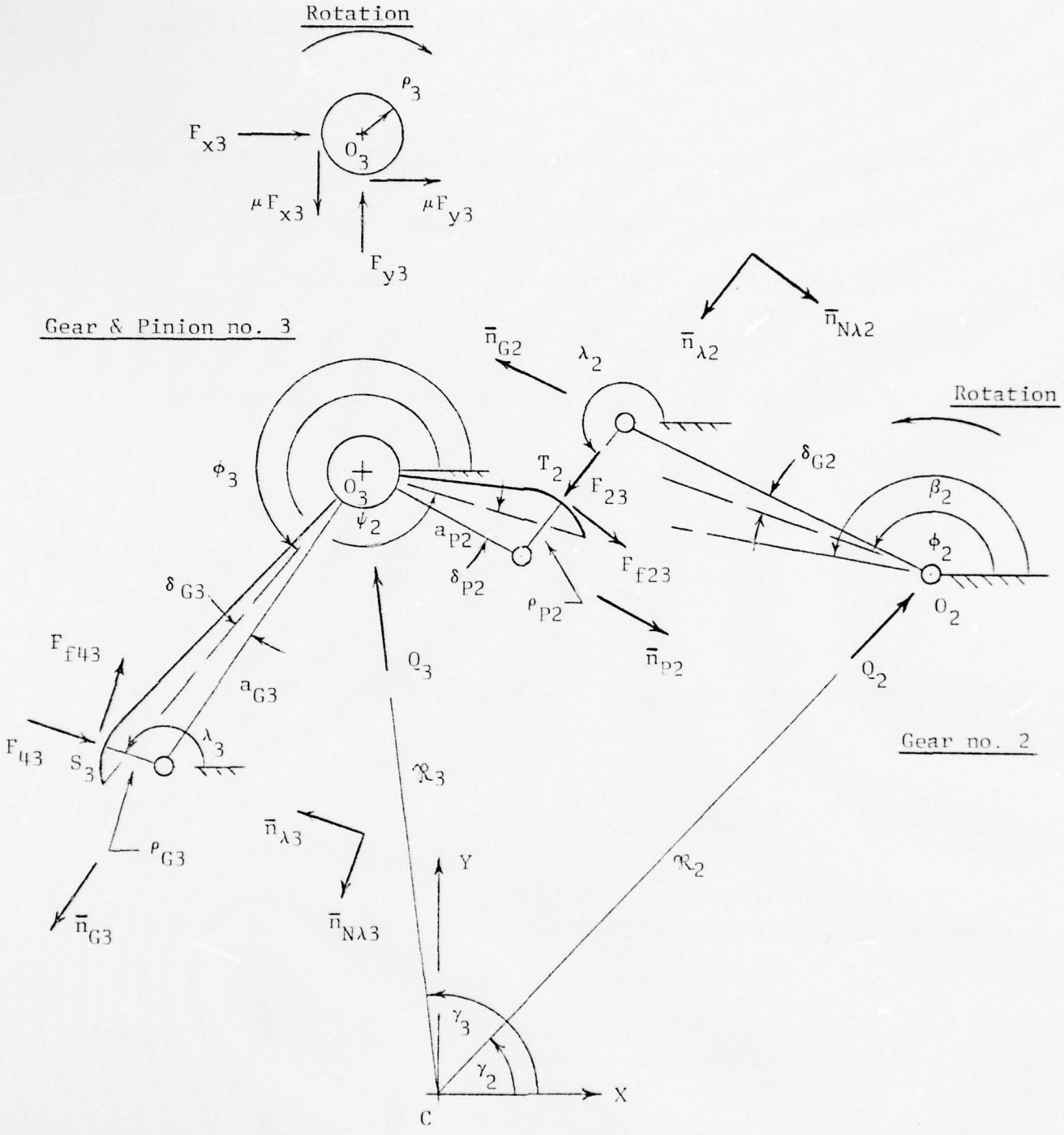

FIGURE H-2

FREE BODY DIAGRAM OF GEAR & PINION NO. 3
MESH NO. 3: ROUND ON ROUND
MESH NO. 2: ROUND ON ROUND

$$\bar{F}_{f23} = \mu s_{2R} F_{23} \bar{n}_{N\lambda 2} \qquad \text{(H-23)}$$

The pivot reactions F_{x3} and F_{y3} as well as the associated friction forces are drawn in a separate diagram in Figure H-2. As was the case earlier, the friction moment due to the friction forces again opposes rotation.

The centrifugal force, due to the mass of the combined gear and pinion no. 3, is given by:

$$\bar{Q}_3 = Q_3(\cos\gamma_3 \bar{i} + \sin\gamma_3 \bar{j}) \qquad \text{(H-24)}$$

where

$$Q_3 = \mathcal{R}_3 m_3 \omega^2 \qquad \text{(H-25)}$$

The force equilibrium of the combination is given by:

$$-F_{34}\bar{n}_{\lambda 3} - \mu s_{3R} F_{34} \bar{n}_{N\lambda 3} + F_{23}\bar{n}_{\lambda 2} + \mu s_{2R} F_{23} \bar{n}_{N\lambda 2} + F_{x3}\bar{i} + \mu F_{y3}\bar{i}$$

$$+ F_{y3}\bar{j} - \mu F_{x3}\bar{j} + \bar{Q}_3 = 0 \qquad \text{(H-26)}$$

The moment equation is given by:

$$\mu\rho_3(\tilde{F}_{x3} + \tilde{F}_{y3})\bar{k} + \left[a_{G3}\bar{n}_{G3} + \rho_{G3}\bar{n}_{\lambda 3}\right] \times \left[-F_{34}\bar{n}_{\lambda 3} - \mu s_{3R}F_{34}\bar{n}_{N\lambda 3}\right]$$

$$+ \left[a_{P2}\bar{n}_{P2} - \rho_{P2}\bar{n}_{\lambda 2}\right] \times \left[F_{23}\bar{n}_{\lambda 2} + \mu s_{2R}F_{23}\bar{n}_{N\lambda 2}\right] = 0 \qquad \text{(H-27)}$$

Equation (H-26) gives the following component expressions:

$$-F_{34}\cos\lambda_3 + \mu s_{3R}F_{34}\sin\lambda_3 + Q_3\cos\gamma_3 + F_{x3} + \mu F_{y3} + F_{23}\cos\lambda_2$$

$$- \mu s_{2R}F_{23}\sin\lambda_2 = 0 \qquad \text{(H-28)}$$

and

$$-F_{34}\sin\lambda_3 - \mu s_{3R}F_{34}\cos\lambda_3 + Q_3\sin\gamma_3 + F_{y3} - \mu F_{x3} + F_{23}\sin\lambda_2$$

$$+ \mu s_{2R}F_{23}\cos\lambda_2 = 0 \qquad \text{(H-29)}$$

The scalar form of the moment equation (H-27) becomes:

$$\mu\rho_3(\tilde{F}_{x3} + \tilde{F}_{y3}) - \mu s_{3R}\rho_{G3}F_{34} - \mu s_{2R}\rho_{P2}F_{23} + a_{G3}F_{34}\left[\sin(\phi_3 + \delta_{G3} - \lambda_3)\right.$$

$$\left. - \mu s_{3R}\cos(\phi_3 + \delta_{G3} - \lambda_3)\right] + a_{P2}F_{23}\left[-\sin(\psi_2 - \delta_{P2} - \lambda_2)\right.$$

$$\left. + \mu s_{2R}\cos(\psi_2 - \delta_{P2} - \lambda_2)\right] = 0 \qquad \text{(H-30)}$$

Simultaneous solution of equations (H-28) and (H-29) for the pivot reactions F_{x3} and F_{y3} gives:

$$F_{x3} = \frac{1}{1 + \mu^2}\left\{F_{34}\left[(1 - \mu^2 s_{3R})\cos\lambda_3 - \mu(1 + s_{3R})\sin\lambda_3\right] + F_{23}\left[\mu(1 + s_{2R})\sin\lambda_2 - (1 - \mu^2 s_{2R})\cos\lambda_2\right] + Q_3\left[\mu\sin\gamma_3 - \cos\gamma_3\right]\right\} \quad \text{(H-31)}$$

and

$$F_{y3} = \frac{1}{1 + \mu^2}\left\{F_{34}\left[(1 - \mu^2 s_{3R})\sin\lambda_3 + \mu(1 + s_{3R})\cos\lambda_3\right] + F_{23}\left[(\mu^2 s_{2R} - 1)\sin\lambda_2 - \mu(1 + s_{2R})\cos\lambda_2\right] - Q_3\left[\sin\gamma_3 + \mu\cos\gamma_3\right]\right\} \quad \text{(H-32)}$$

The sum $\tilde{F}_{x3} + \tilde{F}_{y3}$ of equation (H-30) is now made up of equations (H-31) and (H-32) in the sense of equation (A-3b):

$$\tilde{F}_{x3} + \tilde{F}_{y3} = F_{34}A_5 + F_{23}A_6 + Q_3A_7 + F_{34}A_8 + F_{23}A_9 + Q_3A_{10} \quad \text{(H-33)}$$

where

$$A_5 = \left| \frac{(1 - \mu^2 s_{3R})\cos\lambda_3 - \mu(1 + s_{3R})\sin\lambda_3}{1 + \mu^2} \right| \qquad \text{(H-34)}$$

$$A_6 = \left| \frac{\mu(1 + s_{2R})\sin\lambda_2 - (1 - \mu^2 s_{2R})\cos\lambda_2}{1 + \mu^2} \right| \qquad \text{(H-35)}$$

$$A_7 = \left| \frac{\mu\sin\gamma_3 - \cos\gamma_3}{1 + \mu^2} \right| \qquad \text{(H-36)}$$

$$A_8 = \left| \frac{(1 - \mu^2 s_{3R})\sin\lambda_3 + \mu(1 + s_{3R})\cos\lambda_3}{1 + \mu^2} \right| \qquad \text{(H-37)}$$

$$A_9 = \left| \frac{(\mu^2 s_{2R} - 1)\sin\lambda_2 - \mu(1 + s_{2R})\cos\lambda_2}{1 + \mu^2} \right| \qquad \text{(H-38)}$$

$$A_{10} = \left| \frac{\sin\gamma_3 + \mu\cos\gamma_3}{1 + \mu^2} \right| \qquad \text{(H-39)}$$

Equation (H-33) is now substituted into equation (H-30) and the resulting expression is solved for the contact force F_{23}. Thus,

$$F_{23} = \frac{- F_{34}C_3 - Q_3C_4}{C_5} \qquad \text{(H-40)}$$

where

$$C_3 = \mu\rho_3(A_5 + A_8) - \mu s_{3R}\rho_{G3} + a_{G3}\left[\sin(\phi_3 + \delta_{G3} - \lambda_3) - \mu s_{3R}\cos(\phi_3 + \delta_{G3} - \lambda_3)\right]$$

$$C_4 = \mu\rho_3(A_7 + A_{10})$$

$$C_5 = \mu\rho_3(A_6 + A_9) - \mu s_{2R}\rho_{P2} + a_{P2}\left[\mu s_{2R}\cos(\psi_2 - \delta_{P2} - \lambda_2) - \sin(\psi_2 - \delta_{P2} - \lambda_2)\right]$$

III. FORCE AND MOMENT EQUILIBRIA OF GEAR AND PINION SET NO. 2

Figure H-3 gives the free body diagram of the gear and pinion combination no. 2. In addition, mesh no. 1 is indicated to obtain the directions of the forces of gear no. 1 on pinion no. 2.

The forces of pinion no. 3 on gear no. 2 have directions opposite to those given by equation (H-22) and (H-23) respectively. Thus, the normal force is given by:

$$\bar{F}_{32} = - F_{23}\bar{n}_{\lambda 2} \qquad \text{(H-41)}$$

The friction force of pinion no. 3 on gear no. 2 becomes:

$$\bar{F}_{f32} = - \mu s_{2R} F_{23}\bar{n}_{N\lambda 2} \qquad \text{(H-42)}$$

The contact force of gear no. 1 on pinion no. 2 is given by:

$$\bar{F}_{12} = F_{12}\bar{n}_{\lambda 1} \qquad \text{(H-43)}$$

while the associated friction force of gear no. 1 on pinion no. 2 becomes:

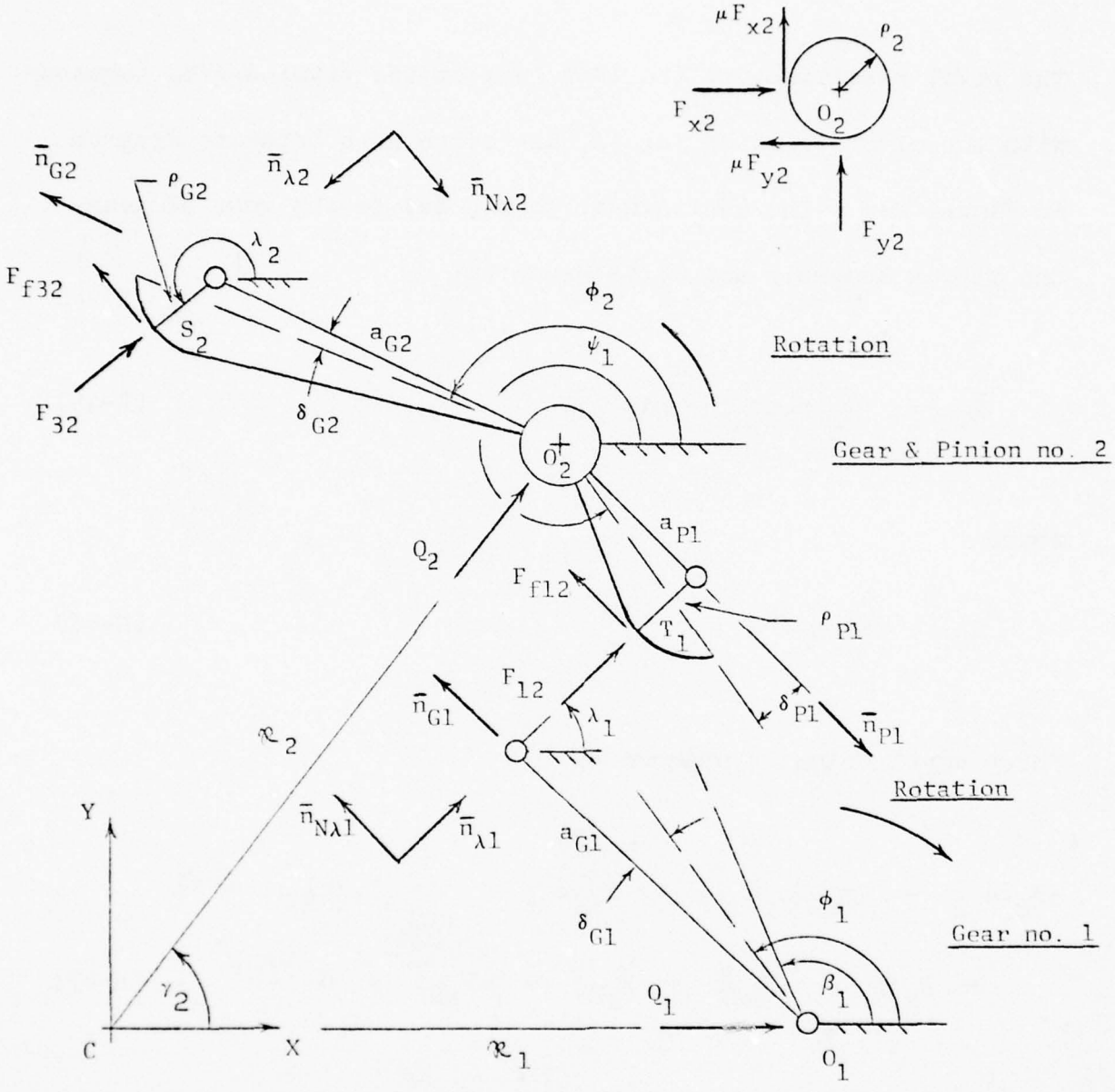

FIGURE H-3

FREE BODY DIAGRAM OF GEAR & PINION NO. 2

MESH NO. 2: ROUND ON ROUND

MESH NO. 1: ROUND ON ROUND

$$\bar{F}_{f12} = \mu s_{1R} F_{12} \bar{n}_{N\lambda 1} \qquad \text{(H-44)}$$

The pivot reactions, of the fuze body on the pivot shaft, together with the pivot friction forces, are shown in a separate diagram in Figure H-3. The centrifugal force, due to the mass of gear and pinion assembly no. 2, is given by:

$$\bar{Q}_2 = Q_2(\cos\gamma_2 \bar{i} + \sin\gamma_2 \bar{j}) \qquad \text{(H-45)}$$

where

$$Q_2 = \mathcal{R}_2 m_2 \omega^2 \qquad \text{(H-46)}$$

Force equilibrium is assured by:

$$-F_{23}\bar{n}_{\lambda 2} - \mu s_{2R} F_{23} \bar{n}_{N\lambda 2} + F_{12}\bar{n}_{\lambda 1} + \mu s_{1R} F_{12} \bar{n}_{N\lambda 1} + \bar{Q}_2 + F_{x2}\bar{i} - \mu F_{y2}\bar{i} + F_{y2}\bar{j} + \mu F_{x2}\bar{j} = 0 \qquad \text{(H-47)}$$

Moment equilibrium must satisfy:

$$-\mu\rho_2(\tilde{F}_{x2} + \tilde{F}_{y2})\bar{k} + \left[a_{G2}\bar{n}_{G2} + \rho_{G2}\bar{n}_{\lambda 2}\right] \times \left[-F_{23}\bar{n}_{\lambda 2} - \mu s_{2R}F_{23}\bar{n}_{N\lambda 2}\right]$$

$$+ \left[a_{P1}\bar{n}_{P1} - \rho_{P1}\bar{n}_{\lambda 1}\right] \times \left[F_{12}\bar{n}_{\lambda 1} + \mu s_{1R}F_{12}\bar{n}_{N\lambda 1}\right] = 0 \qquad \text{(H-48)}$$

Equation (H-47) gives the following component expressions:

$$-F_{23}\cos\lambda_2 + \mu s_{2R}F_{23}\sin\lambda_2 + F_{12}\cos\lambda_1 - \mu s_{1R}F_{12}\sin\lambda_1$$

$$+ Q_2\cos\gamma_2 + F_{x2} - \mu F_{y2} = 0 \qquad \text{(H-49)}$$

and

$$-F_{23}\sin\lambda_2 - \mu s_{2R}F_{23}\cos\lambda_2 + F_{12}\sin\lambda_1 + \mu s_{1R}F_{12}\cos\lambda_1$$

$$+ Q_2\sin\gamma_2 + F_{y2} + \mu F_{x2} = 0 \qquad \text{(H-50)}$$

The scalar form of the moment equation (H-48) becomes:

$$-\mu\rho_2(\tilde{F}_{x2} + \tilde{F}_{y2}) + a_{G2}F_{23}\left[\sin(\phi_2 - \delta_{G2} - \lambda_2) - \mu s_{2R}\cos(\phi_2 - \delta_{G2} - \lambda_2)\right]$$

$$- \mu s_{2R}\rho_{G2}F_{23} + a_{P1}F_{12}\left[-\sin(\psi_1 + \delta_{P1} - \lambda_1) + \mu s_{1R}\cos(\psi_1 + \delta_{P1} - \lambda_1)\right]$$

$$- \mu s_{1R}\rho_{P1}F_{12} = 0 \qquad \text{(H-51)}$$

Simultaneous solution of equations (H-49) and (H-50) for F_{x2} and F_{y2} leads to:

$$F_{x2} = \frac{1}{1 + \mu^2}\left\{F_{23}\left[(1 + \mu^2 s_{2R})\cos\lambda_2 - \mu(s_{2R} - 1)\sin\lambda_2\right]\right.$$

$$+ F_{12}\left[\mu(s_{1R} - 1)\sin\lambda_1 - (1 + \mu^2 s_{1R})\cos\lambda_1\right]$$

$$\left. + Q_2\left[-\cos\gamma_2 - \mu\sin\gamma_2\right]\right\} \qquad \text{(H-52)}$$

and

$$F_{y2} = \frac{1}{1 + \mu^2}\left\{F_{23}\left[(1 + \mu^2 s_{2R})\sin\lambda_2 - \mu(1 - s_{2R})\cos\lambda_2\right]\right.$$

$$+ F_{12}\left[\mu(1 - s_{1R})\cos\lambda_1 - (1 + \mu^2 s_{1R})\sin\lambda_1\right]$$

$$\left. + Q_2\left[\mu\cos\gamma_2 - \sin\gamma_2\right]\right\} \qquad \text{(H-53)}$$

The sum of $\tilde{F}_{x2}$ and $\tilde{F}_{y2}$ of equation (H-51) is now made up of equations (H-52) and (H-53) in the sense of equation (A-3b) of Appendix A:

$$\tilde{F}_{x2} + \tilde{F}_{y2} = F_{23}A_{11} + F_{12}A_{12} + Q_2A_{13} + F_{23}A_{14} + F_{12}A_{15} + Q_2A_{16} \tag{H-54}$$

where

$$A_{11} = \left| \frac{(1 + \mu^2 s_{2R})\cos\lambda_2 - \mu(s_{2R} - 1)\sin\lambda_2}{1 + \mu^2} \right| \tag{H-55}$$

$$A_{12} = \left| \frac{\mu(s_{1R} - 1)\sin\lambda_1 - (1 + \mu^2 s_{1R})\cos\lambda_1}{1 + \mu^2} \right| \tag{H-56}$$

$$A_{13} = \left| \frac{-\cos\gamma_2 - \mu\sin\gamma_2}{1 + \mu^2} \right| \tag{H-57}$$

$$A_{14} = \left| \frac{(1 + \mu^2 s_{2R})\sin\lambda_2 - \mu(1 - s_{2R})\cos\lambda_2}{1 + \mu^2} \right| \tag{H-58}$$

$$A_{15} = \left| \frac{\mu(1 - s_{1R})\cos\lambda_1 - (1 + \mu^2 s_{1R})\sin\lambda_1}{1 + \mu^2} \right| \tag{H-59}$$

$$A_{16} = \left| \frac{\mu \cos\gamma_2 - \sin\gamma_2}{1 + \mu^2} \right| \qquad \text{(H-60)}$$

Equation (H-54) is now substituted into the moment equation (H-51). The resulting expression is then solved for the contact force F_{12}:

$$F_{12} = \frac{- F_{23}C_6 + Q_2C_7}{C_8} \qquad \text{(H-61)}$$

where

$$C_6 = a_{G2}\left[\sin(\phi_2 - \delta_{G2} - \lambda_2) - \mu s_{2R}\cos(\phi_2 - \delta_{G2} - \lambda_2)\right] - \mu\rho_2(A_{11} + A_{14}) - \mu s_{2R}\rho_{G2}$$

$$C_7 = \mu\rho_2(A_{13} + A_{16})$$

$$C_8 = -\left\{a_{P1}\left[\sin(\psi_1 + \delta_{P1} - \lambda_1) - \mu s_{1R}\cos(\psi_1 + \delta_{P1} - \lambda_1)\right] + \mu\rho_2(A_{12} + A_{15}) + \mu s_{1R}\rho_{P1}\right\}$$

IV. FORCE AND MOMENT EQUILIBRIA OF INPUT GEAR NO. 1

Figure H-4 represents the free body diagram of the input gear no. 1 which has the input moment M_{in} acting on it.

The forces of pinion no. 2 on gear no. 1 are given according to equations (H-43) and (H-44):

$$\bar{F}_{21} = - F_{12}\bar{n}_{\lambda 1} \tag{H-62}$$

and

$$\bar{F}_{f21} = - \mu s_{1R} F_{12}\bar{n}_{N\lambda 1} \tag{H-63}$$

The moments due to the friction forces on the pivot oppose rotation as indicated.

The centrifugal force, due to the mass of gear no. 1, is given by:

$$\bar{Q}_1 = Q_1\bar{i} \tag{H-64}$$

where

$$Q_1 = \mathcal{R}_1 m_1 \omega^2 \tag{H-65}$$

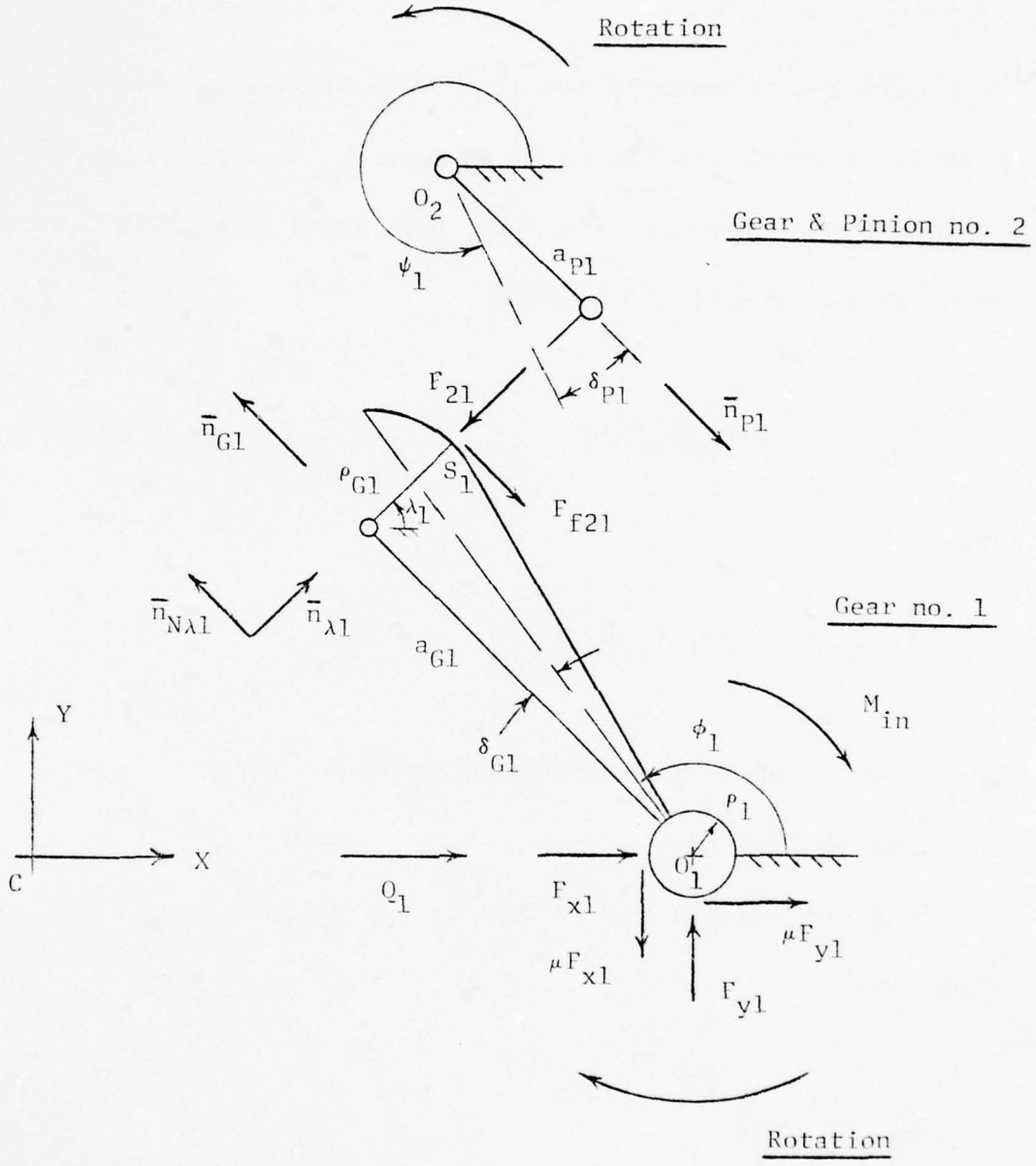

FIGURE H-4

FREE BODY DIAGRAM OF GEAR NO. 1
MESH NO. 1: ROUND ON ROUND

Force equilibrium requires, that:

$$-F_{12}\bar{n}_{\lambda 1} - \mu s_{1R}F_{12}\bar{n}_{N\lambda 1} + \bar{Q}_1 + F_{x1}\bar{i} + \mu F_{y1}\bar{i} + F_{y1}\bar{j} - \mu F_{x1}\bar{j} = 0 \qquad \text{(H-66)}$$

Moment equilibrium is given by:

$$\mu\rho_1(\tilde{F}_{x1} + \tilde{F}_{y1})\bar{k} - M_{in}\bar{k} + \left[a_{G1}\bar{n}_{G1} + \rho_{G1}\bar{n}_{\lambda 1}\right] \times \left[-F_{12}\bar{n}_{\lambda 1} - \mu s_{1R}F_{12}\bar{n}_{N\lambda 1}\right] = 0 \qquad \text{(H-67)}$$

Equation (H-66) furnishes the following component equations:

$$-F_{12}\cos\lambda_1 + \mu s_{1R}F_{12}\sin\lambda_1 + Q_1 + F_{x1} + \mu F_{y1} = 0 \qquad \text{(H-68)}$$

and

$$-F_{12}\sin\lambda_1 - \mu s_{1R}F_{12}\cos\lambda_1 + F_{y1} - \mu F_{x1} = 0 \qquad \text{(H-69)}$$

The scalar form of equation (H-67) becomes:

$$\mu\rho_1(\tilde{F}_{x1} + \tilde{F}_{y1}) - M_{in} + a_{G1}F_{12}\left[\sin(\phi_1 + \delta_{G1} - \lambda_1) - \mu s_{1R}\cos(\phi_1 + \delta_{G1} - \lambda_1)\right] - \mu s_{1R}\rho_{G1}F_{12} = 0 \qquad \text{(H-70)}$$

The simultaneous solution of equations (H-68) and (H-69) furnishes:

$$F_{x1} = \frac{1}{1 + \mu^2}\left\{F_{12}\left[(1 - \mu^2 s_{1R})\cos\lambda_1 - \mu(1 + s_{1R})\sin\lambda_1\right] - Q_1\right\} \tag{H-71}$$

and

$$F_{y1} = \frac{1}{1 + \mu^2}\left\{F_{12}\left[(1 - \mu^2 s_{1R})\sin\lambda_1 + \mu(1 + s_{1R})\cos\lambda_1\right] - \mu Q_1\right\} \tag{H-72}$$

Then, with the same reasoning as before:

$$\tilde{F}_{x1} + \tilde{F}_{y1} = F_{12}A_{17} + Q_1A_{18} + F_{12}A_{19} + Q_1A_{20} \tag{H-73}$$

where

$$A_{17} = \left|\frac{(1 - \mu^2 s_{1R})\cos\lambda_1 - \mu(1 + s_{1R})\sin\lambda_1}{1 + \mu^2}\right| \tag{H-74}$$

$$A_{18} = \left|\frac{1}{1 + \mu^2}\right| \tag{H-75}$$

$$A_{19} = \left| \frac{(1 - \mu^2 s_{1R})\sin\lambda_1 + \mu(1 + s_{1R})\cos\lambda_1}{1 + \mu^2} \right| \qquad \text{(H-76)}$$

$$A_{20} = \left| \frac{\mu}{1 + \mu^2} \right| \qquad \text{(H-77)}$$

Equation (H-73) is now substituted into equation (H-70) and the result is solved for the contact force F_{12}:

$$F_{12} = \frac{M_{in} - Q_1 C_9}{C_{10}} \qquad \text{(H-78)}$$

where

$$C_9 = \mu\rho_1(A_{18} + A_{20})$$

$$C_{10} = \mu\rho_1(A_{17} + A_{19}) + a_{G1}\left[\sin(\phi_1 + \delta_{G1} - \lambda_1) - \mu s_{1R}\cos(\phi_1 + \delta_{G1} - \lambda_1)\right] - \mu s_{1R}\rho_{G1}$$

V. MOMENT INPUT-OUTPUT RELATIONSHIP

Equations (H-61) and (H-78), which are both expressions in F_{12}, are now set equal to each other and the result is solved for F_{23}:

$$F_{23} = \frac{-C_8}{C_6 C_{10}} (M_{in} - Q_1 C_9) + \frac{C_7}{C_6} Q_2 \qquad \text{(H-79)}$$

The above is now equated to equation (H-40) and the result is solved for F_{34}:

$$F_{34} = \frac{C_5 C_8 (M_{in} - Q_1 C_9) - C_5 C_{10} C_7 Q_2 - C_4 C_6 C_{10} Q_3}{C_3 C_6 C_{10}} \qquad \text{(H-80)}$$

Finally equation (H-80) is equated to equation (H-19). This permits the determination of the equilibrant moment M_{o41}:

(for case no. 1: RRR)

$$M_{o41} = M_{in} \frac{C_2 C_5 C_8}{C_3 C_6 C_{10}} - Q_1 \frac{C_2 C_5 C_8 C_9}{C_3 C_6 C_{10}} - Q_2 \frac{C_2 C_5 C_7}{C_3 C_6} - Q_3 \frac{C_2 C_4}{C_3} - Q_4 C_1$$

(H-81)

b. CASE NO. 2: RRF

Since only mesh 1 is now assumed to be in the round on flat phase of motion, the forces F_{34} and F_{23} remain as given by equations (H-19) and (H-40) respectively.

I. FORCE AND MOMENT EQUILIBRIA OF GEAR AND PINION SET NO. 2

Figure H-5 shows the free body diagram of the gear and pinion set with the necessary portions of mesh no. 1.

The forces of pinion no. 3 on gear no. 2 are given by equations (H-41) and (H-42), i.e.:

$$\bar{F}_{32} = - F_{23}\bar{n}_{\lambda 2} \tag{H-82}$$

and

$$\bar{F}_{f32} = - \mu s_{2R} F_{23}\bar{n}_{N\lambda 2} \tag{H-83}$$

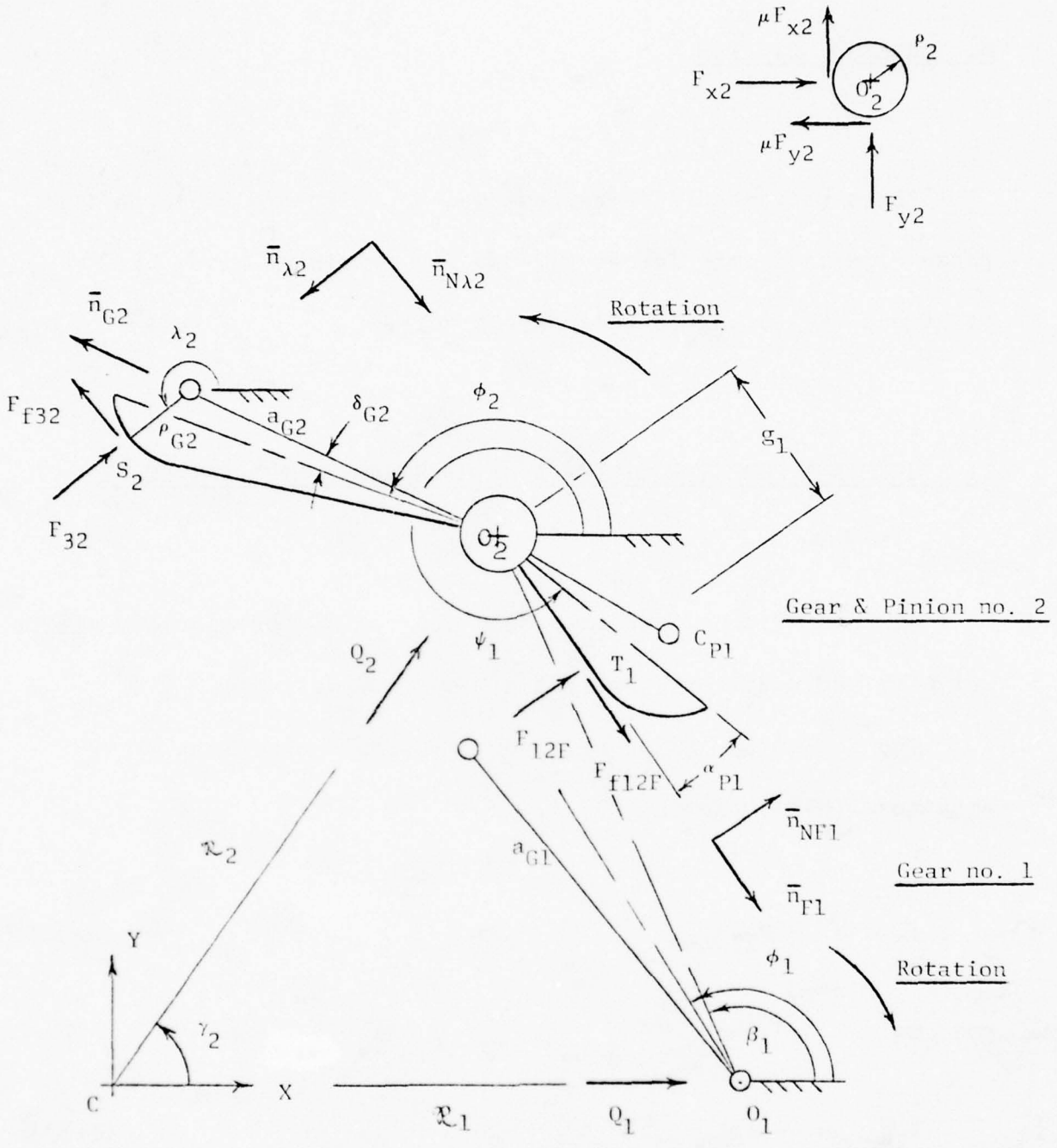

FIGURE H-5

FREE BODY DIAGRAM OF GEAR & PINION NO. 2

MESH NO. 2: ROUND ON ROUND

MESH NO. 1: ROUND ON FLAT

The contact force of gear no. 1 on pinion no. 2 is now given by:

$$\bar{F}_{12F} = F_{12F}\bar{n}_{NF1} \tag{H-84}$$

(Note that the additional subscript F is introduced to distinguish round on flat from round on round contact.)

The associated friction force is given by:

$$\bar{F}_{f12F} = \mu s_{1F} F_{12F}\bar{n}_{F1} \tag{H-85}$$

(See equation (H-2) for s_{1F}.)

The pivot reactions, together with the pivot friction forces, are shown in a separate diagram in Figure H-5. As before, the pivot friction moments oppose rotation.

The centrifugal force $\bar{Q}_2$ is again given by equations (H-45) and (H-46).

Force equilibrium is given by:

$$-F_{23}\bar{n}_{\lambda 2} - \mu s_{2R} F_{23}\bar{n}_{N\lambda 2} + F_{12F}\bar{n}_{NF1} + \mu s_{1F} F_{12F}\bar{n}_{F1} + \bar{Q}_2$$

$$+ F_{x2}\bar{i} - \mu F_{y2}\bar{i} + F_{y2}\bar{j} + \mu F_{x2}\bar{j} = 0 \tag{H-86}$$

Moment equilibrium about point O_2 requires:

$$-\mu\rho_2(\tilde{F}_{x2} + \tilde{F}_{y2})\bar{k} + \left[a_{G2}\bar{n}_{G2} + \rho_{G2}\bar{n}_{\lambda 2}\right] \times \left[-F_{23}\bar{n}_{\lambda 2} - \mu s_{2R}F_{23}\bar{n}_{N\lambda 2}\right]$$

$$+ s_1\bar{n}_{F1} \times F_{12F}\bar{n}_{NF1} = 0 \qquad \text{(H-87)}$$

Note that since the line of action of the friction force F_{f12F} passes through point O_2, this friction force exerts no moment about point O_2.

Equation (H-86) furnishes the following component equations:

$$-F_{23}\cos\lambda_2 + \mu s_{2R}F_{23}\sin\lambda_2 - F_{12F}\sin(\psi_1 - \alpha_{P1}) + \mu s_{1F}F_{12F}\cos(\psi_1 - \alpha_{P1})$$

$$+ F_{x2} - \mu F_{y2} + Q_2\cos\gamma_2 = 0 \qquad \text{(H-88)}$$

and

$$-F_{23}\sin\lambda_2 - \mu s_{2R}F_{23}\cos\lambda_2 + F_{12F}\cos(\psi_1 - \alpha_{P1}) + \mu s_{1F}F_{12F}\sin(\psi_1 - \alpha_{P1})$$

$$+ F_{y2} + \mu F_{x2} + Q_2\sin\gamma_2 = 0 \qquad \text{(H-89)}$$

The scalar form of the moment equation (H-87) becomes:

$$-\mu\rho_2(\tilde{F}_{x2} + \tilde{F}_{y2}) + a_{G2}F_{23}\left[\sin(\phi_2 - \delta_{G2} - \lambda_2) - \mu s_{2R}\cos(\phi_2 - \delta_{G2} - \lambda_2)\right]$$

$$- \mu s_{2R}\rho_{G2}F_{23} + F_{12F}S_1 = 0 \qquad \text{(H-90)}$$

Simultaneous solution of these component equations for F_{x2} and F_{y2} leads to:

$$F_{x2} = \frac{1}{1 + \mu^2}\left\{F_{23}\left[\mu(1 - s_{2R})\sin\lambda_2 + (1 + \mu^2 s_{2R})\cos\lambda_2\right]\right.$$

$$+ F_{12F}\left[(1 - \mu^2 s_{1F})\sin(\psi_1 - \alpha_{P1}) - \mu(1 + s_{1F})\cos(\psi_1 - \alpha_{P1})\right]$$

$$\left. - Q_2\left[\mu\sin\gamma_2 + \cos\gamma_2\right]\right\} \qquad \text{(H-91)}$$

and

$$F_{y2} = \frac{1}{1 + \mu^2}\left\{F_{23}\left[(1 + \mu^2 s_{2R})\sin\lambda_2 - \mu(1 - s_{2R})\cos\lambda_2\right]\right.$$

$$+ F_{12F}\left[-\mu(1 + s_{1F})\sin(\psi_1 - \alpha_{P1}) + (\mu^2 s_{1F} - 1)\cos(\psi_1 - \alpha_{P1})\right]$$

$$\left. + Q_2\left[-\sin\gamma_2 + \mu\cos\gamma_2\right]\right\} \qquad \text{(H-92)}$$

The sum $(\tilde{F}_{x2} + \tilde{F}_{y2})$ of equation (H-90) is now made up of equations (H-91) and (H-92) in the sense of equation (A-3b) of Appendix A:

$$\tilde{F}_{x2} + \tilde{F}_{y2} = F_{23}A_{21} + F_{12F}A_{22} + Q_2A_{23} + F_{23}A_{24} + F_{12F}A_{25} + Q_2A_{26} \tag{H-93}$$

where

$$A_{21} = \left| \frac{\mu(1 - s_{2R})\sin\lambda_2 + (1 + \mu^2 s_{2R})\cos\lambda_2}{\lambda_1 + \mu^2} \right| \tag{H-94}$$

$$A_{22} = \left| \frac{(1 - \mu^2 s_{1F})\sin(\psi_1 - \alpha_{P1}) - \mu(1 + s_{1F})\cos(\psi_1 - \alpha_{P1})}{1 + \mu^2} \right| \tag{H-95}$$

$$A_{23} = \left| \frac{\mu\sin\gamma_2 + \cos\gamma_2}{1 + \mu^2} \right| \tag{H-96}$$

$$A_{24} = \left| \frac{(1 + \mu^2 s_{2R})\sin\lambda_2 - \mu(1 - s_{2R})\cos\lambda_2}{1 + \mu^2} \right| \tag{H-97}$$

$$A_{25} = \left| \frac{-\mu(1 + s_{1F})\sin(\psi_1 - \alpha_{P1}) + (\mu^2 s_{1F} - 1)\cos(\psi_1 - \alpha_{P1})}{1 + \mu^2} \right| \tag{H-98}$$

$$A_{26} = \left| \frac{-\sin\gamma_2 + \mu\cos\gamma_2}{1 + \mu^2} \right| \qquad \text{(H-99)}$$

Equation (H-93) is now substituted into equation (H-90), and the resulting expression is solved for the contact force F_{12F}:

$$F_{12F} = \frac{-F_{23}C_{11} + Q_2C_{12}}{C_{13}} \qquad \text{(H-100)}$$

where

$$C_{11} = a_{G2}\left[\sin(\phi_2 - \delta_{G2} - \lambda_2) - \mu s_{2R}\cos(\phi_2 - \delta_{G2} - \lambda_2)\right] - \mu\rho_2(A_{21} + A_{24}) - \mu s_{2R}\rho_{G2}$$

$$C_{12} = \mu\rho_2(A_{23} + A_{26})$$

$$C_{13} = g_1 - \mu\rho_2(A_{22} + A_{25})$$

II. FORCE AND MOMENT EQUILIBRIA OF INPUT GEAR NO. 1

Figure H-6 represents the free body diagram of input gear no. 1.

The forces of pinion no. 2 on this gear are given according to equations (H-84) and (H-85):

$$\bar{F}_{21F} = - F_{12F}\bar{n}_{NF1} \tag{H-101}$$

and

$$\bar{F}_{f21F} = -\mu s_{1F} F_{12F}\bar{n}_{F1} \tag{H-102}$$

The moments due to the pivot friction forces oppose the indicated rotation due to the moment M_{in}.

The centrifugal force $\bar{Q}_1$ has been defined by equations (H-64) and (H-65).

The force equilibrium equation is given by:

$$-F_{12F}\bar{n}_{NF1} - \mu s_{1F} F_{12F}\bar{n}_{F1} + Q_1\bar{i} + F_{x1}\bar{i} + \mu F_{y1}\bar{i} + F_{y1}\bar{j} - \mu F_{x1}\bar{j} = 0 \tag{H-103}$$

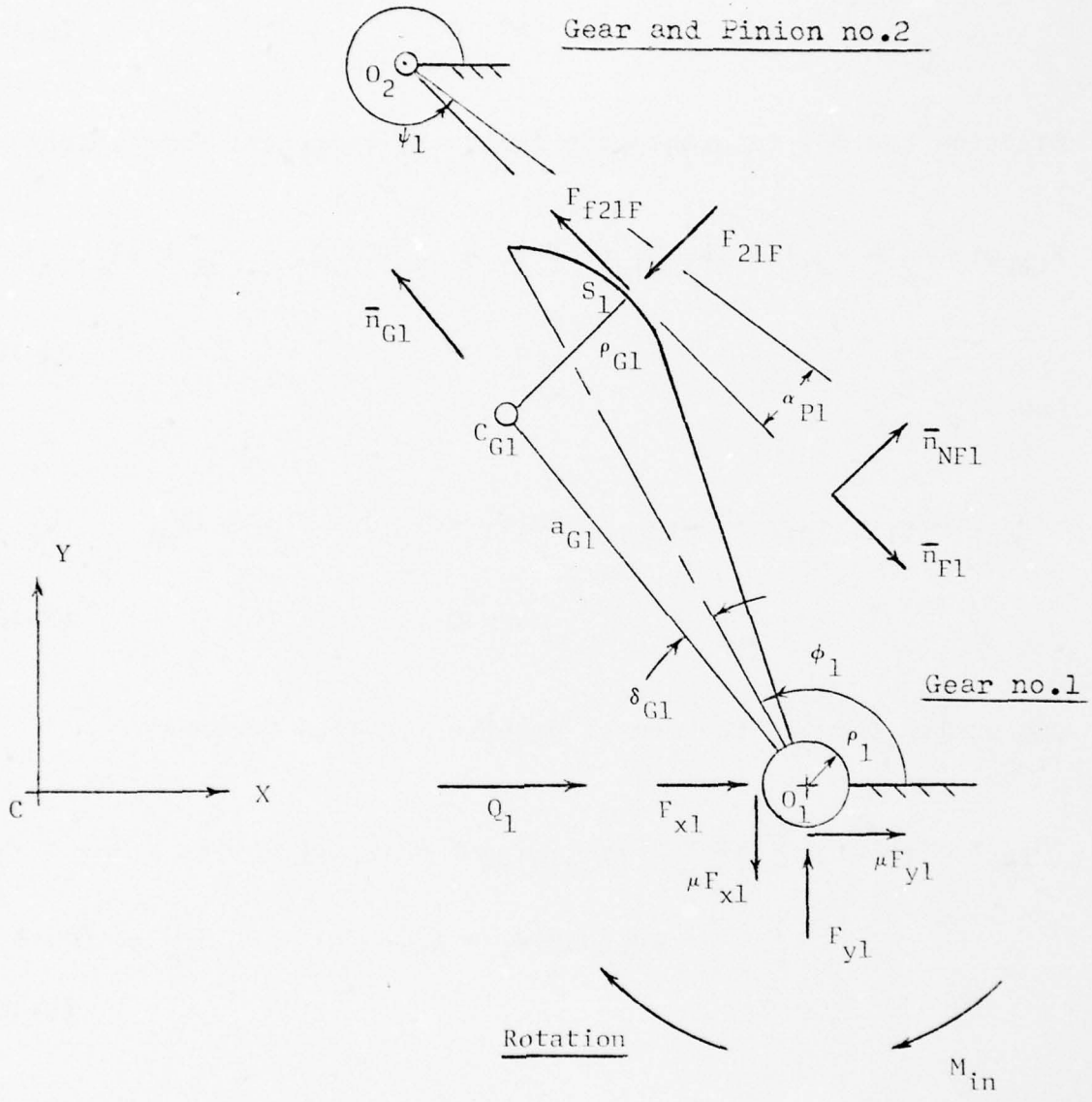

FIGURE H-6

FREE BODY DIAGRAM OF GEAR NO. 1

MESH NO. 1: ROUND ON FLAT

The moment equilibrium equation becomes:

$$-M_{in}\bar{k} + \mu\rho_1(\tilde{F}_{x1} + \tilde{F}_{y1})\bar{k} + \left[a_{G1}\bar{n}_{G1} + \rho_{G1}\bar{n}_{NF1}\right] \times \left[-F_{12F}\bar{n}_{NF1} - \mu s_{1F}F_{12F}\bar{n}_{F1}\right] = 0 \qquad \text{(H-104)}$$

Equation (H-103) furnishes the following component expressions:

$$F_{12F}\sin(\psi_1 - \alpha_{P1}) - \mu s_{1F}F_{12F}\cos(\psi_1 - \alpha_{P1}) + Q_1 + F_{x1} + \mu F_{y1} = 0 \qquad \text{(H-105)}$$

and

$$-F_{12F}\cos(\psi_1 - \alpha_{P1}) - \mu s_{1F}F_{12F}\sin(\psi_1 - \alpha_{P1}) + F_{y1} - \mu F_{x1} = 0 \qquad \text{(H-106)}$$

The scalar form of the moment equation (H-104) becomes:

$$-M_{in} + \mu\rho_1(\tilde{F}_{x1} + \tilde{F}_{y1}) + \mu s_{1F}\rho_{G1}F_{12F} + a_{G1}F_{12F}\left[-\cos(\phi_1 + \delta_{G1} - \psi_1 + \alpha_{P1}) + \mu s_{1F}\sin(\phi_1 + \delta_{G1} - \psi_1 + \alpha_{P1})\right] = 0 \qquad \text{(H-107)}$$

Simultaneous solution of equations (H-105) and (H-106) for F_{x1} and F_{y1} furnishes:

$$F_{x1} = \frac{F_{12F}\left[-(1 + \mu^2 s_{1F})\sin(\psi_1 - \alpha_{P1}) + \mu(s_{1F} - 1)\cos(\psi_1 - \alpha_{P1})\right] - Q_1}{1 + \mu^2} \qquad \text{(H-108)}$$

and

$$F_{y1} = \frac{F_{12F}\left[(1 + \mu^2 s_{1F})\cos(\psi_1 - \alpha_{P1}) + \mu(s_{1F} - 1)\sin(\psi_1 - \alpha_{P1})\right] - \mu Q_1}{1 + \mu^2} \tag{H-109}$$

Now let

$$\tilde{F}_{x1} + \tilde{F}_{y1} = F_{12F}A_{27} + Q_1 A_{28} + F_{12F}A_{29} + Q_1 A_{30} \tag{H-110}$$

where

$$A_{27} = \left| \frac{-(1 + \mu^2 s_{1F})\sin(\psi_1 - \alpha_{P1}) + \mu(s_{1F} - 1)\cos(\psi_1 - \alpha_{P1})}{1 + \mu^2} \right| \tag{H-111}$$

$$A_{28} = \left| \frac{1}{1 + \mu^2} \right| \tag{H-112}$$

$$A_{29} = \left| \frac{\mu(s_{1F} - 1)\sin(\psi_1 - \alpha_{P1}) + (1 + \mu^2 s_{1F})\cos(\psi_1 - \alpha_{P1})}{1 + \mu^2} \right| \tag{H-113}$$

$$A_{30} = \left| \frac{\mu}{1 + \mu^2} \right| \tag{H-114}$$

Equation (H-110) is now substituted into the moment equation (H-107). This furnishes:

$$F_{12F} = \frac{M_{in} - Q_1 C_{14}}{C_{15}} \qquad \text{(H-115)}$$

where

$$C_{14} = \mu\rho_1(A_{28} + A_{30})$$

$$C_{15} = \mu\rho_1(A_{27} + A_{29}) + \mu s_{1F}\rho_{G1}$$

$$+ a_{G1}\left[\mu s_{1F}\sin(\phi_1 + \delta_{G1} - \psi_1 + \alpha_{P1}) - \cos(\phi_1 + \delta_{G1} - \psi_1 + \alpha_{P1})\right]$$

III. MOMENT INPUT-OUTPUT RELATIONSHIP

Equations (H-100) and (H-115), which are both expressions in F_{12F}, are now set equal to each other and the result is solved for F_{23}:

$$F_{23} = \frac{-C_{13}}{C_{11}C_{15}} (M_{in} - Q_1 C_{14}) + Q_2 \frac{C_{12}}{C_{11}} \qquad \text{(H-116)}$$

The above expression is now equated to equation (H-40) and solved for F_{34}:

$$F_{34} = \frac{C_5 C_{13}}{C_3 C_{11} C_{15}} (M_{in} - Q_1 C_{14}) - Q_2 \frac{C_5 C_{12}}{C_3 C_{11}} - Q_3 \frac{C_4}{C_3} \qquad \text{(H-117)}$$

Finally, this expression is set equal to equation (H-19) and the result is solved for the equilibrant moment M_{o42} (for case 2: RRF):

$$M_{o42} = M_{in} \frac{C_2 C_5 C_{13}}{C_3 C_{11} C_{15}} - Q_1 \frac{C_2 C_5 C_{13} C_{14}}{C_3 C_{11} C_{15}} - Q_2 \frac{C_2 C_5 C_{12}}{C_3 C_{11}} - Q_3 \frac{C_2 C_4}{C_3} - Q_4 C_1 \qquad \text{(H-118)}$$

c. CASE NO. 3: RFF

With both meshes no. 1 and no. 2 in the round on flat phase of motion, only force F_{34} of the round on round phase can be incorporated for the present case. The equilibrium equations for gear and pinion set no. 3, gear and pinion set no. 2 and the input gear no. 1 must be newly derived.

I. FORCE AND MOMENT EQUILIBRIA OF GEAR AND PINION SET NO. 3

Figure H-7 shows the free body diagram of gear and pinion set no. 3, together with the necessary outline of mesh no. 2.

The forces of pinion no. 4 on gear no. 3 are given by equations (H-20) and (H-21):

$$\bar{F}_{43} = - F_{34}\bar{n}_{\lambda 3} \tag{H-119}$$

and

$$\bar{F}_{f43} = - \mu s_{3R} F_{34}\bar{n}_{N\lambda 3} \tag{H-120}$$

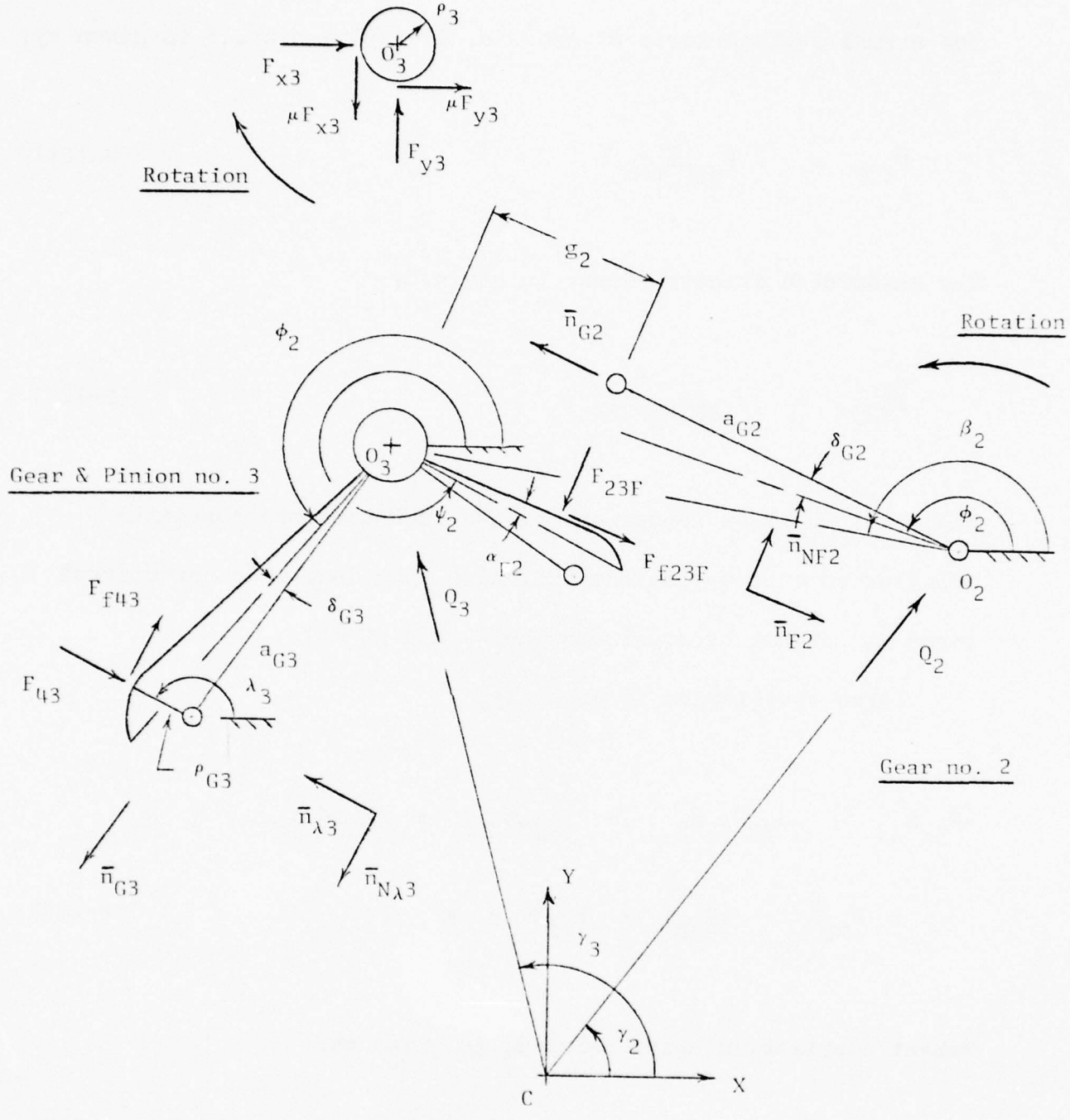

FIGURE H-7

FREE BODY DIAGRAM OF GEAR & PINION NO. 3

MESH NO. 3: ROUND ON ROUND

MESH NO. 2: ROUND ON FLAT

The normal contact force of gear no. 2 on pinion no. 3 is given by:

$$\bar{F}_{23F} = - F_{23F}\bar{n}_{NF2} \qquad \text{(H-121)}$$

The associated friction force is given by:

$$\bar{F}_{f23F} = \mu s_{2F} F_{23F}\bar{n}_{F2} \qquad \text{(H-122)}$$

The pivot friction forces are chosen such that the resulting friction moments oppose the indicated rotation. The centrifugal force $\bar{Q}_3$ is that of equations (H-24) and (H-25).

Force equilibrium is given by:

$$-F_{34}\bar{n}_{\lambda 3} - \mu s_{3R} F_{34}\bar{n}_{N\lambda 3} - F_{23F}\bar{n}_{NF2} + \mu s_{2F} F_{23F}\bar{n}_{F2} + \bar{Q}_3$$

$$+ F_{x3}\bar{i} + \mu F_{y3}\bar{i} + F_{y3}\bar{j} - \mu F_{x3}\bar{j} = 0 \qquad \text{(H-123)}$$

Moment equilibrium about point O_3 is given by:

$$\mu\rho_3(\tilde{F}_{x3} + \tilde{F}_{y3})\bar{k} + \left[a_{G3}\bar{n}_{G3} + \rho_{G3}\bar{n}_{\lambda 3}\right] \times \left[-F_{34}\bar{n}_{\lambda 3} - \mu s_{3R} F_{34}\bar{n}_{N\lambda 3}\right]$$

$$+ g_2\bar{n}_{F2} \times \bar{F}_{23F} = 0 \qquad \text{(H-124)}$$

Note that the friction force F_{f23F} exerts no moment about point O_3.

Equation (H-123) furnishes the following component equations:

$$-F_{34}\cos\lambda_3 + \mu s_{3R}F_{34}\sin\lambda_3 + Q_3\cos\gamma_3 + F_{x3} + \mu F_{y3} + F_{23F}\sin(\psi_2 + \alpha_{P2})$$

$$+ \mu s_{2F}F_{23F}\cos(\psi_2 + \alpha_{P2}) = 0 \qquad \text{(H-125)}$$

and

$$-F_{34}\sin\lambda_3 - \mu s_{3R}F_{34}\cos\lambda_3 + Q_3\sin\gamma_3 + F_{y3} - \mu F_{x3} - F_{23F}\cos(\psi_2 + \alpha_{P2})$$

$$+ \mu s_{2F}F_{23F}\sin(\psi_2 + \alpha_{P2}) = 0 \qquad \text{(H-126)}$$

The scalar form of the moment equation (H-124) becomes:

$$\mu\rho_3(\tilde{F}_{x3} + \tilde{F}_{y3}) + a_{G3}F_{34}\left[\sin(\phi_3 + \delta_{G3} - \lambda_3) - \mu s_{3R}\cos(\phi_3 + \delta_{G3} - \lambda_3)\right]$$

$$- \mu s_{3R}\rho_{G3}F_{34} - \varepsilon_2 F_{23F} = 0 \qquad \text{(H-127)}$$

Simultaneous solution of equations (H-125) and (H-126) for F_{x3} and F_{y3} leads to:

$$F_{x3} = \frac{1}{1+\mu^2}\left\{F_{34}\left[(1-\mu^2 s_{3R})\cos\lambda_3 - \mu(1+s_{3R})\sin\lambda_3\right]\right.$$
$$+ F_{23F}\left[-\mu(1+s_{2F})\cos(\psi_2+\alpha_{P2}) - (1-\mu^2 s_{2F})\sin(\psi_2+\alpha_{P2})\right]$$
$$\left. + Q_3\left[\mu\sin\gamma_3 - \cos\gamma_3\right]\right\} \qquad \text{(H-128)}$$

and

$$F_{y3} = \frac{1}{1+\mu^2}\left\{F_{34}\left[(1-\mu^2 s_{3R})\sin\lambda_3 + \mu(1+s_{3R})\cos\lambda_3\right]\right.$$
$$+ F_{23F}\left[(1-\mu^2 s_{2F})\cos(\psi_2+\alpha_{P2}) - \mu(1+s_{2F})\sin(\psi_2+\alpha_{P2})\right]$$
$$\left. - Q_3\left[\sin\gamma_3 + \mu\cos\gamma_3\right]\right\} \qquad \text{(H-129)}$$

The sum $\tilde{F}_{x3} + \tilde{F}_{y3}$ of equation (H-127) is now made up of equations (H-128) and (H-129) in the sense of equation (A-3b):

$$\tilde{F}_{x3} + \tilde{F}_{y3} = F_{34}A_{31} + F_{23F}A_{32} + Q_3A_{33} + F_{34}A_{34} + F_{23F}A_{35} + Q_3A_{36} \qquad \text{(H-130)}$$

where

$$A_{31} = \left| \frac{(1 - \mu^2 s_{3R})\cos\lambda_3 - \mu(1 + s_{3R})\sin\lambda_3}{1 + \mu^2} \right| \qquad \text{(H-131)}$$

$$A_{32} = \left| \frac{-\mu(1 + s_{2F})\cos(\psi_2 + \alpha_{P2}) - (1 - \mu^2 s_{2F})\sin(\psi_2 + \alpha_{P2})}{1 + \mu^2} \right| \qquad \text{(H-132)}$$

$$A_{33} = \left| \frac{\mu\sin\gamma_3 - \cos\gamma_3}{1 + \mu^2} \right| \qquad \text{(H-133)}$$

$$A_{34} = \left| \frac{(1 - \mu^2 s_{3R})\sin\lambda_3 + \mu(1 + s_{3R})\cos\lambda_3}{1 + \mu^2} \right| \qquad \text{(H-134)}$$

$$A_{35} = \left| \frac{(1 - \mu^2 s_{2F})\cos(\psi_2 + \alpha_{P2}) - \mu(1 + s_{2F})\sin(\psi_2 + \alpha_{P2})}{1 + \mu^2} \right| \qquad \text{(H-135)}$$

$$A_{36} = \left| \frac{\sin\gamma_3 + \mu\cos\gamma_3}{1 + \mu^2} \right| \qquad \text{(H-136)}$$

Equation (H-130) is now substituted into equation (H-127) and the result is solved for F_{23F}:

$$F_{23F} = \frac{- F_{34}C_{16} - Q_3C_{17}}{C_{18}} \qquad \text{(H-137)}$$

where

$$C_{16} = \mu\rho_3(A_{31} + A_{34}) + a_{G3}\left[\sin(\phi_3 + \delta_{G3} - \lambda_3) - \mu s_{3R}\cos(\phi_3 + \delta_{G3} - \lambda_3)\right] - \mu s_{3R}\rho_{G3}$$

$$C_{17} = \mu\rho_3(A_{33} + A_{36})$$

$$C_{18} = \mu\rho_3(A_{32} + A_{35}) - S_2$$

II. FORCE AND MOMENT EQUILIBRIA OF GEAR AND PINION SET NO. 2

Figure H-8 shows the free body diagram of the gear and pinion set no. 2.

The forces of pinion no. 3 on gear no. 2 are equal and opposite to those given by equations (H-121) and (H-122), i.e.:

$$\bar{F}_{32F} = F_{23F}\bar{n}_{NF2} \tag{H-138}$$

and

$$\bar{F}_{f32F} = -\mu s_{2F} F_{23F}\bar{n}_{F2} \tag{H-139}$$

The forces of gear no. 1 on pinion no. 2 are those of equations (H-84) and (H-85).

The pivot friction is accounted for in the usual manner and the centrifugal force $\bar{Q}_2$ is given by equation (H-45).

Force equilibrium is given by:

$$F_{23F}\bar{n}_{NF2} - \mu s_{2F} F_{23F}\bar{n}_{F2} + F_{12F}\bar{n}_{NF1} + \mu s_{1F} F_{12F}\bar{n}_{F1} + \bar{Q}_2 + F_{x2}\bar{i} - \mu F_{y2}\bar{i} + F_{y2}\bar{j} + \mu F_{x2}\bar{j} = 0 \tag{H-140}$$

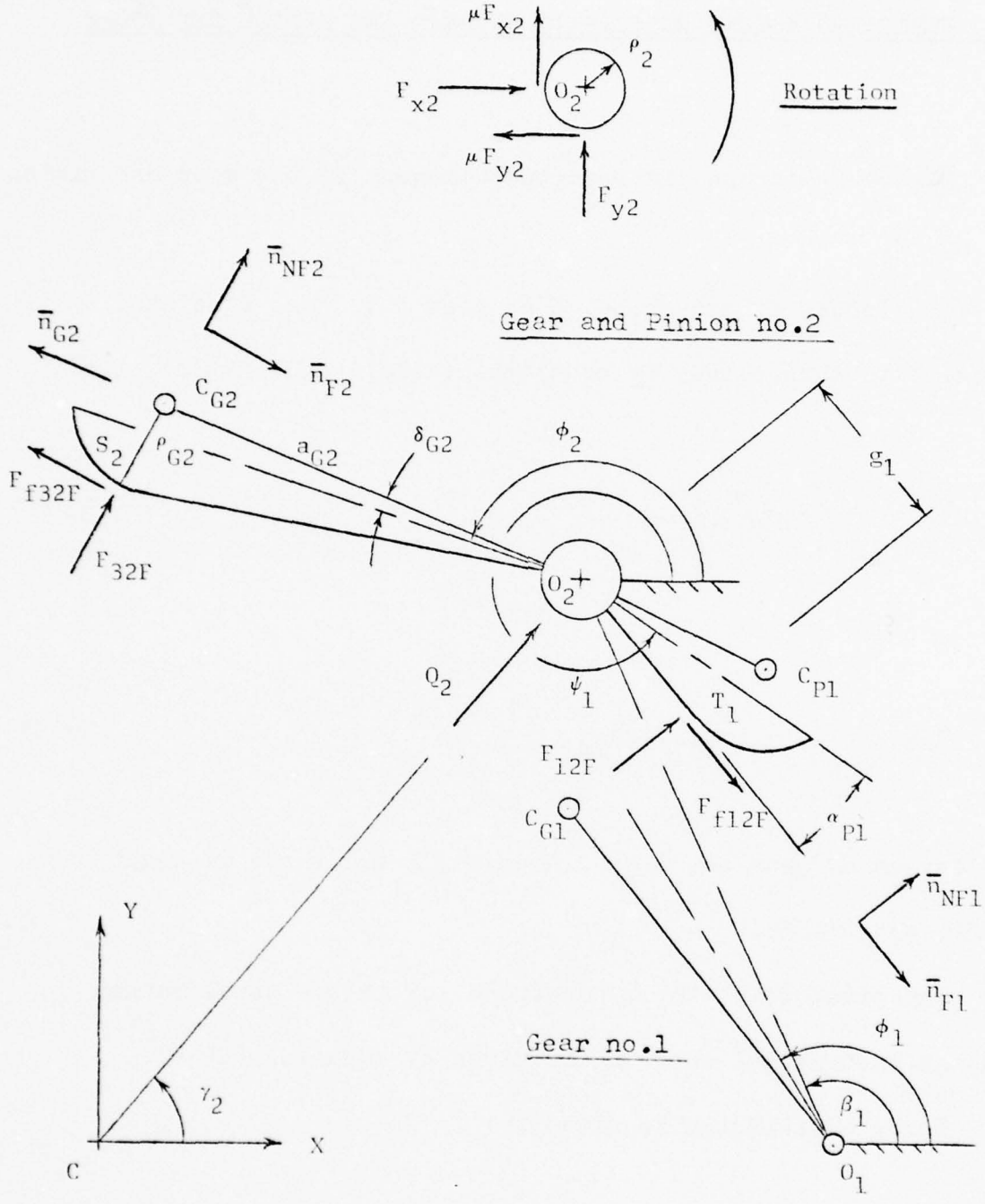

FIGURE H-8

FREE BODY DIAGRAM OF GEAR & PINION NO. 2

MESH NO. 2: ROUND ON FLAT

MESH NO. 1: ROUND ON FLAT

Moment equilibrium about point O_2 requires:

$$-\mu\rho_2(\tilde{F}_{x2} + \tilde{F}_{y2})\bar{k} + [a_{G2}\bar{n}_{G2} - \rho_{G2}\bar{n}_{NF2}] \times [F_{23F}\bar{n}_{NF2} - \mu s_{2F}F_{23F}\bar{n}_{F2}]$$

$$+ \varepsilon_1\bar{n}_{F1} \times F_{12F}\bar{n}_{NF1} = 0 \qquad \text{(H-141)}$$

Equation (H-140) gives the component equations:

$$-F_{23F}\sin(\psi_2 + \alpha_{P2}) - \mu s_{2F}F_{23F}\cos(\psi_2 + \alpha_{P2}) + Q_2\cos\gamma_2 + F_{x2} - \mu F_{y2}$$

$$- F_{12F}\sin(\psi_1 - \alpha_{P1}) + \mu s_{1F}F_{12F}\cos(\psi_1 - \alpha_{P1}) = 0 \qquad \text{(H-142)}$$

and

$$F_{23F}\cos(\psi_2 + \alpha_{P2}) - \mu s_{2F}F_{23F}\sin(\psi_2 + \alpha_{P2}) + Q_2\sin\gamma_2 + F_{y2} + \mu F_{x2}$$

$$+ F_{12F}\cos(\psi_1 - \alpha_{P1}) + \mu s_{1F}F_{12F}\sin(\psi_1 - \alpha_{P1}) = 0 \qquad \text{(H-143)}$$

The scalar form of the moment equation (H-141) becomes:

$$-\mu\rho_2(\tilde{F}_{x2} + \tilde{F}_{y2}) + a_{G2}F_{23F}\left[\cos(\phi_2 - \delta_{G2} - \psi_2 - \alpha_{P2})\right.$$

$$\left. + \mu s_{2F}\sin(\phi_2 - \delta_{G2} - \psi_2 - \alpha_{P2})\right] - \mu s_{2F}\rho_{G2}F_{23F} + g_1F_{12F} = 0$$

(H-144)

Simultaneous solution of the component equations (H-142) and (H-143) for F_{x2} and F_{y2} leads to:

$$F_{x2} = \frac{1}{1 + \mu^2}\left\{F_{23F}\left[(1 + \mu^2 s_{2F})\sin(\psi_2 + \alpha_{P2}) + \mu(s_{2F} - 1)\cos(\psi_2 + \alpha_{P2})\right]\right.$$

$$+ F_{12F}\left[(1 - \mu^2 s_{1F})\sin(\psi_1 - \alpha_{P1}) - \mu(1 + s_{1F})\cos(\psi_1 - \alpha_{P1})\right]$$

$$\left. - Q_2\left[\mu\sin\gamma_2 + \cos\gamma_2\right]\right\} \qquad \text{(H-145)}$$

and

$$F_{y2} = \frac{1}{1 + \mu^2}\left\{F_{23F}\left[\mu(s_{2F} - 1)\sin(\psi_2 + \alpha_{P2}) - (1 + \mu^2 s_{2F})\cos(\psi_2 + \alpha_{P2})\right]\right.$$

$$- F_{12F}\left[\mu(1 + s_{1F})\sin(\psi_1 - \alpha_{P1}) + (1 - \mu^2 s_{1F})\cos(\psi_1 - \alpha_{P1})\right]$$

$$\left. + Q_2\left[\mu\cos\gamma_2 - \sin\gamma_2\right]\right\} \qquad \text{(H-146)}$$

The sum $\tilde{F}_{x2} + \tilde{F}_{y2}$ of equation (H-144) is now made up of equations (H-145) and (H-146) in the sense of equation (A-3b):

$$\tilde{F}_{x2} + \tilde{F}_{y2} = F_{23F}A_{37} + F_{12F}A_{38} + Q_2A_{39} + F_{23F}A_{40} + F_{12F}A_{41} + Q_2A_{42} \tag{H-147}$$

where

$$A_{37} = \left| \frac{(1 + \mu^2 s_{2F})\sin(\psi_2 + \alpha_{P2}) + \mu(s_{2F} - 1)\cos(\psi_2 + \alpha_{P2})}{1 + \mu^2} \right| \tag{H-148}$$

$$A_{38} = \left| \frac{(1 - \mu^2 s_{1F})\sin(\psi_1 - \alpha_{P1}) - \mu(1 + s_{1F})\cos(\psi_1 - \alpha_{P1})}{1 + \mu^2} \right| \tag{H-149}$$

$$A_{39} = \left| \frac{\mu \sin\gamma_2 + \cos\gamma_2}{1 + \mu^2} \right| \tag{H-150}$$

$$A_{40} = \left| \frac{\mu(s_{2F} - 1)\sin(\psi_2 + \alpha_{P2}) - (1 + \mu^2 s_{2F})\cos(\psi_2 + \alpha_{P2})}{1 + \mu^2} \right| \tag{H-151}$$

$$A_{41} = \left| \frac{\mu(1 + s_{1F})\sin(\psi_1 - \alpha_{P1}) + (1 - \mu^2 s_{1F})\cos(\psi_1 - \alpha_{P1})}{1 + \mu^2} \right| \tag{H-152}$$

$$A_{42} = \left| \frac{\mu \cos\gamma_2 - \sin\gamma_2}{1 + \mu^2} \right| \tag{H-153}$$

Equation (H-147) is now substituted into equation (H-144) and the result is solved for F_{12F}:

$$F_{12F} = \frac{- F_{23F}C_{19} + Q_2C_{20}}{C_{21}} \qquad \text{(H-154)}$$

where

$$C_{19} = -\mu\rho_2(A_{37} + A_{40}) + a_{G2}\left[\cos(\phi_2 - \delta_{G2} - \psi_2 - \alpha_{P2}) + \mu s_{2F}\sin(\phi_2 - \delta_{G2} - \psi_2 - \alpha_{P2})\right] - \mu s_{2F}\rho_{G2}$$

$$C_{20} = \mu\rho_2(A_{39} + A_{42})$$

$$C_{21} = -\mu\rho_2(A_{38} + A_{41}) + g_1$$

III. FORCE AND MOMENT EQUILIBRIA OF INPUT GEAR NO. 1

While the numerical values of the force F_{21F} and its associated friction force F_{f12F}, both acting on gear no. 1, are peculiar to the present combination of contact phases, its functional relationship to the input moment M_{in} and the centrifugal force Q_1 is identical to that derived in section 1b-II of this appendix. (See also Figure H-6.)

According to equation (H-115), one obtains for F_{12F}:

$$F_{12F} = \frac{M_{in} - Q_1 c_{14}}{c_{15}} \qquad \text{(H-155)}$$

IV. MOMENT INPUT-OUTPUT RELATIONSHIP

Equations (H-154) and (H-155), both in F_{12F}, are set equal to each other and the result is solved for F_{23F}:

$$F_{23F} = \frac{-C_{21}}{C_{15}C_{19}}(M_{in} - Q_1C_{14}) + Q_2\frac{C_{20}}{C_{19}} \qquad \text{(H-156)}$$

The above is now equated to equation (H-137) and the result is solved for F_{34}:

$$F_{34} = \frac{C_{18}C_{21}}{C_{15}C_{16}C_{19}}(M_{in} - Q_1C_{14}) - Q_2\frac{C_{18}C_{20}}{C_{16}C_{19}} - Q_3\frac{C_{17}}{C_{16}} \qquad \text{(H-157)}$$

Finally, equation (H-157) is equated to equation (H-19), which corresponds to the round on round phase of mesh no. 3. The result is solved for the equilibrant moment M_{043} (for case 3: RFF):

$$M_{043} = M_{in}\frac{C_2C_{18}C_{21}}{C_{15}C_{16}C_{19}} - Q_1\frac{C_2C_{14}C_{18}C_{21}}{C_{15}C_{16}C_{19}} - Q_2\frac{C_2C_{18}C_{20}}{C_{16}C_{19}} - Q_3\frac{C_2C_{17}}{C_{16}}$$

$$- Q_4C_1 \qquad \text{(H-158)}$$

d. CASE NO. 4: RFR

For this contact combination force F_{34} may be taken from the results of case no. 1 [see equation (H-19)], since mesh no. 3 is in the round on round phase of motion. The force F_{23F} of case no. 3, i.e. equation (H-137), also is incorporated.

The input-output relationship of the gear and pinion combination no. 2 must be newly derived, i.e. the force F_{12} must be expressed in terms of the contact force F_{32F} and the centrifugal force Q_2. Finally, the results of the equilibrium equations for the input gear no. 1 of case no. 1 are used. For this case of contact, the force F_{12} is given by equation (H-78).

I. FORCE AND MOMENT EQUILIBRIA OF GEAR AND PINION SET NO. 2

Figure H-9 shows the free body diagram of gear and pinion set no. 2 with the necessary portions of mesh no. 1.

The forces of pinion no. 3 on gear no. 2 were given by equations (H-138) and (H-139):

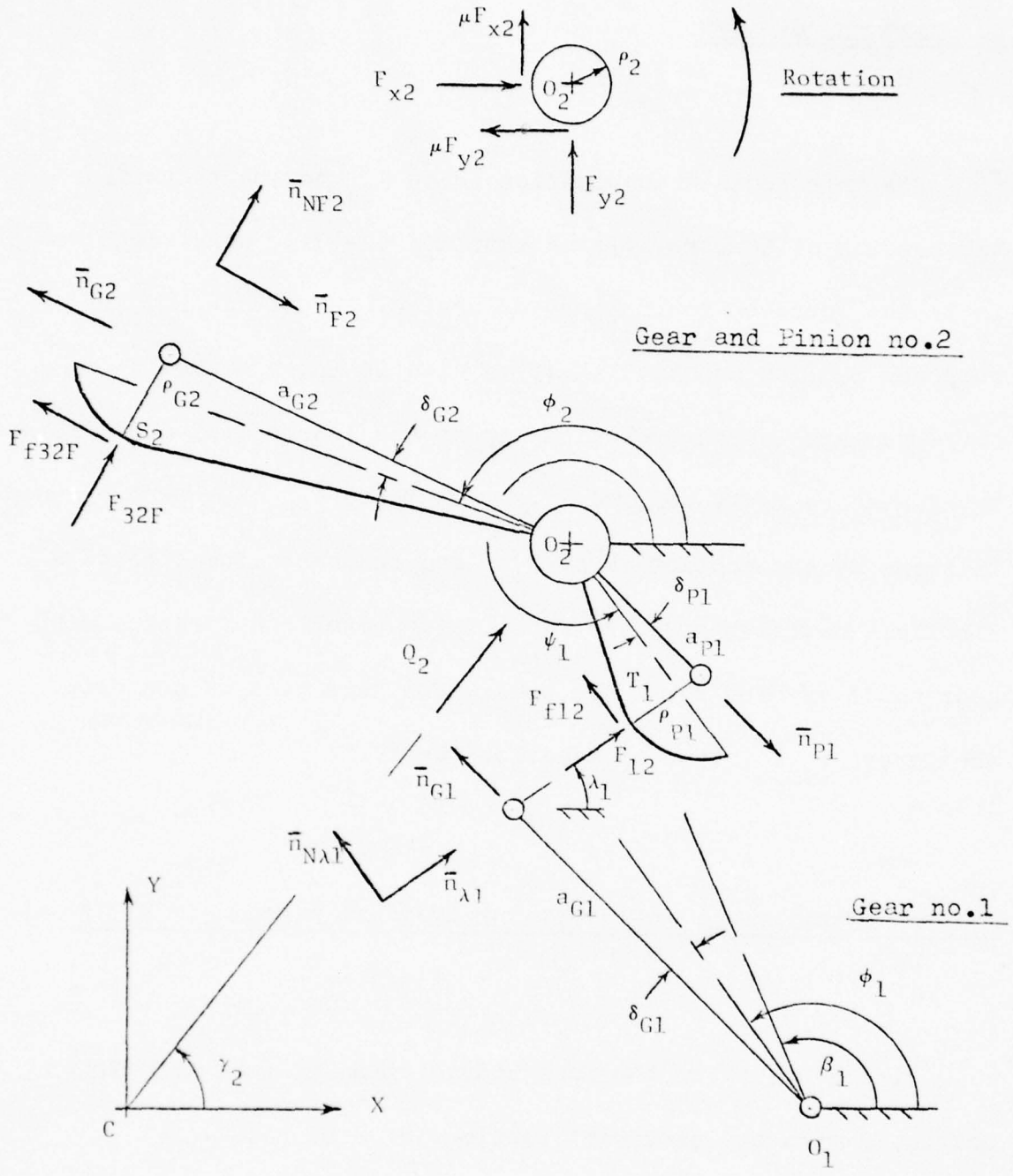

FIGURE H-9

FREE BODY DIAGRAM OF GEAR & PINION NO. 2

MESH NO. 2: ROUND ON FLAT

MESH NO. 1: ROUND ON ROUND

$$\bar{F}_{32F} = F_{23F}\bar{n}_{NF2} \tag{H-159}$$

and

$$\bar{F}_{f32F} = -\mu s_{2F}F_{23F}\bar{n}_{F2} \tag{H-160}$$

The forces of gear no. 1 on pinion no. 2 are given by equations (H-43) and (H-44):

$$\bar{F}_{12} = F_{12}\bar{n}_{\lambda 1} \tag{H-161}$$

and

$$\bar{F}_{f12} = \mu s_{1R}F_{12}\bar{n}_{N\lambda 1} \tag{H-162}$$

The centrifugal force $\bar{Q}_2$ is given by equation (H-45). The pivot reactions and friction forces are handled as before.

Force equilibrium is given by:

$$F_{23F}\bar{n}_{NF2} - \mu s_{2F}F_{23F}\bar{n}_{F2} + F_{12}\bar{n}_{\lambda 1} + \mu s_{1R}F_{12}\bar{n}_{N\lambda 1} + \bar{Q}_2 + F_{x2}\bar{i} - \mu F_{y2}\bar{i} + F_{y2}\bar{j} + \mu F_{x2}\bar{j} = 0 \tag{H-163}$$

Moment equlibrium about point O_2 is given by:

$$-\mu\rho_2(\tilde{F}_{x2} + \tilde{F}_{y2}) + [a_{G2}\bar{n}_{G2} - \rho_{G2}\bar{n}_{NF2}] \times [F_{23F}\bar{n}_{NF2} - \mu s_{2F}F_{23F}\bar{n}_{F2}]$$

$$+ [a_{P1}\bar{n}_{P1} - \rho_{P1}\bar{n}_{\lambda 1}] \times [F_{12}\bar{n}_{\lambda 1} + \mu s_{1R}F_{12}\bar{n}_{N\lambda 1}] = 0 \qquad \text{(H-164)}$$

Equation (H-163) gives the following component equations:

$$-F_{23F}\sin(\psi_2 + \alpha_{P2}) - \mu s_{2F}F_{23F}\cos(\psi_2 + \alpha_{P2}) + F_{x2} - \mu F_{y2} + F_{12}\cos\lambda_1$$

$$- \mu s_{1R}F_{12}\sin\lambda_1 + Q_2\cos\gamma_2 = 0 \qquad \text{(H-165)}$$

and

$$F_{23F}\cos(\psi_2 + \alpha_{P2}) - \mu s_{2F}F_{23F}\sin(\psi_2 + \alpha_{P2}) + F_{y2} + \mu F_{x2} + F_{12}\sin\lambda_1$$

$$+ \mu s_{1R}F_{12}\cos\lambda_1 + Q_2\sin\gamma_2 = 0 \qquad \text{(H-166)}$$

The scalar form of the moment equation (H-164) becomes:

$$- \rho_2(\tilde{F}_{x2} + \tilde{F}_{y2}) + a_{G2}F_{23F}\left[\cos(\phi_2 - \delta_{G2} - \psi_2 - \alpha_{P2}) + \mu s_{2F}\sin(\phi_2 - \delta_{G2} - \psi_2 - \alpha_{P2})\right] - \mu s_{2F}\rho_{G2}F_{23F} - \mu s_{1R}\rho_{P1}F_{12} + a_{P1}F_{12}\left[\mu s_{1R}\cos(\psi_1 + \delta_{P1} - \lambda_1) - \sin(\psi_1 + \delta_{P1} - \lambda_1)\right] = 0 \quad \text{(H-167)}$$

Simultaneous solution of the force component equations (H-165) and (H-166) for F_{x2} and F_{y2} results in:

$$F_{x2} = \frac{1}{1 + \mu^2}\left\{F_{23F}\left[(1 + \mu^2 s_{2F})\sin(\psi_2 + \alpha_{P2}) - \mu(1 - s_{2F})\cos(\psi_2 + \alpha_{P2})\right] + F_{12}\left[\mu(s_{1R} - 1)\sin\lambda_1 - (1 + \mu^2 s_{1R})\cos\lambda_1\right] - Q_2\left[\mu\sin\gamma_2 + \cos\gamma_2\right]\right\} \quad \text{(H-168)}$$

and

$$F_{y2} = \frac{1}{1 + \mu^2}\left\{F_{23F}\left[\mu(s_{2F} - 1)\sin(\psi_2 + \alpha_{P2}) - (1 + \mu^2 s_{2F})\cos(\psi_2 + \alpha_{P2})\right] + F_{12}\left[-(1 + \mu^2 s_{1R})\sin\lambda_1 + \mu(1 - s_{1R})\cos\lambda_1\right] + Q_2\left[-\sin\gamma_2 + \mu\cos\gamma_2\right]\right\} \quad \text{(H-169)}$$

The sum $\tilde{F}_{x2} + \tilde{F}_{y2}$ of equation(H-167) is now made up of equations (H-168) and (H-169) in the usual manner:

$$\tilde{F}_{x2} + \tilde{F}_{y2} = F_{23F}A_{43} + F_{12}A_{44} + Q_2A_{45} + F_{23F}A_{46} + F_{12}A_{47} + Q_2A_{48} \tag{H-170}$$

where

$$A_{43} = \left| \frac{(1 + \mu^2 s_{2F})\sin(\psi_2 + \alpha_{P2}) - \mu(1 - s_{2F})\cos(\psi_2 + \alpha_{P2})}{1 + \mu^2} \right| \tag{H-171}$$

$$A_{44} = \left| \frac{\mu(s_{1R} - 1)\sin\lambda_1 - (1 + \mu^2 s_{1R})\cos\lambda_1}{1 + \mu^2} \right| \tag{H-172}$$

$$A_{45} = \left| \frac{\mu\sin\gamma_2 + \cos\gamma_2}{1 + \mu^2} \right| \tag{H-173}$$

$$A_{46} = \left| \frac{\mu(s_{2F} - 1)\sin(\psi_2 + \alpha_{P2}) - (1 + \mu^2 s_{2F})\cos(\psi_2 + \alpha_{P2})}{1 + \mu^2} \right| \tag{H-174}$$

$$A_{47} = \left| \frac{-(1 + \mu^2 s_{1R})\sin\lambda_1 + \mu(1 - s_{1R})\cos\lambda_1}{1 + \mu^2} \right| \tag{H-175}$$

$$A_{48} = \left| \frac{-\sin\gamma_2 + \mu\cos\gamma_2}{1 + \mu^2} \right| \tag{H-176}$$

Equation (H-170) is now substituted into the moment equation (H-167) and the result is solved for F_{12}:

$$F_{12} = \frac{- F_{23F}C_{22} + Q_2C_{23}}{C_{24}} \qquad \text{(H-177)}$$

where

$$C_{22} = -\mu\rho_2(A_{43} + A_{46}) + a_{G2}\left[\cos(\phi_2 - \delta_{G2} - \psi_2 - \alpha_{P2}) + \mu s_{2F}\sin(\phi_2 - \delta_{G2} - \psi_2 - \alpha_{P2})\right] - \mu s_{2F}\rho_{G2}$$

$$C_{23} = \mu\rho_2(A_{45} + A_{48})$$

$$C_{24} = -\mu\rho_2(A_{44} + A_{47}) + a_{P1}\left[\mu s_{1R}\cos(\psi_1 + \delta_{P1} - \lambda_1) - \sin(\psi_1 + \delta_{P1} - \lambda_1)\right] - \mu s_{1R}\rho_{P1}$$

II. MOMENT INPUT-OUTPUT RELATIONSHIP

Equations (H-177) and (H-78) are now set equal to each other and the result is solved for F_{23F}:

$$F_{23F} = \frac{-C_{24}}{C_{10}C_{22}}(M_{in} - Q_1C_9) + Q_2\frac{C_{23}}{C_{22}} \qquad \text{(H-178)}$$

The above is now equated to equation (H-137) to obtain F_{34}:

$$F_{34} = \frac{C_{18}C_{24}}{C_{10}C_{16}C_{22}}(M_{in} - Q_1C_9) - Q_2\frac{C_{18}C_{23}}{C_{16}C_{22}} - Q_3\frac{C_{17}}{C_{16}} \qquad \text{(H-179)}$$

Finally equations (H-179) and (H-19) are set equal to each other and the equilibrant moment M_{o44} (For case 4: RFR) is determined:

$$M_{o44} = M_{in}\frac{C_2C_{18}C_{24}}{C_{10}C_{16}C_{22}} - Q_1\frac{C_2C_9C_{18}C_{24}}{C_{10}C_{16}C_{22}} - Q_2\frac{C_2C_{18}C_{23}}{C_{16}C_{22}} - Q_3\frac{C_2C_{17}}{C_{16}} - Q_4C_1 \qquad \text{(H-180)}$$

e. CASE NO. 5: FFF

For this contact combination it is necessary to determine new expressions for the force F_{34F}, of gear no. 3 on pinion no. 4, and for force F_{23F}, of gear no. 2 on pinion no. 3.

Equation (H-156), derived for case 3, and which relates force F_{23F} to the input moment M_{in}, may be used for the determination of the final input-output relationship.

I. FORCE AND MOMENT EQUILIBRIA OF PINION NO. 4

Figure H-10 gives the free body diagram of pinion no. 4 in the round on flat phase of motion with gear no. 3.

The equilibrant moment M_{o4} acts in a clockwise direction and opposes the counter-clockwise rotation of the pinion.

The normal contact force $\bar{F}_{34F}$ is given by:

$$\bar{F}_{34F} = F_{34F}\bar{n}_{NF3} \qquad \text{(H-181)}$$

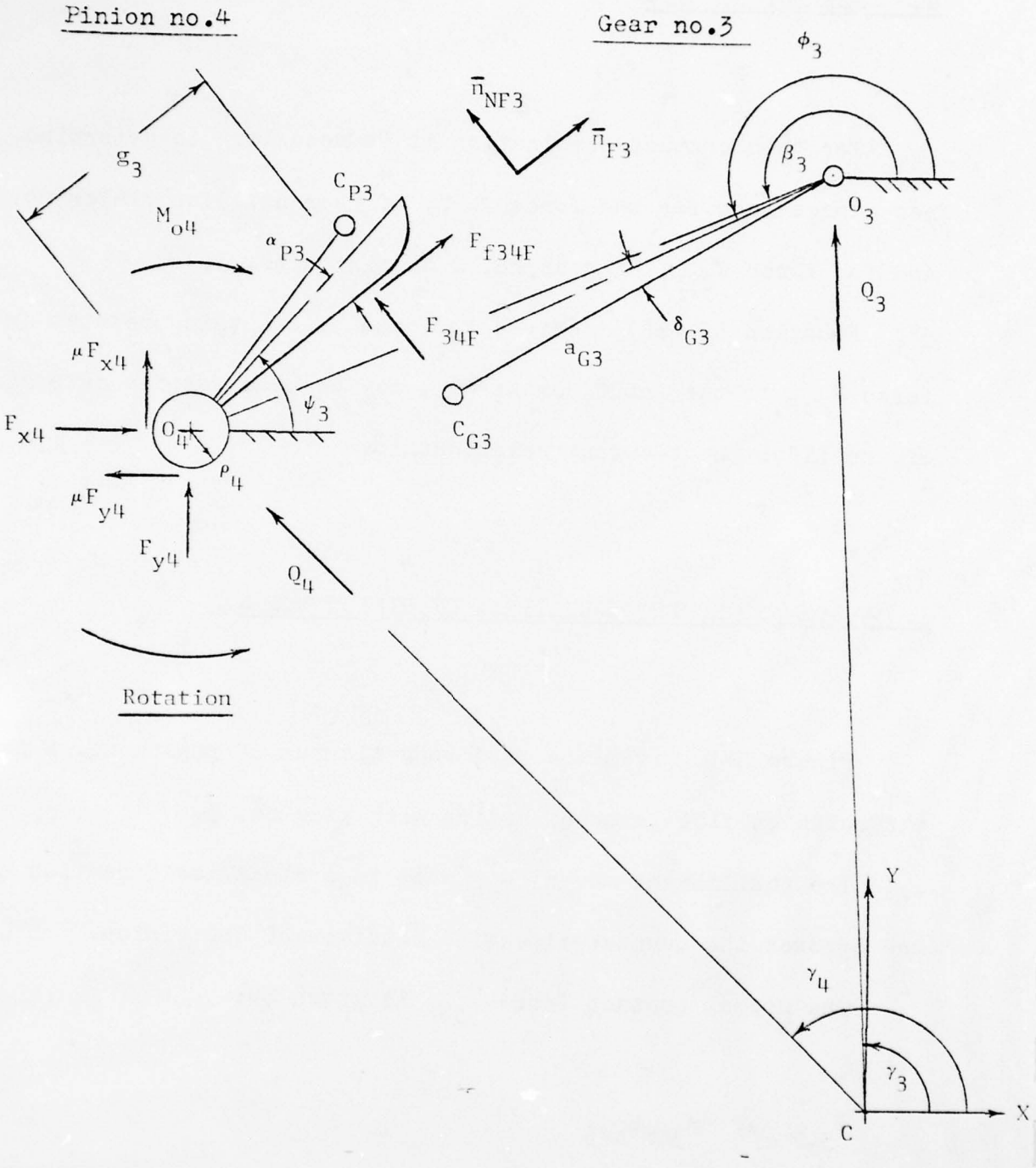

FIGURE H-10

FREE BODY DIAGRAM OF PINION NO. 4

The associated friction force becomes:

$$\bar{F}_{f34F} = \mu s_{3F} F_{34F} \bar{n}_{F3} \qquad \text{(H-182)}$$

The centrifugal force $\bar{Q}_4$ is given by equation (H-5) and the pivot friction forces are chosen such that they oppose rotation.

Force equilibrium is given by:

$$F_{34F}\bar{n}_{NF3} + \mu s_{3F} F_{34F}\bar{n}_{F3} + F_{x4}\bar{i} - \mu F_{y4}\bar{i} + F_{y4}\bar{j} + \mu F_{x4}\bar{j}$$

$$+ Q_4(\cos\gamma_4 \bar{i} + \sin\gamma_4 \bar{j}) = 0 \qquad \text{(H-183)}$$

Moment equilibrium about point O_4 requires that:

$$-M_{o4}\bar{k} - \mu\rho_4(\tilde{F}_{x4} + \tilde{F}_{y4})\bar{k} + s_3\bar{n}_{F3} \times F_{34F}\bar{n}_{NF3} = 0 \qquad \text{(H-184)}$$

Note that the friction force F_{f34F} does not exert a moment about point O_4, since its line of action passes through it.

Equation (H-183) furnishes the following component equations:

$$-F_{34F}\sin(\psi_3 - \alpha_{P3}) + \mu s_{3F} F_{34F}\cos(\psi_3 - \alpha_{P3}) + F_{x4} - \mu F_{y4}$$

$$+ Q_4\cos\gamma_4 = 0 \qquad \text{(H-185)}$$

and

$$F_{34F}\cos(\psi_3 - \alpha_{P3}) + \mu s_{3F}F_{34F}\sin(\psi_3 - \alpha_{P3}) + F_{y4} + \mu F_{x4} + Q_4\sin\gamma_4 = 0 \qquad \text{(H-186)}$$

The scalar form of the moment equation (H-184) becomes:

$$-M_{o4} - \mu\rho_4(\tilde{F}_{x4} + \tilde{F}_{y4}) + g_3F_{34F} = 0 \qquad \text{(H-187)}$$

Simultaneous solution of equations (H-185) and (H-186) for F_{x4} and F_{y4} results in:

$$F_{x4} = \frac{1}{1+\mu^2}\left\{F_{34F}\left[(1-\mu^2 s_{3F})\sin(\psi_3 - \alpha_{P3}) - \mu(1+s_{3F})\cos(\psi_3 - \alpha_{P3})\right] + Q_4\left[-\mu\sin\gamma_4 - \cos\gamma_4\right]\right\} \qquad \text{(H-188)}$$

and

$$F_{y4} = \frac{1}{1+\mu^2}\left\{F_{34F}\left[-\mu(1+s_{3F})\sin(\psi_3 - \alpha_{P3}) - (1-\mu^2 s_{3F})\cos(\psi_3 - \alpha_{P3})\right] + Q_4\left[-\sin\gamma_4 + \mu\cos\gamma_4\right]\right\} \qquad \text{(H-189)}$$

The sum $\widetilde{F}_{x4} + \widetilde{F}_{y4}$ of equation (H-187) is now made up of equations (H-188) and (H-189) in the sense of equation (A-3b):

$$\widetilde{F}_{x4} + \widetilde{F}_{y4} = F_{34F}A_{49} + Q_4A_{50} + F_{34F}A_{51} + Q_4A_{52} \qquad \text{(H-190)}$$

where

$$A_{49} = \left| \frac{(1 - \mu^2 s_{3F})\sin(\psi_3 - \alpha_{P3}) - \mu(1 + s_{3F})\cos(\psi_3 - \alpha_{P3})}{1 + \mu^2} \right| \qquad \text{(H-191)}$$

$$A_{50} = \left| \frac{-\mu\sin\gamma_4 - \cos\gamma_4}{1 + \mu^2} \right| \qquad \text{(H-192)}$$

$$A_{51} = \left| \frac{-\mu(1 + s_{3F})\sin(\psi_3 - \alpha_{P3}) - (1 - \mu^2 s_{3F})\cos(\psi_3 - \alpha_{P3})}{1 + \mu^2} \right| \qquad \text{(H-193)}$$

$$A_{52} = \left| \frac{-\sin\gamma_4 + \mu\cos\gamma_4}{1 + \mu^2} \right| \qquad \text{(H-194)}$$

Equation (H-190) is now substituted into equation (H-187) and the result is solved for F_{34F}:

$$F_{34F} = \frac{M_{04} + Q_4C_{25}}{C_{26}} \qquad \text{(H-195)}$$

where

$$C_{25} = \mu\rho_4(A_{50} + A_{52})$$

$$C_{26} = S_3 - \mu\rho_4(A_{49} + A_{51})$$

II. FORCE AND MOMENT EQUILIBRIA OF GEAR AND PINION SET NO. 3

Figure H-11 gives the free body diagram of gear and pinion combination no. 3. Both mesh 3 and mesh 2 are in their round on flat phase of contact.

The forces of pinion 4 on gear 3 are equal to, but opposite in direction to those given by equations (H-181) and (H-182):

$$\bar{F}_{43F} = - F_{34F}\bar{n}_{NF3} \tag{H-196}$$

and

$$\bar{F}_{f43F} = - \mu s_{3F} F_{34F}\bar{n}_{F3} \tag{H-197}$$

The forces of gear 2 on pinion 3 are given by:

$$\bar{F}_{23F} = - F_{23F}\bar{n}_{NF2} \tag{H-198}$$

and

$$\bar{F}_{f23F} = \mu s_{2F} F_{23F}\bar{n}_{F2} \tag{H-199}$$

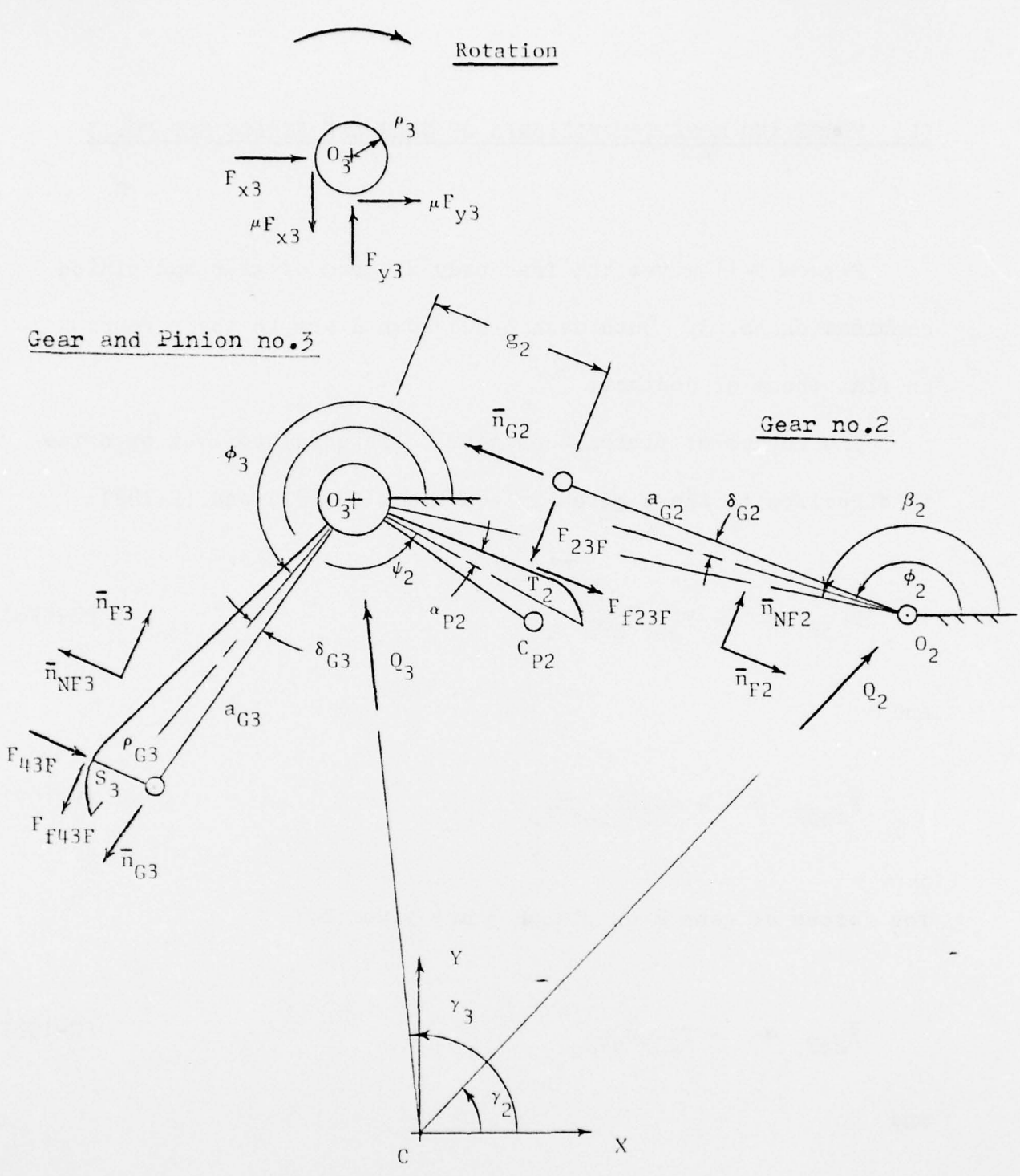

FIGURE H-11

FREE BODY DIAGRAM OF GEAR & PINION NO. 3

MESH NO. 3: ROUND ON FLAT

MESH NO. 2: ROUND ON FLAT

The pivot forces and moments are chosen in the usual manner and the centrifugal force $\bar{Q}_3$ is defined by equation (H-24).

Force equilibrium is given by:

$$-F_{34F}\bar{n}_{NF3} - \mu s_{3F}F_{34F}\bar{n}_{F3} - F_{23F}\bar{n}_{NF2} + \mu s_{2F}F_{23F}\bar{n}_{F2} + \bar{Q}_3 + F_{x3}\bar{i} + \mu F_{y3}\bar{i} + F_{y3}\bar{j} - \mu F_{x3}\bar{j} = 0 \qquad \text{(H-200)}$$

Moment equilibrium about point O_3 requires that

$$\mu\rho_3(\tilde{F}_{x3} + \tilde{F}_{y3})\bar{k} + \left[a_{G3}\bar{n}_{G3} + \rho_{G3}\bar{n}_{NF3}\right] \times \left[-F_{34F}\bar{n}_{NF3} - \mu s_{3F}F_{34F}\bar{n}_{F3}\right] + \beta_2\bar{n}_{F2} \times (-)F_{23F}\bar{n}_{NF2} = 0 \qquad \text{(H-201)}$$

Note that the friction force F_{f23F} does not exert a moment about point O_3.

Equation (H-200) furnishes, after all necessary substitutions, the following component equations:

$$F_{34F}\sin(\psi_3 - \alpha_{P3}) - \mu s_{3F}F_{34F}\cos(\psi_3 - \alpha_{P3}) + Q_3\cos\gamma_3 + F_{x3} + \mu F_{y3} + F_{23F}\sin(\psi_2 + \alpha_{P2}) + \mu s_{2F}F_{23F}\cos(\psi_2 + \alpha_{P2}) = 0 \qquad \text{(H-202)}$$

and

$$-F_{34F}\cos(\psi_3 - \alpha_{P3}) - \mu s_{3F}F_{34F}\sin(\psi_3 - \alpha_{P3}) + Q_3\sin\gamma_3 + F_{y3} - \mu F_{x3}$$

$$- F_{23F}\cos(\psi_2 + \alpha_{P2}) + \mu s_{2F}F_{23F}\sin(\psi_2 + \alpha_{P2}) = 0 \qquad \text{(H-203)}$$

The scalar form of the moment equation (H-201) becomes:

$$\mu\rho_3(\widetilde{F}_{x3} + \widetilde{F}_{y3}) + a_{G3}F_{34F}\left[-\cos(\phi_3 + \delta_{G3} - \psi_3 + \alpha_{P3})\right.$$

$$\left. + \mu s_{3F}\sin(\phi_3 + \delta_{G3} - \psi_3 + \alpha_{P3})\right] + \mu s_{3F}\rho_{G3}F_{34F} - g_2F_{23F} = 0$$

(H-204)

Simultaneous solution of the component equations (H-202) and (H-203) for F_{x3} and F_{y3} gives:

$$F_{x3} = \frac{1}{1 + \mu^2}\left\{F_{34F}\left[-(1 + \mu^2 s_{3F})\sin(\psi_3 - \alpha_{P3}) + \mu(s_{3F} - 1)\cos(\psi_3 - \alpha_{P3})\right]\right.$$

$$+ F_{23F}\left[(\mu^2 s_{2F} - 1)\sin(\psi_2 + \alpha_{P2}) - \mu(1 + s_{2F})\cos(\psi_2 + \alpha_{P2})\right]$$

$$\left. + Q_3\left[\mu\sin\gamma_3 - \cos\gamma_3\right]\right\} \qquad \text{(H-205)}$$

and

$$F_{y3} = \frac{1}{1 + \mu^2}\left\{F_{34F}\left[\mu(s_{3F} - 1)\sin(\psi_3 - \alpha_{P3}) + (1 + \mu^2 s_{3F})\cos(\psi_3 - \alpha_{P3})\right]\right.$$

$$+ F_{23F}\left[-\mu(1 + s_{2F})\sin(\psi_2 + \alpha_{P2}) + (1 - \mu^2 s_{2F})\cos(\psi_2 + \alpha_{P2})\right]$$

$$\left. + Q_3\left[-\sin\gamma_3 - \mu\cos\gamma_3\right]\right\} \qquad \text{(H-206)}$$

The sum $\widetilde{F}_{x3} + \widetilde{F}_{y3}$ is now made up from equations (H-205) and (H-206):

$$\widetilde{F}_{x3} + \widetilde{F}_{y3} = F_{34F}A_{53} + F_{23F}A_{54} + Q_3A_{55} + F_{34F}A_{56} + F_{23F}A_{57} + Q_3A_{58} \qquad \text{(H-207)}$$

where

$$A_{53} = \left|\frac{-(1 + \mu^2 s_{3F})\sin(\psi_3 - \alpha_{P3}) + \mu(s_{3F} - 1)\cos(\psi_3 - \alpha_{P3})}{1 + \mu^2}\right| \qquad \text{(H-208)}$$

$$A_{54} = \left|\frac{(\mu^2 s_{2F} - 1)\sin(\psi_2 + \alpha_{P2}) - \mu(1 + s_{2F})\cos(\psi_2 + \alpha_{P2})}{1 + \mu^2}\right| \qquad \text{(H-209)}$$

$$A_{55} = \left|\frac{\mu\sin\gamma_3 - \cos\gamma_3}{1 + \mu^2}\right| \qquad \text{(H-210)}$$

$$A_{56} = \left| \frac{\mu(s_{3F} - 1)\sin(\psi_3 - \alpha_{P3}) + (1 + \mu^2 s_{3F})\cos(\psi_3 - \alpha_{P3})}{1 + \mu^2} \right| \qquad \text{(H-211)}$$

$$A_{57} = \left| \frac{-\mu(1 + s_{2F})\sin(\psi_2 + \alpha_{P2}) + (1 - \mu^2 s_{2F})\cos(\psi_2 + \alpha_{P2})}{1 + \mu^2} \right| \qquad \text{(H-212)}$$

$$A_{58} = \left| \frac{\sin\gamma_3 + \mu\cos\gamma_3}{1 + \mu^2} \right| \qquad \text{(H-213)}$$

Equation (H-207) is now substituted into equation (H-204). The result is solved for F_{23F}:

$$F_{23F} = \frac{- F_{34F}C_{27} - Q_3 C_{28}}{C_{29}} \qquad \text{(H-214)}$$

where

$$C_{27} = \mu\rho_3(A_{53} + A_{56}) + a_{G3}\left[-\cos(\phi_3 + \delta_{G3} - \psi_3 + \alpha_{P3}) + \mu s_{3F}\sin(\phi_3 + \delta_{G3} - \psi_3 + \alpha_{P3})\right] + \mu s_{3F}\rho_{G3}$$

$$C_{28} = \mu\rho_3(A_{55} + A_{58})$$

$$C_{29} = \mu\rho_3(A_{54} + A_{57}) - \mathcal{E}_2$$

III. MOMENT INPUT-OUTPUT RELATIONSHIP

Equation (H-156) is an expression for F_{23F} as a function of the moment M_{in} and the centrifugal forces Q_1 and Q_2, when both meshes no. 1 and no. 2 are in the round on flat phase of motion. This expression for F_{23F} is now equated to equation (H-214). The result is solved for F_{34F}:

$$F_{34F} = \frac{C_{21}C_{29}}{C_{15}C_{19}C_{27}}(M_{in} - Q_1C_{14}) - Q_2\frac{C_{20}C_{29}}{C_{19}C_{27}} - Q_3\frac{C_{28}}{C_{27}} \qquad \text{(H-215)}$$

The above is now equated to equation (H-195) and the resulting expression is used to determine the equilibrant moment M_{o45} (for Case 5: FFF):

$$M_{o45} = M_{in}\frac{C_{21}C_{26}C_{29}}{C_{15}C_{19}C_{27}} - Q_1\frac{C_{14}C_{21}C_{26}C_{29}}{C_{15}C_{19}C_{27}} - Q_2\frac{C_{20}C_{26}C_{29}}{C_{19}C_{27}}$$

$$- Q_3\frac{C_{26}C_{28}}{C_{27}} - Q_4C_{25} \qquad \text{(H-216)}$$

f. CASE NO. 6: FFR

MOMENT INPUT-OUTPUT RELATIONSHIP

The moment input-output relationship for this contact combination can be assembled entirely from previously derived component relationships. As for case no. 4, mesh no. 1 is in the round on round phase while mesh no. 2 is in the round on flat phase. Therefore, equation (H-178), which relates the force F_{23F} to the input moment M_{in}, may be used. The input-output relationship of the gear and pinion set no. 3, i.e. the relationship between the forces F_{34F} and F_{23F}, is given by equation (H-214) of case no. 5. The force F_{34F} may be obtained from equation (H-195). This expression was also derived for a round on flat contact in case no. 5.

Thus, equation (H-178) is first set equal to equation (H-214) and the result is solved for the force F_{34F}:

$$F_{34F} = \frac{C_{24}C_{29}}{C_{10}C_{22}C_{27}}(M_{in} - Q_1C_9) - Q_2\frac{C_{23}C_{29}}{C_{22}C_{27}} - Q_3\frac{C_{28}}{C_{27}} \qquad \text{(H-217)}$$

The above expression is now set equal to equation (H-195). This then allows the determination of the equilibrant moment M_{046} for the present contact combination.

$$M_{046} = M_{in}\frac{C_{24}C_{26}C_{29}}{C_{10}C_{22}C_{27}} - Q_1\frac{C_9C_{24}C_{26}C_{29}}{C_{10}C_{22}C_{27}} - Q_2\frac{C_{23}C_{26}C_{29}}{C_{22}C_{27}}$$

$$- Q_3\frac{C_{26}C_{28}}{C_{27}} - Q_4C_{25} \qquad \text{(H-218)}$$

AD-A061 862 CITY COLL NEW YORK DEPT OF MECHANICAL ENGINEERING F/G 13/9
OPTIMIZATION OF STEP-UP GEAR TRAINS WITH DIFFERENT KINEMATIC PR--ETC(U)
MAY 78 G G LOWEN DAAG29-77-G-0037

UNCLASSIFIED ARO-14743.1-R-E NL

4 OF 4
ADA
061862

END
DATE
FILMED
3 -79
DDC

g. CASE NO. 7: FRR

For the present contact combination the expression for force F_{34F} may be taken over from equation (H-195) of case no. 5. The input-output relationship of gear and pinion set no. 3, which relates the forces F_{34F} and F_{23}, must be newly derived. The relationship between force F_{23} and the input moment M_{in} is taken from case no. 1 in the form of equation (H-79).

I. FORCE AND MOMENT EQUILIBRIA OF GEAR AND PINION SET NO. 3

Figure H-12 gives the free body diagram of gear and pinion set no. 3. Mesh no. 3 is in the round on flat phase of contact, while mesh no. 2 is in the round on round one.

The forces of pinion no. 4 on gear no. 3 are equal to, but opposite in direction to those given by equations (H-181) and (H-182):

$$\bar{F}_{43F} = - F_{34F}\bar{n}_{NF3} \qquad \text{(H-219)}$$

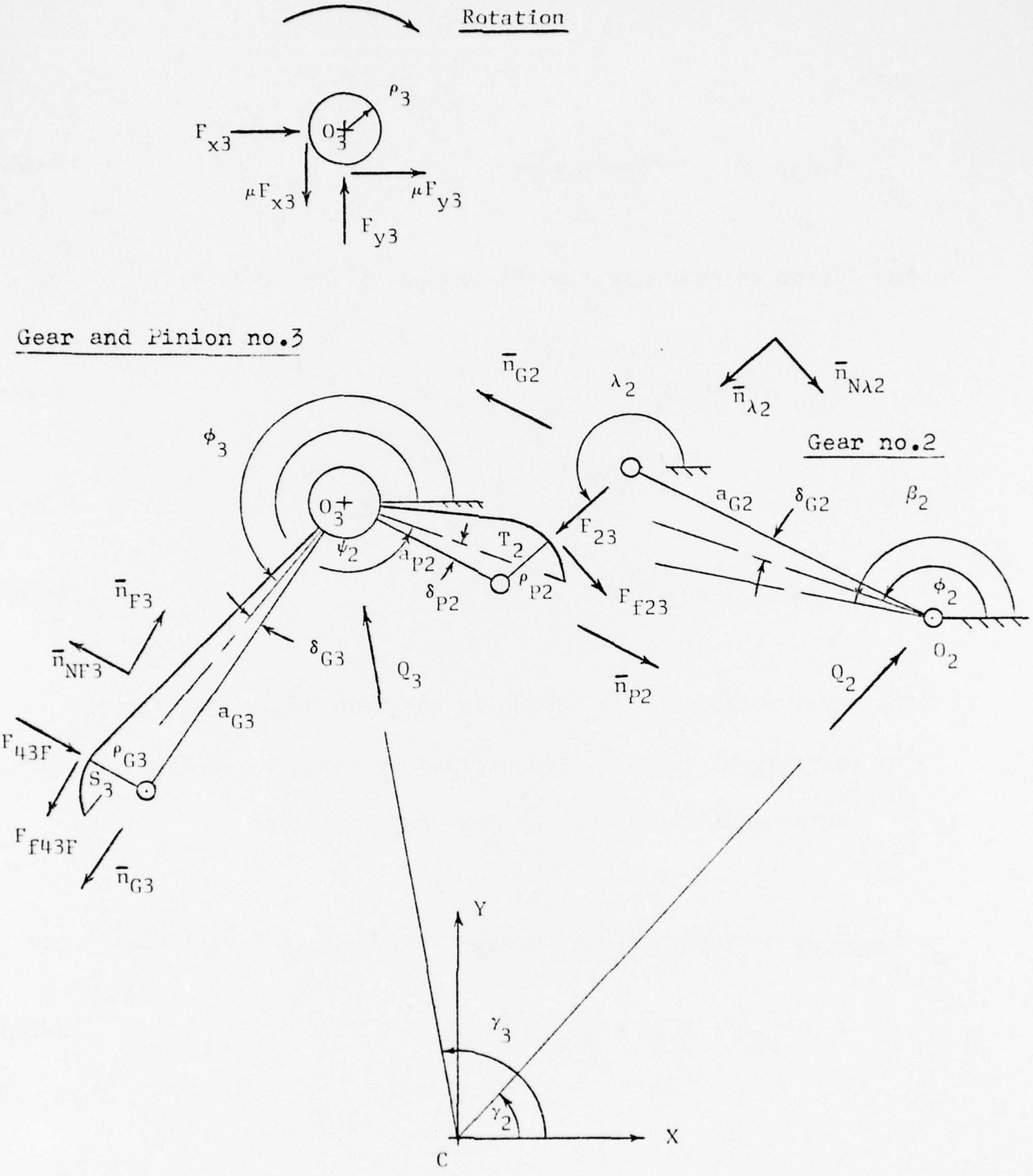

FIGURE H-12

FREE BODY DIAGRAM OF GEAR & PINION NO. 3

MESH NO. 3: ROUND ON FLAT

MESH NO. 2: ROUND ON ROUND

and

$$\bar{F}_{f43F} = -\mu s_{3F} F_{34F} \bar{n}_{F3} \qquad \text{(H-220)}$$

The forces of gear no. 2 on pinion no. 3 are given by:

$$\bar{F}_{23} = F_{23} \bar{n}_{\lambda 2} \qquad \text{(H-221)}$$

and

$$\bar{F}_{f23} = \mu s_{2R} F_{23} \bar{n}_{N\lambda 2} \qquad \text{(H-222)}$$

The pivot reactions are chosen in the same manner as before.

The centrifugal force $\bar{Q}_3$ was defined by equation (H-24).

Force equilibrium of the gear set requires:

$$-F_{34F} \bar{n}_{NF3} - \mu s_{3F} F_{34F} \bar{n}_{F3} + F_{23} \bar{n}_{\lambda 2} + \mu s_{2R} F_{23} \bar{n}_{N\lambda 2} + \bar{Q}_3 + F_{x3} \bar{i}$$

$$+ \mu F_{y3} \bar{i} + F_{y3} \bar{j} - \mu F_{x3} \bar{j} = 0 \qquad \text{(H-223)}$$

Moment equilibrium about point O_3 is given by:

$$\mu\rho_3(\tilde{F}_{x3} + \tilde{F}_{y3})\bar{k} + \left[a_{G3}\bar{n}_{G3} + \rho_{G3}\bar{n}_{NF3}\right] \times \left[-F_{34F}\bar{n}_{NF3} - \mu s_{3F}F_{34F}\bar{n}_{F3}\right]$$

$$+ \left[a_{P2}\bar{n}_{P2} - \rho_{P2}\bar{n}_{\lambda 2}\right] \times \left[F_{23}\bar{n}_{\lambda 2} + \mu s_{2R}F_{23}\bar{n}_{N\lambda 2}\right] = 0 \qquad \text{(H-224)}$$

Equation (H-223) gives the following component expressions:

$$F_{34F}\sin(\psi_3 - \alpha_{P3}) - \mu s_{3F}F_{34F}\cos(\psi_3 - \alpha_{P3}) + Q_3\cos\gamma_3 + F_{x3} + \mu F_{y3}$$

$$+ F_{23}\cos\lambda_2 - \mu s_{2R}F_{23}\sin\lambda_2 = 0 \qquad \text{(H-225)}$$

and

$$-F_{34F}\cos(\psi_3 - \alpha_{P3}) - \mu s_{3F}F_{34F}\sin(\psi_3 - \alpha_{P3}) + Q_3\sin\gamma_3 + F_{y3} - \mu F_{x3}$$

$$+ F_{23}\sin\lambda_2 + \mu s_{2R}F_{23}\cos\lambda_2 = 0 \qquad \text{(H-226)}$$

The scalar form of the moment equation (H-224) becomes:

$$\mu\rho_3(\tilde{F}_{x3} + \tilde{F}_{y3}) + a_{G3}F_{34F}\left[-\cos(\phi_3 + \delta_{G3} - \psi_3 + \alpha_{P3})\right.$$

$$\left. + \mu s_{3F}\sin(\phi_3 + \delta_{G3} - \psi_3 + \alpha_{P3})\right] + \mu s_{3F}\rho_{G3}F_{34F}$$

$$+ a_{P2}F_{23}\left[-\sin(\psi_2 - \delta_{P2} - \lambda_2) + \mu s_{2R}\cos(\psi_2 - \delta_{P2} - \lambda_2)\right]$$

$$- \mu s_{2R}\rho_{P2}F_{23} = 0 \qquad \text{(H-227)}$$

Simultaneous solution of the component equations (H-225) and (H-226) for F_{x3} and F_{y3} results in:

$$F_{x3} = \frac{1}{1 + \mu^2}\left\{F_{34F}\left[-(1 + \mu^2 s_{3F})\sin(\psi_3 - \alpha_{P3}) + \mu(s_{3F} - 1)\cos(\psi_3 - \alpha_{P3})\right]\right.$$

$$+ F_{23}\left[\mu(1 + s_{2R})\sin\lambda_2 + (\mu^2 s_{2R} - 1)\cos\lambda_2\right]$$

$$\left. + Q_3\left[\mu\sin\gamma_3 - \cos\gamma_3\right]\right\} \qquad \text{(H-228)}$$

and

$$F_{y3} = \frac{1}{1 + \mu^2}\left\{F_{34F}\left[\mu(s_{3F} - 1)\sin(\psi_3 - \alpha_{P3}) + (1 + \mu^2 s_{3F})\cos(\psi_3 - \alpha_{P3})\right]\right.$$

$$+ F_{23}\left[(\mu^2 s_{2R} - 1)\sin\lambda_2 - \mu(1 + s_{2R})\cos\lambda_2\right]$$

$$\left. + Q_3\left[-\sin\gamma_3 - \mu\cos\gamma_3\right]\right\} \qquad \text{(H-229)}$$

The sum $\tilde{F}_{x3} + \tilde{F}_{y3}$ in equation (H-227) is now made up from equations (H-228) and (H-229) in the sense of equation (A-3b):

$$\tilde{F}_{x3} + \tilde{F}_{y3} = F_{34F}A_{59} + F_{23}A_{60} + Q_3A_{61} + F_{34F}A_{62} + F_{23}A_{63} + Q_3A_{64} \qquad \text{(H-230)}$$

where

$$A_{59} = \left|\frac{-(1 + \mu^2 s_{3F})\sin(\psi_3 - \alpha_{P3}) + \mu(s_{3F} - 1)\cos(\psi_3 - \alpha_{P3})}{1 + \mu^2}\right| \qquad \text{(H-231)}$$

$$A_{60} = \left|\frac{\mu(1 + s_{2R})\sin\lambda_2 + (\mu^2 s_{2R} - 1)\cos\lambda_2}{1 + \mu^2}\right| \qquad \text{(H-232)}$$

$$A_{61} = \left|\frac{\mu\sin\gamma_3 - \cos\gamma_3}{1 + \mu^2}\right| \qquad \text{(H-233)}$$

$$A_{62} = \left| \frac{\mu(s_{3F} - 1)\sin(\psi_3 - \alpha_{P3}) + (1 + \mu^2 s_{3F})\cos(\psi_3 - \alpha_{P3})}{1 + \mu^2} \right| \qquad \text{(H-234)}$$

$$A_{63} = \left| \frac{(\mu^2 s_{2R} - 1)\sin\lambda_2 - \mu(1 + s_{2R})\cos\lambda_2}{1 + \mu^2} \right| \qquad \text{(H-235)}$$

$$A_{64} = \left| \frac{-\sin\gamma_3 - \mu\cos\gamma_3}{1 + \mu^2} \right| \qquad \text{(H-236)}$$

Equation (H-230) is now substituted into the moment equation (H-227) and the resulting expression is solved for F_{23}:

$$F_{23} = \frac{-F_{34F}C_{30} - Q_3 C_{31}}{C_{32}} \qquad \text{(H-237)}$$

where

$$C_{30} = \mu\rho_3(A_{59} + A_{62}) - a_{G3}\left[\cos(\phi_3 + \delta_{G3} - \psi_3 + \alpha_{P3}) - \mu s_{3F}\sin(\phi_3 + \delta_{G3} - \psi_3 + \alpha_{P3})\right] + \mu s_{3F}\rho_{G3}$$

$$C_{31} = \mu\rho_3(A_{61} + A_{64})$$

$$C_{32} = \mu\rho_3(A_{60} + A_{63}) - a_{P2}\left[\sin(\psi_2 - \delta_{P2} - \lambda_2) - \mu s_{2R}\cos(\psi_2 - \delta_{P2} - \lambda_2)\right]$$

$$- \mu s_{2R}\rho_{P2}$$

II. MOMENT INPUT-OUTPUT RELATIONSHIP

Equation (H-79), which gives the force F_{23} in terms of M_{in}, Q_1 and Q_2 for the appropriate contact combinations, is now set equal to equation (H-237). Subsequently, one finds the following formulation for F_{34F}:

$$F_{34F} = \frac{C_8 C_{32}}{C_6 C_{10} C_{30}}(M_{in} - Q_1 C_9) - Q_2 \frac{C_7 C_{32}}{C_6 C_{30}} - Q_3 \frac{C_{31}}{C_{30}} \qquad \text{(H-238)}$$

The above expression is now set equal to equation (H-195) which gives F_{34F} in terms of M_{04} and Q_4. The determination of the equilibrant moment M_{047} (for case 7: FRR) is now possible. Thus,

$$M_{047} = M_{in} \frac{C_8 C_{26} C_{32}}{C_6 C_{10} C_{30}} - Q_1 \frac{C_8 C_9 C_{26} C_{32}}{C_6 C_{10} C_{30}} - Q_2 \frac{C_7 C_{26} C_{32}}{C_6 C_{30}}$$

$$- Q_3 \frac{C_{26} C_{31}}{C_{30}} - Q_4 C_{25} \qquad \text{(H-239)}$$

h. CASE NO. 8: FRF

MOMENT INPUT-OUTPUT RELATIONSHIP

The input-output relationship for this contact combination can also be assembled entirely from existing expressions. With mesh no. 2 in the round on round phase of contact and mesh no. 1 in the round on flat one, the relationship between force F_{23} and the moment M_{in} is that of case no. 2. Equation (H-116) is applicable. The input-output relationship of gear and pinion set no. 3, which relates F_{34F} to F_{23}, was derived for case no. 7 and is given by equation (H-237). Finally, with mesh no. 3 in the round on flat phase, one uses equation (H-195) for the relationship between force F_{34F} and moment M_{04}.
Thus, equation (H-116) is first set equal to equation (H-237) to obtain an expression for force F_{34F}:

$$F_{34F} = \frac{C_{13}C_{32}}{C_{11}C_{15}C_{30}}(M_{in} - Q_1C_{14}) - Q_2\frac{C_{12}C_{32}}{C_{11}C_{30}} - Q_3\frac{C_{31}}{C_{30}} \qquad \text{(H-240)}$$

The above expression is now set equal to equation (H-195). This allows the determination of M_{o48} (for case 8: FRF):

$$M_{o48} = M_{in}\frac{C_{13}C_{26}C_{32}}{C_{11}C_{15}C_{30}} - Q_1\frac{C_{13}C_{14}C_{26}C_{32}}{C_{11}C_{15}C_{30}} - Q_2\frac{C_{12}C_{26}C_{32}}{C_{11}C_{30}}$$

$$- Q_3\frac{C_{26}C_{31}}{C_{30}} - Q_4C_{25} \qquad \text{(H-241)}$$

2. INPUT-OUTPUT ANALYSIS OF TWO STEP-UP GEAR TRAIN

The following gives derivations for the moment input-output relationships associated with the four possible possible contact combinations of a two step-up gear train. (See Table H-2).

a. CASE NO. 1: RR

For this contact combination, the relationship between the equilibrant moment M_{o3} and force F_{23}, both acting on pinion no. 3, must first be newly obtained. The relationships between forces F_{23} and F_{12} of gear and pinion set no. 2, as well as between force F_{12} and input moment M_{in} of gear no. 1, may be taken from case no. 1 of the three step-up gear train analysis. Equations (H-61) and (H-78), respectively, are applicable.

I. FORCE AND MOMENT EQUILIBRIA OF PINION NO. 3

Figure H-13 shows a schematic free body diagram of pinion no. 3 in the round on round phase of contact. The equilibrant

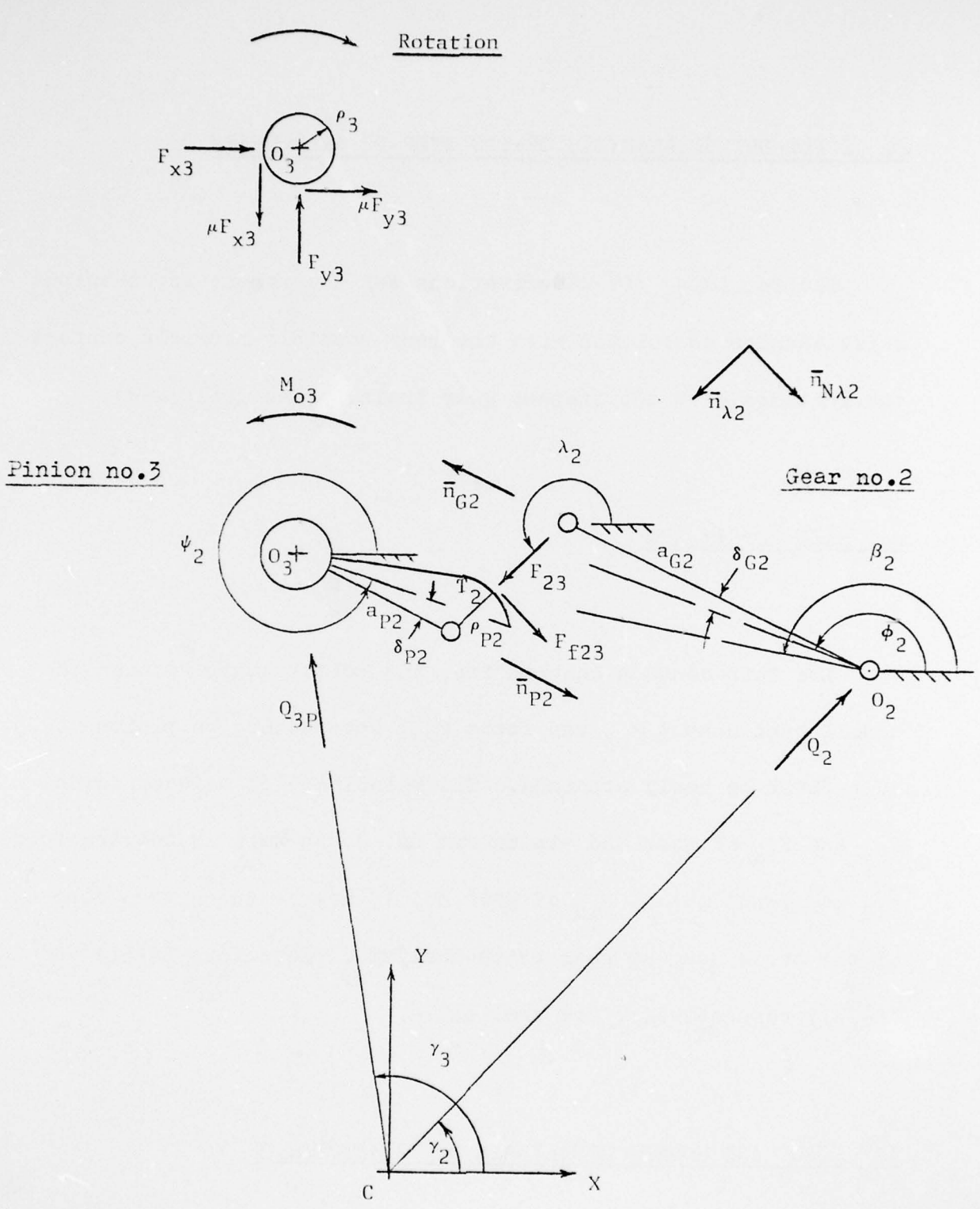

FIGURE H-13

FREE BODY DIAGRAM OF PINION NO. 3
MESH NO. 2: ROUND ON ROUND

moment M_{o3} acts in the direction opposite to the clockwise rotation of the pinion. The normal contact force of gear no. 2 on pinion no. 3 is given by:

$$\bar{F}_{23} = F_{23}\bar{n}_{\lambda 2} \tag{H-242}$$

The associated friction force becomes:

$$\bar{F}_{f23} = \mu s_{2R} F_{23}\bar{n}_{N\lambda 2} \tag{H-243}$$

The pivot reactions are chosen in the usual manner.

The centrifugal force $\bar{Q}_{3P}$ is now due to the mass m_{3P} of the pinion alone, i.e.

$$\bar{Q}_{3P} = Q_{3P}(\cos\gamma_3\bar{i} + \sin\gamma_3\bar{j}) \tag{H-244}$$

where

$$Q_{3P} = m_{3P}\mathcal{R}_3\omega^2 \tag{H-245}$$

Force equilibrium of the pinion is assured by:

$$F_{23}\bar{n}_{\lambda 2} + \mu s_{2R}F_{23}\bar{n}_{N\lambda 2} + F_{x3}\bar{i} + \mu F_{y3}\bar{i} + F_{y3}\bar{j} - \mu F_{x3}\bar{j} + \bar{Q}_{3P} = 0 \qquad \text{(H-246)}$$

Moment equilibrium about point O_3 is given by:

$$\mu\rho_3(\tilde{F}_{x3} + \tilde{F}_{y3})\bar{k} + M_{o3}\bar{k} + \left[a_{P2}\bar{n}_{P2} - \rho_{P2}\bar{n}_{\lambda 2}\right] \times \left[F_{23}\bar{n}_{\lambda 2} + \mu s_{2R}F_{23}\bar{n}_{N\lambda 2}\right] = 0 \qquad \text{(H-247)}$$

Equation (H-246) gives the following component expressions:

$$F_{23}\cos\lambda_2 - \mu s_{2R}F_{23}\sin\lambda_2 + F_{x3} + \mu F_{y3} + Q_{3P}\cos\gamma_3 = 0 \qquad \text{(H-248)}$$

and

$$F_{23}\sin\lambda_2 + \mu s_{2R}F_{23}\cos\lambda_2 + F_{y3} - \mu F_{x3} + Q_{3P}\sin\gamma_3 = 0 \qquad \text{(H-249)}$$

The scalar form of the moment equation (H-247) becomes:

$$\mu\rho_3(\tilde{F}_{x3} + \tilde{F}_{y3}) + M_{o3} - \mu s_{2R}\rho_{P2}F_{23} + a_{P2}F_{23}\left[-\sin(\psi_2 - \delta_{P2} - \lambda_2)\right.$$

$$\left. + \mu s_{2R}\cos(\psi_2 - \delta_{P2} - \lambda_2)\right] = 0 \qquad \text{(H-250)}$$

Simultaneous solution of equations (H-248) and (H-249) for the forces F_{x3} and F_{y3} gives:

$$F_{x3} = \frac{1}{1 + \mu^2}\left\{F_{23}\left[\mu(1 + s_{2R})\sin\lambda_2 + (\mu^2 s_{2R} - 1)\cos\lambda_2\right]\right.$$

$$\left. + Q_{3P}\left[\mu\sin\gamma_3 - \cos\gamma_3\right]\right\} \qquad \text{(H-251)}$$

and

$$F_{y3} = \frac{1}{1 + \mu^2}\left\{F_{23}\left[(\mu^2 s_{2R} - 1)\sin\lambda_2 - \mu(1 + s_{2R})\cos\lambda_2\right]\right.$$

$$\left. + Q_{3P}\left[-\sin\gamma_3 - \mu\cos\gamma_3\right]\right\} \qquad \text{(H-252)}$$

The sum $\tilde{F}_{x3} + \tilde{F}_{y3}$ of equation (H-250) is now made up from equations (H-251) and (H-252) in the sense of equation (A-3b):

$$\tilde{F}_{x3} + \tilde{F}_{y3} = F_{23}A_{65} + Q_{3P}A_{66} + F_{23}A_{67} + Q_{3P}A_{68} \qquad \text{(H-253)}$$

where

$$A_{65} = \left| \frac{\mu(1 + s_{2R})\sin\lambda_2 + (\mu^2 s_{2R} - 1)\cos\lambda_2}{1 + \mu^2} \right| \qquad \text{(H-254)}$$

$$A_{66} = \left| \frac{\mu\sin\gamma_3 - \cos\gamma_3}{1 + \mu^2} \right| \qquad \text{(H-255)}$$

$$A_{67} = \left| \frac{(\mu^2 s_{2R} - 1)\sin\lambda_2 - \mu(1 + s_{2R})\cos\lambda_2}{1 + \mu^2} \right| \qquad \text{(H-256)}$$

$$A_{68} = \left| \frac{-\sin\gamma_3 - \mu\cos\gamma_3}{1 + \mu^2} \right| \qquad \text{(H-257)}$$

Equation (H-253) is now substituted into the moment equation (H-250) and the result is solved for F_{23}:

$$F_{23} = \frac{-M_{03} - Q_{3P}C_{33}}{C_{34}} \qquad \text{(H-258)}$$

where

$$C_{33} = \mu\rho_3(A_{66} + A_{68})$$

$$C_{34} = \mu\rho_3(A_{65} + A_{67}) - \mu s_{2R}\rho_{P2}$$

$$+ a_{P2}\left[\mu s_{2R}\cos(\psi_2 - \delta_{P2} - \lambda_2) - \sin(\psi_2 - \delta_{P2} - \lambda_2)\right]$$

II. MOMENT INPUT-OUTPUT RELATIONSHIP

In the derivation for case 1 of the three step-up gear train it was shown that if one sets equations (H-61) and (H-78) equal to each other, one obtains the following relationship [i.e. equation (H-79)] between force F_{23} and the input moment M_{in}:

$$F_{23} = \frac{-C_8}{C_6 C_{10}} (M_{in} - Q_1 C_9) + Q_2 \frac{C_7}{C_6} \qquad \text{(H-259)}$$

The above expression is now set equal to equation (H-258), and the result is solved for the equilibrant moment M_{o31} (for case 1: RR):

$$M_{o31} = M_{in} \frac{C_8 C_{34}}{C_6 C_{10}} - Q_1 \frac{C_8 C_9 C_{34}}{C_6 C_{10}} - Q_2 \frac{C_7 C_{34}}{C_6} - Q_{3P} C_{33} \qquad \text{(H-260)}$$

b. CASE NO. 2: RF

MOMENT INPUT-OUTPUT RELATIONSHIP

The moment equation for the present case, in which mesh no. 1 is in the round on flat phase and mesh no. 2 in the round on round one, may be derived entirely from existing relationships. Equation (H-116) gives an expression for the force F_{23} in terms of the input moment M_{in} and the centrifugal forces Q_1 and Q_2 for the present combination of contacts in both meshes. When this expression, from case no. 2 of the three step-up gear train, is set equal to equation (H-259) of case no. 1 of the two step-up gear train, one obtains for M_{o32} (case no. 2: RF):

$$M_{o32} = M_{in}\frac{C_{13}C_{34}}{C_{11}C_{15}} - Q_1\frac{C_{13}C_{14}C_{34}}{C_{11}C_{15}} - Q_2\frac{C_{12}C_{34}}{C_{11}} - Q_{3P}C_{33} \qquad \text{(H-261)}$$

c. CASE NO. 3: FF

For this contact combination, where both meshes no. 1 and no.2 are in the round on flat phase, the relationship between the equilibrant moment M_{o3} and the normal contact force F_{23F}, both acting on pinion no. 3, must first be determined. The resulting expression in F_{23F} can then be set equal to the relationship between F_{23F} and the input moment M_{in}, which is given by equation (H-156), and which was derived in conjunction with case no. 3 of the three step-up gear train.

I. FORCE AND MOMENT EQUILIBRIA OF PINION NO. 3

Figure H-14 shows the free body diagram of pinion no. 3 in the round on flat phase of contact. Again, the equilibrant moment M_{o3} acts in a counter-clockwise direction. The normal force F_{23F} of gear no. 2 on pinion no. 3 is given by:

$$\bar{F}_{23F} = - F_{23F}\bar{n}_{NF2} \qquad \text{(H-262)}$$

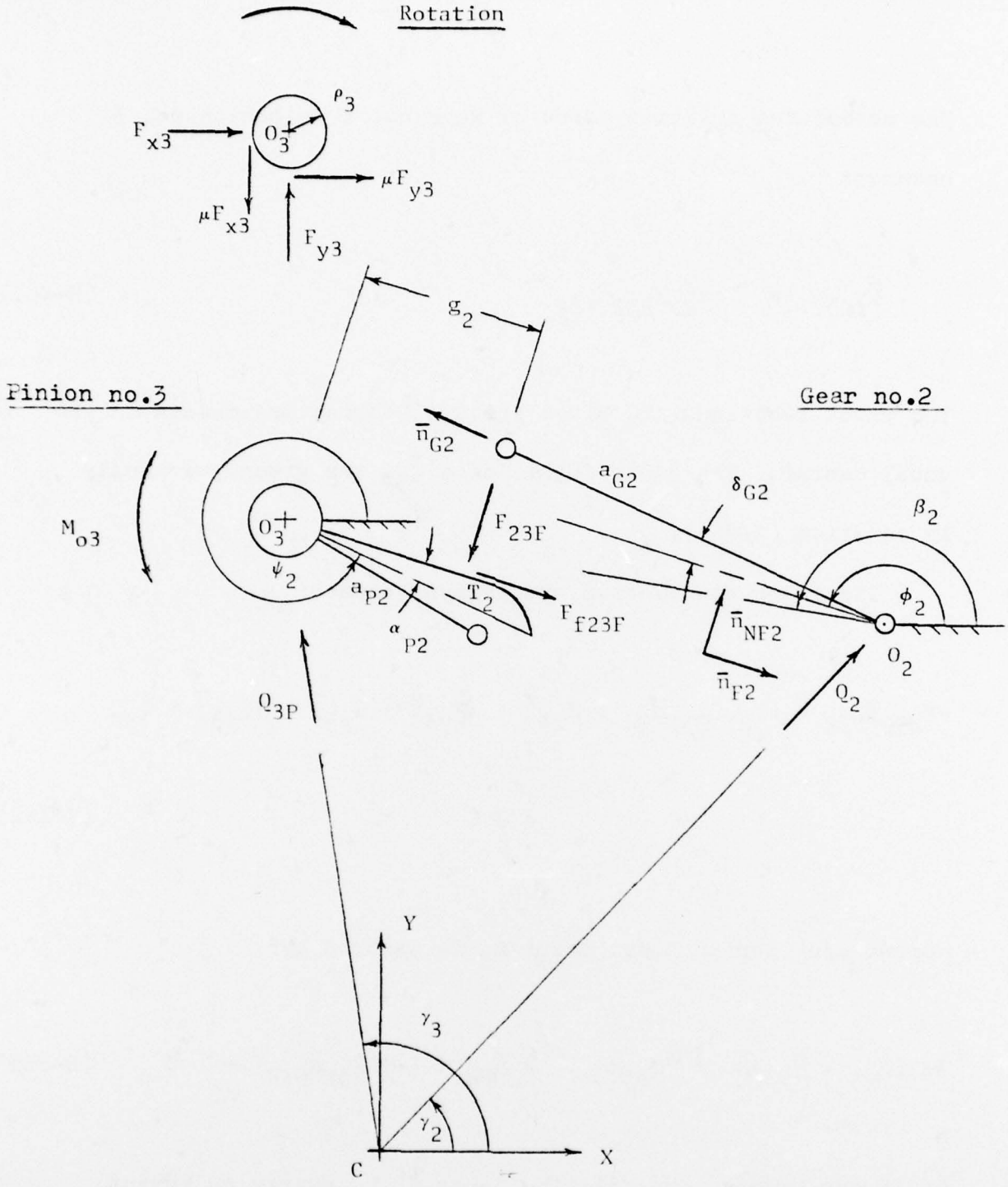

FIGURE H-14

FREE BODY DIAGRAM OF PINION NO. 3

MESH NO. 2: ROUND ON FLAT

The associated friction force of gear no. 2 on pinion no. 3 becomes:

$$\bar{F}_{f23F} = \mu s_{2F} F_{23F} \bar{n}_{F2} \qquad \text{(H-263)}$$

The pivot reactions and pivot friction forces are chosen in the usual manner. The centrifugal force $\bar{Q}_{3P}$ was given previously by equation (H-244).

The force equilibrium expression becomes:

$$-F_{23F}\bar{n}_{NF2} + \mu s_{2F} F_{23F}\bar{n}_{F2} + F_{x3}\bar{i} + \mu F_{y3}\bar{i} + F_{y3}\bar{j} - \mu F_{x3}\bar{j} + \bar{Q}_{3P}$$

$$= 0 \qquad \text{(H-264)}$$

Moment equilibrium about point O_3 is assured by:

$$\mu\rho_3(\tilde{F}_{x3} + \tilde{F}_{y3})\bar{k} + M_{o3}\bar{k} + g_2\bar{n}_{F2} \times (-)F_{23F}\bar{n}_{NF2} = 0 \qquad \text{(H-265)}$$

As always before, the friction force F_{f23F} exerts no moment about point O_3.

Equation (H-264) gives the following component expressions:

$$F_{23F}\sin(\psi_2 + \alpha_{P2}) + \mu s_{2F}F_{23F}\cos(\psi_2 + \alpha_{P2}) + F_{x3} + \mu F_{y3} + Q_{3P}\cos\gamma_3 = 0 \qquad \text{(H-266)}$$

and

$$-F_{23F}\cos(\psi_2 + \alpha_{P2}) + \mu s_{2F}F_{23F}\sin(\psi_2 + \alpha_{P2}) + F_{y3} - \mu F_{x3} + Q_{3P}\sin\gamma_3 = 0 \qquad \text{(H-267)}$$

The scalar form of the moment equation (H-265) is given by:

$$\mu\rho_3(\tilde{F}_{x3} + \tilde{F}_{y3}) + M_{o3} - g_2F_{23F} = 0 \qquad \text{(H-268)}$$

Simultaneous solution of equations (H-266) and (H-267) for F_{x3} and F_{y3} leads to:

$$F_{x3} = \frac{1}{1 + \mu^2}\left\{F_{23F}\left[(\mu^2 s_{2F} - 1)\sin(\psi_2 + \alpha_{P2}) - \mu(1 + s_{2F})\cos(\psi_2 + \alpha_{P2})\right] + Q_{3P}\left[\mu\sin\gamma_3 - \cos\gamma_3\right]\right\} \qquad \text{(H-269)}$$

$$F_{y3} = \frac{1}{1+\mu^2}\left\{F_{23F}\left[-\mu(1+s_{2F})\sin(\psi_2+\alpha_{P2}) + (1-\mu^2 s_{2F})\cos(\psi_2+\alpha_{P2})\right]\right.$$

$$\left. + Q_{3P}\left[-\sin\gamma_3 - \mu\cos\gamma_3\right]\right\} \qquad \text{(H-270)}$$

The sum $\tilde{F}_{x3} + \tilde{F}_{y3}$ of equation (H-268) is now made up of equations (H-269) and (H-270) in the sense of equation (A-3b):

$$\tilde{F}_{x3} + \tilde{F}_{y3} = F_{23F}A_{69} + Q_{3P}A_{70} + F_{23F}A_{71} + Q_{3P}A_{72} \qquad \text{(H-271)}$$

where

$$A_{69} = \left|\frac{(\mu^2 s_{2F} - 1)\sin(\psi_2+\alpha_{P2}) - \mu(1+s_{2F})\cos(\psi_2+\alpha_{P2})}{1+\mu^2}\right| \qquad \text{(H-272)}$$

$$A_{70} = \left|\frac{\mu\sin\gamma_3 - \cos\gamma_3}{1+\mu^2}\right| \qquad \text{(H-273)}$$

$$A_{71} = \left|\frac{-\mu(1+s_{2F})\sin(\psi_2+\alpha_{P2}) + (1-\mu^2 s_{2F})\cos(\psi_2+\alpha_{P2})}{1+\mu^2}\right| \qquad \text{(H-274)}$$

$$A_{72} = \left|\frac{-\sin\gamma_3 - \mu\cos\gamma_3}{1+\mu^2}\right| \qquad \text{(H-275)}$$

Equation (H-271) is now substituted into the moment equation (H-268), and the result is solved for F_{23F}:

$$F_{23F} = \frac{- M_{o3} - Q_{3P}C_{35}}{C_{36}} \qquad \text{(H-276)}$$

where

$$C_{35} = \mu\rho_3(A_{70} + A_{72})$$

$$C_{36} = \mu\rho_3(A_{69} + A_{71}) - g_2$$

II. MOMENT INPUT-OUTPUT RELATIONSHIP

The moment input-output relationship for the present case is obtained, as stated earlier, by setting equation (H-276) equal to equation (H-156) and solving the resulting expression for the equilibrant moment M_{o33} (case no. 3: FF):

$$M_{o33} = M_{in}\frac{C_{21}C_{36}}{C_{15}C_{19}} - Q_1\frac{C_{14}C_{21}C_{36}}{C_{15}C_{19}} - Q_2\frac{C_{20}C_{36}}{C_{19}} - Q_{3P}C_{35} \qquad \text{(H-277)}$$

d. CASE NO. 4: FR

MOMENT INPUT-OUTPUT RELATIONSHIP

The moment input-output relationship for this case, where mesh no. 1 is in round on round contact while mesh no. 2 is in the round on flat phase, may also be derived entirely by assembling existing relationships.

Equation (H-276), of the previous section, gives force F_{23F} in terms of the equilibrant moment M_{o3} when mesh no. 2 is in the round on flat phase. Equation (H-178), derived for case no. 4 (RFR) of the three step-up gear train, relates this force F_{23F} to the input moment M_{in}.

Thus, one first sets equations (H-178) and (H-276) equal to each other and then solves the result for M_{o34} (case 4: FR):

$$M_{o34} = M_{in}\frac{C_{24}C_{36}}{C_{10}C_{22}} - Q_1\frac{C_9C_{24}C_{36}}{C_{10}C_{22}} - Q_2\frac{C_{23}C_{36}}{C_{22}} - Q_{3P}C_{35} \qquad \text{(H-278)}$$